

N°d'ordre NNT:
2018LYSE1185



THESE de DOCTORAT DE L'UNIVERSITE DE LYON

opérée au sein de
l'Université Claude Bernard Lyon 1

Ecole Doctorale N° 206
(Ecole Doctorale de Chimie de Lyon)

Spécialité de doctorat :
Discipline : Chimie des Polymères

Soutenue publiquement le 05/10/2018, par :
HMAYED Ali Al Rida

Radical and catalytic polymerizations of α -olefins: towards CO₂-incorporation

Devant le jury composé de :

Dr. LACROIX-DESMAZES Patrick	Directeur de Recherche-CNRS	Rapporteur
Pr. MARTIN-VACA Blanca	Professeur-Université Paul Sabatier	Rapporteuse
Pr. GIROIR-FENDLER Anne	Professeur-Université Lyon 1	Président du jury
Dr. GUILLAUME Sophie	Directrice de Recherche-CNRS	Examinatrice
Dr. MONTEIL Vincent	Directeur de Recherche-CNRS	Directeur de thèse
Dr. RAYNAUD Jean	Chargé de Recherche-CNRS	Co-directeur de thèse

Acknowledgements:

I would like to thank the members of the jury, Dr. Patrick LACROIX-DESMAZES, Pr. Blanca MARTIN-VACA, Pr. Anne GIROIR-FENDLER, and Dr. Sophie GUILLAUME, for their presence in my PhD defense and their attentive reading of my manuscript.

I express my gratitude to my thesis supervisor, Dr. Jean RAYNAUD for his kind supervision, knowledge, and his featured ideas in this research domain. We spent time on discussing not only work issues but also many other interesting topics, he made the work atmosphere much more comfortable and smooth. For that and for the rest, thanks Jean.

Many thanks to my co-supervisor, Dr. Vincent MONTEIL. His advises and his special experience in polymer chemistry were key elements in the success of this project.

My special thanks go to my teacher Dr. Sébastien NORSIC for teaching me a lot of skills in the practical work. I like to highlight his indispensable help in the laboratory installations for the LCPP group.

I have spent my last three years with exceptional people who are the LCPP group members, I thank them one by one. Particularly, I would like to express my sincere friendly and grateful sentiments to Arne WOLPERS, Aurelien BETHEGNIES, Manel TAAM, Edgar ESPINOSA, Winnie NZAHOU OTTOU, and Cedric YSACCO.

Thanks to the NMR Polymer Center of Institut de Chimie de Lyon for the assistance and access to the NMR facilities.

At the end, my great thanks to my family and my wife for being always there for me, for their moral support, and for their aid that contributed in achieving my PhD diploma.

Abstract

This thesis focuses primarily on the utilization of CO₂ in radical and catalytic polymerizations of α -olefins. Polyethylene was synthesized by a free radical polymerization process in supercritical CO₂ (scCO₂) under mild conditions (T < 100 °C, P < 300 bar) without addition of any initiator diluent, using AIBN, lauroyl peroxide, or benzoyl peroxide to investigate different initiation modes. The decarboxylation of the latter can be suppressed in scCO₂ to yield ester-functionalized polyethylene. Furthermore, an interaction between triethylaluminum (AlEt₃) and radicals was unveiled, the effect of AlEt₃ on ethylene radical polymerization was investigated showing its role as an irreversible chain-transfer agent in this process. This interaction in conjunction with the reactivity of AlEt₃ towards CO₂ were harnessed to allow for CO₂-incorporation within polyethylene chains. Thus, since CO₂ was incorporated within the polyethylene chains using AlEt₃, CO₂ for the first time behaved as an effective reagent in ethylene radical polymerization. On the other hand, ethylene-isoprene random and block copolymerizations *via* iron-catalyzed chain shuttling processes have been achieved. Subsequently, each monomer was polymerized in supercritical CO₂ using its corresponding dedicated iron catalyst in order to achieve sustainable processes to polymerize these monomers, with the ultimate target of incorporating some carboxylic moieties.

Keywords: *Ethylene radical polymerization, supercritical CO₂, triethylaluminum, functionalization, CO₂-incorporation, iron complexes, catalytic chain-transfer copolymerization, catalytic olefin polymerization.*

Résumé

Cette thèse se concentre principalement sur l'activation du CO₂ dans les polymérisations radicalaires et catalytiques des α -oléfines. Le polyéthylène a tout d'abord été synthétisé par un procédé de polymérisation radicalaire dans du CO₂ supercritique (scCO₂) dans des conditions douces ($T < 100$ °C, $P < 300$ bar) sans ajout de solvant organique pour solubiliser l'amorçeur. Nous avons utilisé l'AIBN, le peroxyde de lauryle ou le peroxyde de benzoyle pour étudier différents modes d'amorçage. La décarboxylation de ce dernier peut être supprimée dans le scCO₂ et conduit à la formation de polyéthylène fonctionnalisé par des groupements esters. En outre, une interaction entre le triéthylaluminium (AlEt₃) et les radicaux a été dévoilée, l'effet d'AlEt₃ sur la polymérisation radicalaire de l'éthylène a été étudié, révélant son rôle d'agent de transfert de chaîne irréversible dans ce processus. Cette interaction, en combinaison avec celle d'AlEt₃ avec le CO₂ ont été exploitées pour permettre l'incorporation de CO₂ dans les chaînes de polymère. Ainsi, si le motif CO₂ est présent dans les chaînes de polyéthylène en utilisant AlEt₃, le CO₂ est bien pour la première fois un réactif effectif dans la polymérisation radicalaire de l'éthylène. D'autre part, des copolymérisations statistiques et séquencées d'éthylène-isoprène par des procédés de transferts de chaînes à l'Aluminium catalysés par des complexes de fer ont été réalisées. Ensuite, chaque monomère a été polymérisé indépendamment dans du CO₂ supercritique en utilisant le catalyseur de fer optimal afin d'obtenir des procédés plus écologiques pour la polymérisation de ces monomères dont le but ultime sera l'incorporation de motifs carboxyliques.

Mots-clés: *Polymérisation radicalaire d'éthylène, CO₂ supercritique, triéthylaluminium, fonctionnalisation, incorporation de CO₂, complexes de fer, copolymérisation par transfert de chaînes catalytique, polymérisation catalytique d'oléfines.*

Table of Contents

Résumé	1
Glossary.....	7
Introduction	11
References	16
 A. CHAPTER I. Activation of CO ₂ in Chemistry: The Path towards its Activation in Polymerizations of Olefins.....	17
A.1. History of "CARBON DIOXIDE"	19
A.2. Chemical and Physical Properties of "CO ₂ "	20
A.3. Carbon Dioxide Production	21
A.4. Carbon Dioxide Applications.....	22
A.4.1. In Food Industry	22
A.4.2. In Oil Industry.....	22
A.4.3. In Different Areas	23
A.4.4. In Chemical Industry	23
A.5. Carbon Dioxide in Chemistry	24
A.5.1. Carbon Dioxide as a Reactant or a Monomer	25
A.5.1.1. CO ₂ as a Reactant in Production of Molecules	26
A.5.1.2. CO ₂ as a Monomer in Polymer Synthesis.....	41
A.5.2. Carbon Dioxide as a Polymerization Medium	55
A.5.2.1. Cationic Polymerizations in CO ₂	58
A.5.2.2. Transition Metal-Catalyzed Polymerizations in CO ₂	60
A.5.2.3. Radical Polymerizations in CO ₂	63
A.6. Towards CO ₂ Utilization in Polymerizations of Olefins.....	70

Table of Contents

A.7. ETHYLENE: The Most Important Industrial Olefin.....	71
A.7.1. History of "ETHYLENE"	71
A.7.2. Chemical and Physical Properties of Ethylene	72
A.7.3. Ethylene Production.....	73
A.7.4. Uses of Ethylene.....	74
A.8. POLYETHYLENE	75
A.8.1. History of Polyethylene	76
A.8.2. Structure of Polyethylene.....	77
A.8.3. Properties of Polyethylene	78
A.8.4. Types of Polyethylene and their Synthesis Processes	80
A.8.4.1. LDPE: <i>via Radical Polymerization Processes</i>	81
A.8.4.2. MDPE.....	84
A.8.4.3. HDPE and LLDPE: <i>via Catalytic Polymerization Processes</i>	85
A.8.5. Uses of Polyethylene.....	87
A.9. Kinetic and Thermodynamic Considerations in the Copolymerization of Ethylene and CO₂	88
A.10. Conclusion and Results Obtained at the C2P2 Laboratory	95
A.11. References.....	98
 B. CHAPTER II. Ethylene Free Radical Polymerization in Supercritical CO₂.....	 109
B.1. Abstract.....	110
B.2. Construction and Testing of the High-Pressure Reactor	110
B.2.1. Construction	110
B.2.2. Testing.....	112
B.2.2.1. Pressurizing with Ethylene	114
B.2.2.2. Pressurizing with CO ₂	114

B.2.2.3. Pressurizing with a Mixture of Ethylene and CO ₂	117
B.2.2.4. Average Increase of Pressure.....	119
B.3. Ethylene Free Radical Polymerization in scCO₂.....	119
B.3.1. Recent Work at LCPP: Ethylene Free Radical Polymerization under Mild Conditions by the Effect of Solvent	120
B.3.2. Ethylene Free Radical Polymerization in scCO ₂ under Mild Conditions.	121
B.3.2.1. Radical Initiators	122
B.3.2.2. AIBN-Initiated Reactions.....	124
B.3.2.3. Lauroyl Peroxide-Initiated Reactions.....	128
B.3.2.4. Benzoyl Peroxide-Initiated Reactions	134
B.4. Conclusion	142
B.5. References	144
 C. CHAPTER III. Triethylaluminum-Mediated Ethylene Radical Polymerization: From a Transfer Agent to a CO₂-Incorporating Agent.....	 145
C.1. Abstract	147
C.2. Triethylaluminum-Mediated Ethylene Radical Polymerization: A Chain-Transfer Agent	147
C.2.1. Lewis Acids effect on the Ethylene Radical Polymerization	147
C.2.2. Controlling Agent versus Transfer Agent	148
C.2.3. Definition of a "Controlled Radical Polymerization"	149
C.2.4. Concept of "CRP"	150
C.2.5. Types of "CRP"	151
C.2.5.1. Reversible Termination Mechanism.....	151
C.2.5.2. Degenerative Chain Transfer Mechanism	152
C.2.6. Effect of TEA on the Ethylene Radical Polymerization	154

Table of Contents

C.2.6.1. EPR Analysis: Interaction between TEA and Radicals	154
C.2.6.2. Conventional Ethylene Free Radical Polymerization (blank reaction) and "Aufbau" Reaction.....	156
C.2.6.3. Mn of Polyethylene versus [TEA]	158
C.2.6.4. Mn of Polyethylene versus Conversion	160
C.2.6.5. Variation of Mn as function of [AIBN]	170
C.2.6.6. Quenching the Polymerization Reaction by I ₂	172
C.3. Incorporation of CO ₂ in the Polyethylene Chain Using Triethylaluminum	174
C.3.1. Interaction of Triethylaluminum with CO ₂	174
C.3.2. Ethylene Radical Polymerization in scCO ₂ in the Presence of TEA	175
C.3.3. Hydrolysis of the CO ₂ -Functionalized Polyethylene	182
C.4. Conclusion	185
C.5. References	187
 D. CHAPTER IV. Iron-Catalyzed Ethylene-Isoprene Copolymerization: From a Chain Shuttling Process towards a CO ₂ -Activated Process.	189
D.2. Abstract	191
D.3. Chain Shuttling Copolymerization	191
D.3.1. Definition	191
D.3.2. Concept	191
D.3.3. Literature Review	192
D.4. Iron Complexes	194
D.4.1. Oxidation States of Iron	194
D.4.2. Iron Complexes in Ethylene Polymerization	195
D.4.3. Iron Complexes in Isoprene Polymerization	200
D.5. Ethylene-Isoprene Copolymerization	202

D.6. Ethylene-Isoprene Chain Shuttling Copolymerization via Fe-Al-Fe Transmetallation Reactions	206
D.6.1. Catalysts A and B in Homo-polymerizations	207
D.6.1.1. Ethylene Homo-polymerization Using Catalyst A	207
D.6.1.2. Isoprene Homo-polymerization Using Catalyst B	210
D.6.2. Catalysts A and B in ethylene-Isoprene Copolymerization	213
D.6.2.1. Ethylene-Isoprene Copolymerization Test Using Catalyst A	213
D.6.2.2. Ethylene-Isoprene Copolymerization Test Using Catalyst B	216
D.6.3. Ethylene-Isoprene Chain Shuttling Copolymerization	217
D.6.3.1. Random Copolymerization	218
D.6.3.2. Block Copolymerization	226
D.7. Homo-Polymerizations of Ethylene and Isoprene in scCO₂	236
D.7.1. Iron-Catalyzed Ethylene Polymerization in scCO ₂	236
D.7.2. Iron-Catalyzed Isoprene Polymerization in scCO ₂	238
D.8. Conclusion	241
D.9. References	242
E. Experimental Part.....	245
E.1. Experimental Section of Chapter II	247
E.1.1. Polymerization Method in Supercritical CO ₂	247
E.1.2. Polymerization Method in Dimethylcarbonate	248
E.2. Experimental Section of Chapter III	249
E.2.1. Conventional Ethylene Free Radical Polymerization	249
E.2.2. Polymerization Method of Ethylene Radical Polymerization in Presence of Triethylaluminum	249
E.2.2.1. Quenching the Polymerization Reaction by Iodine	250

Table of Contents

E.2.3. Polymerization Method of Ethylene Radical Polymerization in scCO_2 in Presence of Triethylaluminum	250
E.2.4. Hydrolysis of the CO_2 -Functionalized Polyethylene	251
E.3. Experimental Section of Chapter IV	251
E.3.1. Synthesis of Iron Complexes	251
E.3.1.1. Synthesis of Catalysts A and C	251
E.3.1.2. Synthesis of Catalyst B	253
E.3.2. Homo-Polymerization of Ethylene Using Catalyst A	254
E.3.3. Homo-Polymerization of Isoprene Using Catalyst B	254
E.3.4. Ethylene-Isoprene Copolymerization Test Using Catalyst A	254
E.3.5. Copolymerization Test Using Catalyst B	255
E.3.6. Ethylene-Isoprene Chain Shuttling Random Copolymerization	255
E.3.7. Ethylene-Isoprene Chain Shuttling Block Copolymerization	256
E.3.8. Iron-Catalyzed Ethylene Polymerization in scCO_2	256
E.3.9. Iron-Catalyzed Isoprene Polymerization in scCO_2	257
E.4. Analytical Methods	258
E.4.1. Nuclear Magnetic Resonance (NMR)	258
E.4.2. Size-Exclusion Chromatography (SEC)	258
E.4.3. Differential Scanning Calorimetry (DSC)	258
E.4.4. Fourier Transform Infrared Spectroscopy (FTIR)	259
E.4.5. Electron Paramagnetic Resonance (EPR)	259
Conclusion and Perspectives	261
Conclusion	261
Perspectives	262
References	267

Résumé

Les polyoléfines, la plus grande famille de thermoplastiques, sont des macromolécules formées par la polymérisation d'unités monomères d' α -oléfine (alcène terminal). Au cours des 50 dernières années, les polyoléfines sont devenues les polymères synthétiques les plus utilisés en raison de leur large gamme d'applications dues à leurs propriétés mécaniques uniques et ajustables. Celles-ci comprennent entre autres les domaines de la construction, des biens de consommation et de l'emballage, de l'électronique, de l'électricité et de l'automobile.

Le polyéthylène, le polymère manufacturé le plus commun, est synthétisé à partir de la polymérisation de l'éthylène qui est le monomère oléfinique le plus simple. L'éthylène a toujours retenu l'attention des chimistes des polymères car il est omniprésent, dérivé de combustibles fossiles ou de matières premières renouvelables à cycle de vie court, et permet l'accès à une large gamme de propriétés de matériaux uniquement à partir de sa méthode de polymérisation.

Industriellement, deux stratégies principales sont employées dans la polymérisation de l'éthylène pour produire les différents grades de polyéthylènes semi-cristallins: les procédés radicalaires pour fabriquer du polyéthylène basse densité (LDPE) et les procédés catalytiques pour produire du polyéthylène haute densité (HDPE). Le LDPE, obtenu par des procédés radicalaires à haute température et à haute pression ($> 150^\circ\text{C}$, 1500-3000 bars), donne des matériaux plus mous, composés de chaînes polymères ramifiées, utilisés pour les emballages par exemple. Le HDPE, obtenu par des procédés catalytiques à basse température et pression ($< 100^\circ\text{C}$, < 50 bars), donne des matériaux plus durs, composés de chaînes polymères linéaires, utilisés dans la fabrication de tuyaux par exemple.

Un des cas particulier des α -oléfines sont les diènes, Notamment les diènes 1,3-conjugués, qui cristallisent mieux, sont cruciaux pour l'industrie. Ils y sont souvent polymérisés pour produire des élastomères, vulcanisables pour obtenir les produits finis. Par exemple, le 1,3-butadiène est un précurseur du caoutchouc synthétique utilisé dans les pneumatiques, et l'isoprène est le précurseur des imitations de caoutchouc naturel également utilisées dans la fabrication des pneumatiques.

Le développement de méthodes douces pour la synthèse de polymères utilisant des

matières premières renouvelables est un obstacle technologique majeur sur la voie d'une économie de polymères durables. Le dioxyde de carbone est une des ressources C1 renouvelables des plus attrayantes, et il présente de nombreux avantages pratiques, tels que son abondance, son faible coût et sa relative innocuité. Limiter sa concentration dans l'atmosphère est aussi devenu un enjeu sociétal majeur. Son utilisation en tant que source de carbone est cependant inextricablement inhérent à son caractère inerte du à ses deux doubles liaisons C=O symétriques.

L'objectif principal de ce projet de thèse est de concevoir de nouveaux procédés de polymérisation radicalaire et catalytique des oléfines et d'utiliser avantageusement le CO₂ dans ces procédés (**Figure 1**).

Cette thèse est composée de deux parties principales:

1. Polymérisations radicalaires des oléfines: Le passage des procédés classiques de polymérisation radicalaire des oléfines aux procédés valorisant le CO₂. Cette valorisation comprend l'utilisation de CO₂ comme milieu de polymérisation et comme agent de fonctionnalisation.
2. Polymérisations catalytiques d'oléfin: conception de procédés de polymérisation catalytique d'oléfin fonctionnalisants. D'abord par l'utilisation de complexes de fer, un métal de transition respectueux de l'environnement et abondant; deuxièmement, en activant le CO₂ en tant que milieu de polymérisation/agent de fonctionnalisation dans ces procédés.



Figure 1. Activation du dioxyde de carbone dans les polymérisations radicalaires et catalytiques d'oléfin.

Grâce à la stratégie que nous avons suivie, nous avons visé à développer des procédés durables. Ceci est réalisé en valorisant un déchet (CO₂) dans la polymérisation des

thermoplastiques les plus demandés (polyoléfines) ainsi qu'en substituant partiellement des matières premières à base de pétrole telles que des solvants, plus coûteux, par du CO_2 . En outre, nous dépendons des complexes de fer dans la section catalytique de notre travail, le fer est le moins cher parmi tous les métaux de transition et est respectueux de l'environnement.

Ce manuscrit est composé de quatre chapitres formant une thèse résumée dans le titre: "Polymérisations radicalaires et catalytiques d'oléfines: vers l'incorporation de CO_2 ".

Le premier chapitre représente un examen approfondi de l'utilisation du CO_2 en chimie en tant que réactif, monomère et milieu de polymérisation. Ensuite, la polymérisation de l'éthylène a été revue brièvement car elle a été examinée attentivement dans différentes thèses précédentes et de nombreuses publications récentes. Une revue des considérations cinétiques dans la copolymérisation éthylène- CO_2 a également été mentionnée, expliquant les obstacles à la réalisation de ce processus.

Dans la section des polymérisations radicalaires des oléfines, nous avons étudié l'éthylène, qui représente le modèle oléfinique le plus approprié à étudier car c'est l' α -oléfine la plus simple et la plus applicable sur le plan industriel. La première réalisation expérimentale est détaillée dans le chapitre II, montrant le succès de la polymérisation de l'éthylène par un procédé radicalaire dans le scCO_2 (comme milieu de polymérisation) dans des conditions douces ($< 100^\circ \text{C}$, < 300 bars) sans ajout de diluant pour l'amorceur et donc sans co-solvant organique. Ce travail a été effectué à l'aide de trois initiateurs différents, l'AIBN, le peroxyde de lauryle et le peroxyde de benzoyle, pour étudier différents modes d'amorçage. La décarboxylation de ce dernier a été limitée dans le scCO_2 et a permis la synthèse de polyéthylène fonctionnalisé par un groupement ester.

Ainsi, le CO_2 , ressource ininflammable et disponible, a été valorisé en tant que milieu de polymérisation dans le procédé de polymérisation radicalaire de l'éthylène au lieu des solvants organiques volatils à base de pétrole.

En recherchant un additif capable de briser l'inertie du CO_2 et de l'incorporer dans les chaînes de polyéthylène, nous avons vérifié que le triéthylaluminium (AlEt_3) réagit avec le CO_2 comme mentionné dans la littérature formant des carboxylates d'Al et alcoolates/oxyoles d'Al. Dans le chapitre III, qui comprend deux sous-chapitres, nous

avons découvert une interaction d' AlEt_3 avec les radicaux et son rôle en tant qu'agent de transfert de chaîne irréversible dans la polymérisation radicalaire de l'éthylène dans le premier sous-chapitre.

Utilisant avantageusement ces deux caractéristiques d' AlEt_3 (interaction avec le CO_2 et les radicaux), il a été utilisé dans la polymérisation radicalaire de l'éthylène en milieu scCO_2 pour obtenir du polyéthylène incorporant des motifs esters et carboxylates. Ce travail, qui a été détaillé dans le deuxième sous-chapitre du chapitre 3, a montré qu' AlEt_3 agit comme un agent d'incorporation de CO_2 dans la polymérisation radicalaire de l'éthylène. Le CO_2 a été incorporé dans les chaînes LDPE sous la forme d'esters et de cétales (d'après nos analyses actuelles).

Par conséquent, le CO_2 est valorisable en tant que milieu de polymérisation mais également comme agent de fonctionnalisation dans la polymérisation radicalaire de l'éthylène.

Le chapitre 4 représente la section des polymérisations catalytiques des oléfines, et comprend également deux sous-chapitres. Le premier sous-chapitre traite en détail de la copolymérisation de l'éthylène et de l'isoprène catalysée par des complexes de fer par des procédés de type "transferts de chaînes catalytiques" en utilisant AlEt_3 comme agent de transfert.

Nous nous sommes concentrés sur l'isoprène car sa polymérisation donne un des caoutchoucs synthétiques pouvant remplacer le caoutchouc naturel dans différentes applications (pneumatique, textile, tapis, adhésifs et ballons jouets, etc.) et pour réduire la culture intensive des hévéas. De plus, sa copolymérisation avec l'éthylène donne un matériau qui porte à la fois les caractéristiques du polyéthylène thermoplastique semi-cristallin et de l'élastomère polyisoprène. De tels matériaux pourraient être utilisés dans la fabrication de pneumatiques par exemple, pour améliorer la robustesse et la résistance à l'abrasion, tout en maintenant les propriétés élastomériques.

Dans la deuxième partie de ce chapitre, nous avons présenté des essais réussis de polymérisations de l'éthylène et de l'isoprène catalysées par le fer dans le scCO_2 . Ces tests constituent la base de recherches ultérieures sur l'incorporation de CO_2 dans les chaînes de polymères en utilisant ces mêmes procédés.

Des essais visant à fonctionnaliser le polyéthylène et d'autres polyoléfines avec du CO₂ en utilisant notamment ces diverses stratégies constituent un domaine d'intérêt majeur pour des développements futurs au sein de notre laboratoire.

Glossary

- ABS: acrylonitrile-butadiene-styrene
- AIBN: azobisisobutyronitrile
- atm: atmosphere
- ATRP: atom transfer radical polymerization
- BEMO: bis(ethoxymethyl)oxetane
- BuA: butyl acrylate
- CFC: chlorofluorocarbon
- CHC: cyclohexene carbonate
- CHO: cyclohexene oxide
- COD: cyclooctadiene
- CPO: cyclopentene oxide
- CRP: controlled radical polymerization
- DBU: 1,8-diazobicyclo[5.4.0]undec-7-ene
- dcpe: 1,2-bis(dicyclohexylphosphino)-ethane
- DEC: diethyl carbonate
- DEPC: diethyl peroxydicarbonate
- DEPDC: diethyl peroxydicarbonate
- DFT: density functional theory
- DMAEA: 2-(dimethylamino)ethyl acrylate
- DMAEMA: dimethylaminoethyl methacrylate
- DMAP: (4-dimethylamino)pyridine
- DMAQ: N-N-dimethylaminoquinoline
- DOSY: Diffusion-ordered spectroscopy
- dppf: 1,1'-bis(diphenylphosphino)ferrocene
- dppp: bis(diphenylphosphino)propane
- DSC: Differential Scanning Calorimetry
- dtbpe: 1,2-bis(di-*tert*-butylphosphino)-ethane
- EC: ethylene carbonate
- EO: ethylene oxide

- EPR (ESR): Electron Paramagnetic Resonance (Electron Spin Resonance)
- ESR: Electron spin resonance
- FOA: 1,1-dihydroperfluorooctyl acrylate
- FOMA: perfluorooctylethyl methacrylate
- Fox-7: 3-methyl-3'-[(1,1-dihydroheptafluorobutoxy)methyl]-oxetane
- Freon-113: 1,1,2-trichloro-1,2,2-trifluoroethane
- FRP: free radical polymerization
- FVE: 2- (N-propyl-N-perfluorooctylsulfonamido)ethyl vinyl ether
- HDPE: high-density polyethylene
- HMBC: Heteronuclear Multiple Bond Correlation
- HSQC: Heteronuclear Single Quantum Correlation
- HT-SEC (GPC): High Temperature Size Exclusion Chromatography (Gel Permeation Chromatography)
- IB: isobutylene
- IBVE: isobutyl vinyl ether
- IR spectroscopy: Infrared spectroscopy
- ITP: iodine-transfer polymerization
- LDPE: low-density polyethylene
- LLDPE: linear low-density polyethylene
- MeIm: 1-methylimidazole
- MeOTf: trifluoromethane sulfonate
- MMA: methyl methacrylate
- MOF: metal organic framework
- NMP: nitroxide-mediated polymerization
- NMR: Nuclear Magnetic Resonance
- PBT: polybutylene terephthalate
- Pc: critical pressure
- PC: propylene carbonate
- PCHC: poly(cyclohexene carbonate)
- PCTFE: polychlorotrifluoroethylene
- PE: polyethylene

- PEC: polyethylene carbonate
- PET: polyethylene terephthalate
- PET: polyethylene terphthalate
- PFOS: perfluorooctylsulfonates
- PI: polyisoprene
- PMMA: poly(methyl methacrylate)
- PO: propylene oxide
- PPC: poly(propylene carbonate)
- PPN: bis(triphenylphosphoranylidene)iminium
- PPO: poly(propylene oxide)
- PRE: persistent-radical effect
- PS: polystyrene
- PTFE, teflon: polytetrafluoroethylene
- PVC: polyvinyl chloride
- PVDF: poly(vinylidene difluoride)
- PVF: poly(vinyl fluoride)
- RAFT: reversible addition-fragmentation chain-transfer
- RDRP: reversible-deactivation radical polymerization
- ROMP: ring opening metathesis polymerization
- SBR: styrene-butadiene rubber
- scCO₂: supercritical carbon dioxide
- SO: styrene oxide
- TBD: 1,5,7-triazobicyclo[4.4.0]dec-5-ene
- T_c: critical temperature
- TEA: triethylaluminum
- TERP: tellurium-mediated radical polymerization
- TFE: tetrafluoroethylene
- THF: tetrahydrofuran
- TMDPO: trimethylbenzoyldiphenylphosphineoxide
- TMPCl: 2-(2,4,4-trimethylpentyl)chloride
- TOF: turnover frequency

Glossary

- TON: turnover number
- tos: *p*-toluenesulfonate
- tpp: tetraphenylporphyrin
- VCHO: 4-vinyl-1,2-cyclohexene oxide
- VDF: vinylidene difluoride

Introduction

Polyolefins, the largest family of thermoplastics, are macromolecules formed by the polymerization of olefin (alkene) monomer units. The IUPAC nomenclature term is poly(alkene). During the past 50 years, polyolefins have become, by far, the highest volume in commercial grades of synthetic polymers because of their wide range of applications. These applications include those in construction, consumer goods and packaging, electronics, electrical, and automotive industries.

Polyethylene, the most common manufactured polymer, is synthesized from polymerization of ethylene which is the simplest olefinic monomer. Ethylene has always been the subject of attention of polymer chemists since it is ubiquitous, derived from either fossil fuels or short-lived renewable feedstocks, and allows access to a wide range of material properties solely based on its polymerization method.

Industrially, two main strategies are employed in polymerizing ethylene to produce the different grades of semi-crystalline polyethylenes: radical processes to make low-density polyethylene (LDPE) and catalytic processes to produce high-density polyethylene (HDPE). LDPE obtained *via* radical processes at high temperature and pressures ($> 150^{\circ}\text{C}$, 1500-3000 bar) yields softer materials, composed of branched polymer chains, utilized in packaging for instance. HDPE obtained *via* catalytic processes at low temperature and pressure ($< 100^{\circ}\text{C}$, < 50 bar) yields harder materials, composed of linear polymer chains, utilized in manufacture of pipes for example.

As a side note, dienes are also crucial for industry, in which they are often polymerized to yield elastomers as end-products. For instance, 1,3-butadiene is a precursor to the rubber used in tires, and isoprene is the precursor to natural-rubber mimics also utilized in tire manufacturing.

The development of mild methods for the synthesis of polymers using renewable feedstocks is a critical technological hurdle along the path to a sustainable polymer economy in the future. Carbon dioxide is one of the most attractive renewable C1 resources, and it has many practical advantages, such as abundance, economic efficiency and lack of toxicity. Its favorable nature as a carbon source is, however, inextricably linked to its inherent inertness.

The main objective of this PhD project is performing new radical and catalytic polymerization processes of olefins and advantageously utilizing CO₂ in these processes. This valorization includes not only the use of CO₂ as a polymerization medium but also the more challenging role of its incorporation within the polymer chains, thus its use as effective reagent. Through the strategy that we followed we were aiming at developing sustainable processes. This is achieved by activating a waste product (CO₂) in the polymerization of the most demanded thermoplastics (polyolefins) as well as partially substituting petro-based raw materials such as solvents, which are more costly, by CO₂. In addition, we depend on iron complexes in the catalytic section of our work, iron is the cheapest among all transition metals and is environmentally benign.

In the first chapter, we reviewed extensively the activation of CO₂ in chemistry as a reactant, a monomer, and a polymerization medium. Then, ethylene polymerization was reviewed briefly since it has been reviewed thoroughly in different past theses and a lot of recent publications.¹⁻³ Also, a review of the kinetic considerations in ethylene-CO₂ copolymerization was mentioned, explicating the barriers to achieve this process.

In the search for sustainable polymerization, scientists have turned to supercritical fluids (scf) because of their unique properties combining low viscosity and interesting solvation properties (advantages of both gas and liquid phases). Among these fluids, supercritical carbon dioxide “scCO₂” possesses many properties that made it the most extensively studied scf for polymerization reactions. ScCO₂ represents an environmentally friendly alternative to traditional organic solvents, which are used in radical processes, since it is naturally occurring and abundant. CO₂ has an easily accessible critical point with a T_c of 31.04 °C and a P_c of 72.8 bar. Ethylene also possesses an easily accessible critical point (T_c = 9.44 °C; P_c = 50.49 bar).

Ethylene was therefore polymerized using a radical process under supercritical conditions. CO₂ was expected to minimize transfer reactions and could easily be removed at the end of the polymerization. The second chapter thus deals with ethylene free radical polymerization in scCO₂ under mild conditions ($T < 100$ °C, $P < 300$ bars), which has been achieved without addition of any initiator diluent, using AIBN, lauroyl peroxide, or benzoyl peroxide to investigate different initiation modes (**Figure 1**). Interestingly, the decarboxylation of the latter can be suppressed in scCO₂ to yield ester-functionalized

polyethylene.

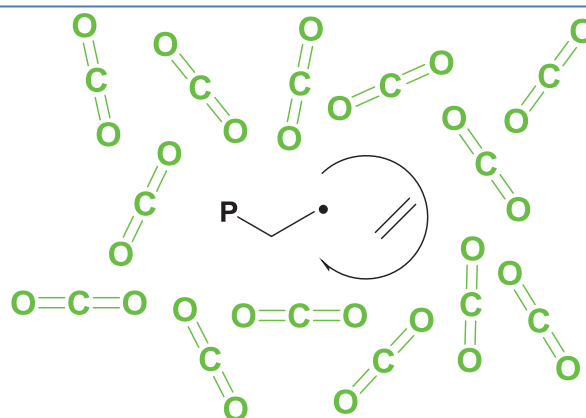


Figure 1. Ethylene free radical polymerization in scCO₂.

While looking for an additive that could break the inertness of CO₂ and incorporate it within the polyethylene chains, we noticed that triethylaluminum (AlEt₃) interacts with CO₂ as reported in the literature.^{4,5} Thus, what was remaining in order to validate this additive (AlEt₃) as a possible CO₂-incorporating agent in ethylene radical polymerization was the proof of its interaction with polyethylenyl radicals.

Chapter III is comprised of two sub-chapters. In the first sub-chapter we investigate the effect of triethylaluminum on the radical polymerization of ethylene. It was proven that AlEt₃ acts as an irreversible chain transfer agent in ethylene radical polymerization (**Figure 2**). Thus, AlEt₃ interacts with polyethylenyl radicals.

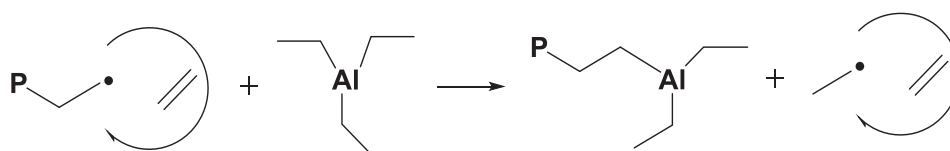


Figure 2. Chain transfer reaction of polyethylene chain to triethylaluminum.

AlEt₃ thus interacts with both radicals and CO₂. We capitalized on this by utilizing AlEt₃ in CO₂-mediated ethylene radical polymerization. This concept yields the incorporation of CO₂ moieties within the polyethylene chains using AlEt₃ (**Figure 3**), this achievement is explained in the second sub-chapter.

Therefore, we upgraded from the utilization of CO₂ as a polymerization medium to its activation and use as a functionalization agent in ethylene radical polymerization (**Figure 4**).

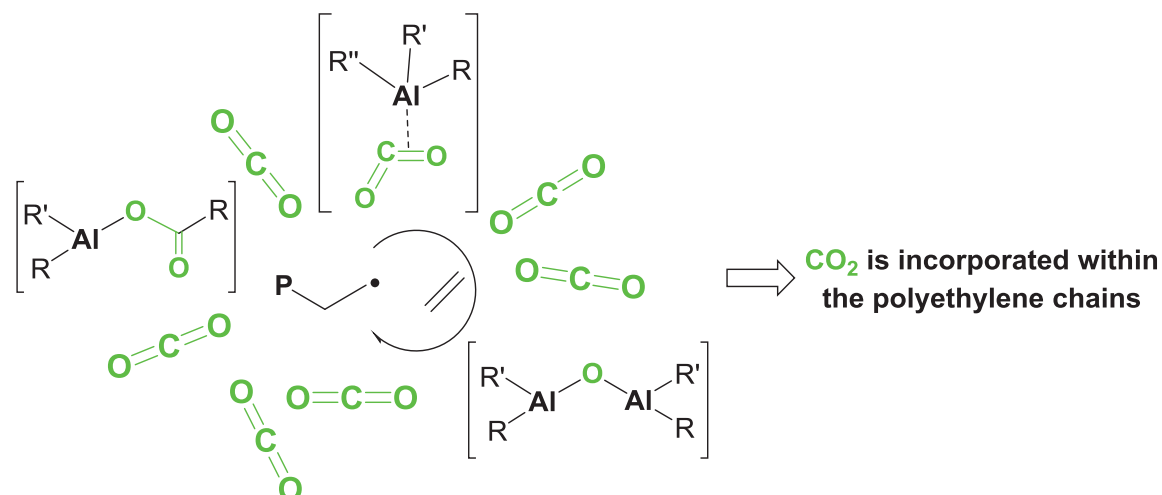


Figure 3. Incorporation of CO₂ within the polyethylene chains using triethylaluminum.

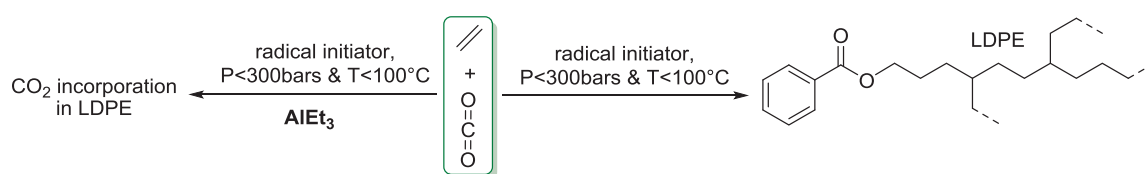


Figure 4. Activation of CO₂ in radical polymerization of ethylene.

Chapter IV represents the catalytic section of this thesis, which depends on iron catalysis. Iron is the most abundant transition metal in the Earth's crust and is environmentally friendly. Thus, to maintain the economic and environmental benefit of iron catalysis we focus on this metal in our work.

Chapter IV is also comprised of two sub-chapters. The first sub-chapter discusses thoroughly the iron-catalyzed ethylene-isoprene copolymerization through chain shuttling processes (**Figure 5**); we reached this methodology in our investigations while testing the corresponding iron catalysts in conventional polymerizations before testing them in CO₂-mediated polymerizations.

We concentrated on isoprene since its polymerization yields one of the synthetic rubbers which has been introduced to replace natural rubber in different applications (textile, carpet industry, adhesives, and toy balloons, etc.) and to reduce the intensive farming of rubber trees. In addition, its copolymerization with ethylene yields a material that bears the characteristics of both the polyethylene thermoplastic and the polyisoprene elastomer. Such materials could be used in the manufacture of tires for instance, to improve robustness and resistance to abrasion.

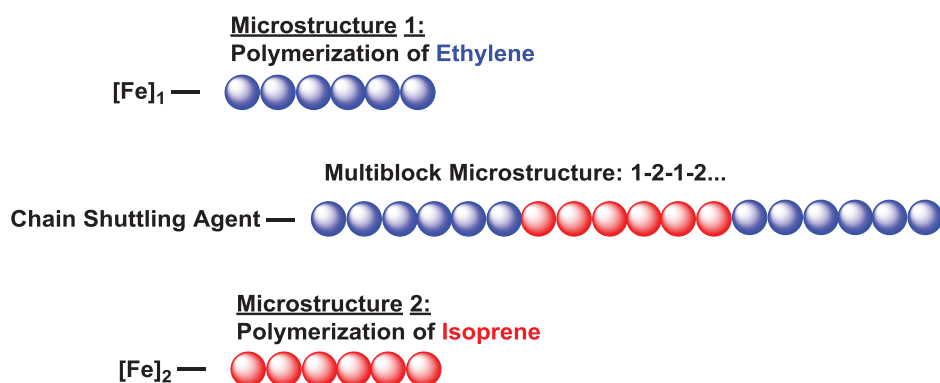


Figure 5. Iron-catalyzed chain shuttling copolymerization of ethylene and isoprene.

In the second part of this chapter we presented successful tests of iron-catalyzed ethylene and isoprene polymerizations in scCO_2 (**Figure 6**). These tests form the basis for further investigations towards CO_2 -incorporation within the polymer chains in these processes.

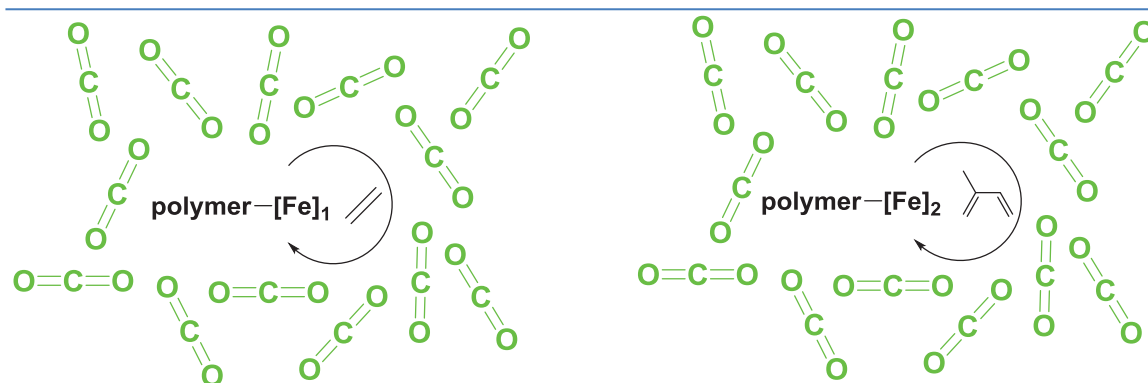


Figure 6. Iron-catalyzed ethylene and isoprene polymerizations in scCO_2 .

Therefore, this thesis, including all its chapters, forms what is mentioned in the title: "Radical and catalytic polymerizations of olefins: towards CO_2 -incorporation".

References

1. Grau, E. Polymerization of Ethylene: From Free Radical Homopolymerization to Hybrid Radical/Catalytic Copolymerization. PhD Thesis, Université Claude Bernard-Lyon I, 2010.
2. McDaniel Max P. Review of the Phillips Chromium Catalyst for Ethylene Polymerization. *Handb. Heterog. Catal.* **2008**, 3733–3792.
3. Böhm Ludwig L. The Ethylene Polymerization with Ziegler Catalysts: Fifty Years after the Discovery. *Angew. Chem. Int. Ed.* **2003**, 42 (41), 5010–5030.
4. J. Weidlein *Angew. Chem.* **1969**, 81, 947.
5. Yur'ev, V. P.; Kuchin, A. V.; Tolstikov, G. A. *Bull. Acad. Sci. USSR Div. Chem. Sci.* **1974**, 23 (4), 817.

A. CHAPTER I. Activation of CO₂ in Chemistry: The Path towards its Activation in Polymerizations of Olefins.

Table of Contents

A.1. History of "CARBON DIOXIDE"	19
A.2. Chemical and Physical Properties of "CO₂"	20
A.3. Carbon Dioxide Production	21
A.4. Carbon Dioxide Applications.....	22
A.4.1. In Food Industry	22
A.4.2. In Oil Industry.....	22
A.4.3. In Different Areas	23
A.4.4. In Chemical Industry	23
A.5. Carbon Dioxide in Chemistry	24
A.5.1. Carbon Dioxide as a Reactant or a Monomer	25
A.5.1.1. CO ₂ as a Reactant in Production of Molecules	26
A.5.1.2. CO ₂ as a Monomer in Polymer Synthesis.....	41
A.5.2. Carbon Dioxide as a Polymerization Medium	55
A.5.2.1. Cationic Polymerizations in CO ₂	58
A.5.2.2. Transition Metal-Catalyzed Polymerizations in CO ₂	60
A.5.2.3. Radical Polymerizations in CO ₂	63
A.6. Towards CO₂ Utilization in Polymerizations of Olefins.....	70
A.7. ETHYLENE: The Most Important Industrial Olefin	71
A.7.1. History of "ETHYLENE"	71
A.7.2. Chemical and Physical Properties of Ethylene	72
A.7.3. Ethylene Production	73

A.7.4. Uses of Ethylene.....	74
A.8. POLYETHYLENE	75
A.8.1. History of Polyethylene	76
A.8.2. Structure of Polyethylene.....	77
A.8.3. Properties of Polyethylene	78
A.8.4. Types of Polyethylene and their Synthetic Processes	80
A.8.4.1. LDPE: <i>via Radical Polymerization Processes</i>	81
A.8.4.2. MDPE.....	84
A.8.4.3. HDPE and LLDPE: <i>via Catalytic Polymerization Processes</i>	85
A.8.5. Uses of Polyethylenes	87
A.9. Kinetic and Thermodynamic Considerations in the Copolymerization of Ethylene and CO ₂	88
A.10. Conclusion and Results Obtained at the C2P2 Laboratory	95
A.11. References.....	98

A.1. History of "CARBON DIOXIDE"

Carbon dioxide (CO₂) is a colorless and odorless gas with a density (1.98 g/L) about 60% higher than that of air (1.225 g/L). At standard conditions of temperature and pressure, it is a gas. Carbon dioxide consists of a carbon atom covalently double bonded to two oxygen atoms. Although its concentration in air varies slightly, a typical concentration in air is about 0.038% or 380 ppm,¹ though continuously rising year after year.

As the source of available carbon in the carbon cycle, atmospheric CO₂ is the primary carbon source for life on Earth and its concentration in Earth's pre-industrial atmosphere was regulated by photosynthetic organisms and geological phenomena.² All aerobic organisms produce CO₂ when they metabolize carbohydrates and lipids to produce energy by respiration.³ Other natural sources of CO₂ include volcanoes and hot springs, and it is freed from carbonate rocks by dissolution in water and acids. Because CO₂ is soluble in water, it occurs naturally in groundwater, rivers, lakes, ice caps, glaciers and seawater. Also, it is present in deposits of petroleum and natural gas.⁴

Carbon dioxide was the first gas to be described as a discrete substance. In 1644, the Flemish chemist Jan Baptist van Helmont observed that when he burned charcoal in a closed vessel, the mass of the resulting ash was much less than that of the original charcoal. His interpretation was that the rest of the charcoal had been transmuted into an invisible substance which he termed a "gas".^{5,6} Then, the properties of carbon dioxide were further studied in the 1750s by the Scottish physician Joseph Black, where he found that limestone (calcium carbonate) could be heated or treated with acids to yield a gas that he called "fixed air". He observed that this gas (fixed air) was denser than air. "Black" also found that when bubbled through limewater (a saturated aqueous solution of calcium hydroxide), it would precipitate calcium carbonate. In 1772, an English chemist, Joseph Priestley, published a paper entitled "Impregnating Water with Fixed Air" in which he described a process of dripping sulfuric acid on chalk in order to produce carbon dioxide, and forcing the gas to dissolve by agitating a bowl of water in contact with the gas.⁷

In Chemistry, Carbon dioxide has different names that it could be described by, even though "Carbon dioxide" is the most popular one (IUPAC name). Other names include: Carbonic acid gas, Carbonic anhydride, Carbonic oxide, Carbon oxide, Carbon(IV) oxide,

and Dry ice (solid phase).

A.2. Chemical and Physical Properties of "CO₂"

The carbon dioxide molecule is linear and centro-symmetric. The carbon-oxygen bond length is 116.3 pm, noticeably shorter than the bond length of a C–O single bond and even shorter than most other C–O multiply-bonded functional groups,⁸ and since it is centro-symmetric, the molecule has no electrical dipole (**Figure 1**).

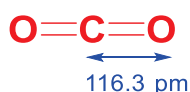


Figure 1. Carbon dioxide molecule.

Carbon dioxide is colorless. It is odorless at low concentrations; however, at sufficiently high concentrations it has a sharp acidic odor.⁹

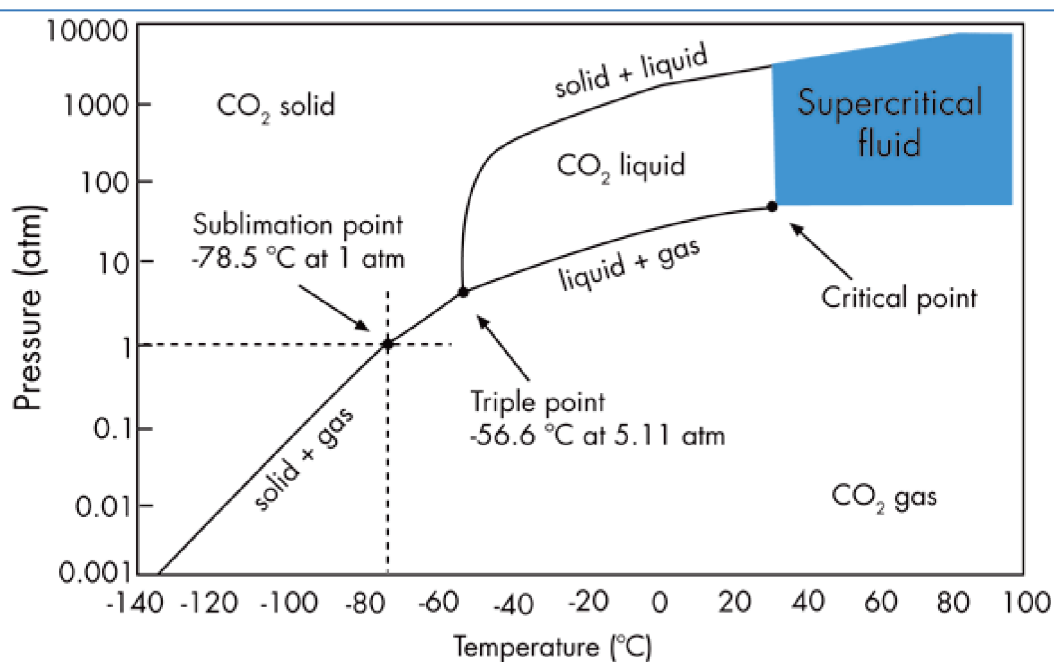


Figure 2. Pressure/Temperature phase diagram of CO₂.

Carbon dioxide was first liquefied (at elevated pressures) in 1823 by Humphry Davy and Michael Faraday.¹⁰ The earliest description of solid carbon dioxide was given by Adrien Jean-Pierre Thilorier, who in 1835 opened a pressurized container of liquid carbon dioxide, only to find that the cooling produced by the rapid evaporation of the liquid yielded a "snow" of solid CO₂.^{11,12}

CO₂ has no liquid state at pressure below 5.1 atm (5.1 atmosphere). At 1 atm, the gas

condenses directly to a solid at temperatures below -78.5 °C. The triple point of CO₂ exists at 5.11 atm / -56.6 °C, and the critical point exists at 72.8 atm / 31.04 °C (**Figure 2**).¹³ At temperatures and pressures above the critical point, carbon dioxide behaves as a supercritical fluid known as "supercritical carbon dioxide" (scCO₂). **Table 1** shows the different physical properties of CO₂.

Table 1. Physical properties of carbon dioxide.

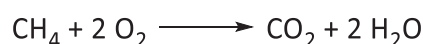
<i>Molecular Weight</i>	<i>44.009 g/mol</i>
<i>Boiling Point</i>	<i>-78.5 °C</i>
<i>Melting Point</i>	<i>-56.6 °C</i>
<i>Liquid Density at 21 °C</i>	<i>0.763 g/cm³</i>
<i>Gas Density at 21 °C</i>	<i>0.001 g/cm³</i>
<i>Critical Temperature</i>	<i>31.04 °C</i>
<i>Critical Pressure</i>	<i>72.8 °C</i>

A.3. Carbon Dioxide Production

Carbon dioxide is produced by many different methods:¹⁴

1. Distillation from air (inefficient method).
2. Combustion of all carbon-based fuels, such as methane (natural gas), petroleum distillates (gasoline, diesel, kerosene, propane), coal, wood and generic organic matter.

Example, Methane combustion:

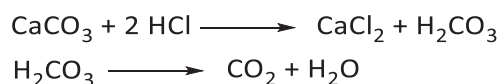


3. Thermal decomposition of limestone (CaCO₃) by heating at about 850°C, in the manufacture of quicklime (calcium oxide, CaO) which has many industrial uses (production of steel, production of glass...):



4. Acids liberate CO₂ from most metal carbonates.

Example, The reaction between hydrochloric acid and calcium carbonate:



5. Carbon dioxide is a by-product of the fermentation of sugar.
6. All aerobic organisms produce CO_2 when they oxidize carbohydrates, fatty acids, and proteins.
7. Direct capture of CO_2 from ambient air in amine-based media, also known as direct air capture (DAC).¹⁵

A.4. Carbon Dioxide Applications

The food industry, the oil industry, the chemical industry, and other different areas use CO_2 .¹⁴

A.4.1. In Food Industry

Carbon dioxide is a food additive used as a propellant and acidity regulator in the food industry. It is approved for usage in the EU (listed as E number E290), US, Australia and New Zealand (listed by its INS number INS290).

Example: Leavening agents cause dough to rise by producing carbon dioxide. Baker's yeast produces carbon dioxide by fermentation of sugars within the dough, while chemical leaveners such as baking powder and baking soda release carbon dioxide when heated or if exposed to acids.

Also, CO_2 is used to produce carbonated soft drinks and soda water. In addition, supercritical CO_2 is used to remove caffeine from coffee.

A.4.2. In Oil Industry

Carbon dioxide is used in enhanced oil recovery where it is injected into producing oil wells, usually under supercritical conditions, when it becomes miscible with the oil. This approach can increase original oil recovery by reducing residual oil saturation by 7% to 23% additional to primary extraction.¹⁶ It acts as a pressurizing agent and when dissolved into the underground crude oil, it significantly reduces its viscosity. Also, it changes surface chemistry allowing the oil to flow more rapidly through the reservoir to the removal well.¹⁷ In mature oil fields, extensive pipe networks are used to carry the

carbon dioxide to the injection points.

A.4.3. In Different Areas

1. Fire Extinguisher: Carbon dioxide can be used to extinguish flames by flooding the environment around the flame with the gas. It does not itself react to extinguish the flame, but starves the flame of oxygen by displacing it. Fire extinguishers designed for electrical fires contain liquid carbon dioxide under pressure. CO₂ extinguishers work well on small flammable liquid and electrical fires, but not on ordinary combustible fires, because although it excludes oxygen, it does not cool the burning substances significantly and when the carbon dioxide disperses, they are free to catch fire upon exposure to atmospheric oxygen.

2. Agricultural Applications: Plants require CO₂ to conduct photosynthesis. The atmospheres of greenhouses must be enriched with additional CO₂ to tolerate and increase the rate of plant growth.¹⁸

3. Medical Uses: CO₂ could be mixed with up to 50% oxygen, forming an inhalable gas, which is known as "Carbogen" and has a variety of medical and research uses.

4. Refrigerant: Liquid and solid CO₂ are important refrigerants, mainly in the food industry, where they are used during the transport and storage of ice cream and other frozen foods.

5. Enhanced Coalbed Methane Recovery: It is a method of producing additional coalbed methane from a source rock, similar to enhanced oil recovery applied in oil fields. Carbon dioxide injected into a black coal bed would occupy pore space and also adsorb onto the carbon in the coal at almost twice the rate of methane, allowing for potential enhanced gas recovery in replacing the trapped methane.¹⁹

A.4.4. In Chemical Industry

1. As an Inert Gas: CO₂ is one of the most commonly used compressed gases for pneumatic (pressurized gas) systems in portable pressure tools. Carbon dioxide is also used as an atmosphere for welding, it reacts to oxidize most metals, it is utilized to assist the weld to penetrate deeper into the parent metal. Usage in the automotive industry is common despite significant evidence that welds made in CO₂ are more brittle than those

made in more inert atmospheres, and that such weld joints deteriorate over time because of the formation of carbonic acid. It is used as a welding gas primarily because it is cheaper than inert gases such as argon or helium.

2. As a Precursor: In the chemical industry, CO₂ is mainly consumed as an ingredient in the production of urea, with a smaller fraction being used to produce methanol and some other products,²⁰ such as metal carbonates and bicarbonates. Some carboxylic acid derivatives such as sodium salicylate are synthesized using CO₂ by the Kolbe-Schmitt reaction.²¹

A.5. Carbon Dioxide in Chemistry

Meeting the world's growing energy demand and changing to a sustainable supply of raw materials are two of nowadays prime challenges. Using CO₂ as one of the roots for the chemical supply chain has been investigated by chemists for a long time, and inventive work towards catalytic transformations of CO₂ as a C1 building block has been envisioned for decades.²²⁻²⁷ The use of CO₂ would be the most direct way to harvest nature's carbon resources, without the by-pass via biomass or fossil resources.²⁸

Due to the discussion of plans to capture CO₂ from flue gases and chemical processes,^{29,30} this area has seen a very dynamic increase in interest most recently. With the employment of carbon capture technologies, CO₂ will become an economically attractive resource, available in huge quantities at acceptable purity. Such technologies include mainly three different configurations: post-combustion capture (removal of CO₂ after combustion of fossil fuels), pre-combustion capture (usually applied in gaseous fuel (H₂, CH₄)), and oxy-fuel combustion capture (the fuel is burned in oxygen instead of air). By using just a small fraction of this massive stream as raw material for chemical production,³¹ waste CO₂ might turn into a valuable feedstock.

Carbon dioxide is a renewable, non-toxic, and cheap C1 building block that can be used for many synthetic applications in chemistry.³²

This part is formed of two main sub-parts explaining the story of carbon dioxide utilization, the first is about using carbon dioxide as a reactant or a monomer, thus activating it, and the second is concerned with its usage as a polymerization medium.

A.5.1. Carbon Dioxide as a Reactant or a Monomer

Although a wide variety of chemical reactions that incorporate CO₂ are known today,³³⁻³⁶ many more can be envisioned. Thus, there is a continuing requirement to develop new chemistries based on the CO₂ molecule. As such, industrially applicable target molecules can be identified and technological progresses can be directed towards promising application areas.

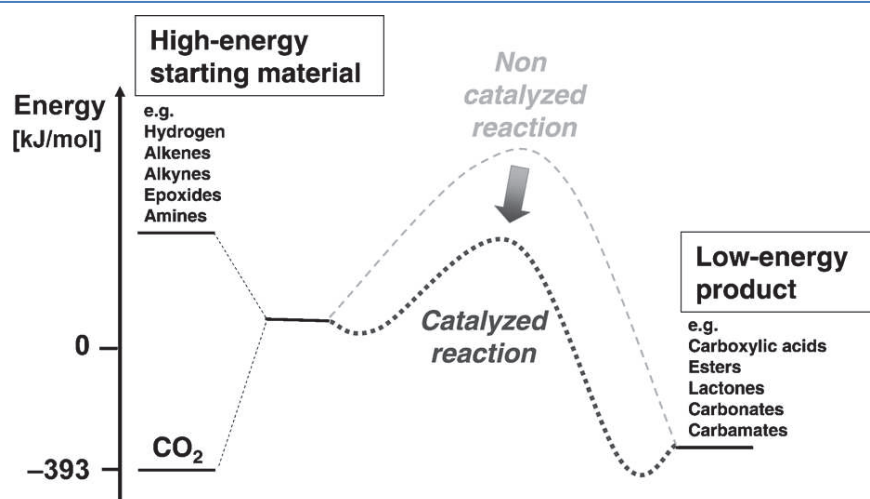
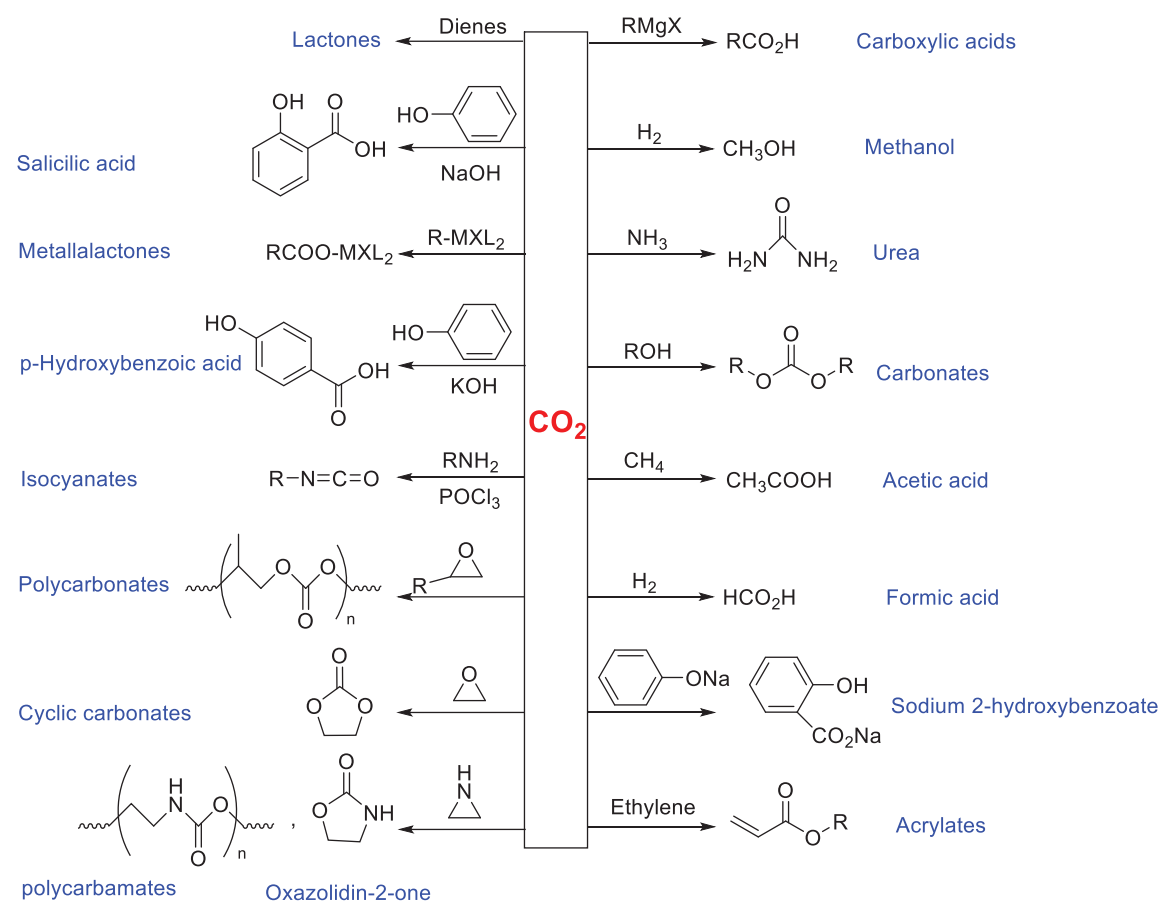


Figure 3. Schematic illustration of the energy balance for chemical fixation of CO₂ with energy-rich reactants. Martina Peters, Burkhard Kçhler, Wilhelm Kuckshinrichs, Walter Leitner, Peter Markewitz, and Thomas E. Muller: Chemical Technologies for Exploiting and Recycling Carbon Dioxide into the Value Chain. CHEMSUSCHEM. 2011. 4. 1216-1240. Copyright Wiley-VCH Verlag GmbH & Co. KGaA. Reproduced with permission.

By concentrating on the use of CO₂ as a C1-building block, Muller and coworkers³⁷ mentioned that there are three major scientific and technological challenges which can be recognized on the way to industrial implementation of activating CO₂, based on the simplified general analysis of CO₂ transformation. **(1) Identifying pathways and products:** as aforementioned, by continuing the development of new chemistries based on CO₂. **(2) Understanding and developing new catalysts:** Highly effective catalysts are required in many reactions including CO₂ as a reactant to enable, accelerate, and control reactions using CO₂ as C1-building block. The importance of using catalysts in this field is often associated with the low reactivity of the CO₂ molecule, looking for methods of direct CO₂ activation. **(3) Addressing energetic constraints:** When using CO₂ as C1-building block in the chemical industry, its low energy level is an important aspect (**Figure 3**). Typically, a high-energy reactant such as hydrogen, unsaturated compounds,

or strained cyclic molecules can be used to drive the chemical reactions towards low energy products.^{38,39} Therefore, the high-energy reactant should to be carefully considered to assess whether or not a given transformation has the possibility to lead to a reduction of CO₂.

Scheme 1. Transformations of CO₂ as C1-building block.



Beller and co-workers have reported a review which describes the most recent advances made in the area of CO₂ activation under mild conditions. They have focused mainly on the application of CO₂ as C1 building block in organic synthesis.⁴⁰

There are numerous chemical reactions for synthesizing organic molecules from CO₂, **Scheme 1** summarizes a number of these reactions. In this part, some selected reactions will be discussed, showing CO₂ as a reactant in synthesis of molecules (part A.5.1.1) and as a monomer in polymers synthesis (part A.5.1.2).

A.5.1.1. CO₂ as a Reactant in Production of Molecules

a- Synthesis of Urea. Urea is quantitatively the most important product of the

chemical industry nowadays for which CO₂ is used as a C1 building block. In the annual production of about 153 million metric tonnes of urea (in 2011),⁴¹ 112 million metric tonnes of CO₂ are utilized as feedstock. Urea is produced from CO₂ and ammonia under high pressure and high temperature (**Scheme 1**).⁴² Usually the urea production takes place nearby units for synthesizing ammonia, as large amounts of pure CO₂ are separated during the production of hydrogen *via* synthesis gas. The largest quantities of urea are currently used as agricultural fertilizers.

In urea production reaction, ammonia and CO₂ react to form ammonium carbamate which is then dehydrated to urea. In the process, ammonia and CO₂ are fed to the synthesis reactor which operates at around 180-210 °C and 150 bar. The reaction mixture containing ammonia, ammonium carbamate and urea is first stripped of the ammonia and the resulting solution passes through a number of decomposers operating at progressively reduced pressures. Then, the unconverted carbamate is decomposed back to ammonia and CO₂ and recycled to the reactor. The urea solution is concentrated by crystallisation, and the crystals can be melted to yield pure urea in the form of granules.⁴²

b- Synthesis of Methanol. Methanol is the most important transformed product of synthesis gas which is a mixture of CO and H₂. CO and H₂ react over a catalyst to produce methanol ($\text{CO} + 2 \text{H}_2 \rightarrow \text{CH}_3\text{OH}$). Nowadays, the most extensively used catalyst is a mixture of copper and zinc oxides supported on alumina. The production of synthesis gas from methane produces three moles of hydrogen for every mole of carbon monoxide, whereas the synthesis consumes only two moles of hydrogen gas per mole of carbon monoxide. Thus, it is dealt with the excess hydrogen by injection of CO₂ into the methanol synthesis reactor, where it, too, reacts to form methanol according to the equation: $\text{CO}_2 + 3 \text{H}_2 \rightarrow \text{CH}_3\text{OH} + \text{H}_2\text{O}$.^{43,44}

A Catalytic hydrogenation of CO₂ to methanol in a Lewis pair functionalized metal organic framework (MOF) has been reported by Johnson and coworkers.⁴⁵ They have used density functional theory (DFT) to computationally design a catalyst capable of producing methanol from CO₂ and H₂, including calculating the reaction pathways and barriers of each step. The catalyst consists of a microporous metal organic framework (UiO-67) functionalized with catalytically active Lewis pair functional groups.

In 2017, Beller and co-workers have developed a homogeneous cobalt/Triphos-based system able to hydrogenate CO₂ to methanol at 100 °C, which is unprecedented.⁴⁶

Recently, Liu and coworkers specified the active sites over commercial copper/zinc oxide/aluminum oxide (Cu/ZnO/Al₂O₃) catalysts for CO₂ hydrogenation to methanol.⁴⁷ They reported a direct comparison between the activity of ZnCu and ZnO/Cu model catalysts for methanol synthesis.

c- Synthesis of Salicylic Acid and *p*-Hydroxybenzoic acid. Salicylic acid is synthesized *via* the Kolbe-Schmitt method,⁴⁸ in which sodium phenolate reacts with CO₂ at high temperatures and pressures (**Scheme 1**). The high ortho-selectivity of salicylic acid is caused by the chelate effect of sodium ions.⁴⁹ In contrast, potassium phenolate almost exclusively yields *p*-hydroxybenzoic acid.⁵⁰

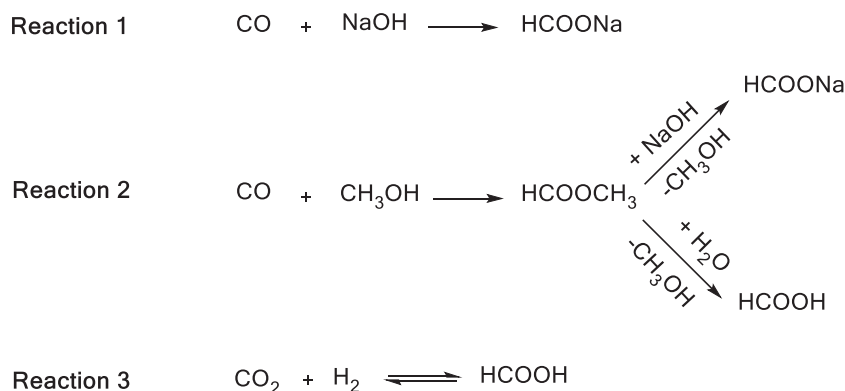
Salicylic acid is used in production of acetyl salicylic acid commonly known as analgesic, and *p*-Hydroxybenzoic acid is used mainly in production of its esters, the parabens, that are applied as preservatives. Liquid-crystalline polyester used as high-performance materials in the electronic industry can be built up from 50-80% *p*-hydroxybenzoic acid.^{51,52}

Therefore, the application these acids as co-monomers in production of polyesters seems promising.

d- Synthesis of Formic Acid. The conventional synthesis of formic acid was by the reaction of CO with alkali hydroxides and subsequent transformation of the formate with sulfuric acid. Nowadays, the common applied method is the reaction of CO with methanol and subsequent cleavage of the methylester with sodium hydroxide or water (**Scheme 2**).

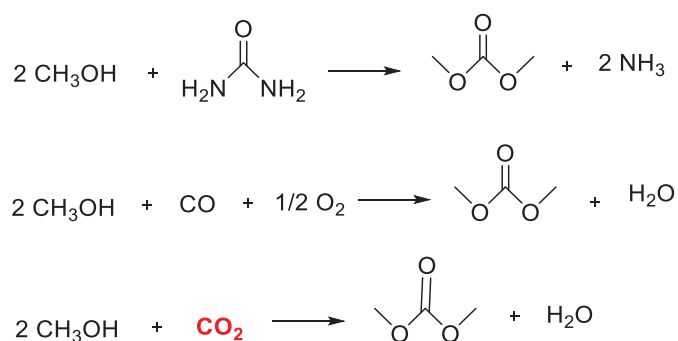
The selective hydrogenation of CO₂ would form an alternative path to produce formic acid (**Scheme 2**).⁵³ The challenge in the direct hydrogenation of CO₂ is that it is an exothermic but endergonic reaction under normal conditions ($\Delta H_{298K} = -31.6$ kJ/mol and $\Delta G_{298K} = 32.9$ kJ/mol).

The catalyst development is well advanced,⁵⁴⁻⁵⁶ however the isolation of formic acid remains a problem. Most recent developments include iron hydride catalysts with tetradentate phosphine ligands⁵⁷ and iridium complexes with pincer ligands.⁵⁵

Scheme 2. Synthesis of formic acid.

Thus, upgrading from CO to CO₂ as a reactant for the production of formic acid could be a green route for the production of relatively wide range of chemicals.

e- Synthesis of Dialkyl and Cyclic Carbonates (Dimethylcarbonate, Ethylene Carbonate). Dialkylcarbonates, in particular dimethylcarbonate, are widely used intermediates for organic synthesis and production of polymers.⁵⁸ Currently, dialkylcarbonates are commercially produced mostly from the corresponding alcohol and phosgene.⁵⁹ Other routes include the reaction of alcohols with urea (**Scheme 3**).⁶⁰ Also, the oxidative carbonylation of aliphatic alcohols has been commercialized.⁶¹ The carboxylation of aliphatic alcohols with tin- and titanium-based catalysts has been described.^{62,63} As the reaction is equilibrium limited, the produced water must to be removed from the process to achieve good conversions.^{64,65} This forms a main difficulty for implementation of the carboxylation reaction.

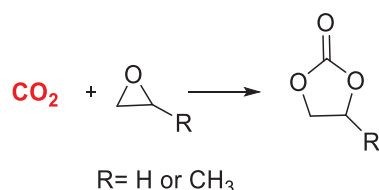
Scheme 3. Routes for dimethylcarbonate synthesis.

Using a suitable catalyst, epoxides react readily with CO₂ to form five-membered ring carbonates (**Scheme 4**),⁶⁵⁻⁶⁷ where the energy for the reaction is supplied by the ring-opening of the epoxide. Vice versa, this means that energy has to be expended during

the production of the epoxides. For example, ethylene oxide is produced by direct oxidation of ethylene with air in an exothermic reaction. But the production of propylene carbonate is more difficult, because the starting material propylene oxide cannot be produced directly by air-oxidation of propylene. It is produced either through a hydrochlorination reaction (which proceeds *via* the conversion of propylene to propylene chlorohydrin which is then converted into propylene oxide by a dehydrochlorination reaction) or by an oxidation reaction (which is done by oxidation of propylene with an organic peroxide).⁶⁸

Cyclic carbonates can be synthesized from renewable feedstock, for example, combining epoxidized soybean oil or oleic acid methyl ester with CO₂. These methods abide with the principles of CO₂-fixation and renewable resources. An alternative access to cyclic carbonates is the oxidative carbonylation of diols.⁶⁹

Scheme 4. Synthesis of cyclic carbonates (ethylene and propylene carbonate).



The use of dimethylcarbonate as an active carbonic acid derivative is very promising in polymer applications such as polycarbonate and polyurethane synthesis. Also, cyclic carbonates can serve as building blocks for polymers; six-membered ring carbonates can be directly polymerized via ring opening polymerization. Moreover, cyclic carbonates react with bifunctional primary or secondary amines to produce urethane groups and thus towards synthesis of polyurethanes (non-isocyanate polyurethanes (NIPUS)). Synthesis of polycarbonates using CO₂ as a monomer will be discussed in part A.5.1.2.

f- Synthesis of Acrylates and Lactones. Acrylate synthesis from CO₂ harnesses oxidative coupling as an activation process for the production of molecules of interest (monomers in particular). In this section, a series of reports published from the 1980s until nowadays will be discussed. Syntheses of corresponding lactones are limited.

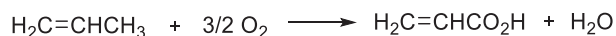
Scheme 5 represents the methods used commercially to produce acrylic acid (the simplest molecule in the family of acrylates). Acrylic acid is commonly produced from oxidation of propylene, and because propane is a significantly cheaper raw material than

propylene, considerable research efforts are undertaken to develop a process based on the one-step selective oxidation of propane to acrylic acid.^{70,71}

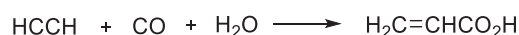
An initial method was the hydrocarboxylation of acetylene (Reppe chemistry) which requires nickel carbonyl and high pressures of carbon monoxide.⁷²

Scheme 5. Routes for production of acrylic acid.

Oxidation of propylene:



Hydrocarboxylation of acetylene (Reppe chemistry):



Transition-metal-catalyzed coupling of CO₂ and ethylene toward acrylate formation has been recognized as an alternative to the currently used propylene oxidation technology since the reports of Hoberg and Carmona in the 1980s (**Figure 4**).^{73,74} These pioneers pursued new methods for CO₂-ethylene coupling using zero-valent nickel⁷¹⁻⁷³ and group VI metals,^{75,76} however catalytic activity remained elusive.

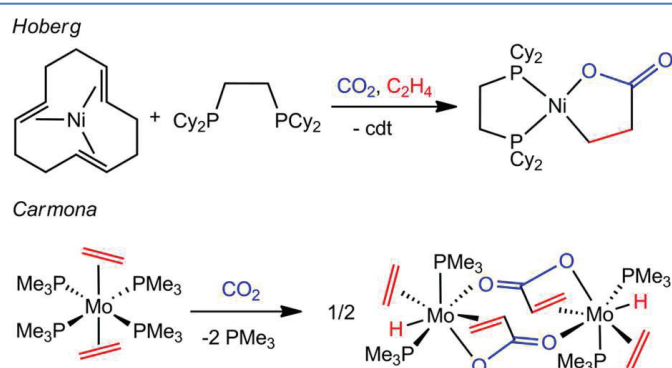


Figure 4. Pioneering reports of CO₂-ethylene coupling at transition metals complexes.

"Adapted with permission from (Jin, D.; Schmeier, T. J.; Williard, P. G.; Hazari, N.; Bernskoetter, W. H. *Organometallics* **2013**, 32 (7), 2152-2159.). Copyright (2013) American Chemical Society."

Different experimental and computational mechanistic studies on these reactions propose that the early and late metal complexes likely share several common intermediates on the desired catalytic pathway, but are challenged by different steps in the proposed cycle (**Figure 5**).⁷⁷⁻⁸¹ In the case of group VI metals, the oxidative coupling of CO₂ and ethylene appears relatively easy, occurring at ambient temperature and pressure. The couplings at molybdenum and tungsten have consistently produced acrylate products, indicating that β-H elimination from computationally predicted

metallalactone intermediates is quick.⁸² But the strong oxophilicity of molybdenum and tungsten has hampered reductive acrylate elimination using methods compatible with catalysis, as proven examples of acrylate liberation require either a strong base (i.e. butyllithium) or a methylating agent (i.e. iodomethane).^{75,82}

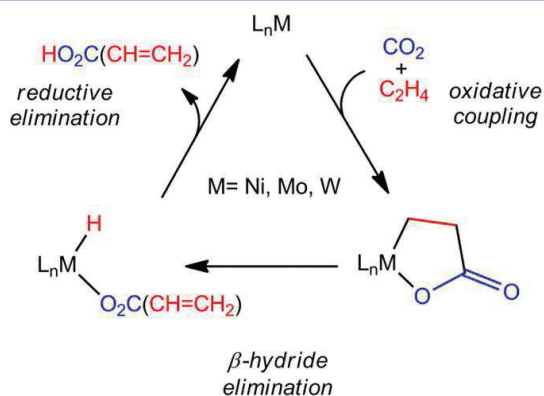


Figure 5. General proposition of a catalytic cycle for production of acrylic acid from CO₂ and ethylene. "Adapted with permission from (Jin, D.; Schmeier, T. J.; Williard, P. G.; Hazari, N.; Bernskoetter, W. H. *Organometallics* **2013**, 32 (7), 2152-2159.). Copyright (2013) American Chemical Society."

In contrast, elimination of acrylate from nickel should be easier due to its lower oxophilicity and reduction potential as well as its greater tolerance toward protic functional groups. The principal difficulties for catalytic acrylate formation at nickel seem to lie in the high pressures required for most oxidative couplings (up to 40 bar) and a hardness to have β -hydride elimination from the nickelalactone intermediates. The pressures typically required for nickel-catalyzed CO₂-ethylene coupling could be achieved in autoclave reactors, but some undesired side reactions could occur, such as ligand degradation and multiple CO₂ insertions.⁸³⁻⁸⁵ The high CO₂ pressure can also interfere with the last steps required to achieve catalytic acrylate production.⁸⁶ However, it appears that β -H elimination from nickelalactone complexes is the hardest step.

The origin of stability to β -hydride elimination in square planar nickelalactone species is mostly the result of two interconnected factors: the strain energy associated with distorting the five-membered lactone ring and the absence of an accessible low-lying orbital for a β -agostic interaction. Crystallographic evidence from multiple nickelalactone structures shows that the key C-H bonds in the β position to the metal are oriented away from the nickel and would likely require significant twisting of the

five-membered ring to be brought within a covalent interaction distance.^{77,86,87} Brookhart, Green, and others have shown that β -H elimination in late transition metals occurs *via* formation of an agostic intermediate, which requires an empty orbital on the metal to accept electron donation from the target C-H bond.⁸⁸ Thus coordination of the β C-H bond in nickelalactone complexes would require the use of a higher-energy empty orbital or significant ligand rearrangement.

Limbach and co-workers⁸⁶ have circumvented these barriers to β -hydride elimination by adding external bases such as sodium tert-butoxide to diphosphine nickelalactone species, which deprotonate the β -carbon directly without requiring transfer of the hydride to nickel. This approach produces sodium acrylate (NaCO₂CHCH₂) in relatively good yield, and by repeated sequential additions of CO₂, ethylene, and base, several equivalents of sodium acrylate may be obtained in one reaction vessel. Unfortunately, the strong sodium base required for the deprotonation is not compatible with the high CO₂ pressure needed for nickelalactone formation. Thus, there is no constant set of reaction conditions under which catalytic production could be achieved.

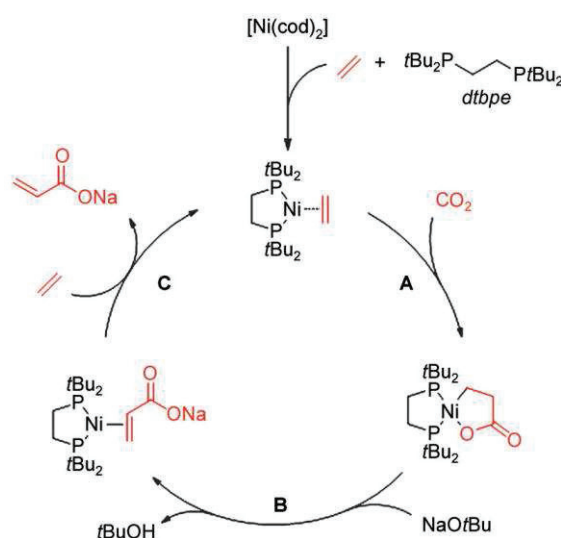


Figure 6. Catalytic cycle for the formation of sodium acrylate from CO₂, ethylene, and a base. Michael L. Lejkowski, Ronald Lindner, Takeharu Kageyama, Gabriella E. Bodizs, Philipp N. Plessow, Imke B. Muller, Ansgar Schäfer, Frank Rominger, Peter Hofmann, Cornelia Futter, Stephan A. Schunk, and Michael Limbach: The First Catalytic Synthesis of an Acrylate from CO₂ and an Alkene—A Rational Approach. *CHEMISTRY A EUROPEAN JOURNAL*. 2012. 18. 14017 – 14025. Copyright Wiley-VCH Verlag GmbH & Co. KGaA. Reproduced with permission.

Figure 6 represents the catalytic cycle proposed by Limbach and co-workers, and

similar cycles were proposed in all the reports published on production of acrylates from CO₂ and ethylene by the effect of a base.

Scheme 6. Ni-catalyzed formation of sodium acrylate with the highest TON from CO₂, ethylene, and a base.

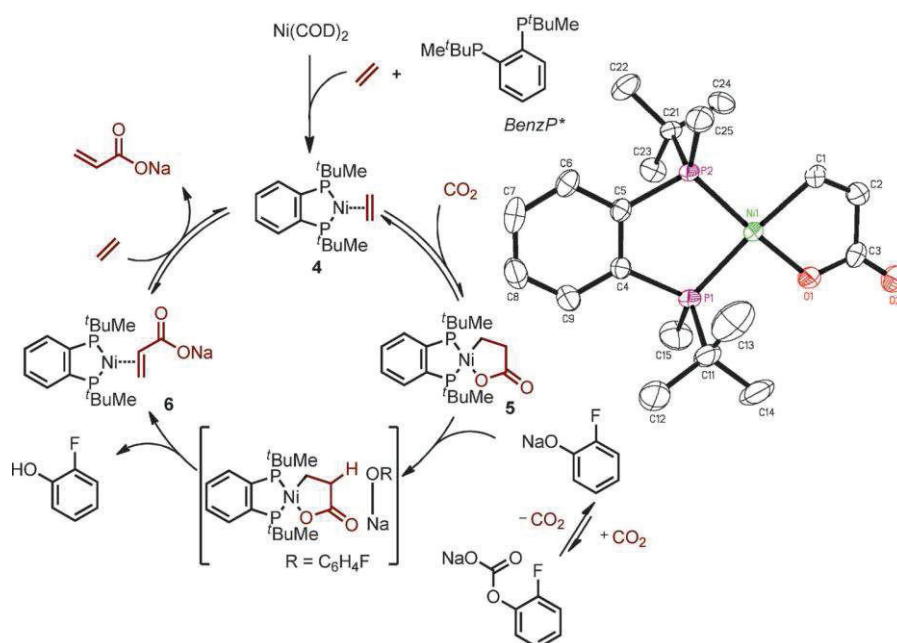
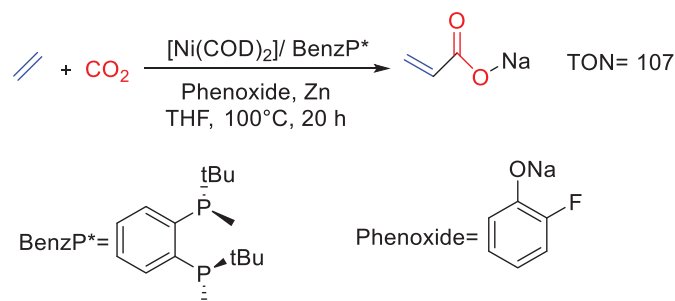


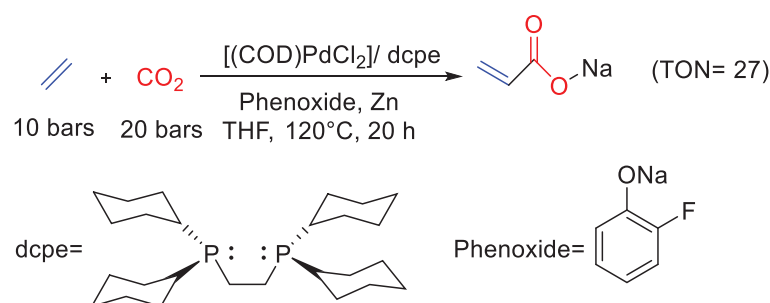
Figure 7. Catalytic cycle of Ni-catalyzed formation of sodium acrylate from CO₂ and ethylene with the highest TON and solid-state structure of lactone 5. Nfflria Huguet, Ivana Jevtovikj, Alvaro Gordillo, Michael L. Lejkowski, Ronald Lindner, Miriam Bru, Andrey Y. Khalimon, Frank Rominger, Stephan A. Schunk, Peter Hofmann, and Michael Limbach: Nickel-Catalyzed Direct Carboxylation of Olefins with CO₂: One-Pot Synthesis of α,β -Unsaturated Carboxylic Acid Salts. *CHEMISTRY A EUROPEAN JOURNAL*. 2014, 20, 16858 – 16862. Copyright Wiley-VCH Verlag GmbH & Co. KGaA. Reproduced with permission.

In addition, Limbach and co-workers⁸⁹ have found a strong nickel catalyst and reaction setup for the one-pot, direct carboxylation of activated alkenes, such as ethylene, styrenes, and 1,3-dienes with CO₂. They mentioned that strong N-bases such as DBU react irreversibly with CO₂ to form carbamates. Phenoxides are less nucleophilic, which makes them suitable bases to work with under CO₂-pressure conditions. To the best of

our knowledge, the highest TON (turnover number) (TON= 107) was obtained in this work.⁸⁹ After testing a series of ligands under constant conditions, BenzP* gave the highest yield (**Scheme 6; Figure 7**). Using Ni(COD)₂ (COD= cyclooctadiene) as a precursor with BenzP* ligand and zinc (reductant) under 20 bars of CO₂ and 10 bars of ethylene at 100°C in THF different phenoxides were tested, the reaction using sodium 2-fluoro phenoxide gave the highest yield (TON= 107) (**Scheme 6**).

Also, Limbach and co-workers⁹⁰ have synthesized a palladium catalyst for the catalytic synthesis of sodium acrylates or $\alpha,\beta,\gamma,\delta$ -unsaturated carboxylates from CO₂, alkenes or 1,3-dienes and a base (in the same manner: using a base to force metallalactone ring opening) characterized by a TON > 20 relative to Pd. **Scheme 7** represents the Pd-catalyzed formation of sodium acrylate with the highest yield (TON= 27), where (COD)₂PdCl₂ was the precursor with the ligand dcpe and the base sodium 2-fluoro phenoxide.

Scheme 7. Pd-catalyzed formation of sodium acrylate with the highest TON from CO₂, ethylene and a base.⁹⁰

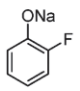
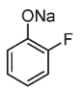
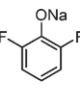
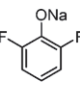
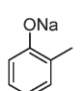
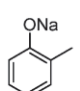
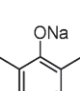
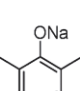


Schaub and co-workers⁹¹ showed a screening of nickel and palladium precursors with different ligands, bases, and temperatures, **Table 2** summarizes this screening.

Buntine and co-workers⁹² performed DFT calculations for Ni-mediated oxidative coupling of CO₂ and C₂H₄ with DBU as ligand. Their calculations suggest an energy drop at the nickelalactone formation step (-14.7 kcal/mol relative to C₂H₄ and CO₂), with the steps of nickelalactone ring opening and β -H elimination being thermodynamically less favored (+13.6, +7.6, and +7.3 kcal/mol relative to L₂Ni, C₂H₄, and CO₂, respectively). The β -H elimination step involves a transition state that is very high in energy (ΔG = 42.6 kcal/mol) due to the strain of the five-membered ring. Buntine and co-workers reported that the reaction from the metallalactone to the acrylate can proceed *via* scission of the

Ni-O bond, allowing β -H atoms to approach the Ni center.

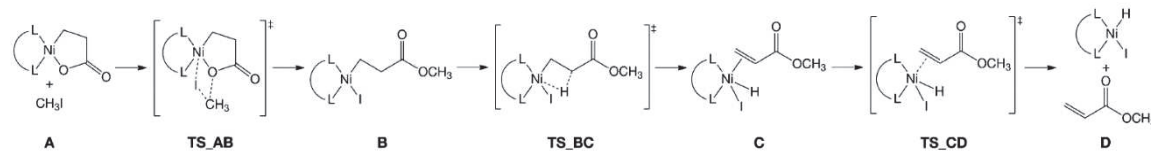
Table 2. Screening for nickel and palladium catalysts. Simone Manzini, Núria Huguet, Oliver Trapp, and Thomas Schaub: Palladium- and Nickel-Catalyzed Synthesis of Sodium Acrylate from Ethylene, CO₂, and Phenolate Bases: Optimization of the Catalytic System for a Potential Process. *European Journal of Organic Chemistry*. 2015, 7122–7130. Copyright Wiley-VCH Verlag GmbH & Co. KGaA. Reproduced with permission.

$\text{CH}_2=\text{CH}_2 + \text{CO}_2 \xrightarrow[\text{Base (20 or 30 mmol), THF, 20 h}]{\text{Catalyst (0.2 mmol), Ligand (0.22 mmol)}} \text{CH}_2=\text{CH}-\text{CO}_2\text{Na}$						
Entry ^[a]	Catalyst	Ligand	T(°C)	Zn (mmol)	Base	TON ^[c]
1 ^[b,d]	Ni(COD) ₂	BenzP*	120	10		107
2 ^[e]	PdCl ₂ (COD)	dcpe	145	10		24
3 ^[b,d]	Ni(COD) ₂	BenzP*	80	–		1
4	PdCl ₂ (COD)	dcpe	145	10		1
5 ^[b,d]	Ni(COD) ₂	BenzP*	80	–		4
6	PdCl ₂ (COD)	dcpe	145	10		31
7 ^[b,d]		BenzP*	80	–		4
8	Ni(COD) ₂		145	10		43
9		dcpe	145	10		69
10	PdCl ₂ (COD)	dcpe	145	10		38

[a] Reaction conditions: base (20 mmol), catalyst (0.2 mmol), ligand (0.22 mmol), THF (30 mL), ethylene (10 bar), CO₂ (20 bar), 20 h. [b] As [a] but 30 mmol of base was added. [c] TON determined based on ¹H NMR analysis in D₂O as solvent and using 3-(trimethylsilyl)propionic-2,2,3,3-d⁴ acid sodium salt (0.125 mmol) as internal standard. [d] Result from previous work in Schaub's laboratory.¹¹⁴ [e] Result from previous work in Schaub's laboratory.¹¹⁷

Based on this result, Rieger and co-workers⁹³ force the metallalactone (nickelalactone) ring opening by the addition of methyl iodide, a strong methylating agent to react with the slightly polarized Ni-O bond. They used dppp (bis(diphenylphosphino)propane) ligand to form the nickel complex because of its good solubility in organic solvents. Even though their achievement is not yet a complete catalytic cycle and the yields obtained are far from quantitative, the *in situ* methylation investigated was a way that enables the β -H elimination and liberation of acrylates. Further investigations will be necessary to find an appropriate ligand system and reaction conditions (CO₂ pressure, ethylene pressure, solvent, etc.) to obtain good TONs.

Scheme 8. Pathway from the nickelalactone (A) to the free methyl acrylate (D). S. Y. Tina Lee, Mirza Cokoja, Markus Drees, Yang Li, Janos Mink, Wolfgang A. Herrmann, and Fritz E. Kuhn: Transformation of Nickelalactones to Methyl Acrylate: On the Way to a Catalytic Conversion of Carbon Dioxide. *ChemSusChem*. 2011, 1275–1279. Copyright Wiley-VCH Verlag GmbH & Co. KGaA. Reproduced with permission.



Kuhn and co-workers⁹⁴ also reported a formation of methyl acrylate *via* a nickel-catalyzed reaction forcing the nickelalactone ring opening by MeI (**Scheme 8**). They showed that ligand variation at nickelalactones has a major effect on the production of methyl acrylate, and that high excess of methyl iodide is also necessary to overcome the high reaction barriers in the β -H elimination reaction to produce methyl acrylate. The maximum yield (40%) was obtained using the ligand bis(dimethylamino)ethane and addition of 100 equivalent of MeI in 3 h. The results presented prove that nickelalactones bearing chelating diamines or diphosphines undergo successfully β -H elimination to produce methyl acrylate.

After this report, Kuhn and co-workers⁹⁵ reported a liberation of methyl acrylate from metallalactone complexes *via* M-O ring opening (M= Ni, Pd) with methylating agents. The ring opening of various nickela- and pallada-lactones induced by the cleavage of the M-O bond by methyl trifluoromethanesulfonate (MeOTf) and methyl iodide was investigated. MeOTf shows higher efficiency in the lactone ring opening than MeI.

Hofmann and co-workers⁹⁶ studied the mechanistic aspects of the nickel-mediated formation of acrylates from CO₂, ethylene and methyl iodide, where they proposed an extended mechanism for this reaction on the basis of theoretical and experimental studies for the bidentate ligand 1,2-bis(di-tert-butylphosphino)ethane (dtbpe). They were able to isolate reactive intermediates and to verify the existence of their proposed reaction pathways. They insured that the strong binding of acrylate to nickel prevents a catalytic cycle, at least for the chosen ligand.

Another method has been reported by Vogt and co-workers,⁹⁷ where a nickel-catalyzed conversion of CO₂ and ethylene to acrylate has been achieved in combination with a hard Lewis acid (Lithium iodide) to force β -H elimination, the highest TON

achieved by this method was 21. Lithium acrylate was formed in up to 73% yield after $[(dppe)Ni(C_3H_4O_2)]$ was reacted with 5 equivalents of LiI in dichloromethane for 24 h. Lithium propionate was formed as a by-product, its production was avoided by the addition of an excess of triethyl amine (Et_3N), the yield increases till 95%. Vogt and co-workers mentioned that the choice of ligand and a higher ethylene/ CO_2 pressure ratio have a beneficial effect on the production of acrylate, and good TONs can be achieved without the need to add zinc.

Bernskoetter and co-workers⁹⁸ suggest another solution to force β -H elimination by addition of the Lewis acid tris(pentafluorophenyl)borane which has been found to promote rapid β -H elimination from a nickelalactone species, $(dppf)Ni(CH_2CH_2CO_2)$ (**A**; **Figure 8**), under ambient conditions, where dppf is 1,1'-bis(diphenylphosphino)ferrocene. The reversible β -hydride elimination results in the formation of the thermodynamically stable 2,1-acryl borate insertion product $(dppf)Ni(CH(CH_3)CO_2BAr^F_3)$ (**Figure 8**). The coordinated borate-substituted acrylate may easily be substituted by ethylene, but the resulting $(dppf)Ni$ complex shows resistance to CO_2 -ethylene coupling. However, as Bernskoetter mentioned, the ability to both ring-open the nickelalactone with a discrete Lewis acid and promote acrylate liberation with more mild bases provides a key step toward establishing a viable catalytic process that can withstand the high CO_2 pressure conditions typical of nickel-promoted couplings. Also, demonstration of a sequential Lewis acid-base addition to enable acrylate liberation from a nickelalactone increases the attention of cocatalysts, such as frustrated Lewis pairs, for promoting a functional catalytic system for CO_2 -ethylene to acrylate at nickel and other metals. **Figure 8** represents the hypothetical cycle for Lewis acid/base promoted coupling of CO_2 and ethylene to form acrylate.

Furthermore, Bernskoetter and co-workers⁹⁹ studied the effect of sodium cation on metallacycle β -H elimination in CO_2 -ethylene coupling to acrylate in a sodium tetrakis[3,5-bis(trifluoromethyl)phenyl]borate ($NaBAr^F_4$) promoted reaction. Their results are consistent with the suggestion that as the Lewis acidity of the promoter increases and a stronger acid-oxygen bond (in this case: Na-O bond) is formed, the process of β -hydride elimination becomes easier. Thus, a key for effective catalytic CO_2 -olefin coupling to acrylate is the use of Lewis acid cocatalysts, which can promote β -H

elimination, but still bind weakly enough to allow their removal from the substrate.

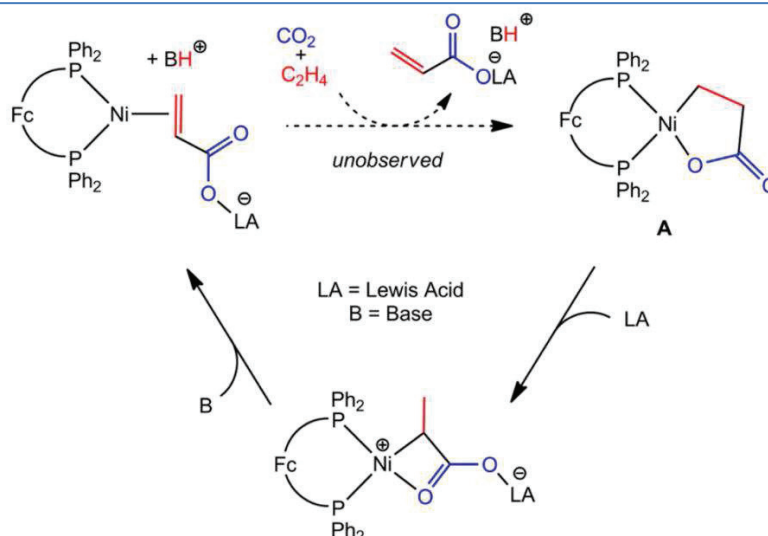


Figure 8. Hypothetical cycle for Lewis acid/base promoted coupling of CO₂ and ethylene to form acrylate. "Adapted with permission from (Jin, D.; Schmeier, T. J.; Williard, P. G.; Hazari, N.; Bernskoetter, W. H. *Organometallics* **2013**, 32 (7), 2152-2159.). Copyright (2013) American Chemical Society."

A theoretical study was reported by Hofmann and co-workers¹⁰⁰ about the formation of acrylates from CO₂ and ethylene mediated by nickel complexes. Their studies concluded that strongly anionic bases lead to a kinetically and thermodynamically favorable cleavage of the lactone (mainly nickelalactones with bidentate ligands) via direct deprotonation.

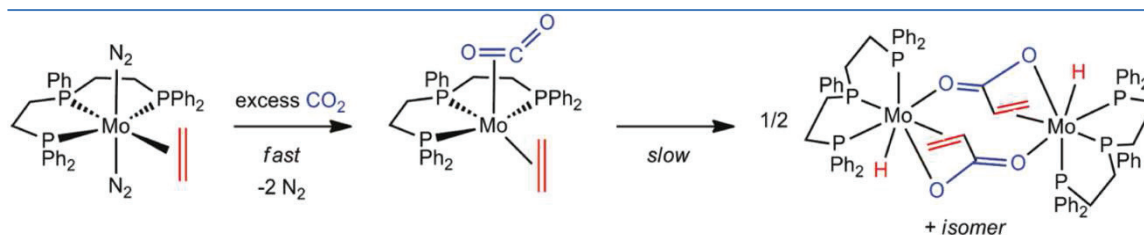


Figure 9. Formation of the dimerized molybdenum complex for acrylate production. "Adapted with permission from (Bernskoetter, W. H.; Tyler, B. T. *Organometallics* **2011**, 30, 520.). Copyright (2011) American Chemical Society."

Bernskoetter and Tyler⁷⁷ reported a study of the kinetics and mechanism of molybdenum-mediated acrylate formation from carbon dioxide and ethylene, where a new (Ph₂PCH₂CH₂)₂PPh-supported bis(dinitrogen)molybdenum ethylene complex has been synthesized and found to promote C-C bond coupling with CO₂ to give a binuclear acrylate hydride species. The reduction of CO₂ (**Figure 9**), although qualitatively slower than the similar transformations inspired by Carmona over two decades ago, provided a

stage for the first experimental examination of the mechanism for this CO₂ functionalization. Verifying the conversion to acrylate hydride complex (**Figure 9**) afforded direct characterization of an intermediate molybdenum carbon dioxide ethylene adduct, establishing pre-coordination of both substrates as a likely requirement for CO₂ functionalization by ethylene at early transition metals.

A series of different metals were used to produce acrylates from ethylene and CO₂. As aforementioned, acrylates formation catalyzed by nickel, palladium, and group VI metals (molybdenum and tungsten) was investigated by different research groups showing that the main barrier was in metallalactone ring opening and β -H elimination. Other metals were an area of investigation to produce metallacycles but these studies are still considered narrow.

In 1985, a report was published by Cohen and Bercaw¹⁰¹ on the the formation of titanacycles derived from reductive coupling of nitriles, alkynes, acetaldehyde, and carbon dioxide with bis(pentamethylcyclopentadienyl)(ethylene)titanium(II). Another report was done in 1990 by Denner and Alt¹⁰² on the reaction of the zirconium complexes, Cp₂Zr(PMe₃)₂ and Cp₂Zr(C₂H₄)(PMe₃), with acetylenes, olefins, 1,2-dihydroxybenzene and carbon dioxide to give five-membered metallacycles. Also, Teuben and co-workers¹⁰³ reported a cyclopentadienylvanadium(I) complexes, CpV(L)(PMe₃)₂ (L = η^2 -ethene, η^2 -alkyne), to produce a metallalactone. In addition, a rhodium-catalyzed production of metallacycles was reported by Aresta and Quaranta.¹⁰⁴ Even though these reports are interesting, none of them managed to overcome the barrier of ring opening toward production of monomers.

To the best of our knowledge, the only report investigating iron-catalyzed coupling of olefins with carbon dioxide was done by Hoberg and co-workers,¹⁰⁵ where they showed a C-C coupling between CO₂ and butadiene catalyzed by iron(0) complexes forming a route toward production of dicarboxylic acids.

Nozaki and co-workers¹⁰⁶ reported the synthesis of a metastable lactone, 3-ethylidene-6-vinyltetrahydro-2H-pyran-2-one, which is formed by the palladium-catalyzed coupling of carbon dioxide and 1,3-butadiene. This lactone was synthesized as an intermediate toward copolymerization of CO₂ and butadiene as a strategy to circumvent the thermodynamic and kinetic barriers for such copolymerization reactions (to be discussed

in section A.5.1.2).

A.5.1.2. CO₂ as a Monomer in Polymer Synthesis

Over the last twenty years, many efficient catalysts that are active towards CO₂/epoxide couplings have been developed¹⁰⁷⁻¹¹² for the stereocontrolled synthesis of functional cyclic carbonates^{113,114} in addition to stereoregular functional polymers.^{115,116} Furthermore, some of these catalytic systems are currently employed in commercially feasible industrial processes that exploit CO₂ fixation using ethylene and propylene oxide as reactants. These processes give access to poly(ethylene carbonates), poly(propylene carbonates), and polyethercarbonate-polyol mixtures with narrow molar mass distributions, which are of further use in polyurethane synthesis.¹¹⁷

The applicability of this type of polymerization reactions is still limited to the synthesis of polycarbonates and polyethercarbonates, the preparation of polyesters by direct copolymerization of CO₂ with ethylene or dienes is still far. This copolymerization reaction is particularly attractive since it represents a link between different renewable resources, such as CO₂, and cheap, widely available petroleum-derived alkenes, that can also be derived from short-life cycle resources, thus allowing a potential evolution towards more sustainable materials. The main obstacles that prevent a successful copolymerization of these monomers include: 1) a high energy barrier associated with the alternating copolymerization between ethylene/polyene and CO₂, which requires excess ethylene insertion to ensure endergonic CO₂ insertion, and 2) a kinetic barrier that arises from the high activation energy for CO₂ insertion into the growing polymeric chain relative to polyethylene or polypropylene chain growth.¹¹⁸⁻¹²⁰

a- Copolymerization of CO₂ and Epoxides. In 1969, Inoue and co-workers made the discovery that a mixture of ZnEt₂ and H₂O was active for catalyzing the alternating copolymerization of propylene oxide (PO) and CO₂, designing the beginning of epoxide-CO₂ coupling chemistry.^{121,122}

Then, Inoue investigated the use of dihydric sources, including resorcinol,^{123,124} dicarboxylic acids,¹²⁵ and primary amines,¹²⁶ in mixtures with ZnEt₂ for PO-CO₂ copolymerization. These systems showed TOFs of 0.17, 0.43, and 0.06 h⁻¹, respectively.

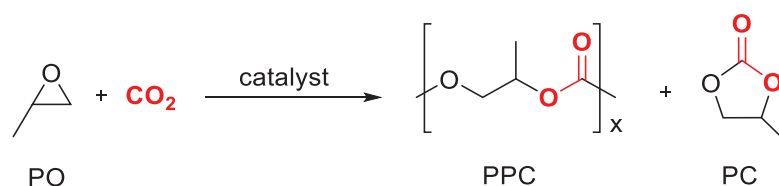
After Inoue's discoveries, Kuran and co-workers settled a copolymerization system

using ZnEt_2 and trihydric phenols, including pyrogallol and 4-bromopyrogallol, that produced PPC with TOFs up to 0.3 h^{-1} at 35°C and 60 atm CO_2 .^{127,128} Looking forward to develop more active catalysts, Hattori and co-workers synthesized a heterogeneous catalyst from Zn(OH)_2 and glutaric acid. Under 30 atm CO_2 and 60°C , the Zn(OH)_2 /glutaric acid mixture yielded PPC with a TOF of 1.1 h^{-1} ($M_n = 12000 \text{ g/mol}$).¹²⁹

Even though these results have been achieved, the active species responsible for polymer and cyclic formation remained unknown. However, several mechanistic studies support the theory that multi-site catalysts are active in the alternating copolymerization of CO_2 and epoxides.¹³⁰⁻¹³²

Different metals are active for the coupling of epoxides and CO_2 , including Al, Mn, Ni, Mg, V, Zr, Cr, Co, Zn, and others such as Cd and Cu (**Scheme 9**). Studies have shown that large differences in catalytic efficiency result from the organic frameworks surrounding these metals, especially in the case of zinc.

Scheme 9. Alternating copolymerization of propylene oxide (as a model) with CO_2 producing poly(propylene carbonate) and propylene carbonate.



Aluminum and Manganese Catalysts. In 1978, Inoue synthesized the first single-site catalysts for epoxide- CO_2 copolymerization based on a tetraphenylporphyrin (tpp) ligand framework, (**1a-d**; **Figure 10**).¹³³ $[(\text{tpp})\text{AlCl}]$ (**1a**) and $[(\text{tpp})\text{AlOMe}]$ (**1b**) reacted with PO to form poly(propylene oxide) (PPO) in a living polymerization with dispersities of 1.07-1.15. Only **1b** copolymerized PO and CO_2 , at 20°C and 8 atm of CO_2 , giving PPC ($M_n = 3900 \text{ g/mol}$; $M_w/M_n = 1.15$) with 40% carbonate linkages in 19 days.^{134,135} Although molar masses were low and reaction times were long, this reaction was the first example of polycarbonates having narrow dispersities.

Similar to **1a**, $[(\text{tpp})\text{AlOR}]$ (**1d**), where R is an oligomer of PO, did not react with CO_2 . The addition of ethylene oxide (EO) and CO_2 to **1d** catalytically produced cyclic ethylene carbonate (EC).¹³⁶

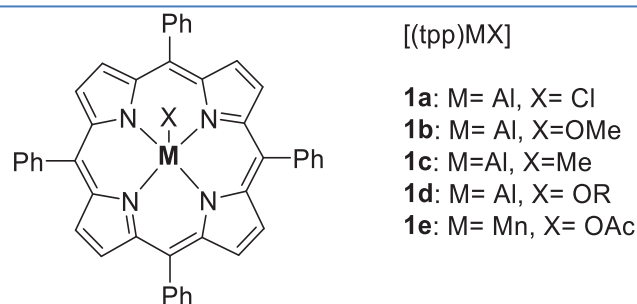


Figure 10. Aluminum and manganese porphyrins for the homopolymerization of epoxides and copolymerization of epoxides and CO₂. (R= alkyl, oligomer of PPO)

In 1999, Chang and co-workers also tested metalloporphyrins for PO-CO₂ copolymerization. They mentioned that **1a** and Et₄NBr cocatalyst gave PPC (Mn= 1900 g/mol, Mw/Mn= 1.1) with only 75% carbonate linkages at 20 °C and 52 atm of CO₂.¹³⁷

In addition, Kleij and co-workers^{138,139} reported the formation of carbonates from CO₂ and epoxides by different aluminum catalysts with high activities, this forms a step toward using such catalysts in polycarbonates production.

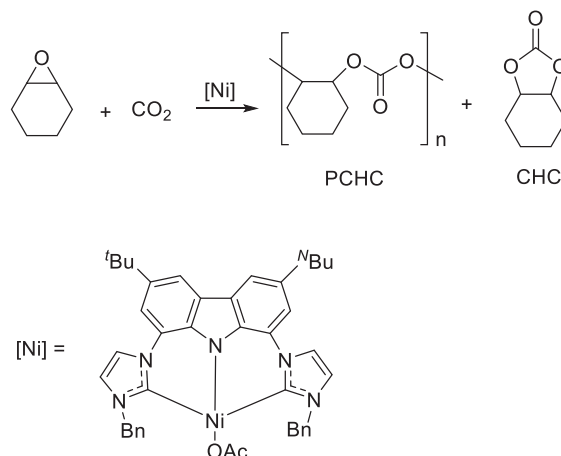
In 2003, Inoue and co-workers reported an active related porphyrin system utilizing manganese as a metal center.¹⁴⁰ At 80 °C, [(tpp)MnOAc] (**1e**) reacted with CHO and 50 atm of CO₂ to produce PCHC (poly(cyclohexene carbonate)) (99% carbonate linkages; Mn= 6700 g/mol, Mw/Mn= 1.3) with a TOF of 16.3 h⁻¹.

Nickel, Magnesium, and Zirconium Catalysts. Nickel-catalyzed CO₂/epoxides copolymerization reactions have been recently an area of investigation for Lin and co-workers¹⁴¹ who reported in 2016 the synthesis and structural characterization of efficient bimetallic nickel catalysts that bear diamine-bis(benzotriazole phenolate) derivatives for these copolymerizations. A thermally robust di-nickel catalyst was an effective catalyst for the alternating copolymerization of CHO with CO₂ to give TOFs >400 h⁻¹.

Then, in 2017, Huang and co-workers¹⁴² reported the synthesis, characterization, and catalytic studies for CO₂/epoxide coupling *via* nickel acetates based on carbazolidine-bis(NHC) (NHC= N-heterocyclic carbene). These Ni complexes were verified to be active catalysts for coupling of CHO and CO₂ without cocatalysts (**Scheme 10**). Also, a series of structurally well-defined dinickel carboxylate complexes based on the ^RBiIBTP derivatives [^RBiIBTP= bis(benzotriazole iminophenolate)] were synthesized and

developed for copolymerization of CO₂ and epoxides by Ko and co-workers.¹⁴³

Scheme 10. Coupling of CHO and CO₂ catalyzed by carbene nickel(II) complex. "Adapted with permission from (Lee, T.-Y.; Lin, Y.-J.; Chang, Y.-Z.; Huang, L.-S.; Ko, B.-T.; Huang, J.-H. *Organometallics* **2017**, 36 (2), 291.). Copyright (2017) American Chemical Society."



Magnesium- and zirconium-catalyzed copolymerization reactions are rarely studied. Sakai and co-workers¹⁴⁴ have reported the synthesis of a highly active magnesium catalyst for the synthesis of cyclic carbonates from CO₂ and epoxides under solvent-free conditions.

A selected report in Zr-catalyzed reactions is the one done by Ramkumar and co-workers,¹⁴⁵ where they have synthesized new Zr-alkoxide complexes containing salan-type diamine bis(phenolato) ligands. All the complexes have exhibited activity for the copolymerization of CO₂ and epoxides (CHO and PO), yielding polymers with moderate molar masses and narrow dispersities.

Chromium Catalysts. Kruper and Dellar¹⁴⁶ discovered that [(tpp)CrX] (**2a**, **2b**; **Figure 11**) in mixtures with a Lewis-basic amine cocatalyst (such as 1-methylimidazole (Melm) or (4-dimethylamino)pyridine (DMAP)) are moderately active for the cyclization of epoxides and CO₂. A wide range of epoxides, including PO, trans-2-butene oxide, epichlorohydrin, CHO, and cyclopentene oxide (CPO), were rapidly converted to the corresponding cyclic carbonates.

Following this report, Holmes and co-workers¹⁴⁷ synthesized [(tfpp)CrCl] (**3**; **Figure 11**), which showed TOF up to 173 h⁻¹ for the alternating copolymerization of CHO and CO₂ at 225 atm of CO₂ (scCO₂) and 110 °C. The fluorinated aromatic moieties improved catalyst solubility in scCO₂, and therefore increased the yields of PCHC. Similar to aluminum-

porphyrin catalysts utilized in epoxide-CO₂ copolymerization, these chromium analogs produced polycarbonates with narrow dispersities ($M_w/M_n = 1.08-1.50$) and low molar masses ($M_n = 1500-9400$ g/mol). Besides, the produced PCHC contains high percentages of carbonate linkages (97%).

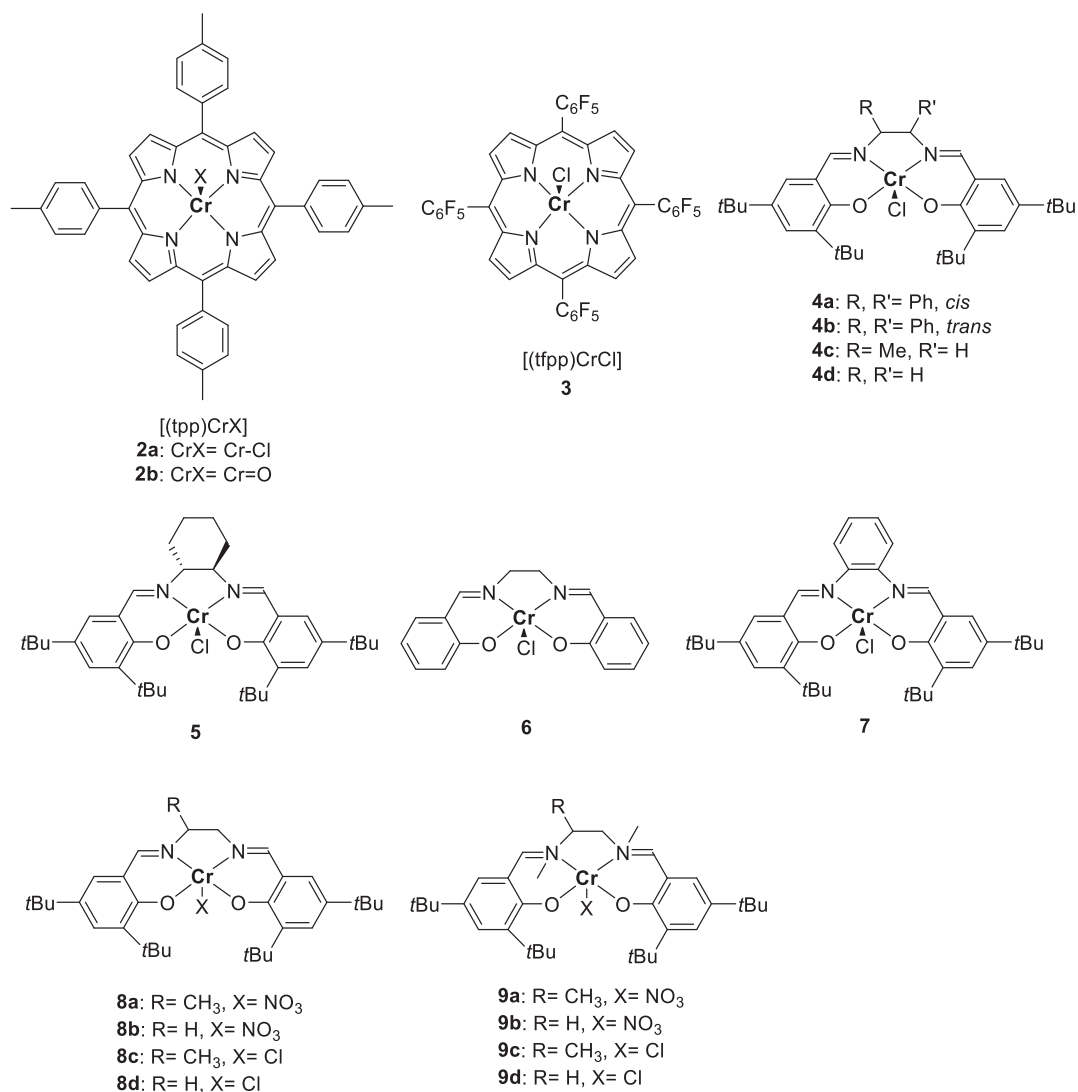


Figure 11. Chromium catalysts used in the epoxides/CO₂ copolymerization.

Jacobsen and co-workers found $[(\text{salen})\text{CrCl}]$ complexes to be highly active in the asymmetric ring opening of epoxides.¹⁴⁸ Nguyen and Paddock reported highly active $[(\text{salen})\text{CrCl}]/\text{DMAP}$ based systems, **4a-c** and **5** (Figure 11), for the cycloaddition of CO₂ and a variety of terminal aliphatic epoxides, including PO, epichlorohydrin, butadiene monoepoxide, and styrene oxide (SO).¹⁴⁹ Nguyen also stated that cycloaliphatic epoxides such as CHO are copolymerized with CO₂ by $[(\text{salen})\text{CrCl}]$ complexes. Holmes and Mang reported the conversion of glycidol derivatives to cyclic carbonates using **5**/DMAP.¹⁵⁰

Then, He and co-workers reported the synthesis of ethylene carbonate using **6** (**Figure 11**)/cocatalyst mixtures.¹⁵¹

Darensbourg and Yarbrough reported that complex **5** is an active catalyst for the alternating copolymerization of CHO and CO₂.¹⁵⁰ At 80 °C and 60 atm of CO₂, compound **5** converted CHO to PCHC with a moderate TOF of 10.4 h⁻¹. Analysis of the polycarbonate indicated nearly 100% carbonate linkages, Mn= 8900 g/mol and Mw/Mn= 1.2.

Silylated aliphatic epoxides, such as 2-(3,4-epoxycyclohexyl)ethyl-trimethoxysilane, and CO₂ can also be copolymerized by salen-chromium complexes and Melm as a cocatalyst.¹⁵² At 80 °C and 55 atm of CO₂, **4d** (**Figure 11**) and Melm catalyzed the production of the silylated polycarbonate with a TOF of 12.0 h⁻¹. Subsequent work detailed the energetics of polymer versus cyclic-species formation using compound **5**.¹⁵³

Rieger and co-workers found that complex **7** [(salen)CrCl] (**Figure 11**), and DMAP cocatalyst rapidly copolymerize PO and CO₂ (TOFs up to 226 h⁻¹) at 75 °C and 35 atm of CO₂.¹⁵⁴ The PPC produced have molar masses up to 16700 g/mol with dispersities as low as 1.4, and carbonate linkages up to 98%. They discovered that the DMAP/**7** ratio highly affected the product distribution in the coupling process, no conversion to PC or PPC was observed in absence of DMAP.

There is a lack of agreement regarding the mode of operation of these catalysts. Different mechanisms were proposed to explain the behavior of these catalysts.^{148-150,152,153}

In 2005, Phelps and Darensbourg studied the copolymerization of PO and CO₂ using various (salen)CrX catalysts with PCy₃ or PPN⁺ ((C₆H₅)₃P)₂N⁺) azide and chloride salts as cocatalysts.¹⁵⁵ After that, Rao and co-workers reported that [salanCrX] (salan= reduced salen) complexes (**8a-d**, **Figure 11**), with DMAP as a co-catalyst, were much more active than the salen counterparts (**9a-d**) in the copolymerization of PO and CO₂.¹⁵⁶

More recently, Duchateau and co-workers¹⁵⁷ have used a few chromium complexes of pyrrole and pyridine-based ligand systems as catalysts for CO₂-epoxide copolymerization. Two complexes of these catalysts revealed high activity, producing polymers with moderate molar masses, a high percentage of carbonate linkages, and moderate TOFs.

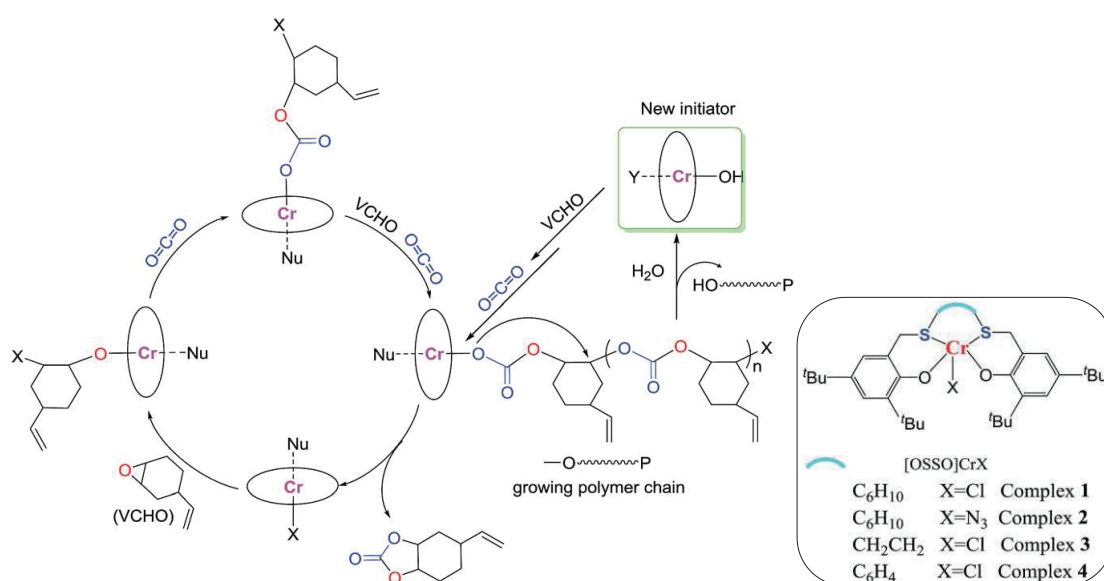


Figure 12. Proposed mechanism by Liu et al. for the copolymerization of VCHO with CO₂. [Si, G.; Zhang, L.; Han, B.; Zhang, H.; Li, X.; Liu, B. *RSC Adv.* **2016**, 6 (27), 22821.] Reproduced by permission of The Royal Society of Chemistry.

Liu and co-workers¹⁵⁸ used four chromium complexes with [OSSO] ligands (**Figure 12**) in combination with a Lewis base and an onium salt, where they were active catalysts in the copolymerization of CO₂ and VCHO with TOF up to 134 h⁻¹ and carbonate linkage more than 95%. A complex supported by [OSSO] ligand with ethylene backbone showed a higher activity than the complexes bearing cyclohexylene- or phenylene-bridges. Their proposed mechanism of the copolymerization reaction is represented in **Figure 12**.

Cobalt Catalysts. In 1979, Ikeda et al. have reported that Co(OAc)₂ copolymerizes PO and CO₂ with a very low TOF (0.06 h⁻¹).¹⁵⁹ After that, some reports about cobalt-catalyzed coupling of epoxides and CO₂ have been published. In 2002-2003, He and co-workers reported the synthesis of ethylene carbonate using **10** (**Figure 13**) with cocatalyst mixtures.^{160,161} Shi and co-workers reported that related salen-cobalt complexes such as **11** (**Figure 13**) can be activated with Lewis bases such as amines for the synthesis of PC.¹⁶² Then, Coates and co-workers published that salen-cobalt complexes **12a-c** (**Figure 13**) showed moderate TOF (up to 81 h⁻¹ with **12a**) in the copolymerization of PO and CO₂.¹⁶³

After that, Lu and Wang¹⁶⁴ increased the catalytic efficiency of **12c** in the copolymerization of PO and CO₂ by addition of *n*-Bu₄NBr. At ambient temperature and

20 bar of CO₂, the TOF for polycarbonate and cyclic carbonate was equal to 228 h⁻¹. Then, Paddock and Nguyen¹⁶⁵ reported that a (salen)CoX (**13a**; **Figure 13**)/Lewis base catalyst system selectively produced PPC from PO and CO₂ under mild conditions.

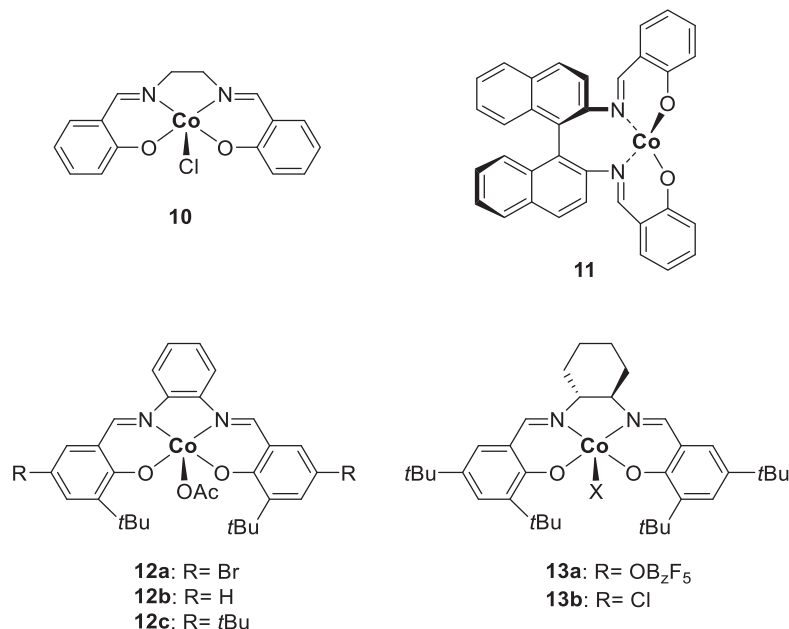


Figure 13. Cobalt catalysts used in epoxides/CO₂ copolymerizations.

Lu and co-workers have examined extensively the asymmetric alternating copolymerization of *rac*-PO and CO₂ using the chiral (salen)CoX complex with strong N-base as co-catalysts.¹⁶⁶

In an additional contribution, Cohen and Coates have reported that complexes **13a** and **13b** showed TOFs up to 720 h⁻¹ at 22 °C for *rac*-PO/CO₂ copolymerization in the presence of [PPN]Cl or [PPN]OBzF₅.¹⁶⁷ Then a communication on this topic has been published by Nozaki and co-workers involving the highly selective synthesis of PPC from PO and CO₂.¹⁶⁸

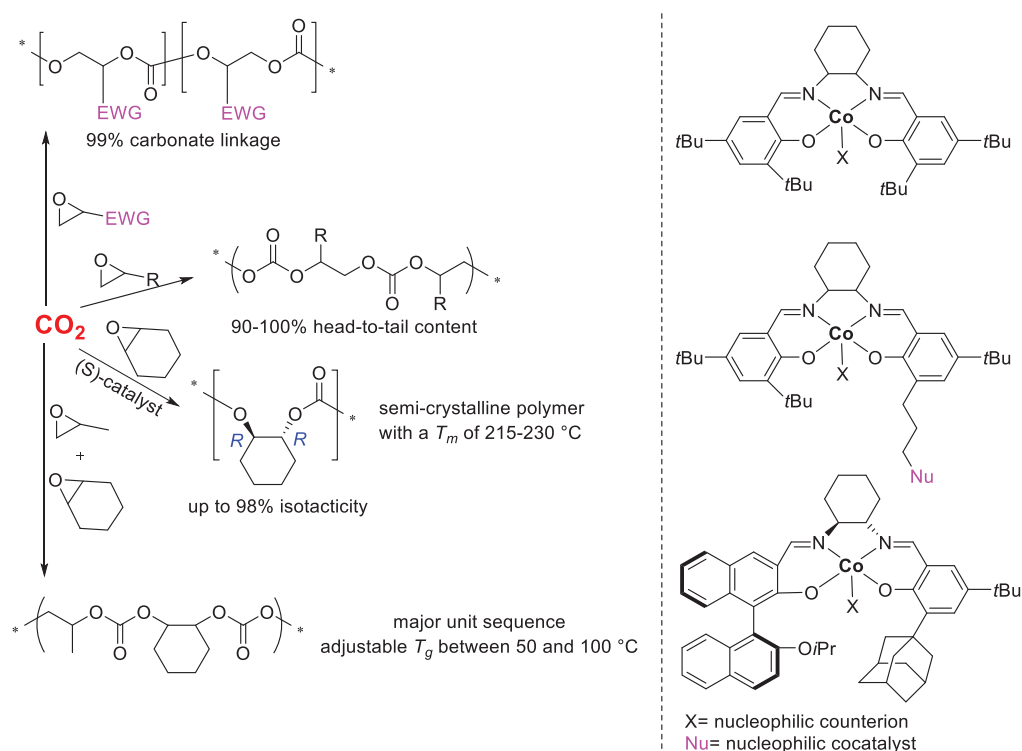
Lu and co-workers have also reported the copolymerization of CHO and CO₂ under mild reaction conditions (25 °C and 15 bars) using chiral (salen)CoX catalysts in the presence of [PPN]Cl as a cocatalyst.¹⁶⁹

In 2011, Darensbourg and co-workers¹⁷⁰ have reported an alternating copolymerization of CO₂ and epichlorohydrin (for post-functionalization of the copolymer) using cobalt(III)-based catalyst systems.

Then, Wu and co-workers¹⁷¹ have proven that trivalent cobalt complexes of

salicylaldimine are highly active catalysts in the copolymerization of CO₂ and epoxides to selectively produce the corresponding perfectly alternating polycarbonates, mainly in the presence of an intra- or intermolecular nucleophilic co-catalyst. The most important characteristics of these Co(III)-based catalysts are broad substrate scope including epoxides bearing an electron-withdrawing group, and the high regioselectivity for epoxide ring-opening, which permits the synthesis of stereoregular CO₂ copolymers (**Scheme 11**). They mentioned that these complexes work under the mechanism that the Co(III) complex works as a Lewis acidic metal ion (electrophile) to activate the epoxide, and the nucleophilic counter-ion or cocatalyst as a nucleophile to initiate the polymer chain growth.

Scheme 11. CO₂/ epoxides copolymerization using Co(III) catalysts reported by Wu and co-workers. (EWG= electron withdrawing group). "Adapted with permission from (Lu, X.-B.; Ren, W.-M.; Wu, G.-P. *Acc. Chem. Res.* 2012, 45 (10), 1721.). Copyright (2012) American Chemical Society."



In 2015, Rieger and co-workers¹⁷² reported a study on the deactivation of cobalt(III)-based porphyrin and salen catalysts by reduction to cobalt(II) species in the copolymerization of PO and CO₂.

Then, in 2016, Chen and co-workers¹⁷³ have compared the mononuclear and dinuclear catalysts systems in PO/CO₂ copolymerization. The dinuclear catalyst system was very active and selective, and PPC produced with high molar masses. A mechanism based on

the dinuclear structure was proposed. The induction period and low CO₂ pressure effect were the typical features of proposed mechanism. Finally, Nozaki and co-workers¹⁷⁴ have developed an *in situ* oxidation method to produce Co(III)-salicyl complexes and use them in the copolymerization of PO with CO₂.

Zinc Catalysts. The majority of the reports in the area of epoxides/CO₂ coupling has been done using zinc complexes.

As aforementioned, the first active species for the alternating epoxides/CO₂ copolymerization were based on mixtures of ZnEt₂ with di- and tri-hydric sources, and mixtures of carboxylic acids and Zn(OH)₂.¹²¹⁻¹²⁶ In 1999, Ree and co-workers¹⁷⁵ reported a variant of the Zn(OH)₂/glutaric acid system using ZnO as the zinc source. A TOF= 3.4 h⁻¹ was achieved for PO/CO₂ copolymerization at 60 °C and 25 atm of CO₂, which at that time was the highest activity reported for zinc carboxylates. Analysis of the PPC showed a Mn= 210 000 g/mol, Mw/Mn= 1.3.

A similar system was reported by Beckman and co-workers,¹⁷⁶ who observed that ZnO and a highly fluorinated carboxylic acid derived from a monoester of maleic acid (**14a**; **Figure 14**) is efficient in copolymerizing alternately CHO with scCO₂. The fluorination increased the solubility of the catalyst mixture and helped in PCHC production, the TOF obtained was 8.8 h⁻¹ at 135 atm of CO₂ and 100 °C. Additionally, **14b** (**Figure 14**), a Zn(II)-based compound, produced PCHC (Mn= 2150 g/mol, Mw/Mn= 4.4) with a low TOF of 1.2 h⁻¹ at 90 °C and 110 atm of CO₂.¹⁷⁷

Heterogeneous systems are often characterized by poor reproducibility and the formation of non-uniform polymers due to the presence of many different types of active sites that yield polymers with different activities and selectivities. To solve these problems, Darensbourg and Holtcamp reported in 1995 the first discrete zinc complexes for epoxides/CO₂ alternating copolymerizations.¹⁷⁸ This finding forms a key step in the development of catalysts for CO₂/epoxides copolymerization. Compound **15a** (**Figure 14**), which was synthesized from 2,6-diphenylphenol and Zn[N(SiMe₃)₂]₂, crystallized as a bis((2,6-diphenyl)phenoxy)zinc complex containing two diethyl ether solvent molecules coordinated to a tetrahedral zinc center. Under 55 atm of CO₂ at 80 °C, PCHC (91% carbonate linkages, Mn= 38000 g/mol, Mw/Mn= 4.5) was produced with a TOF= 2.4 h⁻¹.

Subsequent work studied steric effects of N-aryl substituents, including 2,4,6-tri-tert-butyl (15b; **Figure 14**), 2,6-di-tert-butyl (15c; **Figure 14**), and 2,4,6-trimethyl (15d; **Figure 14**), on CHO/CO₂ copolymerization.¹⁷⁹ Complex 15d exhibited the highest TOF (9.6 h⁻¹), thus proving that bulky ortho-substituents were not important for high copolymerization rates.¹⁸⁰ Compound 16a (**Figure 14**) showed a moderate TOF equal to 7.6 h⁻¹. The PCHC produced has molar masses of 42 000 g/mol and Mw/Mn= 6.0, with >99% carbonate linkages.^{181,182}

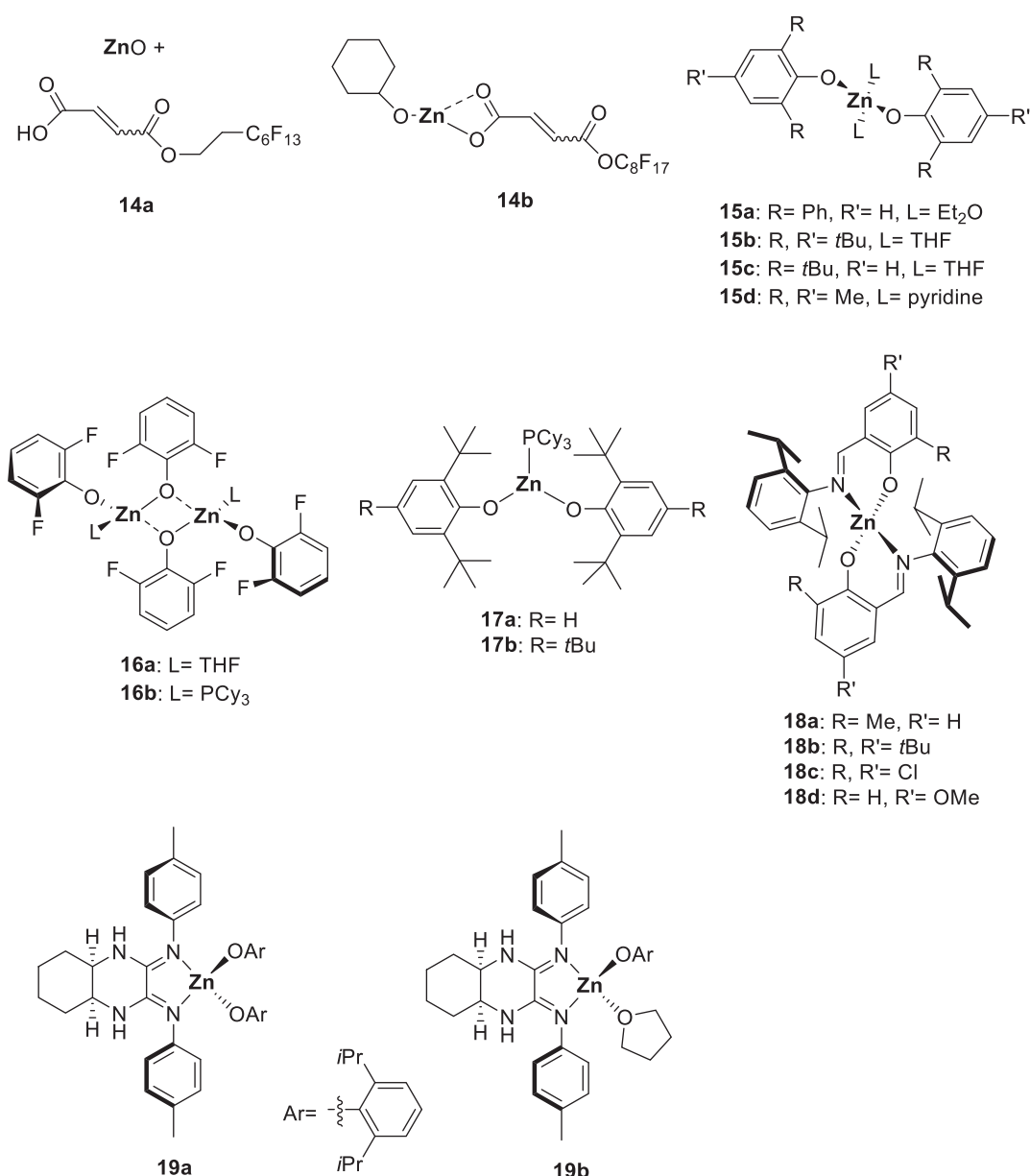


Figure 14. Zinc complexes used in CO₂/epoxides copolymerizations.

Darensbourg and co-workers proposed that two coordination sites were necessary for polyether formation from epoxides polymerization, while only one was required for

copolymer formation.^{182,183} To examine this theory, phosphane (PCy₃, PMe₃, etc.) adducts of the zinc phenoxides were synthesized, where these have only one open coordination site.¹⁸³ Compounds **17a** and **17b** (**Figure 14**) were found to be three-coordinate zinc compounds. **17b** produced PCHC with 100% carbonate linkages without loss of catalytic activity. Moreover, **16a**, which possesses only one open coordination site, generated PCHC with 100% carbonate linkages, but **16b** (the PCy₃ adduct of **16a**) was not active in CHO/CO₂ copolymerization.

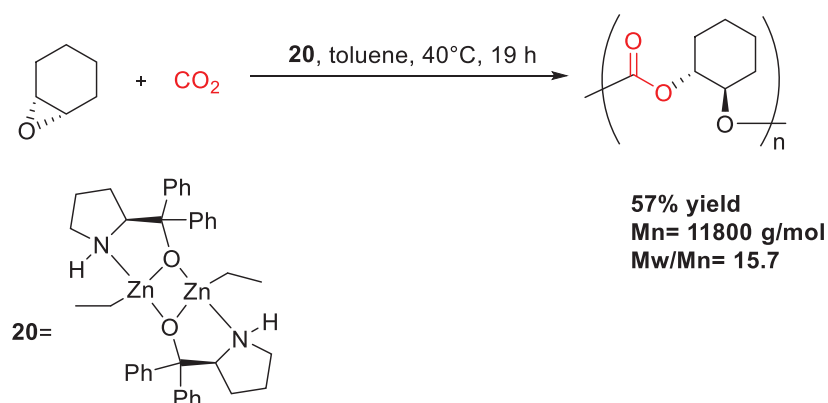
Then, Darensbourg and coworkers investigated zinc benzoate,¹⁸⁴ (dialkylamino)ethyltetramethylcyclopentadienyl zinc derivatives,¹⁸⁶ and bis(salicylaldiminato)zinc (**18a-d**; **Figure 14**).¹⁸⁵ A number of bis(salicylaldiminato)zinc complexes (**18a-d**) were synthesized by reaction of Zn[N(SiMe₃)₂]₂ with salicylaldimines. Complex **18a** was the most active catalyst in CHO/CO₂ copolymerization, it produced PCHC with > 99 % carbonate linkages, Mn= 41000 g/mol, and Mw/Mn= 10.3; TOF equal to 6.9 h⁻¹.

After that, Hampel and co-workers reported the usage of quinoxaline-derived zinc alkoxide complexes (**19a**, **19b**; **Figure 14**) in CHO/CO₂ copolymerization but with low activities.¹⁸⁷ At 80 °C and 80 atm of CO₂, compounds **19a** and **19b** showed TOFs of 4.9 h⁻¹ and 3.6 h⁻¹, respectively. The PCHC produced by **19a** have 97 % carbonate linkages, Mn= 13500 g/mol, and Mw/Mn= 4.59.

Coates and co-workers discovered a highly active epoxide/CO₂ copolymerization system using bulky β-diiminate zinc catalysts, under low pressure and temperature (7 atm of CO₂ and 50 °C).^{188,189}

There is a major attention on controlling the stereochemistry of the ring-opening in epoxide/CO₂ copolymerization for several reasons, mainly because the microstructure directly affects polymer properties.¹⁹⁰ In 1999, Nozaki and coworkers reported that a mixture of ZnEt₂ and (S)-α,α-diphenylpyrrolidine-2-yl-methanol was efficient in stereoselective CHO/CO₂ copolymerization at 40 °C and 30 atm of CO₂.¹⁹¹

Hiyama and co-workers¹⁰⁸ have reported a CHO/CO₂ alternating copolymerization using chiral dimeric zinc complexes **20** (**Scheme 12**). This dimeric zinc complex was active in CHO/CO₂ alternating copolymerization to give optically active polycarbonate.

Scheme 12. Asymmetric alternating copolymerization of CO₂ and cyclohexene oxide.

In 2009, Williams and co-workers¹⁹² reported a new macrocyclic di-zinc complex that shows very high activity in CHO/CO₂ copolymerization at just 1 atm of CO₂. Then, in 2015, they reported a number of dinuclear zinc salen complexes that are efficient catalysts for CO₂/CHO ring opening copolymerization. The studies concentrate on the effect of the ligand structures on the catalytic activity and the stability of the dinuclear complexes. Ligands containing imine moieties gave complexes that were more stable than the amine counterparts. Also, the complexes with imine substituents exhibited better selectivities, producing perfectly alternating copolymers, whereas complexes with amine substituents gave higher ether linkage content.¹⁹³ Chang and co-workers¹⁹⁴ have proved the use of intramolecular dinuclear zinc-azephenol catalyst synthesized *in situ* in the cyclopentene oxide/CO₂ copolymerization to produce completely alternating poly(cyclopentene carbonate).

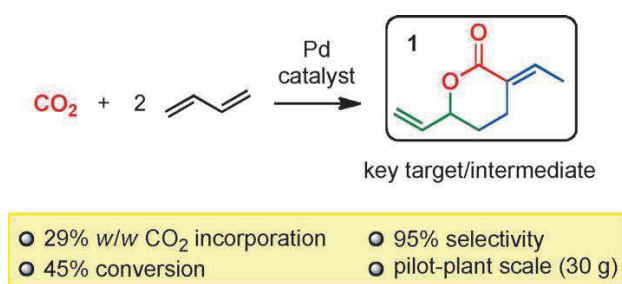
Therefore, there is a wide range of catalysts capable of copolymerizing epoxides and CO₂, which represents a green alternative route for the production of polycarbonates that are crucial for industry, they are used heavily in electronics and automotive industry for instance.

b- Copolymerization of CO₂ and Dienes. To the best of our knowledge, the only report that published a copolymerization of CO₂ with dienes is the one reported by Nozaki and co-workers,¹⁰⁶ where they copolymerized CO₂ and butadiene *via* a lactone intermediate.

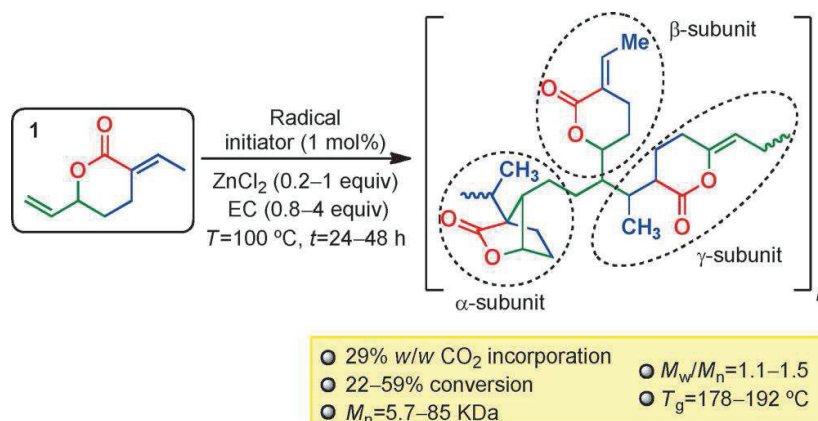
Nozaki and co-workers have reported a procedure for the preparation of CO₂/diene copolymers.^{106,120} The key of this success was the inventive use of an alternative polymerization strategy that circumvents the thermodynamic and kinetic barriers

associated with direct CO₂/butadiene copolymerization. In particular, they have used a known δ -lactone, 3-ethylidene-6-vinyltetrahydro-2H-pyran-2-one (**A**),¹⁹⁵ which is obtained by telomerization of CO₂ and butadiene in the presence of a palladium/phosphine ligand catalytic system (**Scheme 13**).

Scheme 13. Synthesis of δ -lactone A. The allylic moiety and the vinyl moiety are highlighted in blue and green, respectively. Giulia Fiorani and Arjan W. Kleij: Preparation of CO₂/Diene Copolymers: Advancing Carbon Dioxide Based Materials. *Angewandte Chemie International Edition*. 2014, 53, 7402-7404. Copyright Wiley-VCH Verlag GmbH & Co. KGaA. Reproduced with permission.



Scheme 14. Synthesis of and data for poly-A and poly-A'. Giulia Fiorani and Arjan W. Kleij: Preparation of CO₂/Diene Copolymers: Advancing Carbon Dioxide Based Materials. *Angewandte Chemie International Edition*. 2014, 53, 7402-7404. Copyright Wiley-VCH Verlag GmbH & Co. KGaA. Reproduced with permission.



Nozaki and co-workers discovered that δ -lactone **A** can be polymerized *via* a thermally initiated radical polymerization reaction using V-40 [1,1'-azobis(cyclohexane-1-carbonitrile)] as a radical initiator. Moderate conversion (17 %) occurred, and the polymer **poly-A** was obtained (**Scheme 14**). **Poly-A** was characterized by a moderate M_n (5700 g/mol) and a narrow dispersity ($M_w/M_n=1.3$). The presence of the Lewis acid ZnCl₂, and an additional solvent, such as ethylene carbonate (EC), increased the reaction rate and improved the yield to 48 % and M_n values to 62000-85000 g/mol, while retaining a good dispersity. However, the morphology of the resulting polymer (**poly-A'**) was also affected, **Poly-A'** include different isomeric subunits (α , β , and γ in **Scheme 14**).

According to Kleij,¹⁹⁶ their presence is due to Lewis acid stabilization of the radical in the α -position to the ester carbonyl group or hydrogen abstraction from the vinyl moiety of **A**. Both **poly-A** and **poly-A'** display relatively high CO₂ incorporation (29 %) and high glass transition temperatures (T_g= 178-192 °C). These new polymers could be used as alternatives for polylactones in biomedical applications.

The following section represents the utilization of CO₂ as a medium in different polymerization reactions to be a green alternative of organic solvents.

A.5.2. Carbon Dioxide as a Polymerization Medium

The synthesis and processing required to manufacture polymers consume energy, produce waste streams, and contribute in polluting the environment, even if measures are taken by the producers and also lawmakers to minimize harmful side effects. However, with a multi-million ton polymer production, we would be well advised to do better regarding sustainable routes to commodity polymers. It has been pointed out that performing polymer chemistry in liquid or supercritical CO₂ may be one of the required actions to diminish environmental impact of polymer industry.^{197,198} Supercritical carbon dioxide (scCO₂) has different properties that have permitted it to be the most widely studied supercritical fluid for polymerization reactions. Supercritical fluids possess two valuable features: they can have gas-like diffusivities (which have significant effects for reaction kinetics) while having liquid-like densities that allow for solvation of many compounds. They show changes in solvent density with small changes in temperature or pressure without altering solvent composition.¹⁹⁹

When CO₂ is used as a supercritical solvent, different advantages can be recognized. The chemical industry has become increasingly aware of environmental concerns over the use of volatile organic solvents and chlorofluorocarbons in the manufacture of commercial polymers. The use of water relieves these problems somewhat, but still results in large amounts of harmful aqueous waste that require treatment. Because of these environmental concerns, scCO₂ represents a more environmentally benign alternative to conventional solvents. CO₂ is naturally occurring and abundant where it exists in natural reservoirs of high purity located all over the world. In addition, it is generated in large quantities as a by-product in ammonia, hydrogen, and ethanol plants

and in electrical power generation stations that burn fossil fuels.²⁰⁰ CO₂ has an easily reachable critical point with a critical temperature (T_c) of 31.04 °C and a critical pressure (P_c) of 72.8 bar. As it is an ambient gas, CO₂ can be simply recycled after use as a solvent to avoid any contribution to greenhouse effects. Lastly, it is relatively nontoxic, non-flammable, and inexpensive, making it an attractive solvent for large-scale production.

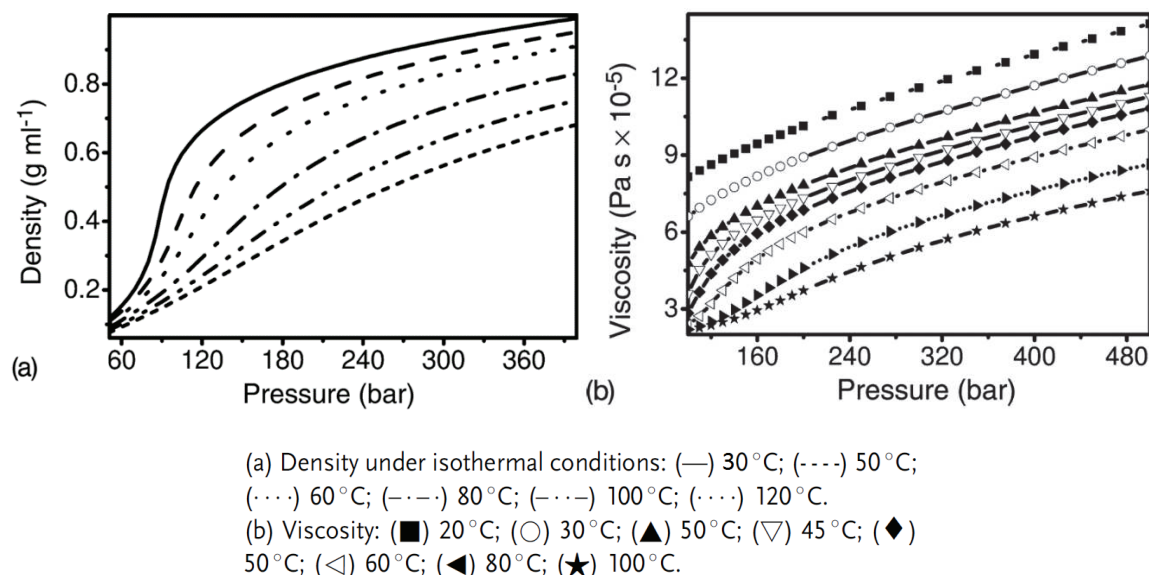


Figure 15. Pressure dependence of CO₂ physical properties.²⁰¹ Paul T. Anastas, Walter Leitner, Philip G. Jessop: Handbook of Green Chemistry, Volume 4, Green Solvents, Supercritical Solvents. 478 pages, 2010. Copyright Wiley-VCH Verlag GmbH & Co. KGaA. Reproduced with permission.

Solubility plays a major role in the synthesis of polymers in scCO₂, and the ability of a solvent to dissolve solutes depends strongly on its density; as aforementioned, changes in temperature or pressure can significantly alter the density of scCO₂ without variation of its composition.¹⁹⁹ For example, the density of CO₂ can be varied from gas-like ($\rho < 0.2$ g/cm³) to liquid-like values ($\rho > 0.6$ g/cm³) as shown in **Figure 15** (a). Furthermore, the viscosity of scCO₂ is much lower than that of liquid solvents and it varies strongly with changes in pressure and temperature (**Figure 15** (b)). Because of these properties, supercritical fluids (SCF) diffusion coefficients are similar to those of gases. As shown in **Figure 16**, any small change in temperature or pressure, mainly near the critical point, has a large effect on the diffusivities, a factor that can have strong consequences on reaction kinetics.

While CO₂ is a good solvent for most nonpolar and some polar molecules of low molar masses,²⁰³ it is a poor solvent for most polymers of high molar masses under mild

conditions (<100 °C, <350 bar). For example, poly(methyl acrylate) needs 2000 bars of CO₂ at 100 °C for a 10⁵ g/mol polymer to dissolve in CO₂.²⁰⁴ Such high pressures are not useful and are too costly in polymers manufacturing. The main polymers that show good solubility in CO₂ under mild conditions are amorphous fluoropolymers and silicones.^{199,205,206}

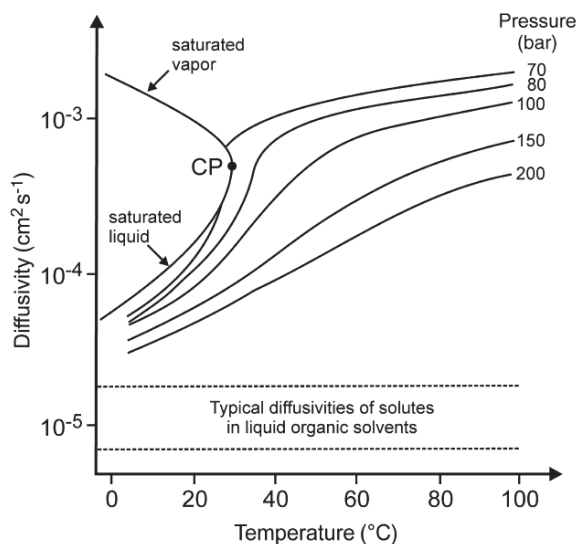


Figure 16. Temperature and pressure dependence of low molecular weight solute diffusivity in CO₂.²⁰² "CP: critical point". Paul T. Anastas, Walter Leitner, Philip G. Jessop: Handbook of Green Chemistry, Volume 4, Green Solvents, Supercritical Solvents. 478 pages, 2010. Copyright Wiley-VCH Verlag GmbH & Co. KGaA. Reproduced with permission.

Even though step-growth reactions are far away from our area of investigation; as a brief side-comment, step-growth reactions in CO₂ have been reported for the production of polycarbonates, polyamides, polyesters, polypyrrole, polyphenoxides, and silica gels *via* different polymerization processes (melt-phase condensation, sol-gel, and oxidative coupling).²⁰⁷⁻²¹⁴

Chain-growth polymerization reactions have been well investigated in CO₂. The major types of chain-growth polymerization methods include free radical, cationic, anionic, and metal catalyzed reactions. Most chain-growth polymerizations in CO₂ have focused on free-radical polymerizations, but there is a number of reports in the areas of cationic and metal-catalyzed reactions. To the best of our knowledge, anionic polymerizations in CO₂ have been rarely studied, for obvious reactivity issues of strong anions with CO₂ the main study was on anionic ring opening polymerization of oxiranes in scCO₂.²¹⁵

A.5.2.1. Cationic Polymerizations in CO₂.

Cationic polymerizations represent an area of interest in polymer science since they allow for the synthesis of unique polymers (such as polyisobutylene and polyvinyl ethers); their implementation to supercritical fluids field has been challenging. The high reactivity of carbocations results in fast polymerization reactions, but also leads to undesirable side reactions such as chain transfer and termination. These side reactions limit the use of cationic polymerizations. The basicity of monomers that are capable of being polymerized cationically and the acidity of the protons α to the carbocation on the polymer growing chain make proton abstraction by the monomer an important side reaction that is difficult to overcome. These side reactions are often reduced by decreasing the reaction temperature.

Living cationic polymerization methods have been developed to produce well-defined polymers.²¹⁶ These living methods allow the control of molar masses, dispersities, end group functionality, polymer microstructure, and reactivity. Winstein developed an ion pair spectrum to describe the active site in cationic polymerizations.²¹⁷ A classical nonliving carbocationic polymerization is found to have solvent separated ion pairs, while living systems have contact ion pairs. Solvent choice plays an important role in cationic polymerizations because it affects the equilibrium between contact pairs and solvent-separated ion pairs and the activation energy of transfer and termination reactions. Nonpolar solvents are generally required for cationic polymerizations since they minimize ion separation.

Because of the tunable properties of scCO₂ such as dielectric constant, it constitutes an interesting medium for studying cationic reactions. One disadvantage is the T_c of CO₂ (31.04 °C), since cationic polymerizations are usually done at low temperatures (-70 to -30 °C) to avoid side reactions, thus cationic polymerizations in scCO₂ are inherently difficult. Generally, most of the early experiments using CO₂ as a solvent for cationic reactions were performed in liquid CO₂ at low temperatures. However, it has been shown that good results could be obtained in liquid and supercritical CO₂. Moreover, CO₂ has been shown to be inert to cationic polymerization conditions.²¹⁸

A 1960 report by Biddulph and Plesch explored the heterogeneous polymerization of isobutylene in liquid CO₂ at -50 °C.²¹⁹ Two catalyst systems were shown to be active,

AlBr₃ and TiCl₄ using ethyl bromide and isopropyl chloride, respectively, as co-solvents. The AlBr₃-catalyzed reactions proceeded rapidly, but were incomplete and gave molar masses of about 500 000 g/mol. The low conversion corresponds to the catalyst becoming embedded in the polymer precipitate. The TiCl₄ reaction was slower, but proceeded to completion and gave molar masses of about 30 000 g/mol.

A series of papers in the late 1960s that form the first systematic study of cationic polymerizations in compressed liquid reported the precipitation polymerization of formaldehyde in liquid and supercritical CO₂. A carboxylic acid, such as acetic or trifluoroacetic acid, was added to catalyze the polymerization.²²⁰⁻²²² The polymerization reactions were conducted at 20-50 °C with a 50-60 % conversions. CO₂ was inert to the propagating cationic species.

Kennedy, depending on earlier work by Plesch,²¹⁹ reported the polymerization of isobutylene (IB) in supercritical CO₂ using 2-(2,4,4-trimethylpentyl)chloride (TMPCl) as an initiator and a Lewis acid catalyst such as BCl₃, TiCl₄, or SnCl₄ as a co-initiator.²²³ Polymerizations were done at 32.5-36 °C and 75-135 bar. Methyl chloride was added as a co-solvent (3%) to solubilize the ionic species, and its presence lead to higher conversions and narrower dispersities. The conversions were up to 30-35 % and polymers with Mn= 1000-2500 g/mol and Mw/Mn= 1.5-3.1 were produced.

An isobutylene/styrene copolymer was also synthesized in CO₂ using methylchloride as a cosolvent and TMPCl/TiCl₄ was the initiating system.²²⁴ A conversion of 15 % was obtained, but Mn and dispersities were not reported, where the authors only mentioned that by increasing reaction times polymers with higher molar masses were obtained.

The first example of electrophilic aromatic alkylation in scCO₂ is the synthesis of phenol-terminated polyisobutylene.²²⁵ TMPCl and Cl-terminated polyisobutylene (Mn= 2000 g/mol) were alkylated by phenol at 32.5 °C and 140 bar in the presence of BF₃.OEt₂ for 24 h, with yields of 75 % and 60 % respectively were observed. Also, the isomerization polymerization of 3-methyl-1-butene and 4-methyl-1-pentene has been investigated in scCO₂.^{226,227} The reactions were done at 140 bar CO₂ and 32.5 °C with residual water and AlCl₃ as the catalyst system. Similar to IB polymerization, a co-solvent (5% methyl chloride or 10% ethyl chloride) was used to obtain better results. For 3-methyl-1-butene, the conversion obtained was 40 % with a molar mass of 1000 g/mol

and $M_w/M_n = 1.41$; for 4-methyl-1-pentene the results were 70 %, 1700 g/mol, and 2.16.

DeSimone and his coworker reported a study of cationic polymerization of vinyl ethers in $scCO_2$,^{228,229} where both precipitation and homogeneous polymerizations were reported. The initiation system was based on Higashimura's living cationic polymerization method developed for hydrocarbon solvents. This method uses the Lewis acid ethyl aluminum dichloride and the acetic acid adduct of isobutyl vinyl ether (IBVE) as the initiator in the presence of a Lewis base deactivator such as ethyl acetate.²³⁰ The polymerization of IBVE started homogeneously, but became heterogeneous as the polymer precipitated. Yields obtained of the polymer synthesized in CO_2 were similar to those obtained of the polymer synthesized in cyclohexane, but with broader dispersities. At 60 °C, the dispersities of the polymers produced in CO_2 increased to greater than 9, indicating no molar mass control, mostly due to increased chain transfer to monomer and lower CO_2 density, which would permit faster precipitation of polymer.

The homogeneous polymerization of 2-(*N*-propyl-*N*-perfluorooctylsulfonamido)ethyl vinyl ether (FVE) was also realized.^{231,232} The polymerizations were homogeneous during the reaction and gave molar masses of, for example, 4000 g/mol with a dispersity of 1.6. The narrow dispersities reached with the CO_2 -soluble fluorinated polymer compared to the broad ones obtained with the CO_2 -insoluble poly(IBVE) show that the solubility of the resulting polymer plays an important role in determining the dispersity in these cationic polymerizations in $scCO_2$.

In addition, DeSimone and coworkers reported a cationic dispersion polymerization of styrene in CO_2 to overcome the problems evidenced by SEM analysis for poly(BEMO) and poly(IB) where they observed an absence of well-defined particles in SEM images.²³³

Cansell and coworkers reported a ring opening cationic polymerization of cyclosiloxane and phenyloxazoline in $scCO_2$.²¹⁵ More recent, Antunes and coworkers reported a study on the cationic polymerization of styrene in $scCO_2$ using $AlCl_3$ as an initiator, these reactions yielded low monomer conversion rates (about 50%) and a molar mass of 2000 g/mol at room temperature.²³⁴

A.5.2.2. Transition Metal-Catalyzed Polymerizations in CO_2

Catalytic polymerizations in CO_2 as a polymerization medium have been an area of

investigation in transition metal-catalyzed polymerization domain.

The ring-opening metathesis polymerization (ROMP) of bicyclo[2.2.1]-hept-2-ene (norbornene) in CO₂ was catalyzed by ruthenium and molybdenum carbene catalysts reported by Grubbs²³⁵⁻²³⁷ and Schrock,²³⁸ respectively (**Figure 17**).²³⁹ While the Ru catalyst appeared insoluble in CO₂, the Mo catalyst was partially soluble. These catalysts gave a yield of 94 % of polynorbornene in CO₂ (using toluene as a co-solvent a yield of 97 % obtained) and molar masses equal to 10⁵-10⁶ g/mol at much milder reaction conditions of 25-45 °C and around 100 bar. The Ru catalyst gave about 25% *cis* content with no real dependence on density while the Mo catalyst gave 66 % *cis* content at a density of 0.57 g/mL and 82 % at 0.72 g/mL. The ruthenium carbene catalyst was also used to polymerize *cis*-cyclooctene with a yield of 50% and a molar mass of 10⁵ g/mol. The polymers produced in CO₂ were similar in molecular weight and microstructure to those produced in dichloromethane.

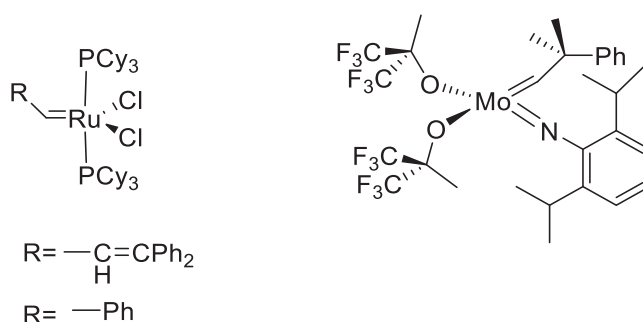
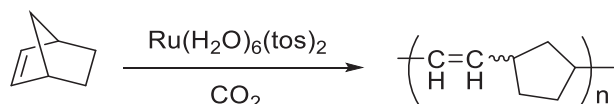


Figure 17. Catalysts for ROMP of norbornene in supercritical CO₂. "Adapted with permission from (Kendall, J. L.; Canelas, D. Q.; Young, J. L.; DeSimone, J. M. *Chem. Rev.* 1999, 99, 543-563.). Copyright (1999) American Chemical Society."

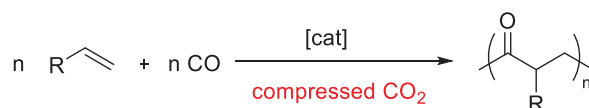
DeSimone and co-workers reported a ROMP of norbornene in CO₂ catalyzed by [Ru(H₂O)₆(tos)₂] (tos= *p*-toluenesulfonate) (**Scheme 15**).^{240,241} The reactions were performed at 65 °C with pressures of 60-345 bar. The insoluble polymer precipitated, and there was no obvious relation between pressure and molar mass (which varied from 10⁴ to 10⁵ g/mol), yields= 30-76 %, or dispersities of 2.0-3.6. The [Ru(H₂O)₆(tos)₂] catalyst is insoluble in CO₂, but could be solubilized by the addition of methanol. When the polymerization was undertaken with methanol (up to 16 wt %) as a co-solvent, the Mn and the dispersity were similar to those of the polynorbornene produced in the absence of methanol, but the yields increased by increasing methanol content. For example, the reaction with 16 wt % methanol gave in 5 h a similar yield to what the reaction without

methanol gave in 16 h, thus, the reaction was much faster in the presence of methanol. Also, a deep effect on polymer microstructure was found with increasing methanol content, where the presence of methanol decreased the *cis*-vinylene content in the produced polymer (83% *cis* without methanol and 33% *cis* with 16 wt % methanol).

Scheme 15. ROMP of norbornene in supercritical CO₂. "Adapted with permission from (Kendall, J. L.; Canelas, D. Q.; Young, J. L.; DeSimone, J. M. *Chem. Rev.* **1999**, 99, 543-563.). Copyright (1999) American Chemical Society."

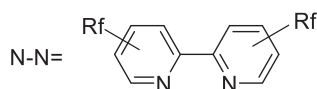


Scheme 16. CO/Vinyl Arene copolymerization via cationic Pd(II) in the presence of carbon dioxide. "Adapted with permission from (Campos-Carrasco, A.; Estorach, C. T.; Bastero, A.; Reguero, M.; Masdeu-Bultó, A. M.; Franciò, G.; Leitner, W.; D'Amora, A.; Milani, B. *Organometallics* **2011**, 30 (24), 6572-6586.). Copyright (1999) American Chemical Society."



R = C₆H₅, 4-*tert*-BuC₆H₄

[cat] = [Pd(N-N)₂X]₂, [Pd(CH₃)(NCCH₃)(N-N)][X]



More recent, Milani and co-workers reported a synthesis of a cationic Palladium(II) complex for CO/vinyl arenes copolymerization in the presence of CO₂ (**Scheme 16**), where they synthesized new bipyridine ligands bearing one or two perfluorinated ponytails and examined their coordination chemistry with Palladium(II) precursors by synthesizing two series of complexes, one involving monocationic complexes and the other dicationic complexes with various counterions, such as tosylate, hexafluorophosphate, and BArF⁻. Both series of complexes were investigated as precatalysts for the copolymerization of CO/vinyl arene in scCO₂ and in CO₂-expanded substrate. For both series of complexes, the best results were obtained from the polymerization that was performed in CO₂-expanded substrate. Some catalyst precursors were active up to 1.5 kg copolymer/g Pd for the monocationic precatalysts and 6.1 kg copolymer/g Pd for the dicationic precatalysts in production of syndiotactic polyketones, with molar mass equal to 149 500 g/mol for the monocationic precatalyst and 222 000 g/mol for the dicationic one. The good catalytic data found in CO₂ showed

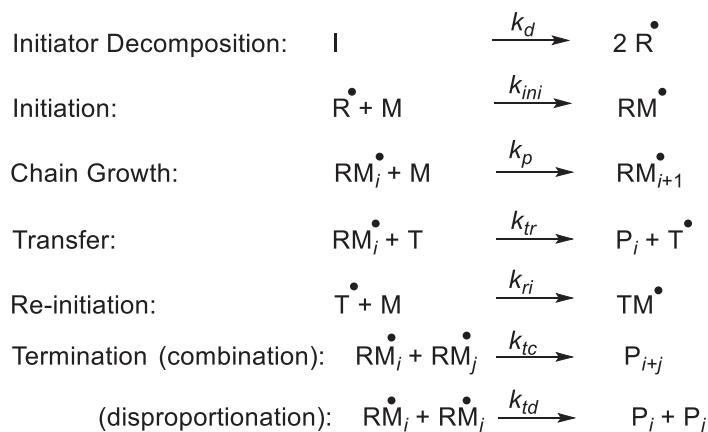
that compressed CO₂ is a potential appropriate medium for this reaction.²⁴²

Note that, CO₂ is used to quench early transition metals-catalyzed reactions, which means that it is used as a poison that blocks the active sites and this form a main obstacle for performing such reactions in presence of CO₂. It is used as a selective tag which can label the growing polymer chains in early transition metals catalytic polymerizations.²⁴³ CO₂ as tag is believed to be a more suitable agent for one component catalysts (e.g. TiCl₃) because the tag does not accumulate in the polymer.²⁴⁴ Besides, as a tag, it is much more effective than CO in the ethylene polymerization catalyzed by Zr(C₃H₅)₄/Al₂O₃, Zr(C₃H₅)₄/SiO₂ and TiBz₄/Al₂O₃ systems.²⁴⁵

A.5.2.3. Radical Polymerizations in CO₂

In a chain-growth polymerization reaction, an active species is formed which subsequently grows by successive addition of monomer molecules. With free radical polymerization, the active species are electrically neutral radicals that are continuously formed by decomposition of a radical initiator, and are continuously consumed by radical-radical termination reactions (**Scheme 17**).

Scheme 17. Reaction steps in a free radical polymerization mechanism. I= initiator, M= monomer, T= transfer agent, RM= growing chain, P= unreactive polymer chain.



Under homogeneous conditions, all constituents such as initiator, monomer, radicals, and polymer are dissolved during the whole reaction time, where the reaction can be performed in bulk or in solution. The reaction kinetics of homogeneous free radical polymerization (FRP) in scCO₂ have been investigated, starting with the decomposition kinetics of the initiator azobisisobutyronitrile (AIBN). The decomposition rate of the initiator (k_d , **Scheme 17**) was reduced by a factor of 2.5 compared with benzene as a

solvent, but the initiator efficiency, describing how many growing chain radicals are formed per decomposed initiator molecule, increased by 50% due to the reduced cage effect.²⁴⁶ Also, a reactor with continuous stirring was used to determine the rate constant of decomposition and the initiator efficiency of diethyl peroxydicarbonate (DEPC). Between 65 and 85 °C, first-order kinetics were confirmed, characterized by an energy of activation $E_A^{(DEPC)} = 132 \text{ kJ/mol}$. The rate constant obeyed the Arrhenius equation $K_d^{(DEPC)} = 6.3 \times 10^{16} \text{ s}^{-1} \exp(E_A/RT)$ and the initiator efficiency was $f = 0.6$.²⁴⁷

The light-induced degeneration and subsequent addition to methyl methacrylate of the photoinitiator trimethylbenzoyldiphenylphosphine oxide (TMDPO) was measured with time-resolved ESR spectroscopy (electron spin resonance spectroscopy) in liquid CO₂ and scCO₂ at an excitation wavelength of 308 nm. Measurement of the ESR line resulted in the rate of initiation $k_{ini} = (5.5 \pm 0.5) \times 10^7 \text{ M}^{-1} \text{ s}^{-1}$ in liquid CO₂ and $(6.1 \pm 0.6) \times 10^7 \text{ M}^{-1} \text{ s}^{-1}$ in scCO₂. These values were close to those obtained in acetonitrile $[(8.1 \pm 1.6) \times 10^7 \text{ M}^{-1} \text{ s}^{-1}]$ and toluene $[(4.0 \pm 0.4) \times 10^7 \text{ M}^{-1} \text{ s}^{-1}]$ as solvents.²⁴⁶

Since solubility turned out to be an important factor for scCO₂ mediated reactions, CO₂-soluble azo initiators have been designed and tested. At 215 bar, bis(perfluoroalkylethyl) 4,4'-azobis-4-cyanovalerate decomposes with first-order kinetics and an activation energy of decomposition of 76 kJ/mol between 60 and 80 °C. The decomposition constant at 70 °C was $1.56 \times 10^{-6} \text{ s}^{-1}$.²⁴⁸ The thermal decomposition of diethyl peroxydicarbonate (DEPDC) was examined by in situ attenuated total reflection Fourier transform infrared (ATR-FTIR) spectroscopy in heptane and in scCO₂. In both solvents the decomposition followed first-order kinetics with an activation energy of 115 kJ/mol (T= 40-74 °C) in heptane and 118 kJ/mol in scCO₂ (T= 40 to 60 °C). When the CO₂ was vented, the unstable intermediate decomposition product monoethyl carbonate was decarboxylated and derivatized mainly into ethanol.²⁴⁹ Investigations on the rate of polymerization with the examples of styrene,²⁵⁰ FOA,²⁵¹ MMA, and butyl acrylate²⁵² showed that the rate constant of propagation k_p (**Scheme 17**) remains at the order of magnitude for bulk polymerizations, indicating that CO₂ does not interfere with the polymerization reaction. However, the termination constants k_t (both k_{tc} and k_{td}) (**Scheme 17**) increase in cases where CO₂ is a poor solvent for the generated polymer.²⁵³

It is a particular advantage of CO₂ that it is inert with respect to radical transfer

reactions, that is, k_{tr} in **Scheme 17** can be regarded as zero. Therefore the free radical polymerization kinetics in the homogeneous solution phase of scCO₂ are very similar to those done in non-polar liquid solvents.²⁵³

Different classes of polymers have been synthesized in CO₂ as a polymerization medium:

a- Side-chain Fluoropolymers. Perfluorinated compounds represent a unique class of compounds as they are immiscible with water, do not mix with hydrocarbons,²⁵⁴ form low-energy surfaces, and have extreme chemical resistance. These advantages turn into problems upon production of their corresponding polymers, since either environmentally dangerous chlorofluorocarbon (CFC) solvents have to be used in solution polymerizations, or emulsion polymerizations have to be carried out and require perfluorinated surfactants such as perfluorooctylsulfonates (PFOS) or perfluoroalkylcarboxylates.²⁵⁵ Also, more problems are caused by side reactions of growing fluorinated radicals with solvents which decrease the product quality.^{256,257} CO₂ offers different advantages, since it is a non-toxic and non-reactive solvent that can be removed from the final product without an energetic cost.²¹⁸ Macromolecules with perfluoroalkyl side-chains are of technical importance for the production of non-sticky surfaces, soil- and water-repelling coatings, and "easy to clean" applications, in addition to their applications in electronics.^{256,257}

As the polymers become soluble in CO₂ below 300 bar upon exceeding a minimum fluoro-side-chain molar fraction, the polymers can be synthesized under homogeneous solution conditions by FRP in scCO₂.²⁵⁸ 1,1-Dihydroperfluorooctyl acrylate (FOA) has been polymerized with AIBN as a radical initiator in scCO₂ solution at 60 °C and 207 bar to produce high molecular weight polyFOA with high yields that were soluble in CO₂.²⁰⁵

Also, styrene monomers with perfluoroalkyl side-chains have been polymerized in scCO₂. The polymers produced were identical with the polymers produced in solution polymerization in 1,2,2-trifluoroethane (Freon-113).^{205,218}

Monomers with fluorinated side groups have been copolymerized with nonfluorinated monomers such as methyl methacrylate (MMA), butyl acrylate (BuA), ethylene, and styrene in scCO₂.²⁵⁹⁻²⁶² FOA was also copolymerized with 2-(dimethylamino)ethyl

acrylate (DMAEA) and 4-vinylpyridine to produce CO₂-soluble polymeric amines,^{263,264} 3-O-methacryloyl-D-glucopyranose^{265,266} and poly (ethylene oxide) monomethacrylate to give CO₂-philic/hydrophilic macromolecules.²⁶⁷ Perfluorooctylethyl methacrylate (FOMA) was copolymerized in scCO₂ with 2-hydroxyethyl methacrylate, oligoethylene oxide monomethacrylate and dimethylaminoethyl methacrylate (DMAEMA) to produce CO₂-soluble amphipathic copolymers.²⁶⁸ Also, the homo- and copolymerization behavior of bis(trifluoromethyl)phenyl acrylate/hexafluoroisopropylidene was examined.²⁶⁹

Controlled radical polymerization reactions have also been done in scCO₂. Perfluoroalkane acrylates and methacrylates such as FOA and FOMA have been polymerized by means of atom transfer radical polymerization (ATRP), using a bipyridine ligand with perfluoroalkyl substituents to render it CO₂-soluble. PolyFOMA of Mn = 16 800 g/mol and a narrow dispersity of Mw/Mn = 1.01 was obtained with a yield of 83%. Note that with CO₂-insoluble ligands, lower yields (<65%) and much broader dispersities (Mw/Mn = 5.9) have been obtained. The controlled nature of the reaction was demonstrated by synthesis of a well-defined amphiphilic polyFOMA-*b*-polyMMA diblock copolymer.²⁷⁰ The specific importance of these CO₂-soluble homo- and co-polymers lies in their possible application as emulsifiers, or stabilizers for emulsion or dispersion polymerization in scCO₂.

Lacroix-Desmazes et al.²⁷¹ reported the synthesis of different gradient fluorinated copolymers by reversible addition fragmentation chain transfer (RAFT) polymerization in α,α,α -trifluorotoluene, and they proved their high solubility in scCO₂ to allow using them as complexing surfactants in many applications. They took the advantage of this solubility to synthesize a gradient copolymer by RAFT polymerization directly in CO₂ medium. Poly(1,1,2,2-tetra-hydroperfluorodecyl acrylate-co-acetoacetoxyethyl methacrylate) (poly(FDA-co-AAEM)) gradient copolymer was successfully synthesized in scCO₂ with a good control, the living and controlled character of the polymerization wasn't affected by the CO₂ medium.

Also, Lacroix-Desmazes et al.²⁷² reported a reverse iodine-transfer polymerization (RITP) of 1,1,2,2-tetrahydroperfluorodecyl acrylate (FDA) in scCO₂ at 70 °C under a CO₂ pressure of 300 bar. The increase of Mn (from 10 000 to 100 000 g/mol) went with a decrease of the dispersity of the polymers (from 2.06 to 1.33), which is consistent with a

controlled radical polymerization.

Since our work is concerned with polyolefins, we concentrate in this part (side-chain fluoropolymers) on the polymerizations of fluoroolefins (fluorinated analogs of olefins) in CO₂, where fluorinated monomers are the most studied monomers in CO₂-mediated polymerizations.

Fluoroolefin Polymers. Commercialized perfluorinated materials such as polytetrafluoroethylene (PTFE, Teflon), polychlorotrifluoroethylene (PCTFE), poly(vinylidene difluoride) (PVDF), and poly(vinyl fluoride) (PVF) are produced in large amounts by aqueous emulsion polymerizations of the corresponding fluoroolefins (Figure 18).^{254,256}

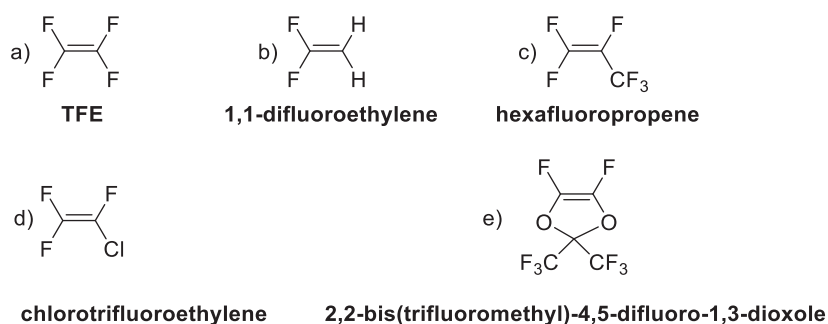


Figure 18. Some fluoro-monomers polymerized in scCO₂.

The main disadvantages of this process are (i) the necessary use of environmentally risky perfluorinated surfactants,²⁷³ (ii) the generation of large waste water streams, (iii) the energy requirement for product drying (more than 2.3×10^9 kJ/m³ of evaporated water), and (iv) side reactions due to the high electrophilicity of the growing perfluorinated chain radicals, causing the formation of, for example, acid fluoride or carbonic acid end groups.²⁵⁵

1) *Polytetrafluoroethylene*. PTFE, the perfluorinated analog of polyethylene, as characterized by a Tg of -73 °C and an irreversible melting temperature above 335 °C,²⁷⁴ can be used between -269 and 260 °C.

The monomer, TFE, tends to undergo auto-polymerization, which may causes explosions. Upon dilution with CO₂ the mixture becomes stable, but can still be polymerized.²⁷⁵ The polymerization of TFE in scCO₂ has been studied and patented extensively.²⁷⁶ PTFE is insoluble in scCO₂ because of its high crystallinity and melting

temperature. The polymerization proceeds in the form of a dispersion polymerization, where the polymer becomes insoluble.

Tetrafluoroethylene copolymerizations^{277,278} with perfluoro(propyl vinyl ether) and with hexafluoropropylene or homopolymerizations²⁷⁹ have been done in CO₂, resulting in high molar mass (>10⁶ g/mol) polymers with high yields. The two major advantages of this process, absence of chain transfer to solvent and absence of undesirable end-groups (such as -Cl from transfer to halogenated solvents), have been reviewed.²⁸⁰

2) *Poly(vinylidene fluoride)*. PVDF is a semi-crystalline thermoplastic polymer.²⁸¹ Technical PVDF exhibits melting ranges between 154 and 180 °C; its maximum continuous used temperature is reported to be 150 °C.²⁸² PVDF remains tough even at temperatures below 0 °C with a T_g= -40 °C.

Commercially, the polymer is produced either in emulsion or suspension polymerization reactions at monomer pressures of 10-200 bars and temperatures from 10 to 130 °C.²⁸¹ For emulsion polymerization, fluorinated surfactants have been used in combination with organic percarbonates and peroxides.²⁸³ Highly regular PVDF with 94-97% alteration of -CH₂- and -CF₂- groups crystallizes well and is soluble only in high-boiling polar solvents such as DMF, and DMSO.²⁸¹ Solution polymerizations of vinylidene fluoride (VDF) have been reported, initiated by radical initiators or ionizing irradiation such as γ-rays,^{284,285} but are not possible with respect to economy.

VDF has been polymerized in the homogeneous phase in scCO₂ at 120 °C and 1500 bar in the presence of perfluorohexyl iodide as a transfer agent to keep the molecular weight below the precipitation limit. The molecular weight increased linearly with the reaction time during the initial stage of the polymerization, while the dispersity remained around 1.2-1.5, indicating a controlled polymerization reaction.²⁸⁶

Since pressures beyond 1000 bar exceed technical feasibility, most studies focused on milder conditions in which the PVDF formed cannot be dissolved by scCO₂. The homopolymerization of VDF in scCO₂ was shown to be of the precipitation polymerization type,^{287,288} characterized by multimodal molecular weight distributions, and low powder density.^{289,290}

3) *Copolymerizations of perfluoroolefins*. A brief part to mention the copolymerizations of

perfluoroolefins in CO₂. PTFE, for example, is difficult to process and exhibits only moderate mechanical strength due to its plasticity. Copolymerization allows the properties of polymers to be improved and tailored more for specific applications. Therefore, a series of perfluorinated copolymers have been introduced, in particular copolymers of TFE with hexafluoropropene,²⁹¹ ethylene,²⁹² 2,2-bis(trifluoromethyl)-4,5-difluoro-1,3-dioxole,²⁹³ and perfluorovinyl ether.²⁹⁴ The copolymers have attracted a great deal of attention in ferroelectric materials, since the polymer samples change their length in electric fields, which is an important feature for producing actuators.

b- Poly(methyl methacrylate). Atactic poly(methyl methacrylate) (PMMA) as produced by FRP is an amorphous thermoplastic with a T_g= 105 °C. The polymerization of MMA has become the most studied polymerization reaction in scCO₂. PMMA is insoluble in scCO₂ under conventional polymerization conditions (P= 350 bar, T= 60-100 °C),^{295,296} and early studies showed that precipitation polymerization resulted in low monomer conversions (10-40 %), and also a PMMA with molar masses of 77 000-149 000 g/mol and uncontrolled particle shapes and particle size distributions.^{297,298}

The effects of pressure and temperature on the precipitation polymerization of MMA in scCO₂ were investigated, and the importance of phase equilibrium for the product yield and properties was confirmed.²⁹⁹

The first free radical dispersion polymerization of MMA in scCO₂ was reported in 1994, using polyFOMA as a steric stabilizer. The polymerization was initiated with either AIBN or a fluorinated AIBN derivative at 65 °C and 207 bars. Nearly complete monomer conversion was obtained, the M_n increased to 190 000-325 000 g/mol, and the PMMA precipitated in the form of spherical particles with a narrow diameter distribution between 1 and 3 μm. The key role of polyFOA and its methacrylate analog polyFOMA as stabilizers that allowed for control of the reaction rate and the reaction products particle morphology was associated by a subsequent work.³⁰⁰

In 2008, Hu and co-workers³⁰¹ studied the effect of pressure on the FRP of MMA in CO₂ fluid from ambient atmosphere pressure to 285 bar. It was found that, when the polymerization of MMA was performed under 118-285 bar, the MMA conversion and the M_n of PMMA were relatively low and MMA-CO₂ mixture was in a homogeneous phase. However, while the polymerization was carried out at or below 92 bar, in which

the MMA-CO₂ mixture was at vapor-liquid equilibrium state, the PMMA with high Mn was synthesized at quite high MMA conversion.

c- Polystyrene. Polystyrene (PS) produced from FRP is an atactic, amorphous, thermoplastic material with a T_g= 100 °C. As PS and modified PS make up about 4 % of the total polymer production,³⁰² the replacement of the organic solvent-based production for sustainable manufacture seems worthwhile.

Pulsed laser spectroscopy was applied to measure the propagation rate constant k_p of the FRP of styrene in the homogeneous scCO₂ phase. At 65 °C and 180 bar, a k_p = 460 ± 70 L/mol.s was obtained, which is close to that for styrene bulk polymerization.²⁵⁰ However, since PS rapidly precipitates from scCO₂ reaction mixtures, most studies concentrated at precipitation or dispersion polymerization reactions. At 58 °C and 100 bar, solvent mixtures consisting of THF-CO₂ or cyclohexene-CO₂ have been investigated in precipitation polymerizations, where in these investigations the effect of CO₂ as a non-solvent was purposed to reduce the dispersity of the produced polymer.³⁰³ In ethanol-CO₂ mixtures, the precipitation polymerization of styrene was limited to low yields (15-60 %) of low molar masses (Mn < 26 000 g/mol),³⁰⁴ showing that efficient stabilization of the polymer particles is required. Different stabilizers were tested in polymerization of styrene in scCO₂, as an example, polyFOA is one of the best stabilizers used.³⁰³

d- Polyethylene. To the best of our knowledge, the polymerization of polyethylene (PE) in CO₂ as a reaction medium *via* a free radical process was reported only once in 1969 by Kagiya and co-workers, where they used 1.22 mmol of azobisisobutyronitrile (AIBN) as an initiator, the reaction was performed under a total pressure (ethylene + CO₂) of 392 bar at 55 °C for 4 h, and the yield obtained was 3 g, but they added 10 mL of 2-ethyl-hexyl adipate as an initiator diluent.³⁰⁵

Therefore, CO₂ seems to be a successful green alternative to organic solvents in different radical polymerization reactions, its usage could lead to more sustainable production of a variety of polymers.

A.6. Towards CO₂ Utilization in Polymerizations of Olefins

Polyolefins form the largest class of the thermoplastics commodity. They are polymers

of simple alkenes such as ethylene, propylene, butenes, and pentenes, and copolymers thereof. Their production reaches hundreds of millions of tons annually, they are incorporated in most of our daily use materials (in packaging, building and construction, electronics, electrical, and automotive industries...). Because of this importance, polymer chemists are looking forward to develop more environmentally friendly processes in the production of polyolefins. One way to adjust the balance between the huge world demand of polyolefins and preserving environment is to avoid the use of components in the polymerization processes that produce unnecessary wastes. One of the possible producing-waste components are the organic solvents, CO₂ could be regarded as an alternative, both at the synthetic and at the recycling stage of polyolefins.

As aforementioned, CO₂ has been used as a solvent in different polymerization processes but it is rarely used in olefin polymerizations (apart from styrene polymerization).

Moreover, we worked not only to utilize CO₂ as a solvent in ethylene polymerization, but also on overcoming the CO₂ inertness in order to force its incorporation in the polymer backbone. Thus, in such a dual use of CO₂, as a solvent and a functionalization agent in synthesis of polyolefins, a link between different renewable resources, such as CO₂, and cheap, widely available alkenes is made, targeting a potential evolution towards more sustainable materials.

Even though ethylene and polyethylene are widely reviewed, for clarity in introducing our work the following two parts will deal with a brief review about ethylene as a model for olefins (simplest olefin) and polyethylene (the most important industrial polyolefin).

A.7. ETHYLENE: The Most Important Industrial Olefin

A.7.1. History of "ETHYLENE"

Ethylene is a hydrocarbon which has the formula C₂H₄ (H₂C=CH₂). It is a colorless flammable gas with a faint odor when pure. Ethylene is one of the most important building blocks of the chemical industry, it is the simplest olefin. It is used as the basic building block to produce a wide range of plastics, solvents, cosmetics and other

products. The market demand in 2016 is greater than 150 million tons with a global growth rate of around 3.5 % estimated over the 5 years following.³⁰⁶

Ethylene seems to be discovered by "Johann Joachim Becher" in 1669, who produced it by heating ethanol with sulfuric acid.³⁰⁷ "Joseph Priestley" also mentioned the gas in his *Experiments and observations relating to the various branches of natural philosophy: with a continuation of the observations on air* (1779), where he reported that "Jan Ingenhousz" saw ethylene synthesized in the same way by "Mr. Enée" in Amsterdam in 1777 and that "Ingenhousz" after produced the gas himself.³⁰⁸

The properties of ethylene were studied in 1795 by four Dutch chemists, Johann Rudolph Deimann, Adrien Paets van Troostwyck, Anthoni Lauwerenburgh and Nicolas Bondt, who found that it differs from hydrogen gas and that it contains both carbon and hydrogen atoms. This group also discovered that ethylene could be combined with chlorine to produce the *oil of the Dutch chemists*, 1,2-dichloroethane; this discovery gave ethylene the name used for it at that time, *olefiant gas* (oil-making gas).³⁰⁷

In the 19th century, the suffix *-ene* (an ancient Greek root added to the end of female names meaning "daughter of") was commonly used to refer to a molecule that contains one fewer hydrogen atoms than the molecule being modified. Thus, "ethylene" (C₂H₄) was the "daughter of ethyl" (C₂H₅). The name "ethylene" was used from 1852.

In 1866, the German chemist "August Wilhelm von Hofmann" proposed a system of hydrocarbon nomenclature in which the suffixes *-ane*, *-ene*, *-ine*, *-one*, and *-une* were used to denote the hydrocarbons with 0, 2, 4, 6, and 8 fewer hydrogens than their parent alkane.³⁰⁹ In this system, ethylene became "ethene". Hofmann's system eventually became the basis for the Geneva nomenclature approved by the International Congress of Chemists in 1892, which remains at the core of the IUPAC nomenclature. However, by that time, the name ethylene was deeply rooted, and it remains in wide use today.³¹⁰

A.7.2. Chemical and Physical Properties of Ethylene

Ethylene is a hydrocarbon that has four hydrogen atoms bound to a pair of carbon atoms that are connected by a double bond. All six atoms that comprise ethylene are coplanar (in the same plane). The H-C-H angle is 117.4° (**Figure 19**), near 120° which is

the angle of ideal sp² hybridized carbon. The molecule is also relatively rigid, where the rotation around the C-C bond is a high energy process that requires breaking the π -bond.

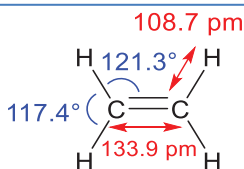


Figure 19. Ethylene molecule.

The π -bond in the ethylene molecule has a useful reactivity. It is a region of high electron density, therefore it is susceptible to attack by electrophiles. Many reactions of ethylene are catalyzed by transition metals, which bind easily to the ethylene using both the π and π^* orbitals.

Table 3 shows the different physical properties of ethylene.

Table 3. Physical Properties of Ethylene.

<i>Molecular Weight</i>	<i>28.05 g/mol</i>
<i>Boiling Point</i>	<i>-103.3 °C</i>
<i>Melting Point</i>	<i>-168.9 °C</i>
<i>Liquid Density at 21 °C</i>	<i>0,568 g/cm³</i>
<i>Gas Density at 21 °C</i>	<i>0.001 g/cm³</i>
<i>Critical Temperature</i>	<i>9.44 °C</i>
<i>Critical Pressure</i>	<i>50.49 °C</i>

A.7.3. Ethylene Production

Briefly, ethylene is produced in the petrochemical industry by steam cracking, where gaseous or light liquid hydrocarbons are heated to 750-950 °C, inducing numerous free radical reactions followed by immediate quench to stop these reactions. This process converts large hydrocarbons into smaller ones and introduces unsaturation. Ethylene is separated from the obtained mixture by repeated compression and distillation.³¹¹

Note that there is three main types of steam cracking: 1) The steam cracking of ethane and propane (from natural gas and from crude oil); 2) the steam cracking of naphtha from crude oil (naphtha is an intermediate hydrocarbon liquid stream derived from the

refining of crude oil); 3) the catalytic cracking of gas oil from crude oil.³¹²



Figure 20. A plant for ethylene production by steam cracking of naphtha at Grangemouth in Scotland (INEOS Company).

As aforementioned, the market demand in 2016 is greater than 150 million tons with a global growth rate of around 3.5 % estimated over the 5 years following,³⁰⁶ where ethylene is produced by around 120 companies in 32 countries in order to cover this demand. This gigantic production shows the importance of this molecule, where it is considered as the most important manufactured organic chemical. It is the building block for a wide range of chemicals from plastics to solvents.

Figure 20 shows a plant at Scotland for steam cracking of naphtha to produce ethylene.³¹²

A.7.4. Uses of Ethylene

Ethylene is widely used in the chemical industry, it is a raw material for different organic chemicals and polymers, which are used in a wide variety of industrial and consumer markets.

The largest outlet, accounting for around 60% of ethylene demand globally, is polyethylene. Low density polyethylene (LDPE) and linear low density polyethylene (LLDPE) mainly go into film applications such as food and non-food packaging, shrink and stretch film, and non-packaging uses. High density polyethylene (HDPE) is used primarily in blow molding and injection molding applications such as containers, drums,

household goods, caps and pallets. HDPE can also be extruded into pipes for water, gas and irrigation, and films for refuse sacks, carrier bags and industrial lining.³¹³ Polyethylene production will be explained in part A.8.

The next largest consumer of ethylene is ethylene oxide (EO) production, which is consequently primarily used to make ethylene glycol. The majority of the monoethylene glycol is used to make polyester fibres for textile applications, polyethylene terephthalate (PET) resins for bottles and polyester films. Monoethylene glycol is also used in antifreeze applications. Other EO derivatives include ethoxylates (for use in shampoo, kitchen cleaners, etc), glycol ethers (solvents, fuels and others) and ethanolamines (surfactants, personal care products and others).

Ethylene dichloride is made by the chlorination of ethylene and can then be cracked to make vinyl chloride monomer. Almost all the amounts of the vinyl chloride produced are used to make polyvinyl chloride (PVC) which has its main applications in the construction industry. Also, it reacts with benzene to make ethylbenzene which is further processed into styrene. The main products obtained from styrene are polymers and synthetic rubbers such as polystyrene (PS), acrylonitrile-butadiene-styrene (ABS) and styrene-butadiene rubber (SBR).

Other ethylene derivatives include alpha olefins which are used in LLDPE production, detergent alcohols and plasticizer alcohols; vinyl acetate where its polymer is used in adhesives, paints, and paper coatings; and industrial ethanol which is used as a solvent or in the manufacture of chemical intermediates such as ethyl acetate and ethyl acrylate.

A.8. POLYETHYLENE

It is hard to imagine our present life without polyethylene. As the largest volume polymer, polyethylene is critical to every part of our daily life today. From electricity transmission lines to natural gas transport, from food packaging and preservation to construction, from infra structure to agriculture. Its low cost, highly desirable functional qualities and ease of processing into films, pipes, molded articles of different forms and shapes has enabled it to become what it is today.

As a definition, polyethylene or polyethene (abbreviated PE) is a polymer composed of

ethylene as the repeated unit, it is the most common plastic used mainly in packaging and insulation.

A.8.1. History of Polyethylene

The first known synthesis of polyethylene occurred accidentally in 1894 by Hans von Peckmann,³¹⁴ where an accidental decomposition of diazomethane yielded a white powder. Peckmann's colleagues, Eugen Bamberger and Friedrich Tschirner, analyzed this powder, they recognized that it was made up of hydrogen and carbon atoms with long chains of methylenes, $-CH_2-$, and they termed it polymethylene.

In 1929, Friedrich and Marvel made low molecular weight polyethylene by heating ethylene with BuLi while they were examining reactions between alkali metal alkyls and quaternary arsonium salts.³¹⁵

In 1933, two researchers at Imperial Chemical Industries (ICI) in England, "Eric Fawcett" and "Reginald Gibson", were investigating ethylene and benzaldehyde mixture at very high temperatures, observed a sudden loss of pressure in the vessel. Being afraid of a leak, upon opening the reactor they noticed a white waxy solid and realized that they just made polyethylene.³¹⁶ This was the first polymerization of ethylene by a free radical mechanism initiated by trace oxygen contamination in the system. Fawcett and Gibson, not knowing it was the oxygen contamination that caused the polymerization, were unable to repeat their work in a controlled way. The work continued in ICI and finally in 1935 Michael Perrin was able to develop this accident into a reproducible high-pressure synthesis for polyethylene that became the basis for industrial LDPE production beginning in 1939 by ICI in England.

The freshly produced PE was of great interest as an insulation material to the defense industries during World War II. The primary industrial application was for the development of air born radar and as an insulator for the underwater cables. Polyethylene enabled such a decrease in the weight of the radar equipment so that it could be placed in the aircraft. This was particularly valuable for locating enemy aircraft in adverse weather conditions and was one of the big secrets of World War II. DuPont in the USA was collaborating with ICI from early days and was receiving samples regularly, this collaboration enabled DuPont to develop a tubular process for the manufacture of

LDPE. Although the tubular process had significant problems, it eventually became one of the two key processes for the manufacture of LDPE.³¹⁷

The production of LDPE initially started in the USA in 1943 funded by the USA government for the war effort. Just after, Union Carbide started production of LDPE by a tubular process. By end of 1947 both DuPont and Union Carbide were commercially supplying LDPE and the annual sales reached 10 million lbs (4536 tons). Then, in the early 1950's, Dow Chemical Company joined the ranks of new producers of LDPE and licensed the ICI autoclave process.³¹⁷

A.8.2. Structure of Polyethylene

Depending on the definition of a polymer, a polyethylene is a macromolecule formed by the covalent bonding between ethylene molecules in which ethylene is the repeated unit (**Figure 21**).

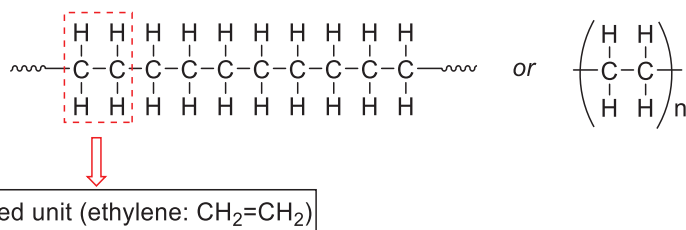


Figure 21. The general structural formula of polyethylene.

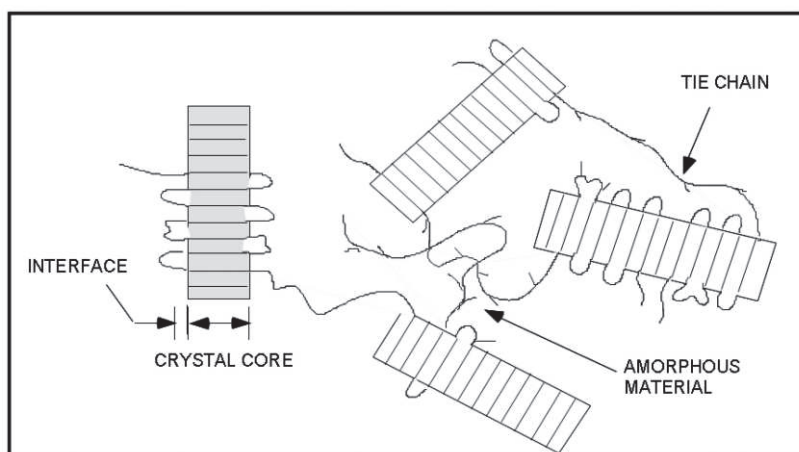


Figure 22. Graphical description of the tie chains. "Adapted with permission from (Demirors, M. In *100+ Years of Plastics. Leo Baekeland and Beyond*; ACS Symposium Series; American Chemical Society, 2011; Vol. 1080, pp 115-145.). Copyright (2011) American Chemical Society."

The sensitive morphological structure that determines most of the properties of polyethylene is the semi-crystalline structure of this polymer. The molecular connection

between the amorphous part and crystalline part and the interconnected nature of crystalline network defines most of the physical properties of PE (**Figure 22**).

A tie chain is defined as a molecule that has parts of it embedded in the core of two or more crystals.^{318,319} The development of this concept has been very helpful in understanding the system (**Figure 22**).^{320,321}

This connectivity confirms that any stress applied gets distributed in the system between the amorphous phase and the crystalline phase. This concept also explains well the effect of changing the fundamental molecular features (molecular weight, density and co-monomer content) on the properties. For example, generally, high molecular weight molecules of a given co-monomer content are more capable of forming tie chains as their length is long enough to participate in two or more crystals. If molecules are not long enough then they cannot function as tie chains. The optimum physical strength is obtained when the tie chain concentration is at its maximum. This requires that the crystal size is in a certain range where a balance between crystal strength and tie chain concentration is achieved. This optimum is achieved around a density of 0.905-0.915 g/cm³. The tie chain concentration also depends on the co-monomer type used, where the longer the short chain branch, the more tie chains occur.³²²

A.8.3. Properties of Polyethylene

Polyethylene consists of nonpolar and saturated hydrocarbons. The individual macromolecules are not covalently linked. Because of their symmetric molecular structure, they tend to crystallize; overall polyethylene is partially crystalline. Higher crystallinity increases density and mechanical and chemical stability.

Polyethylene usually can be dissolved at elevated temperatures in aromatic hydrocarbons such as toluene or xylene, or in chlorinated solvents such as trichloroethane or trichlorobenzene. PE absorbs almost no water. The gas and water vapor permeability (only polar gases) is lower than most plastics; oxygen and carbon dioxide on the other hand can pass it easily.

PE can become brittle when exposed to sunlight, carbon black is usually used as a UV stabilizer. It burns slowly with a blue flame having a yellow tip and gives off an odor of paraffin (similar to candle flame). The material continues burning on removal of the

flame source and produces a drip.

Density: Density plays a serious role in defining solid state properties of PE to the level that PE resins are generally classified depending on their density. **Table 4** summarizes the main classification of polyethylenes based on density. There is also ultra-high molecular weight PE (UHMWPE), it has extremely long chains with molar masses usually between 3.5 and 7.5 million g/mol. It expresses all the characteristics of HDPE with the added traits of being resistant to concentrated acids and alkalis, as well as numerous organic solvents.

Table 4. Classification of Polyethylene Families by Density.

<i>PE Family</i>	<i>Lower Density Limit (g/cm³)</i>	<i>Higher Density Limit (g/cm³)</i>
High Density Polyethylene (HDPE)	0.941	0.975
Medium Density Polyethylene (MDPE)	0.928	0.941
Low Density Polyethylene (LDPE) and Linear Low Density Polyethylene (LLDPE)	0.915	0.928
Very Low Density Polyethylene (VLDPE)	0.900	0.915

Polyethylene is a semi crystalline composite material with amorphous and crystalline region. The totally amorphous region has a density of around 0.865 g/cm³ while the pure crystal structure has a density of 1.00 g/cm³. In any case a 100% crystallinity is not reached as some amorphous material exists in between crystals.

The major crystalline form of polyethylene is orthorhombic even though both hexagonal and monoclinic forms exist.³²³ The detailed studies showed that branches larger than a methyl groups are excluded from the crystal structure.^{324,325}

Tensile properties: Tensile properties of polyethylene are the most important properties for a large number of applications. They provide a guide to how the material will respond to an external deformation in terms of resistance to deformation, load bearing characteristics as well as ability to accommodate deformation.^{326,327} Tensile properties are determined by subjecting a dog bone type test specimen to extension and

recording the response of the material as a stress strain curve.

Dart and Tear Properties: Dart and tear are two resistance properties of PE. Those properties are mainly important for film applications such as food packaging. Dart impact strength represents the high speed impact environment such as dropping a package from a certain height and is an indication of the capacity of the resin to survive such an impact and continue to protect the contents of packaging. Dart impact generally depends on density and the molar mass of the polymer. There is a high degree of correlation between tie chains and dart impact of the polymer, where the presence of long chain branching is usually harmful to dart impact strength.

Tear resistance is a measure of the energy needed to generate certain length of tear in a thin film normalized to a 25 micron thickness. It is an important property for films. Tear resistance like other properties greatly depends on the molecular structure of the polymer.³²⁸

Thermal Properties: The melting point of polyethylene depends on the type of polyethylene. **Table 5** shows the most two important thermal properties of the most two applicable types of polyethylene.

Table 5. Thermal Properties of Polyethylene.

<i>Thermal Property</i>	<i>LDPE</i>	<i>HDPE</i>
Approximate Melting Temperature (°C)	110	135
Maximum Operating Temperature (°C)	71	82

Electrical Properties: Polyethylene is a good electrical insulator. It offers good tracking resistance; however, it becomes easily electrostatically charged (which can be reduced by additions of graphite).

Optical Properties: PE can vary between almost clear (transparent), milky-opaque (translucent) or opaque. Thereby, LDPE owns the greatest, LLDPE slightly less and HDPE the least transparency.

A.8.4. Types of Polyethylene and their Synthetic Processes

Polyethylene is commonly categorized into one of several major compounds of which

the most common include LDPE, LLDPE, and HDPE (some classifications include also MDPE and UHMWPE). Other variants include ultra-low molecular weight polyethylene (ULMWPE or PE-WAX), high-molecular weight polyethylene (HMWPE), high density cross-linked polyethylene (HDXLPE), cross-linked polyethylene (PEX or XLPE), Very low density polyethylene (VLDPE), and Chlorinated polyethylene (CPE). **Figure 23** represents the structures of the main types of PE.

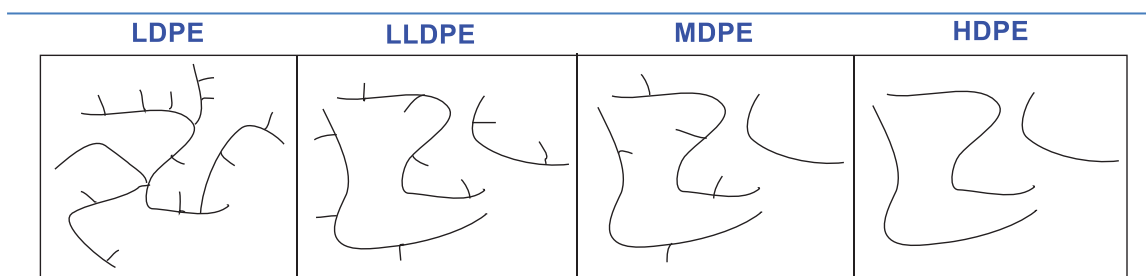


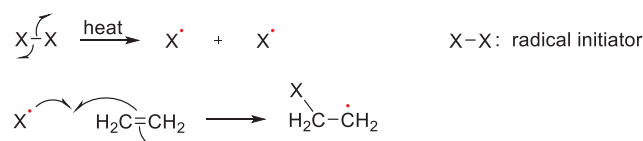
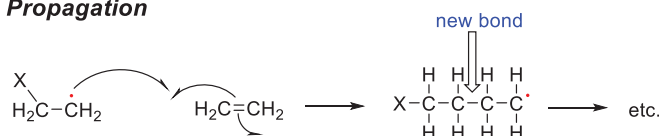
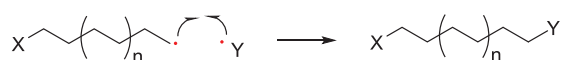
Figure 23. Schematic representation of the structures of the different types of PE.

A.8.4.1. LDPE: via Radical Polymerization Processes

LDPE was the first polyethylene commercially used. It is the only one made using **free radical chemistry** under high temperatures and pressures. There are four industrial methods of radical polymerization:

- *Bulk polymerization*: reaction mixture contains only initiator and monomer, no solvent.
- *Solution polymerization*: reaction mixture contains solvent, initiator, and monomer.
- *Suspension polymerization*: reaction mixture contains an aqueous phase, water-insoluble monomer, and initiator soluble in the monomer droplets (both the monomer and the initiator are hydrophobic).
- *Emulsion polymerization*: similar to suspension polymerization except that the initiator is soluble in the aqueous phase rather than in the monomer droplets (the monomer is hydrophobic, and the initiator is hydrophilic). An emulsifying agent is also needed.

Scheme 18 represents the mechanism of the free radical polymerization process of ethylene which is formed of three main steps.

Scheme 18. Mechanism of the free radical polymerization of ethylene.
Initiation**Propagation****Termination**

Y: a radical source such as a propagating chain

1) Initiation: it is the first step of the radical polymerization process; during this step an active center is created from which a polymer chain (polyethylene chain) is generated, this active center (radicalized center) is produced usually by thermal decomposition or photo-decomposition of the initiator. **2) Propagation:** after the radical initiator is formed, it attacks a monomer. In an ethylene monomer, one electron pair is held securely between the two carbons in a *sigma* bond and the other is more loosely held in a *pi* bond. The free radical uses one electron from the pi bond to form a more stable bond with the carbon atom. The other electron returns to the second carbon atom, turning the whole molecule into another radical. This begins the polymer chain, a polymer spends most of its time in increasing its chain length (propagating) during polymerization. **3) Termination:** chain termination will occur unless the reaction is completely free of contaminants, however, due to the high reactivity of radicals, termination can occur by several different mechanisms:

- Combination of two active chain ends: one or both of the following processes may occur. a) *Combination*: two chain ends simply couple together to form one long chain; b) *disproportionation*: a hydrogen atom from one chain end is abstracted to another, producing a polymer with a terminal unsaturated group and a polymer with a terminal saturated group.
- Combination of an active chain end with an initiator radical.
- Interaction with impurities or inhibitors. For example, Oxygen is the common

inhibitor. The growing chain will react with molecular oxygen, producing an oxygen radical, which is much less reactive, thus the rate of propagation slows down.

A different mode of termination reactions is the **Chain Transfer**. There are several types of chain transfer mechanisms:

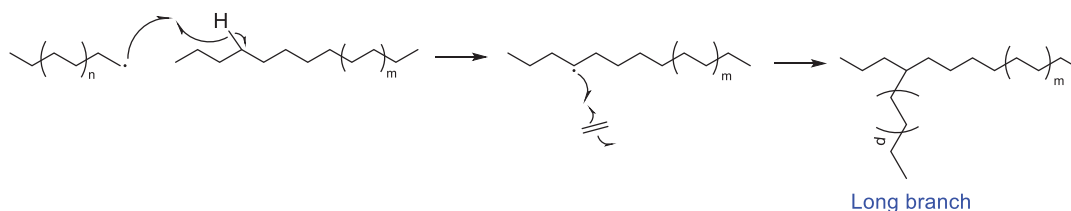
- *Transfer to solvent:* a hydrogen atom is abstracted from a solvent molecule, resulting in the formation of radical on the solvent molecules. The effectiveness of chain transfer involving solvent molecules depends on the amount of solvent present (more solvent leads to greater probability of transfer), the strength of the bond involved in the abstraction step (weaker bond leads to greater probability of transfer), and the stability of the solvent radical that is formed (greater stability leads to greater probability of transfer). Halogens, except fluorine, are easily transferred.
- *Transfer to monomer:* a hydrogen atom is abstracted from a monomer. While this does create a radical on the affected monomer, resonance stabilization of this radical discourages further propagation. This doesn't occur in ethylene polymerization.
- *Transfer to initiator:* a polymer chain reacts with an initiator, which terminates that polymer chain, but creates a new radical initiator. This initiator can then begin new polymer chains. Therefore, contrary to the other forms of chain transfer, chain transfer to the initiator does allow for further propagation. Peroxide initiators are especially sensitive to chain transfer.
- *Transfer to polymer:* the radical of a polymer chain abstracts a hydrogen atom from somewhere on another polymer chain. This terminates the growth of one polymer chain, but allows the other to branch and resume growing.

Note that the most obvious effect of chain transfer is a decrease in the polymer chain length.

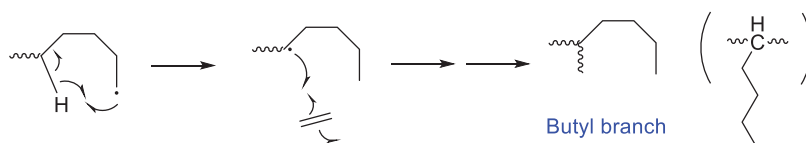
The structure of LDPE contains long chain branching which makes it highly required in the production of thin films either by itself or blends with other types of polyethylenes. Its long chain branching (LCB) is a result of the high pressure process where

intermolecular hydrogen abstraction by a growing chain end from another polyethylene is the source of this highly desirable properties (**Scheme 19**).

Scheme 19. Mechanism of SCB and LCB formation in LDPE process.



Intermolecular Hydrogen Abstraction: LCB Formation



Intramolecular Hydrogen Abstraction (back biting mechanism): SCB Formation

The density of LDPE is also adjusted by means of a back biting mechanism, the growing polymer radical intramolecularly abstracts a hydrogen atom usually 3 to 6 carbon atoms from the radical center forming short chain branching (SCB) (**Scheme 19**). The process of back biting can be controlled by reaction conditions such as pressure and temperature providing the ability to target the required densities through changes to the process conditions. This provides a relatively limited density variation leading to a small density range for LDPE from about 0.915 g/cm³ to 0.928 g/cm³.³²⁹

LDPE has the highest level of branching between PE families, this branching has a significant impact on the rheology of LDPE, mainly the LCB. For example, the presence of LCB increases the shear thinning of the polymer, which means that at high shear rates the polymer has lower viscosity than expected while at low shear rates the polymer has higher viscosity than expected.

A.8.4.2. MDPE

Only some classifications consider MDPE from the main types of PE so we mentioned it just briefly. It is a type of polyethylene defined by a density range of 0.928-0.941 g/cm³. It is less dense than HDPE, which is more common.

MDPE can be produced by chromium/silica catalysts, Ziegler-Natta catalysts or metallocene catalysts (same catalysts that produce HDPE and LLPE). MDPE has good

shock and drop resistance properties. It is typically used in gas pipes and fittings, sacks, shrink film, packaging film, and carrier bags.

A.8.4.3. **HDPE and LLDPE: via Catalytic Polymerization Processes**

Unlike LDPE which uses free radical chemistry, high density polyethylene and linear low density polyethylene are produced through catalysis utilizing coordination chemistry. Three basic chemistries are used for the production of HDPE and LLDPE: Chromium catalysts (Phillips catalyst), Ziegler-Natta catalysts, and metallocene catalysts. Since these types of catalytic polymerizations are very well known and reviewed in the literature, and since our work doesn't depend on any of these catalysis, we will mention just a brief history of each and reference some of the recent reviews corresponding to each type. Then section will be concerned with post-metallocene catalysts (the introduction of chapter IV will concentrate on the iron complexes corresponding to this type of catalysts).

Chromium Catalysts: By early 1950's LDPE has become available with a number of manufacturers in US and Europe. The new plastic was starting to make inroads into new applications, especially films. The major issue remained the fact that the LDPE process required such high pressures and temperatures to operate. Thus the race was on the development of an alternative way to polymerize ethylene at lower pressures and temperatures. This would make production of polyethylene much less challenging from an engineering perspective.

The first major discovery in low pressure polymerization came in 1951. Two chemists working in Phillips Petroleum, Robert Banks and J. P. Hagen, discovered a catalyst based on chromium trioxide (consisting essentially of Cr/silica and Cr/silica-alumina) that could polymerize ethylene at 80 to 110 °C and at pressures less than 1000 psi (69 bar).³³⁰ Polymers with densities of 0.95–0.97 g/cm³ were obtained, indicating linear PE. Phillips Company immediately developed a commercial process, which was licensed in less than 4 years after the discovery. Nowadays, the Phillips supported chromium catalyst is used to produce some 40-50% of the world's HDPE.³³¹

A series of reviews have been reported on Phillips catalyst by McDaniel et al.³³¹⁻³³³

Ziegler-Natta Catalysts: Two years after Phillips catalyst discovery, Karl Ziegler, a

German chemist, discovered that a combination of TiCl_4 and $\text{Al}(\text{C}_2\text{H}_5)_3$ gave comparable activities to that of Phillips catalyst in the production of polyethylene. A polymer density of about 0.94 g/mL was reported.³³¹ Then, Giulio Natta, an Italian chemist, used crystalline $\alpha\text{-TiCl}_3$ in combination with $\text{Al}(\text{C}_2\text{H}_5)_2\text{Cl}$ to produce the first isotactic polypropylene.

In the 1970s, magnesium chloride was discovered to greatly enhance the activity of the titanium-based catalysts. These MgCl_2 -supported TiCl_4 catalysts generated high performance high-density polyethylene, linear low-density polyethylene, and highly isotactic polypropylene.³³⁴

Two broad classes of Ziegler–Natta catalysts are employed, distinguished by their solubility: Heterogeneous supported catalysts based on titanium compounds are used in polymerization reactions in combination with co-catalysts, organoaluminum compounds such as triethylaluminium. This class of catalyst dominates in the industry. And homogeneous catalysts usually based on complexes of Ti or Zr mainly, they are usually used in combination with a different organoaluminum co-catalyst, methylaluminoxane (MAO) such as group IV metallocenes described in the next paragraph.

A lot of reviews reported the development of Ziegler-Natta catalytic polymerization.³³⁵⁻³³⁷

Metallocene Catalysts: According to the IUPAC definition, a metallocene contains a transition metal and two cyclopentadienyl ligands coordinated in a sandwich structure, i.e., the two cyclopentadienyl anions are on parallel planes with equal bond lengths and strengths.

The first metallocene to be classified was ferrocene, and was discovered simultaneously in 1951 by Kealy and Pauson,³³⁸ and Miller and coworkers.³³⁹ The structure of " $\text{C}_{10}\text{H}_{10}\text{Fe}$ " was determined by Wilkinson and coworkers and by Fischer and coworkers.³⁴⁰

Closely related to the metallocenes are the metallocene derivatives, such as titanocene dichloride, vanadocene dichloride. Certain metallocenes and their derivatives exhibit catalytic properties, where these well-defined complexes with alkylaluminum activators (e.g., $\text{Cp}_2\text{TiCl}_2/\text{AlR}_n\text{Cl}_{3-n}$) found use as homogeneous olefin polymerization

catalysts.^{341,342} However, group IV metallocenes activated with alkylaluminum were not considered as practical catalysts due to their low activities. The discovery of the combination of group IV metallocenes and MAO by Sinn and Kaminsky in 1980 made the application of group IV metallocenes as polymerization catalysts industrially practical.^{343,344}

Post-Metallocene Catalysts: Ever since, the great potential of well-defined transition metal complexes for olefin polymerization demonstrated by the group IV metallocene catalysts has driven many researchers to investigate highly active post-metallocene catalysts.³⁴⁵ The first post-metallocene catalysts, which are truly comparable to the metallocene catalysts in terms of catalytic activities and polymer molar masses, are probably the nickel complexes with diimine ligands discovered by Brookhart and coworkers in 1995.³⁴⁶ Their discovery accelerated the research on post-metallocene catalysts.

In 1998, Brookhart and Gibson reported that iron or cobalt complexes with diimine-pyridine ligands exhibited very high ethylene polymerization activities.^{347,348} Then, nickel complexes with phenoxy-imine ligands (Grubbs and coworkers), and group IV transition metal complexes having phenoxy-imine ligands (Fujita and coworkers), were reported as high performance olefin polymerization catalysts.³⁴⁹

As aforementioned, the synthesis and activities of Fe post-metallocene catalysts will be discussed thoroughly in the introduction of chapter IV.

A.8.5. Uses of Polyethylenes

Table 6 illustrates the applications of the three main types of polyethylene.

Table 6. Industrial applications of the main types of polyethylene.

Method/ Process	LDPE	HDPE	LLDPE
Film making	For milk carton lining, production of cling films...	Manufacture of shopping plastic bags and food packaging plastics	Manufacture of stretchable films

Injection molding process	Manufacture of bowls and buckets	Manufacture of crates and dustbins	Production of food boxes of different capacities
Blow molding process	Production of squeezable bottles such as ketchup containers...	Production of drums and detergent bottles	-
Process of extrusion	Manufacture of flexible water pipes and cables jacketing	Manufacture of water pipes of varying capacities	Coating cables

A.9. Kinetic and Thermodynamic Considerations in the Copolymerization of Ethylene and CO₂

Incorporating CO₂ into useful polymers not only takes advantage of a renewable, relatively cheap, and extremely abundant C1 building block, it helps to remove a greenhouse gas from the atmosphere. Since Inoue's discovery of catalysts for the copolymerization of CO₂ and epoxides in 1969,¹²¹ extensive research effort has been directed toward developing other catalysts that are capable of incorporating CO₂ into polymer chains. There have been multiple reports of copolymerizing CO₂ with high-energy comonomers such as epoxides and aziridines to form polycarbonates and polyurethanes, respectively.³⁵⁰ However, no success of direct copolymerization of CO₂ with ethylene or dienes has been reported. This copolymerization reaction is particularly attractive since it represents a link between different renewable resources, such as CO₂, and cheap, broadly available alkenes such as ethylene, thus allowing a potential development towards more sustainable materials.

The main obstacles that prevent a successful copolymerization of these monomers include: **a)** a high energy barrier associated with the alternating copolymerization between ethylene (or any alkene) and CO₂, which requires excess ethylene insertion to ensure endergonic CO₂ insertion, and **b)** a kinetic barrier that arises from the high activation energy for CO₂ insertion into the growing polymeric chain relative to

polyethylene chain growth.¹¹⁸⁻¹²⁰ To the best of our knowledge, only two reports discussed the kinetic and thermodynamic considerations of ethylene/CO₂ copolymerizations.

The first report was done by Miller and co-workers in 2006,¹¹⁸ they calculated the thermodynamic parameters for the incorporation of carbon dioxide into a polyethylene chain using average bond dissociation energies, the Benson additivity method, and DFT calculations. These calculations show that the formation of the perfectly alternating ethylene/CO₂ copolymer is thermodynamically impossible at reasonable polymerization temperatures. However, the favorable thermodynamics for ethylene can offset the unfavorable thermodynamics of CO₂ and polymers with ethylene/CO₂ quotients greater than 2.37 (less than 29.7 mol % CO₂) should be feasible at room temperature (from DFT analysis).

Table 7. Average bond dissociation energies (BDE) used to calculate ethylene/carbon dioxide copolymerization thermodynamics. "Adapted with permission from (Price, C. J.; Reich, B. J. E.; Miller, S. A. *Macromolecules* 2006, 39, 2751-2756.). Copyright (2006) American Chemical Society."

reaction	BDE ^a
$\text{CH}_2=\text{CH}_2 \rightarrow \cdot\text{CH}_2\text{CH}_2\cdot$	$148 - 81 = 67$
$\cdot\text{CH}_2\text{CH}_2\cdot \rightarrow \text{polyethylene}$	- 81
$\text{CH}_2=\text{CH}_2 \rightarrow \text{polyethylene}$	$67 - 81 = -14$
$\text{CH}_2=\text{CH}_2 \rightarrow 2 \cdot\text{CH}_2$	148
$\text{CO}_2 \rightarrow \cdot\text{C}(=\text{O})\text{O}\cdot$	$172 - 84 = 88$
$2 \cdot\text{CH}_2 + \cdot\text{C}(=\text{O})\text{O}\cdot \rightarrow \cdot\text{CH}_2\text{C}(=\text{O})\text{O}\cdot$	$-81 + -84 = -165$
$\cdot\text{CH}_2\text{C}(=\text{O})\text{O}\cdot \rightarrow \text{poly(ethylene carbonate)}$	-81
$\text{CH}_2=\text{CH}_2 + \text{CO}_2 \rightarrow \text{poly(ethylene carbonate)}$	$148 + 88 - 165 - 81 = -10$
$C \text{ CO}_2 + E \text{ CH}_2=\text{CH}_2 \rightarrow \text{copolymer}$	
$\Delta H_{\text{poly}} = [C(-10) + (E - 1)(-14)]/(C + E)$ (eq 1)	
$\Delta G_{\text{poly}} = [C(-10 \text{ kcal/mol}) + (E - 1)(-14 \text{ kcal/mol})]/(C + E) - [T(-0.030 \text{ kcal/molK})]$ (eq 2)	

^a Energies are in kcal/mol.

Table 7 shows the average bond dissociation energies used to calculate ethylene/CO₂ copolymerization thermodynamics (for the simplified polymer microstructure that avoids adjacent carbon dioxide monomers, a thermodynamically unfavorable arrangement).^{351,352} This approach yields eq 1, which gives the polymerization enthalpy per monomer as a function of the ethylene/CO₂ (*E/C*) quotient. The value of ΔG_{poly} (per monomer) can be determined by substituting eq 1 into $\Delta G = \Delta H - T\Delta S$ and assuming that $\Delta S = -0.030$ kcal/(mol K) per monomer incorporated (eq 2).³⁵³ This method predicts an exergonic copolymerization for *E/C* \approx 2.56 or greater, suggesting that the perfectly alternating copolymer is thermodynamically inaccessible at reasonable polymerization temperatures. However, it is clear that average bond dissociation energies poorly estimate the enthalpy of ethylene homopolymerization. This estimation suggests -14 kcal/mol, but the measured value is -22.348 kcal/mol.³⁵⁴

Table 8. Supergroups based on Benson groups simplifying the thermodynamic treatment of polymerization systems such as the copolymerization of ethylene and carbon dioxide.^a "Adapted with permission from (Price, C. J.; Reich, B. J. E.; Miller, S. A. *Macromolecules* 2006, 39, 2751-2756.). Copyright (2006) American Chemical Society."

supergroup	component groups	group additivity ΔH	supergroup additivity ΔH	supergroup ΔH_{poly}	group additivity <i>S</i>	supergroup additivity ^b <i>S</i>	supergroup ΔS_{poly}
	C-(C) ₂ (H) ₂ C-(C) ₂ (H) ₂	-5.0 -5.0	-10.0	-10.0 - (12.5) = -22.5	9.42 9.42	18.84	18.84 - (52.42) = -33.6
	C-(H) ₂ (C)(CO) CO-(C)(O) O-(C)(CO) C-(H) ₂ (O)(C)	-5.2 -35.2 -43.1 -8.1	-91.6	-91.6 - (12.5 - 94.0) = -10.1	9.6 14.78 8.39 10.3	43.07	43.07 - (52.43 + 51.10) = -60.5

$$C \text{ CO}_2 + E \rightleftharpoons \left[\text{C} \text{---} \text{C(=O)O} \right]_C \left[\text{CH}_2\text{CH}_2 \right]_{E-1}$$

$$\Delta H_{\text{poly}} = [C(-10.1 \text{ kcal/mol}) + (E-1)(-22.5 \text{ kcal/mol})]/(C + E) \quad (\text{eq 3})$$

$$\Delta G_{\text{poly}} = [C(-10.1 \text{ kcal/mol}) + (E-1)(-22.5 \text{ kcal/mol})]/(C + E) - T[C(-0.0605 \text{ kcal/molK}) + (E-1)(-0.0336 \text{ kcal/molK})]/(C + E) \quad (\text{eq 4})$$

^a Units given for enthalpy are kcal/mol; units given for entropy are cal/(mol K). The following experimental data are in kcal/mol: $\Delta H_f^\circ(\text{ethylene}) = 12.5$ kcal/mol; $\Delta H_f^\circ(\text{CO}_2) = -94.0$ kcal/mol; $S^\circ(\text{ethylene}) = 52.42$ cal/(mol K); $S^\circ(\text{CO}_2) = 51.10$ cal/(mol K). ^b The entropic correction to *S* (given by $-R \ln \sigma$) is 0 since the symmetry number (σ) is 1 for these supergroups.

As they mentioned, a generally more reliable thermodynamic method employs Benson's group additivity rules.³⁵⁵ In the thermodynamic analysis of polymers, the Benson method can be modified to account for "supergroups" instead of simple groups. Miller et al. stated that in the present case, one supergroup is taken as C-CH₂CH₂-C and a second is taken as C-CH₂C(O)OCH₂-C (**Table 8**). These groupings simplify the resultant enthalpic formula for copolymerization and predict the net enthalpy (in kcal/mol) per

monomer incorporated as shown in eq 3. Note that this method does not address the possibility of adjacent CO₂ monomers. This exclusion is done because of the considerable endothermicity known for this kind of enchainment.^{351,352} The formation of hypothetical poly(carbon dioxide) from carbon dioxide is calculated to be endothermic by 18.6 kcal/mol ($\text{CO}-(\text{O})_2 + \text{O}-(\text{CO})_2 - \Delta H^\circ_f(\text{CO}_2) = (-29.2) + (-46.2) - (-94.0)$).

The value of ΔG_{poly} (per monomer) can be estimated by substituting eq 3 into $\Delta G = \Delta H - T\Delta S$ and calculating ΔS_{poly} from entropic Benson group additivity values.³⁵⁶ The result is eq 4, and it is apparent that formation of the perfectly alternating copolymer is thermodynamically forbidden at room temperature, but its formation at -106 °C (the ceiling temperature) and below is exergonic. Of course, most polymerization kinetics at this temperature are infinitely slow. However, copolymers with greater *E/C* quotients are thermodynamically possible at room temperature. The Benson additivity method predicts that the copolymerization is exergonic for *E/C* \approx 1.64 and greater at room temperature. Simply stated, the exergonic polymerization of ethylene compensates for the endergonic incorporation of carbon dioxide. The previous two paragraphs are reproduced with permission from reference 118 (Adapted with permission from (Price, C. J.; Reich, B. J. E.; Miller, S. A. *Macromolecules* **2006**, 39, 2751-2756.). Copyright (2006) American Chemical Society.)

The second report was done by Muller et al. in 2016,³⁵⁷ where they depend on DFT analysis to study the copolymerization of CO₂ and ethylene. They did their study using a palladium(II) catalyst with the chelating 2-[bis(2-methoxyphenyl)-phosphine]-benzenesulfonato ligand (1) [Pd(Et)(1)] (**Figure 24**), which is highly effective in the copolymerization of CO and ethylene to polyketones.³⁵⁸ A majority of the following part is reproduced with permission from reference 357 (Verena Moha, Daniela Cozzula, Markus Hçlscher, Walter Leitner, and Thomas E. Müller: A DFT Study on the Co-Polymerization of CO₂ and Ethylene: Feasibility Analysis for the Direct Synthesis of Polyethylene Esters. *CHEMSUSCHEM*. 2016, 9, 1614–1622. Copyright Wiley-VCH Verlag GmbH & Co. KGaA. Reproduced with permission.).

They have calculated the catalytic cycle for the ethylene homopolymerization with [Pd(Et)(1)] as the catalytically active species.³⁵⁷ The generally accepted Cossee-Arlman mechanism³⁵⁹ for olefin polymerization was readily reproduced. For comparison with the co-polymerization profiles, they showed the energy profile for the ethylene

homopolymerization (**Figure 24**). The *trans* insertion, whereby ethylene molecule is inserted *trans* to the O atom of the bidentate ligand, is energetically favored (intermediate IIa). The energy span (the largest energy difference in the profile representing the effective activation barrier) is found for the insertion of the first (IIa-IIIa) and the second C₂H₄ molecules (Va-IVa). The respective values of 17.8 and 19.2 kcal/mol correspond to an active catalyst that, in agreement with experiment,³⁶⁰ is very active.

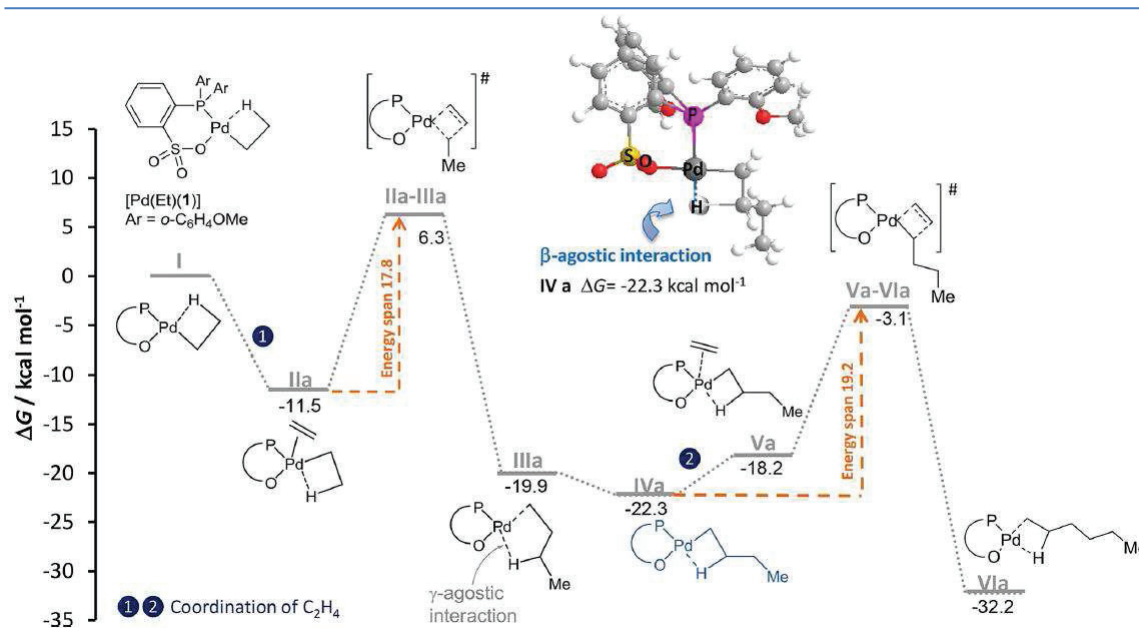


Figure 24. Gibbs free energy profile (gas phase) of the C₂H₄ homopolymerization with catalyst [Pd(Et)(1)]. Verena Moha, Daniela Cozzula, Markus Hçlscher, Walter Leitner, and Thomas E. Müller: A DFT Study on the Co-Polymerization of CO₂ and Ethylene: Feasibility Analysis for the Direct Synthesis of Polyethylene Esters. CHEMSUSCHEM. 2016, 9, 1614–1622. Copyright Wiley-VCH Verlag GmbH & Co. KGaA. Reproduced with permission.

Then, they studied the copolymerization of carbon monoxide with ethylene using [Pd(Et)(1)] (**Figure 25**). During the initiation step, CO coordinates in an exergonic reaction at the catalytically active species I to yield intermediate IIb ($\Delta G = -23.0$ kcal/mol). Subsequently, CO inserts into the Pd-C bond of IIb *via* transition state IIb-IIIb (-13.5 kcal/mol). The coordination of ethylene to the Pd center of IIIb results in IVb (-22.5 kcal/mol), followed by isomerization to intermediate Vb with a lower energy (-26.6 kcal/mol). Then, the ethylene molecule inserts *via* precursor state VIb and transition state VIb-VIIb (-5.8 kcal/mol) into the Pd-C bond. Coordination of the next CO molecule (IXb) followed by the transition state IXb-Xb (-23.2 kcal/mol) leads to insertion of the next CO molecule.³⁵⁷

The energy difference between *cis* and *trans* insertion of CO was calculated to be $\Delta G = 11.4$ kcal/mol in favor of the *trans* insertion (IIb-IIIb). Similarly, the energy difference between *cis* and *trans* insertion of ethylene was calculated to be $\Delta G = 11.8$ kcal/mol in favor of the *trans* insertion (IVb). The *cis* insertions are characterized by larger distances between the Pd center and the co-monomers CO and ethylene compared to the corresponding *trans* insertion.

The energy span between intermediate Vb and transition state Vlb-VIIb was calculated to be $\Delta G = 20.8$ kcal/mol. The relatively low energy span suggests that [Pd(Et)(1)] is a good catalyst for the copolymerization reaction. The anticipated high reaction rates are in full agreement with the experiment.³⁶¹ Due to the disparate barrier for insertion of CO and ethylene, a non-alternating polyketone with short polyethylene segments will be obtained when the two substrates CO and C₂H₄ are available in similar concentrations.

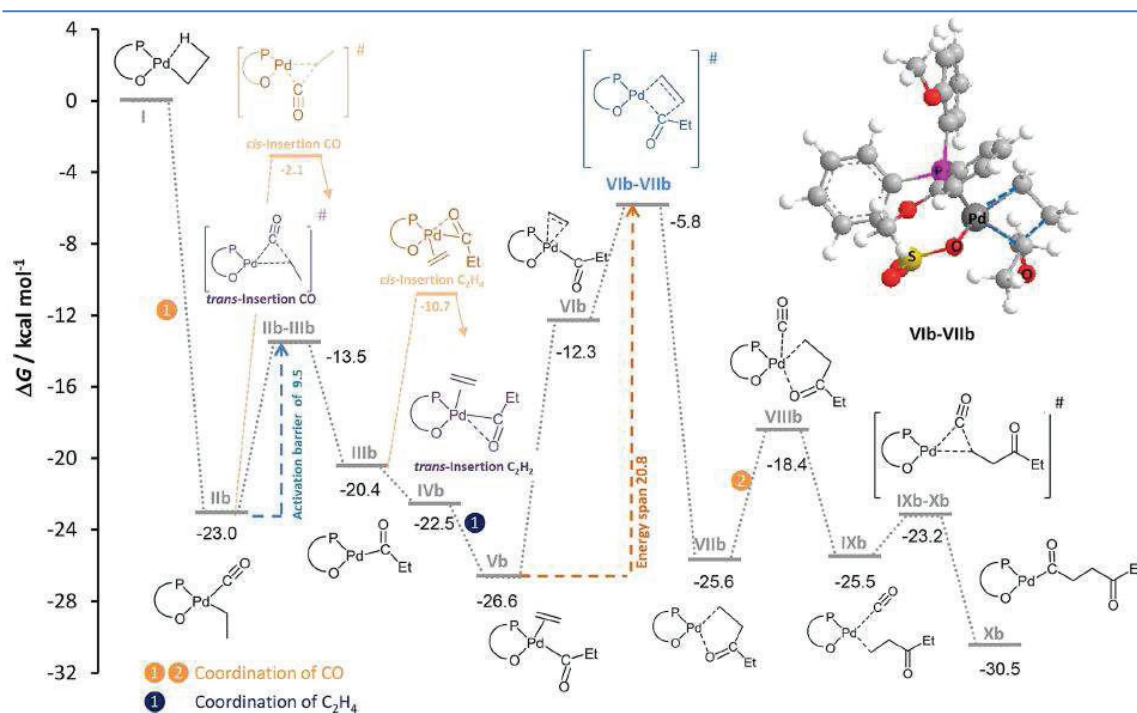


Figure 25. Gibbs free energy profile (gas phase) of the CO/C₂H₄ copolymerization with catalyst [Pd(Et)(1)]. Verena Moha, Daniela Cozzula, Markus Hçlscher, Walter Leitner, and Thomas E. Müller: A DFT Study on the Co-Polymerization of CO₂ and Ethylene: Feasibility Analysis for the Direct Synthesis of Polyethylene Esters. CHEMSUSCHEM. 2016, 9, 1614–1622. Copyright Wiley-VCH Verlag GmbH & Co. KGaA. Reproduced with permission.

On the basis of the calculated C₂H₄ homopolymerization and CO/ethylene copolymerization sequences, Muller et al. devised the catalytic cycle for the CO₂/ethylene copolymerization (**Figure 26**). End-on coordination of CO₂ to the Pd center

of [Pd(Et)(1)] provides intermediate II (-7.6 kcal/mol). Isomers of II with side-on coordinated CO₂ could not be localized. CO₂ then inserts into the Pd-alkyl bond *via* transition state II-III (31.4 kcal/mol). The activation barrier for this reaction ($\Delta G = 39.0$ kcal/mol) is much higher than the barrier for the corresponding CO insertion ($\Delta G = 9.5$ kcal/mol, **Figure 25**), indicating that this transition state is a key step, which needs to be lowered by catalyst design. Complex III rearranges *via* intermediate IV to intermediate V. Ethylene coordination yields VI, which relaxes to the complexes VII and VIII. Intermediates VIII and V are equally stable, indicating that coordination of ethylene and monodentate carboxylate (VIII) is energetically equivalent to the bidentate coordination mode of the carboxylate (V). Then, the subsequent insertion of ethylene proceeds readily *via* transition state VIII-IX. The activation energy is much lower ($\Delta G = 19.2$ kcal/mol) than the barrier for CO₂ insertion ($\Delta G = 39.0$ kcal/mol). Transition state VIII-IX leads to complex IX, which rearranges to the more stable intermediate X (0.5 kcal/mol).³⁵⁷

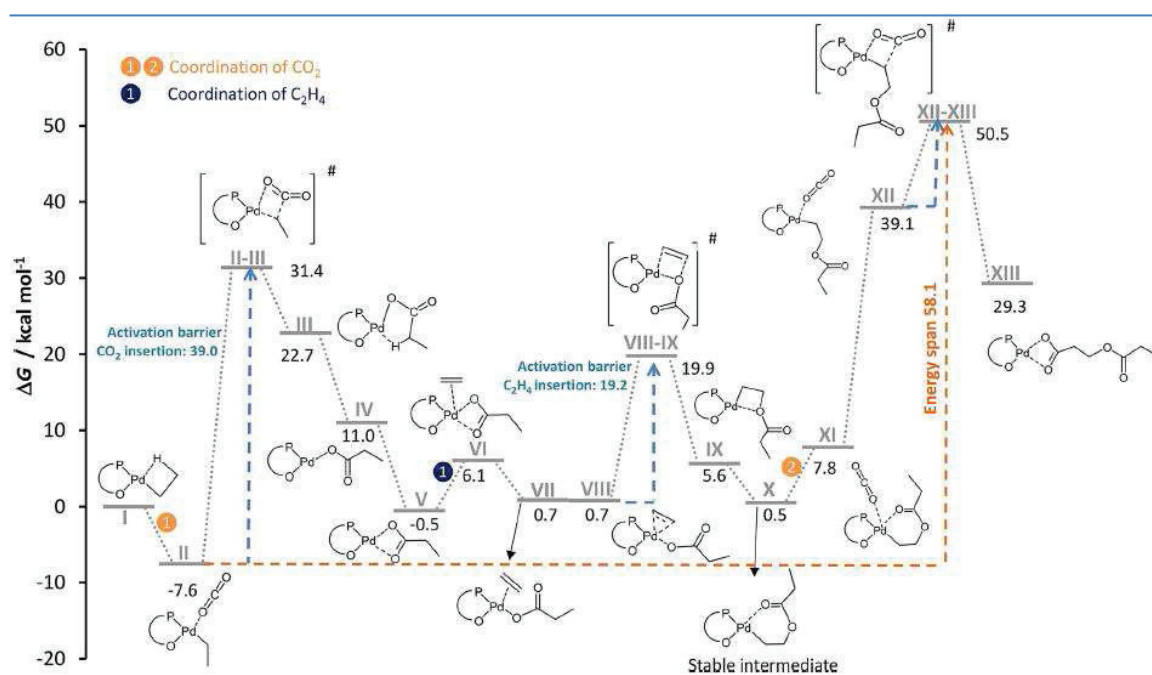


Figure 26. Gibbs free energy profile (gas phase) of the CO₂/C₂H₄ copolymerization with catalyst [Pd(Et)(1)]. Verena Moha, Daniela Cozzula, Markus Hçlscher, Walter Leitner, and Thomas E. Müller: A DFT Study on the Co-Polymerization of CO₂ and Ethylene: Feasibility Analysis for the Direct Synthesis of Polyethylene Esters. CHEMSUSCHEM. 2016, 9, 1614–1622. Copyright Wiley-VCH Verlag GmbH & Co. KGaA. Reproduced with permission.

In contrast to the first coordination of CO₂, which is exergonic ($\Delta G = -7.6$ kcal/mol), the subsequent coordination of CO₂ generating XI is endergonic ($\Delta G = 7.3$ kcal/mol). The insertion of the second CO₂ molecule proceeds *via* transition state XII-XIII and requires

an activation energy of 11.4 kcal/mol. The energy span of 58.1 kcal/mol between the most stable intermediate II and the highest transition state XII-XIII is clearly too high to enable productive turnover frequencies.

Also, this report explored the *cis* and *trans* insertion of the two co-monomers into the growing polymer chain. For insertion of the first CO₂ molecule, the energy difference for the transition state (II-III) is 0.4 kcal/mol in favor of the *trans* insertion. *Trans* insertion is also preferred for the insertion of a second CO₂ molecule ($\Delta G = 2.0$ kcal/mol). In contrast, the energy difference between *cis* and *trans* insertion of ethylene is much larger ($\Delta G = 31.1$ and 19.9 kcal/mol, respectively). Accordingly, the *trans* insertion of ethylene will be the preferred pathway.³⁵⁷

These calculations show that the insertion of CO₂ into the Pd-alkyl bond is a key step. According to Muller et al.,³⁵⁷ the corresponding barrier strongly depends on the choice of the ligand. By the use of a ligand set with electron-donating substituents and, consequently, an electron-rich palladium center the energy barrier is significantly lowered. Noteworthy, after insertion of three equivalents of ethylene prior to the insertion of the next CO₂ molecule, favorable Gibbs free activation barriers as low as 29.3 kcal/mol were derived for the non-alternating copolymerization. However, analysis of potential termination steps showed that for successful CO₂/C₂H₄ copolymerization the propensity for β -hydride elimination needs to be further reduced.

A.10. Conclusion and Results Obtained at the C2P2 Laboratory

After scanning the literature, the utilization of CO₂ in the polymerization of olefins, mainly ethylene polymerization, appears to be one of the most challenging goals in polymer chemistry nowadays, whether this utilization is as a polymerization medium or as a functionalization agent, in which the former is the primary step for the latter (using CO₂ as a polymerization medium in olefin polymerization processes is a step towards the achievement of CO₂-incorporation in the polyolefin backbone).

Here is our goal, to activate CO₂ in olefin polymerization reactions, radical and catalytic, starting by its utilization as a polymerization medium towards its incorporation in the polymer chain.

Our team elected this methodology because of its relevance from environmental and industrial stand points. First, the utilization of CO₂ as an alternative to organic solvents is a sustainable alternative that is already one of the components of the air (readily available) in place of petroleum-derived solvents that produce harmful wastes for the environment. Polyolefins (mainly PE and PP) account for about 60% of the thermoplastics produced annually, thus this development could be applied to the production of millions of tons of polymers and reduce a huge amount of wastes.

On the other hand, the incorporation of CO₂ in the polyolefin chain will open the door for the production of sustainable materials depending on a daily-renewable gas (CO₂) and relatively environmentally friendly monomers (olefins). These materials could form in the future an alternative to the other functionalized materials synthesized from toxic substrates such as the copolymerizations of olefins with carbon monoxide.

From an industrial stand point, the utilization of CO₂ as a polymerization medium in olefin polymerization processes will lead to cheaper and easier production of polyolefins (excluding the polyolefins produced in gas phase reactions). Commercially, part of the olefin polymerization processes can be conducted in organic solvents (catalytic processes) and the other part without any solvent (e.g. ethylene radical polymerization processes or gas-phase processes for catalytic systems); in both cases utilizing CO₂ is beneficial, in the first case it can replace solvents that are also harder to remove from the medium, and in the second case it could improve the productivity of the processes and its removal would be almost similar to the removal of any gaseous monomer.

Also, the incorporation of CO₂ in the polyolefin chain will pave the road towards the synthesis of different types of copolymers through the functionality added to the backbone of the polyolefin. And it will be an important step towards the direct copolymerization of CO₂ with olefins.

In this work, we concentrate mainly on the activation of CO₂ in ethylene polymerization due to the knowledge of our research team in ethylene polymerization processes and since ethylene is the simplest olefin (a model olefin) and it is the most industrially applicable monomer.

This thesis will discuss first the ethylene free radical polymerization in CO₂ (chapter II),

showing that this process could occur using different initiators and initiation modes, and comparing it to the conventional processes.

Then, chapter III will be comprised of two major parts: the first is about triethylaluminum-mediated radical polymerization of ethylene, this idea originated from a previous study at LCPP about the interaction of aluminum alkyls with radicals, thus our team investigated the effect of this Lewis acid and alkylating reagent in the radical polymerization of ethylene. From this point, we tried to use triethylaluminum as a means to incorporate CO₂ in the polyethylene chains, which is developed in the second part of chapter III.

The last chapter (chapter IV) will deal with another strategy of our work which is the catalytic approach. This chapter is also comprised of two major parts: the first part forms the basis for the second, it deals with the chain shuttling copolymerization of ethylene and isoprene using iron complexes. Before testing these iron complexes in CO₂ we tested them in conventional polymerization processes but we went further to copolymerize ethylene with isoprene (isoprene is chosen as a model of conjugated dienes: it is one of the most important industrial dienes used in production of elastomers) *via* a new method using cheap and environmentally benign iron complexes in order to get new materials having common properties of both homopolymers. Then, starting from this achievement, we tested these complexes in polymerization processes in scCO₂ to gain the advantage of utilizing CO₂ as an alternative to organic solvents in these catalytic processes.

This is a brief summary of what will be presented in the following chapters, the whole study is therefore entitled: "Radical and catalytic polymerizations of α -olefins: towards CO₂-incorporation".

A.11. References

1. US Department of Commerce, N. ESRL Global Monitoring Division - Global Greenhouse Gas Reference Network <https://www.esrl.noaa.gov/gmd/ccgg/trends/>.
2. Odum, E. P. *Q. Rev. Biol.* **1994**, 69 (3), 418.
3. Food Factories - www.legacyproject.org
<http://www.legacyproject.org/activities/foodfactories.html>.
4. good-plant-design-and-operation-onshore-carbon-capture-installations-and-onshore-pipelines.pdf <http://hub.globalccsinstitute.com/sites/default/files/publications/7276/good-plant-design-and-operation-onshore-carbon-capture-installations-and-onshore-pipelines.pdf>.
5. Harris, D. F.; Glas, M. D.; Lond, B. Sc.; F. R. S. E. *The Lancet* **1910**, 176, 906-908.
6. History of Industrial Gases | Ebbe Almquist | Springer
<http://www.springer.com/la/book/9780306472770>.
7. Priestley, J.; Hey, W. *Philos. Trans.* **1772**, 62, 147.
8. Chemistry of the Elements - 2nd Edition <https://www.elsevier.com/books/chemistry-of-the-elements/greenwood/978-0-7506-3365-9>.
9. Carbon Dioxide - Product Stewardship Summary - product-summary-carbon-dioxide.pdf
<http://www.airproducts.com/~media/Files/PDF/company/product-summary-carbon-dioxide.pdf?la=en>.
10. Davy, H. *Phil. Trans. R. Soc. Lond.* **1823**, 113, 199-205.
11. Adrien Jean Pierre THILORIER - Stammbaum Raynald CHANCE - Geneanet
<http://gw.geneanet.org/rcfb?lang=de&p=adrien+jean+pierre&n=thilorier>.
12. *Philos. Mag.* **1836**, 8 (48), 446.
13. Carbon dioxide <http://webbook.nist.gov/cgi/cbook.cgi?ID=C124389&Mask=4>.
14. Pierantozzi, R. Carbon Dioxide. In *Kirk-Othmer Encyclopedia of Chemical Technology*; John Wiley & Sons, Inc., 2000.
15. Darunte, L. A.; Oetomo, A. D.; Walton, K. S.; Sholl, D. S.; Jones, C. W. *ACS Sustain. Chem. Eng.* **2016**, 4 (10), 5761-5768.
16. Appendix A: CO2 for use in enhanced oil recovery (EOR) | Global CCS Institute
<https://hub.globalccsinstitute.com/publications/accelerating-uptake-ccs-industrial-use-captured-carbon-dioxide/appendix-co2-use>.
17. Blunt, M.; Fayers, F. J.; Orr, F. M. *Energy Convers. Manag.* **1993**, 34 (9), 1197.
18. Stafford, N. *Nature* **2007**, 448 (7153), 526-528.
19. Wickstrom, L. H.; Slucher, E. R.; Baranoski, M. T.; Mullett, D. J. *Rep. Submitt. Ohio Dep. Nat. Resour. Div. Geol. Surv. Open-File Rep.* **2008**, 1, 56.
20. Metz, B.; Davidson, O.; de Coninck, H.; Loos, M.; Meyer, L. *IPCC Special Report on Carbon Dioxide Capture and Storage*; Cambridge University Press, Cambridge, United Kingdom and New York, NY, USA, 2005; p 442.
21. Lindsey, A. S.; Jeskey, H. *Chem. Rev.* **1957**, 57 (4), 583-620.
22. *Transformation and Utilization of Carbon Dioxide*; Bhanage, B. M., Arai, M., Eds.; Green Chemistry and Sustainable Technology; Springer-Verlag: Berlin Heidelberg, 2014.
23. Das, S.; Wan Daud, W. M. A. *Renew. Sustain. Energy Rev.* **2014**, 39, 765-805.
24. Plasseraud, L. *ChemSusChem* **2010**, 3 (5), 631.
25. Bertau, M.; Offermanns, H.; Menges, G.; Keim, W.; Effenberger, F. X. *Chem. Ing. Tech.* **2010**, 82 (12), 2055.
26. Keim, W.; Offermanns, H. *Nachrichten Aus Chem.* **2010**, 58 (4), 434.
27. Mikkelsen, M.; Jørgensen, M.; C. Krebs, F. *Energy Environ. Sci.* **2010**, 3 (1), 43.
28. Weiss, M.; Neelis, M.; Blok, K.; Patel, M. *Clim. Change* **2009**, 95, 369-394.
29. Ho, M. T.; Allinson, G. W.; Wiley, D. E. *Ind. Eng. Chem. Res.* **2008**, 47 (14), 4883-4890.
30. Yazaydin, A. Ö.; Snurr, R. Q.; Park, T.-H.; Koh, K.; Liu, J.; LeVan, M. D.; Benin, A. I.; Jakubczak, P.; Lanuza, M.; Galloway, D. B.; et al. *J. Am. Chem. Soc.* **2009**, 131 (51), 18198-18199.
31. Peters, M.; Muller, T. E.; Leitner, W. *Tce* **2009**, 813, 46-47.
32. Sakakura, T.; Choi, J.-C.; Yasuda, H. *Chem. Rev.* **2007**, 107 (6), 2365-2387.
33. Patil, Y. P.; Tambade, P. J.; Jagtap, S. R.; Bhanage, B. M. *Front. Chem. Eng. China* **2010**, 4, 213-235.

34. Ricci, M. Carbon Dioxide as a Building Block for Organic Intermediates: An Industrial Perspective. In *Carbon Dioxide Recovery and Utilization*; Springer, Dordrecht, 2003; pp 395–402.
35. Aresta, M.; Dibenedetto, A. *Dalton Trans.* **2007**, 28, 2975–2992.
36. Aresta, M.; Dibenedetto, A. Carbon Dioxide Fixation into Organic Compounds. In *Carbon Dioxide Recovery and Utilization*; Springer, Dordrecht, 2003; pp 211–260.
37. Peters, M.; Köhler, B.; Kuckshinrichs, W.; Leitner, W.; Markewitz, P.; Müller, T. E. *ChemSusChem* **2011**, 4 (9), 1216–1240.
38. Leitner, W. *Coord. Chem. Rev.* **1996**, 153, 257–284.
39. Sakakura, T.; Choi, J.; Yasuda, H. *Chem. Rev.* **2007**, 107, 2365–2387.
40. Liu, Q.; Wu, L.; Jackstell, R.; Beller, M. *Nat. Commun.* **2015**, 6, 5933.
41. P. Heffer, M. Prud'homme, 79th IFA Annual Conference, Montreal (Canada), 23– 25 May 2011.
42. Pagani, G. *Hydrocarbon Process. Int. Ed.* **1982**, 61, 87– 91.
43. Deutschmann, O.; Knözinger, H.; Kochloefl, K.; Turek, T. Heterogeneous Catalysis and Solid Catalysts, 3. Industrial Applications. In *Ullmann's Encyclopedia of Industrial Chemistry*; Wiley-VCH Verlag GmbH & Co. KGaA, 2011.
44. Keim, W.; Offermanns, H. *Nachr. Chem.* **2010**, 58, 434 –435.
45. Ye, J.; Johnson, J. K. *Catal. Sci. Technol.* **2016**, 6 (24), 8392–8405.
46. Schneidewind, J.; Adam, R.; Baumann, W.; Jackstell, R.; Beller, M. *Angew. Chem. Int. Ed.* **2017**, 56 (7), 1890–1893.
47. Kattel, S.; Ramírez, P. J.; Chen, J. G.; Rodriguez, J. A.; Liu, P. *Science* **2017**, 355 (6331), 1296–1299.
48. Hunt, S. E.; Jones, J. I.; Lindsey, A. S.; Killoh, D. C.; Turner, H. S. *J. Chem. Soc.* **1958**, 3152 –3160.
49. Markovic, Z.; Engelbrecht, J. P.; Markovic, S.; Naturforsch. Z. A: *Phys. Sci.* **2002**, 57, 812–818.
50. Markovic, Z.; Markovic, S.; Manojlovic, N.; Predojevic-Simovic, J. J. *Chem. Inf. Model.* **2007**, 47, 1520 – 1525.
51. Minkova, L. I.; Milie, R.; Filippi, S.; Polacco, G. *Int. J. Polym. Mater.* **2001**, 50, 373–386.
52. Kang, T.-K.; Kim, Y.; Cho, W.-J.; Ha, C.-S. *J. Appl. Polym. Sci.* **2001**, 80, 1085–1095.
53. Jessop, P. G.; Ikariya, T.; Noyori, R. *Chem. Rev.* **1995**, 95, 259–272.
54. Hutschka, F.; Dedieu, A.; Leitner, W. *Angew. Chem. Int. Ed. Engl.* **1995**, 34, 1742–1745.
55. Tanaka, R.; Yamashita, M.; Nozaki, K. *J. Am. Chem. Soc.* **2009**, 131, 14168–14169.
56. Jessop, P. G.; Ikariya, T.; Noyori, R. *Chem. Rev.* **1999**, 99, 475–493.
57. Federsel, C.; Boddien, A.; Jackstell, R.; Jennerjahn, R.; Dyson, P. J.; Scopelliti, R.; Laurenczy, G.; Beller, M. *Angew. Chem. Int. Ed.* **2010**, 49, 9777–9780.
58. Arico, F.; Tundo, P. *Russ. Chem. Rev.* **2010**, 79, 479–489.
59. Zevenhoven, R.; Eloneva, S.; Teir, S. *Catal. Today* **2006**, 115, 73–79.
60. Zhao, W.; Peng, W.; Wang, D.; Zhao, N.; Li, J.; Xiao, F.; Wei, W.; Sun, Y. *Catal. Commun.* **2009**, 10 (5), 655–658.
61. Ballivet-Tkatchenko, D.; Chambrey, S.; Keiski, R.; Ligabue, R.; Plasseraud, L.; Richard, P.; Turunen, M. *Catal. Today* **2006**, 115, 80–87.
62. Plasseraud, L.; Ballivet-Tkatchenko, D.; Cattey, H.; Chambrey, S.; Ligabue, R.; Richard, P.; Willem, R.; Biesemans, M. *J. Organomet. Chem.* **2010**, 695, 1618–1626.
63. Sakakura, T.; Kohno, K. *Chem. Commun.* **2009**, 11, 1312 –1330.
64. Honda, M.; Kuno, S.; Sonehara, S.; Fujimoto, K.-i.; Suzuki, K.; Nakagawa, Y.; Tomishige, K. *ChemCatChem* **2011**, 3, 365–370.
65. Takahashi, T.; Watahiki, T.; Kitazume, S.; Yasuda, H.; Sakakura, T. *Chem. Commun.* **2006**, 15, 1664 –1666.
66. Dengler, J. E.; Lehenmeier, M. W.; Klaus, S.; Anderson, C. E.; Herdtweck, E.; Rieger, B. *Eur. J. Inorg. Chem.* **2011**, 336– 343.
67. Liang, S.; Liu, H.; Jiang, T.; Song, J.; Yang, G.; Han, B. *Chem. Commun.* **2011**, 47, 2131 –2133.
68. Kahlich, D.; Wiechern, U.; Lindner, J. Propylene Oxide. In *Ullmann's Encyclopedia of Industrial Chemistry*; American Cancer Society, 2000.
69. Doro, F.; Winnertz, P.; Leitner, W.; Prokofieva, A.; Muller, T. E. *Green Chem.* **2011**, 13, 292 –295.
70. Naumann d'Alnoncourt, R.; Csepei, L.-I.; Hävecker, M.; Girgsdies, F.; Schuster, M. E.; Schlögl, R.; Trunschke, A. *J. Catal.* **2014**, 311, 369–385.
71. Amakawa, K.; Kolen'ko, Y. V.; Villa, A.; Schuster, M. E.; Csepei, L.-I.; Weinberg, G.; Wrabetz, S.; Naumann d'Alnoncourt, R.; Girgsdies, F.; Prati, L.; Schlögl, R.; Trunschke, A. *ACS Catal.* **2013**, 3 (6), 1103–1113.

72. Ohara, T.; Sato, T.; Shimizu, N.; Prescher, G.; Schwind, H.; Weiberg, O.; Marten, K.; Greim, H. Acrylic Acid and Derivatives. In *Ullmann's Encyclopedia of Industrial Chemistry*; Wiley-VCH Verlag GmbH & Co. KGaA, 2003.
73. Hoberg, H.; Schaefer, D. J. *Organomet. Chem.* **1983**, 251, C51.
74. Alvarez, R.; Carmona, E.; Cole-Hamilton, D. J.; Galindo, A.; Gutierrez-Puebla, E.; Monge, A.; Poveda, M. L.; Ruiz, C. *J. Am. Chem. Soc.* **1985**, 107 (19), 5529-5531.
75. Alvarez, R.; Carmona, E.; Galindo, A.; Gutierrez, E.; Marin, J. M.; Monge, A.; Poveda, M. L.; Ruiz, C.; Savariault, J. M. *Organometallics* **1989**, 8, 2430.
76. Galindo, A.; Pastor, A.; Perez, P.; Carmona, E. *Organometallics* **1993**, 12, 4443.
77. Bernskoetter, W. H.; Tyler, B. T. *Organometallics* **2011**, 30, 520.
78. Graham, D. C.; Mitchell, C.; Bruce, M. I.; Metha, G. F.; Bowie, J. H.; Buntine, M. A. *Organometallics* **2007**, 26, 6784.
79. Papai, I.; Schubert, G.; Mayer, I.; Besenyi, G.; Aresta, M. *Organometallics* **2004**, 23, 5252.
80. Schubert, G.; Papai, I. *J. Am. Chem. Soc.* **2003**, 125, 14847.
81. Dedieu, A.; Ingold, F. *Angew. Chem., Int. Ed. Engl.* **1989**, 28, 1694.
82. Wolfe, J. M.; Bernskoetter, W. H. *Dalton Trans.* **2012**, 41, 10763.
83. Hoberg, H.; Ballesteros, A.; Sigan, A.; Jegat, C.; Barhausen, D.; Milchereit, A. *J. Organomet. Chem.* **1991**, 407, C23.
84. Hoberg, H.; Ballesteros, A. *J. Organomet. Chem.* **1991**, 411, C11.
85. Hoberg, H.; Peres, Y.; Kruger, C.; Tsay, Y. H. *Angew. Chem., Int. Ed. Engl.* **1987**, 26, 771.
86. Lejkowski, M. L.; Lindner, R.; Kageyama, T.; Bódizs, G. É.; Plessow, P. N.; Müller, I. B.; Schäfer, A.; Rominger, F.; Hofmann, P.; Futter, C.; Schunk, S. A.; Limbach, M. *Chem. – Eur. J.* **2012**, 18 (44), 14017.
87. Langer, J.; Walther, D.; Malassa, A.; Westerhausen, M.; Gorls, H. *Eur. J. Inorg. Chem.* **2010**, 275.
88. Brookhart, M.; Green, M. L. H.; Parkin, G. *Proc. Natl. Acad. Sci.* **2007**, 104, 6908.
89. Huguet, N.; Jevtovikj, I.; Gordillo, A.; Lejkowski, M. L.; Lindner, R.; Bru, M.; Khalimon, A. Y.; Rominger, F.; Schunk, S. A.; Hofmann, P.; Limbach, M. *Chem. – Eur. J.* **2014**, 20 (51), 16858-16862.
90. Stieber, S. C. E.; Huguet, N.; Kageyama, T.; Jevtovikj, I.; Ariyananda, P.; Gordillo, A.; Schunk, S. A.; Rominger, F.; Hofman, P.; Limbach, M. *Chem. Commun.* **2015**, 51, 10907-10909.
91. Manzini, S.; Huguet, N.; Trapp, O.; Schaub, T. *Eur. J. Org. Chem.* **2015**, 2015 (32), 7122-7130.
92. Graham, D. C.; Mitchell, C.; Bruce, M. I.; Metha, G. F.; Bowie, J. H.; Buntine, M. A. *Organometallics* **2007**, 26, 6784.
93. Bruckmeier, C.; Lehenmeier, M. W.; Reichardt, R.; Vagin, S.; Rieger, B. *Organometallics* **2010**, 29 (10), 2199-2202.
94. Lee, S. Y. T.; Cokoja, M.; Drees, M.; Li, Y.; Mink, J.; Herrmann, W. A.; Kühn, F. E. *ChemSusChem* **2011**, 4 (9), 1275-1279.
95. Lee, S. Y. T.; Ghani, A. A.; D'Elia, V.; Cokoja, M.; Herrmann, W. A.; Basset, J.-M.; Kühn, F. E. *New J. Chem.* **2013**, 37 (11), 3512-3517.
96. Plessow, P. N.; Weigel, L.; Lindner, R.; Schäfer, A.; Rominger, F.; Limbach, M.; Hofmann, P. *Organometallics* **2013**, 32 (11), 3327-3338.
97. Hendriksen, C.; Pidko, E. A.; Yang, G.; Schöffner, B.; Vogt, D. *Chem. – Eur. J.* **2014**, 20 (38), 12037-12040.
98. Jin, D.; Schmeier, T. J.; Williard, P. G.; Hazari, N.; Bernskoetter, W. H. *Organometallics* **2013**, 32 (7), 2152-2159.
99. Jin, D.; Williard, P. G.; Hazari, N.; Bernskoetter, W. H. *Chem. – Eur. J.* **2014**, 20 (11), 3205-3211.
100. Plessow, P. N.; Schäfer, A.; Limbach, M.; Hofmann, P. *Organometallics* **2014**, 33 (14), 3657-3668.
101. Cohen, S. A.; Bercaw, J. E. *Organometallics* **1985**, 4, 1006.
102. Alt, H. G.; Denner, C. E. *J. Organomet. Chem.* **1990**, 390, 53.
103. Hessen, B.; Meetsma, A.; Bolhuis, F.; Teuben, J.; Helgesson, G.; Janger, S. *Organometallics* **1990**, 9, 1925.
104. Aresta, M.; Quaranta, E. *J. Organomet. Chem.* **1993**, 463, 215.
105. Hoberg, H.; Jenni, K.; Krüger, C.; Raabe, E. *Angew. Chem. Int. Ed. Engl.* **1986**, 25 (9), 810-811.
106. Nakano, R.; Ito, S.; Nozaki, K. *Nat. Chem.* **2014**, 6 (4), 325-331.
107. Cheng, M.; Moore, D. R.; Reczek, J. J.; Chamberlain, B. M.; Lobkovsky, E. B.; Coates, G. W. *J. Am. Chem. Soc.* **2001**, 123 (36), 8738.
108. Nakano, K.; Nozaki, K.; Hiyama, T. *J. Am. Chem. Soc.* **2003**, 125 (18), 5501-5510.

109. Darensbourg, D. J.; Wilson, S. J. *Green Chem.* **2012**, *14*, 2665-2671.
110. Darensbourg, D. J. *Chem. Rev.* **2007**, *107*, 2388-2410.
111. Lu, X.-B.; Ren, W.-M.; Wu, G.-P. *Acc. Chem. Res.* **2012**, *45*, 1721-1735.
112. Whiteoak, C. J.; Kielland, N.; Laserna, V.; Escudero-Adan, E. C.; Martin, E.; Kleij, A.W. *J. Am. Chem. Soc.* **2013**, *135*, 1228-1231.
113. Ren, W.-M.; Wu, G.-P.; Lin, F.; Jiang, J.-Y.; Liu, C.; Luo, Y.; Lu, X.-B. *Chem. Sci.* **2012**, *3*, 2094-2102.
114. Whiteoak, C. J.; Martin, E.; Escudero-Adan, E.; Kleij, A.W. *Adv. Synth. Catal.* **2013**, *355*, 2233-2239.
115. Liu, Y.; Wang, M.; Ren, W.-M.; He, K.-K.; Xu, Y.-C.; Liu, J.; Lu, X.-B. *Macromolecules* **2014**, *47*, 1269-1276.
116. Nakano, K.; Hashimoto, S.; Nakamura, M.; Kamada, T.; Nozaki, K. *Angew. Chem. Int. Ed.* **2011**, *50*, 4868-4871.
117. Kember, M. R.; Williams, C. K. *J. Am. Chem. Soc.* **2012**, *134*, 15676-15679.
118. Price, C. J.; Reich, B. J. E.; Miller, S. A. *Macromolecules* **2006**, *39*, 2751-2756.
119. Nakano, R.; Ito, S.; Nozaki, K. *Nat. Chem.* **2014**, *6*, 325-331.
120. Dove, A. P. *Nat. Chem.* **2014**, *6* (4), 276-277.
121. Inoue, S.; Koinuma, H.; Tsuruta, T. *J. Polym. Sci. Part B* **1969**, *7*, 287-292.
122. Inoue, S.; Koinuma, H.; Tsuruta, T. *Makromol. Chem.* **1969**, *130*, 210-220.
123. Kobayashi, M.; Inoue, S.; Tsuruta, T. *Macromolecules* **1971**, *4*, 658-659.
124. Kobayashi, M.; Tang, Y. L.; Tsuruta, T.; Inoue, S.; *Makromol. Chem.* **1973**, *169*, 69-81.
125. Kobayashi, M.; Inoue, S.; Tsuruta, T. *J. Polym. Sci. Polym. Chem. Ed.* **1973**, *11*, 2383-2385.
126. Inoue, S.; Kobayashi, M.; Koinuma, H.; Tsuruta, T. *Makromol. Chem.* **1972**, *155*, 61-73.
127. Kuran, W.; Pasynkiewicz, S.; Skupinska, J.; Rokicki, R. *Macromol. Chem. Phys.* **1976**, *177*, 11-20.
128. Gorecki, P.; Kuran, W. *J. Polym. Sci. Part C* **1985**, *23*, 299-304.
129. Soga, K.; Imai, E.; Hattori, I. *Polym. J.* **1981**, *13*, 407-410.
130. Kuran, W.; Listos, T. *Macromol. Chem. Phys.* **1994**, *195*, 977-984.
131. Kuran, W.; Listos, T. *Macromol. Chem. Phys.* **1994**, *195*, 1011-1015.
132. Kuran, W.; Listos, T.; *Pol. J. Chem.* **1994**, *68*, 1071-1083.
133. Inoue, S. *J. Polym. Sci. Part A* **2000**, *38*, 2861-2871.
134. Takeda, N.; Inoue, S. *Makromol. Chem.* **1978**, *179*, 1377-1381.
135. Aida, T.; Inoue, S. *Macromolecules* **1982**, *15*, 682-684.
136. Aida, T.; Inoue, S. *J. Am. Chem. Soc.* **1983**, *105*, 1304-1309.
137. Jung, J. H.; Ree, M.; Chang, T. *J. Polym. Sci. Part A* **1999**, *37*, 3329-3336.
138. Whiteoak, C. J.; Kielland, N.; Laserna, V.; Escudero-Adán, E. C.; Martin, E.; Kleij, A. W. *J. Am. Chem. Soc.* **2013**, *135* (4), 1228.
139. Whiteoak, C. J.; Kielland, N.; Laserna, V.; Castro-Gómez, F.; Martin, E.; Escudero-Adán, E. C.; Bo, C.; Kleij, A. W. *Chem. – Eur. J.* **2014**, *20* (8), 2264.
140. Sugimoto, H.; Ohshima, H.; Inoue, S. *J. Polym. Sci. Part A* **2003**, *41*, 3549-3555.
141. Lin, P.-M.; Chang, C.-H.; Chuang, H.-J.; Liu, C.-T.; Ko, B.-T.; Lin, C.-C. *ChemCatChem* **2016**, *8* (5), 984.
142. Lee, T.-Y.; Lin, Y.-J.; Chang, Y.-Z.; Huang, L.-S.; Ko, B.-T.; Huang, J.-H. *Organometallics* **2017**, *36* (2), 291.
143. Huang, L.-S.; Tsai, C.-Y.; Chuang, H.-J.; Ko, B.-T. *Inorg. Chem.* **2017**, *56* (11), 6141.
144. Ema, T.; Miyazaki, Y.; Koyama, S.; Yano, Y.; Sakai, T. *Chem. Commun.* **2012**, *48* (37), 4489.
145. Mandal, M.; Chakraborty, D.; Ramkumar, V. *RSC Adv.* **2015**, *5* (36), 28536.
146. Kruper, W. J.; Dellar, D. V. *J. Org. Chem.* **1995**, *60*, 725-727.
147. Mang, S.; Cooper, A. I.; Colclough, M. E.; Chauhan, N.; Holmes, A. B. *Macromolecules* **2000**, *33*, 303-308.
148. Jacobsen, E. N. *Acc. Chem. Res.* **2000**, *33*, 421-431.
149. Paddock, R. L.; Nguyen, S. T. *J. Am. Chem. Soc.* **2001**, *123*, 11498-11499.
150. Darensbourg, D. J.; Yarbrough, J. C. *J. Am. Chem. Soc.* **2002**, *124*, 6335-6342.
151. Lu, X. B.; Feng, X. J.; He, R. *Appl. Catal. A* **2002**, *234*, 25-33.
152. Darensbourg, D. J.; Rodgers, J. L.; Fang, C. C. *Inorg. Chem.* **2003**, *42*, 4498-4500.
153. Darensbourg, D. J.; Yarbrough, J. C.; Ortiz, C.; Fang, C. C. *J. Am. Chem. Soc.* **2003**, *125*, 7586-7591.
154. R. Eberhardt, M. Allmendinger, B. Rieger, *Macromol. Rapid Commun.* **2003**, *24*, 194 – 196.
155. Darensbourg, D. J.; Phelps, A. L. *Inorg. Chem.* **2005**, *44*, 4622.

156. Bertocco, A. Precipitation and Crystallization Techniques. In *Chemical Synthesis Using Supercritical Fluids*; Jessop, P. G., Leitner, W., Eds.; Wiley-VCH: Weinheim, 1999; p 108.
157. Gurnham, J.; Gambarotta, S.; Korobkov, I.; Jasinska-Walc, L.; Duchateau, R. *Organometallics* **2014**, 33 (17), 4401.
158. Si, G.; Zhang, L.; Han, B.; Zhang, H.; Li, X.; Liu, B. *RSC Adv.* **2016**, 6 (27), 22821.
159. Soga, K.; Uenishi, K.; Ikeda, S. *J. Polym. Sci. Polym. Sci. Ed.* **1979**, 17, 415-423.
160. Lu, X.-B.; Feng, X.-J.; He, R. *Appl. Catal. A* **2002**, 234, 25.
161. Lu, X. B.; He, R.; Bai, C. X. *J. Mol. Catal. A* **2002**, 186, 1-11.
162. Shen, Y. M.; Duan, W. L.; Shi, M. *J. Org. Chem.* **2003**, 68, 1559-1562.
163. Qin, Z.; Thomas, C. M.; Lee, S.; Coates, G. W. *Angew. Chem., Int. Ed.* **2003**, 42, 5484.
164. Lu, X.-B.; Wang, Y. *Angew. Chem., Int. Ed.* **2004**, 43, 3574.
165. Paddock, R. L.; Nguyen, S. T. *Macromolecules* **2005**, 38, 6251.
166. Lu, X.-B.; Shi, L.; Wang, Y.-M.; Zhang, R.; Zhang, Y.-J.; Peng, X.-J.; Zhang, Z.-C.; Li, B. *J. Am. Chem. Soc.* **2006**, 128, 1664.
167. Cohen, C. T.; Coates, G. W. *J. Polym. Sci. Part A* **2006**, 44, 5182.
168. Nakano, K.; Kamada, T.; Nozaki, K. *Angew. Chem., Int. Ed.* **2006**, 45, 7274.
169. Shi, L.; Lu, X.-B.; Zhang, R.; Peng, X.-J.; Zhang, C.-Q.; Li, J.-F.; Peng, X.-M. *Macromolecules* **2006**, 39, 5679.
170. Wu, G.-P.; Wei, S.-H.; Ren, W.-M.; Lu, X.-B.; Xu, T.-Q.; Darensbourg, D. J. *J. Am. Chem. Soc.* **2011**, 133 (38), 15191.
171. Lu, X.-B.; Ren, W.-M.; Wu, G.-P. *Acc. Chem. Res.* **2012**, 45 (10), 1721.
172. Xia, W.; Salmeia, K. A.; Vagin, S. I.; Rieger, B. *Chem. – Eur. J.* **2015**, 21 (11), 4384.
173. Li, X.; Duan, R.; Pang, X.; Gao, B.; Wang, X.; Chen, X. *Appl. Catal. B Environ.* **2016**, 182, 580.
174. Hatazawa, M.; Nakabayashi, K.; Ohkoshi, S.; Nozaki, K. *Chem. – Eur. J.* **2016**, 22 (38), 13677.
175. Soga, K.; Imai, E.; Hattori, I. *Polym. J.* **1981**, 13, 407-410.
176. Super, M. S.; Berluche, E.; Costello, C.; Beckman, E. J. *Macromolecules* **1997**, 30, 368-372.
177. Sarbu, T.; Beckman, E. J. *Macromolecules* **1999**, 32, 6904-6912.
178. Darensbourg, D. J.; Holtcamp, M. W. *Macromolecules* **1995**, 28, 7577-7579.
179. Darensbourg, D. J.; Holtcamp, M. W.; Struck, G. E.; Zimmer, M. S.; Niezgoda, S. A.; Rainey, P.; Robertson, J. B.; Draper, J. D.; Reibenspies, J. H. *J. Am. Chem. Soc.* **1999**, 121, 107-116.
180. Darensbourg, D. J.; Wildeson, J. R.; Yarbrough, J. C.; Reibenspies, J. H. *J. Am. Chem. Soc.* **2000**, 122, 12487-12496.
181. Koning, C.; Wildeson, J.; Parton, R.; Plum, B.; Steeman, P.; Darensbourg, D. J. *Polymer* **2001**, 42, 3995-4004.
182. Darensbourg, D. J.; Wildeson, J. R.; Yarbrough, J. C.; Reibenspies, J. H. *J. Am. Chem. Soc.* **2000**, 122, 12487-12496.
183. Darensbourg, D. J.; Zimmer, M. S.; Rainey, P.; Larkins, D. L. *Inorg. Chem.* **2000**, 39, 1578-1585.
184. Darensbourg, D. J.; Wildeson, J. R.; Yarbrough, J. C. *Inorg. Chem.* **2002**, 41, 973-980.
185. Darensbourg, D. J.; Rainey, P.; Yarbrough, J. C. *Inorg. Chem.* **2001**, 40, 986-993.
186. Darensbourg, D. J.; Wildeson, J. R.; Yarbrough, J. C. *Organometallics* **2001**, 20, 4413-4417.
187. Hampel, O.; Rode, C.; Walther, D.; Beckert, R.; Gorts, H. Z. *Naturforsch.* **2002**, 57, 946-956.
188. Cheng, M.; Lobkovsky, E. B.; Coates, G. W. *J. Am. Chem. Soc.* **1998**, 120, 11018-11019.
189. Moore, D. R.; Cheng, M.; Lobkovsky, E. B.; Coates, G. W. *J. Am. Chem. Soc.* **2003**, 125, 11911-11924.
190. Nakano, K.; Kosaka, N.; Hiyama, T.; Nozaki, K. *Dalton Trans.* **2003**, 4039-4050.
191. Nozaki, K.; Nakano, K.; Hiyama, T. *J. Am. Chem. Soc.* **1999**, 121, 11008-11009.
192. Kember, M. R.; Knight, P. D.; Reung, P. T. R.; Williams, C. K. *Angew. Chem. Int. Ed.* **2009**, 48 (5), 931.
193. Thevenon, A.; Garden, J. A.; White, A. J. P.; Williams, C. K. *Inorg. Chem.* **2015**, 54 (24), 11906.
194. Hua, Y.-Z.; Yang, X.-C.; Liu, M.-M.; Song, X.; Wang, M.-C.; Chang, J.-B. *Macromolecules* **2015**, 48 (6), 1651.
195. Musco, A.; Perego, C.; Tartari, V. *Inorg. Chim. Acta* **1978**, 28, L147-L148.
196. Fiorani, G.; Kleij, A. W. *Angew. Chem. Int. Ed.* **2014**, 53 (29), 7402-7404.
197. Kemmere, M. F. Supercritical Carbon Dioxide for Sustainable Polymer Processes. In *Supercritical Carbon Dioxide*; Kemmere, M. F., Meyer, M. T., Eds.; Wiley-VCH Verlag GmbH & Co. KGaA, 2005; pp 1-14.

198. DeSimone, J. M. and Turmas, W. (eds) (2003) *Green Chemistry Using Liquid and Supercritical Carbon Dioxide*, Oxford University Press, Oxford.
199. McHugh, M. A.; Krukonis, V. J. *Supercritical Fluid Extraction: Principles and Practice*, 2nd ed.; Butterworth-Heinemann: Stoneham, 1993.
200. Barer, S. J.; Stern, K. M. In *Catalytic Activation of Carbon Dioxide*; Ayers, W. M., Ed.; American Chemical Society: Washington, DC, 1988; p 1.
201. Filardo, G.; Galia, A.; Giaconia, A. Modification of Polymers in Supercritical Carbon Dioxide. In *Carbon Dioxide Recovery and Utilization*; Springer, Dordrecht, 2003; pp 197–207.
202. Fleming, O. S.; Kazarian, S. G. Polymer Processing with Supercritical Fluids. In *Supercritical Carbon Dioxide*; Kemmere, ir artje F., Meyer, M. T., Eds.; Wiley-VCH Verlag GmbH & Co. KGaA, 2005; pp 205–238.
203. Hyatt, J. A. *J. Org. Chem.* **1984**, *49*, 5097–5101.
204. Rindfleisch, F.; DiNoia, T.; McHugh, M. A. *Polym. Mater. Sci. Eng.* **1996**, *74*, 178.
205. DeSimone, J. M.; Guan, Z.; Elsbernd, C. S. *Science* **1992**, *257*, 945–947.
206. Guan, Z.; Combes, J. R.; Menciloglu, Y. Z.; DeSimone, J. M. *Macromolecules* **1993**, *26*, 2663–2669.
207. Odell, P. G.; Hamer, G. K. *Polym. Prepr.* **1997**, *38*, 470–471.
208. Hedrick, J. L.; Mulcahey, L. J.; Taylor, L. T. *ACS Symp. Ser.* **1992**, *488*, 206–220.
209. Sharp, K. G. *J. Sol-Gel Sci. Technol.* **1994**, *2*, 35–41.
210. Loy, D. A.; Shea, K. J.; Russick, E. M. *Mater. Res. Soc. Symp. Proc.* **1992**, *271*, 699–704.
211. Kerton, F. M.; Lawless, G. A.; Ames, S. P. *J. Mater. Chem.* **1997**, *7*, 1965–1966.
212. Tan, B.; Woods, H. M.; Licence, P.; Howdle, S. M.; Cooper, A. I. *Macromolecules* **2005**, *38* (5), 1691–1698.
213. Gross, S. M.; Roberts, G. W.; Kiserow, D. J.; DeSimone, J. M. *Macromolecules* **2000**, *33* (1), 40–45.
214. Shi, C.; DeSimone, J. M.; Kiserow, D. J.; Roberts, G. W. *Macromolecules* **2001**, *34* (22), 7744–7750.
215. Mingotaud, A.; Dargelas, F.; Cansell, F. *Macromol. Symp.* **2000**, *153*, 77–86.
216. Higashimura, T.; Sawamoto, M.; Miyamoto, M. *Macromolecules* **1984**, *17*, 265.
217. Winstein, S.; Chippinger, B.; Fainberg, A. H.; Robinson, G. C. *J. Am. Chem. Soc.* **1954**, *76*, 2597.
218. Kendall, J. L.; Canelas, D. Q.; Young, J. L.; DeSimone, J. M. *Chem. Rev.* **1999**, *99*, 543–563.
219. Biddulph, R.; Plesch, P. *J. Chem. Soc.* **1960**, 3913.
220. Yokota, H.; Kondo, M.; Kagiya, T.; Fukui, K. *J. Polym. Sci.: Part A-1* **1968**, *6*, 425–434.
221. Yokota, H.; Kondo, M.; Kagiya, T.; Fukui, K. *J. Polym. Sci.: Part A-1* **1968**, *6*, 435–446.
222. Yokota, H.; Kondo, M.; Kagiya, T.; Fukui, K. *Bull. Chem. Soc. Jpn.* **1969**, *42*, 1412–1416.
223. Pernecker, T.; Kennedy, J. P. *Polym. Bull. (Berlin)* **1994**, *32*, 537–543.
224. Kennedy, J. P.; Pernecker, T. United States Patent 5,376,744, 1994.
225. Deák, G.; Pernecker, T.; Kennedy, J. P. *Macromol. Rep.* **1995**, *A32*, 979–984.
226. Pernecker, T.; Deak, G.; Kennedy, J. P. *Polym. Prepr. (Am. Chem. Soc., Div. Polym. Chem.)* **1995**, *36*, 243–244.
227. Pernecker, T.; Deak, G.; Kennedy, J. P. *Macromol. Rep.* **1995**, *A32*, 969–978.
228. Clark, M. R.; DeSimone, J. M. *Polym. Prepr. (Am. Chem. Soc., Div. Polym. Chem.)* **1994**, *35*, 482–483.
229. Clark, M. R.; DeSimone, J. M. *Macromolecules* **1995**, *28*, 3002–3004.
230. Higashimura, T.; Sawamoto, M.; Miyamoto, M. *Macromolecules* **1984**, *17*, 265.
231. Clark, M. R.; DeSimone, J. M. *Polym. Prepr. (Am. Chem. Soc., Div. Polym. Chem.)* **1994**, *35*, 482–483.
232. Clark, M. R.; DeSimone, J. M. *Macromolecules* **1995**, *28*, 3002–3004.
233. Clark, M. R.; Kendall, J. L.; DeSimone, J. M. *Macromolecules* **1997**, *30*, 6011–6014.
234. Bueno, C.; Cabral, V. F.; Cardozo-Filho, L.; Dias, M. L.; Antunes, O. A. C. *J. Supercrit. Fluids* **2009**, *48* (2), 183–187.
235. Nguyen, S. T.; Grubbs, R. H.; Ziller, J. W. *J. Am. Chem. Soc.* **1993**, *115*, 9858.
236. Schwab, P.; France, M. B.; Ziller, J. W.; Grubbs, R. H. *Angew. Chem., Int. Ed. Engl.* **1995**, *34*, 2039.
237. Schwab, P.; Grubbs, R. H.; Ziller, J. W. *J. Am. Chem. Soc.* **1996**, *118*, 100.
238. Schrock, R. R.; Murdzek, J. S.; Bazan, G. C.; Robbins, J.; DiMare, M.; O'Regan, M. *J. Am. Chem. Soc.* **1990**, *112*, 3875.
239. Furstner, A.; Koch, D.; Langemann, K.; Leitner, W.; Six, C. *Angew. Chem., Int. Ed. Engl.* **1997**, *36*, 2466–2469.

240. Mistele, C. D.; Thorp, H. H.; DeSimone, J. M. *Polym. Prepr. (Am. Chem. Soc., Div. Polym. Chem.)* **1995**, 36, 507-508.
241. Mistele, C. D.; Thorp, H. H.; DeSimone, J. M. *J. Macromol. Sci. A* **1996**, 33, 953-960.
242. Campos-Carrasco, A.; Estorach, C. T.; Bastero, A.; Reguero, M.; Masdeu-Bultó, A. M.; Franciò, G.; Leitner, W.; D'Amora, A.; Milani, B. *Organometallics* **2011**, 30 (24), 6572-6586.
243. Ranieri, M. M. E. Measuring on Main Kinetic Parameters of Molecular Catalyst for Olefin Polymerization Using High-Pressure-Type Quenched Flow Reactor. PhD Thesis, Université Claude Bernard-Lyon I, 2012.
244. Bukatov, G. D.; Zakharov, V. A.; Yermakov, Y. I. *Die Makromolekulare Chemie* **1978**, 179, 2097-2101.
245. Zakharov, V. A.; Bukatov, G. D.; Dudchenko, V. K.; Minkov, A. I.; Yermakov, Y. I. *Die Makromolekulare Chemie* **1974**, 175, 3035-3040.
246. Forbes, M.D.E.; Yashiro, H. *Macromolecules* **2007**, 40, 1460-1465.
247. Charpentier, P.A.; DeSimone, J. M.; Roberts, G.W. *Chemical Engineering Science* **2000**, 55, 5341-5349.
248. Bilgin, N.; Baysal, C.; Menciloglu, Y. Z. *Journal of Polymer Science Part A Polymer Chemistry* **2005**, 43, 5312-5322.
249. Xu, W. Z.; Li, X.; Charpentier, P.A. *Polymer* **2007**, 48, 1219-1228.
250. van Herk, A. M.; Manders, B.G.; Canelas, D.A.; Quadir, M.; DeSimone, J. M. *Macromolecules* **1997**, 30, 4780-4782.
251. Ryan, J.; Erkey, C.; Shaw, M. *Polym. Prepr.* **1997**, 38, 428-429.
252. Beuermann, S.; Buback, M.; Schmaltz, C.; Kuchta, F.-D. *Macromol. Chem. Phys.* **1998**, 199 (6), 1209.
253. Beuermann, S.; Buback, M. Kinetics of Free-Radical Polymerization in Homogeneous Phase of Supercritical Carbon Dioxide. In *Supercritical Carbon Dioxide: in Polymer Reaction Engineering*; Wiley-VCH Verlag GmbH & Co. KGaA, 2006; pp 55-80.
254. Lewandowski, G.; Meissner, E.; Milchert, E. *J. Hazard. Mater.* **2006**, 136 (3), 385-391.
255. Cassidy, P. E. *J. Am. Chem. Soc.* **2005**, 127 (9), 3233-3234.
256. Nishino, T.; Urushihara, Y.; Meguro, M.; Nakamae, K. *J. Colloid Interface Sci.* **2004**, 279 (2), 364-369.
257. Urushihara, Y.; Nishino, T. *Langmuir* **2005**, 21 (6), 2614-2618.
258. Wood, C. D.; Yarbrough, J. C.; Roberts, G.; DeSimone, J. Production of Fluoropolymers in Supercritical Carbon Dioxide. In *Supercritical Carbon Dioxide: in Polymer Reaction Engineering*; Wiley-VCH Verlag GmbH & Co. KGaA, 2006; pp 189-204.
259. Fink, R.; Beckman, E. J. High-Pressure Reaction Equipment Design. In *Chemical Synthesis Using Supercritical Fluids*; Jessop, P. G., Leitner, W., Eds.; Wiley-VCH Verlag GmbH, 1999; pp 67-87.
260. Forbes, M. D. E.; Yashiro, H. *Macromolecules* **2007**, 40, 1460-1465.
261. Guan, Z.; Combes, J. R.; Menciloglu, Y. Z.; DeSimone, J. M. *Macromolecules* **1993**, 26, 2663-2669.
262. Guan, Z.; Combes, J. R.; Elsbernd, C. S.; DeSimone, J. M. *Polym. Prepr.* **1993**, 34, 446-447.
263. Ehrlich, P. *Chemtracts: Organic Chemistry* **1993**, 6, 92-94.
264. Kapellen, K. K.; Mistele, C. D.; DeSimone, J. M. *Macromolecules* **1996**, 29, 495-496.
265. Hwang, H. S.; Yuvaraj, H.; Kim, W. S.; Lee, W.-K.; Gal, Y.-S.; Lim, K. T. *J. Polym. Sci. Part Polym. Chem.* **2008**, 46 (4), 1365.
266. Ye, W.; DeSimone, J. M. *Ind. Eng. Chem. Res.* **2000**, 39, 4564-4566.
267. Ye, W.; Wells, S.; DeSimone, J. M. *J. Polym. Sci. Part Polym. Chem.* **2001**, 39 (21), 3841.
268. Yoshida, E.; Imamura, H. *Colloid and Polymer Science* **2007**, 285, 1463-1470.
269. Ganapathy, H. S.; Hwang, S. S.; Lee, M. Y.; Jeong, Y. T.; Gal, Y. S.; Lim, K. T. *J. Mater. Sci.* **2008**, 43, 2300-2306.
270. Yoshida, E.; Imamura, H. *Colloid and Polymer Science* **2007**, 285, 1463-1470.
271. Ribaut, T.; Lacroix-Desmazes, P.; Fournel, B.; Sarrade, S. *J. Polym. Sci. Part Polym. Chem.* **2009**, 47 (20), 5448-5460.
272. Bouilhac, C.; Chirat, M.; Joly-Duhamel, C.; Lacroix-Desmazes, P. *Macromol. Chem. Phys.* **2013**, 214 (20), 2259-2265.
273. Xia, J.; Johnson, T.; Gaynor, S. G.; Matyjaszewski, K.; DeSimone, J. *Macromolecules* **1999**, 32 (15), 4802.
274. Lau, S. F.; Wesson, J. P.; Wunderlich, B. *Macromolecules* **1984**, 17 (5), 1102.
275. Kennedy, K. A.; Roberts, G. W.; DeSimone, J. M. *Adv. Polym. Sci.* **2005**, 175, 329-346.

276. Du, L.; Kelly, J. Y.; Roberts, G. W.; DeSimone, J. M. *J. Supercrit. Fluids* **2009**, 47 (3), 447–457.
277. Romack, T. J.; DeSimone, J. M. *Macromolecules* **1995**, 28, 8429–8431.
278. DeYoung, J. P.; Romack, T. J.; DeSimone, J. M. *Polym. Prepr (Am. Chem. Soc., Div. Polym. Chem.)* **1997**, 38, 424–425.
279. Romack, T. J.; Kipp, B. E.; DeSimone, J. M. *Macromolecules* **1995**, 28, 8432–8434.
280. Canelas, D. A.; DeSimone, J. M. *Adv. Polym. Sci.* **1997**, 133, 103–140.
281. Giaconia, A.; Scialdone, O.; Apostolo, M.; Filardo, G.; Galia, A. *J. Polym. Sci. Part Polym. Chem.* **2008**, 46 (1), 257.
282. Humphrey, J. S.; Amin-Sanayei, R. Vinylidene Fluoride Polymers. In *Encyclopedia of Polymer Science and Technology*, 3rd ed.; Mark, H. F., Ed.; Wiley: New York, 2004; Vol. 4, pp 510–533.
283. Lin, B.; Giurgiutiu, V. *Proc. SPIE* **2005**, 5765, 1033–1044.
284. Pantani, R.; Speranza, V.; Besana, G.; Titomanlio, G. *J. Appl. Polym. Sci.* **2003**, 89 (12), 3396.
285. Doll, W. W.; Lando, J. B. *J. Appl. Polym. Sci.* **1970**, 14, 1767–1773.
286. Glass, A. French Patent 1,570,233, 1969.
287. Charpentier, P. A.; Kennedy, K.; DeSimone, J. M.; Roberts, G. W. *Macromolecules* **1999**, 32, 5973–5975.
288. Beginn, U.; Najjar, R.; Ellmann, J.; Möller, M. *Chem. Ing. Tech.* **2011**, 83 (9), 1419–1442.
289. Liu, J.; Tai, H.; Howdle, S. M. *Polymer* **2005**, 46 (5), 1467.
290. Ahmed, T. S.; DeSimone, J. M.; Roberts, G. W. *Chem. Eng. Sci.* **2004**, 59 (22), 5139.
291. Tai, H.; Wang, W.; Martin, R.; Liu, J.; Lester, E.; Licence, P.; Woods, H. M.; Howdle, S. M. *Macromolecules* **2005**, 38 (2), 355.
292. Gangal, S. V.; Brothers, P. D. Perfluorinated Polymers, Perfluorinated Ethylene–Propylene Copolymers. In *Encyclopedia of Polymer Science and Technology*; John Wiley & Sons, Inc., 2002.
293. Gangal, S. V. Perfluorinated Polymers, Tetrafluoroethylene–Ethylene Copolymers. In *Encyclopedia of Polymer Science and Technology*; John Wiley & Sons, Inc., 2002.
294. Gangal, S. V.; Brothers, P. D. Perfluorinated Polymers, Tetrafluoroethylene–Perfluorodioxole Copolymers. In *Encyclopedia of Polymer Science and Technology*; John Wiley & Sons, Inc., 2002.
295. Rindfleisch, F.; DiNoia, T. P.; McHugh, M. A. *Polym. Mater. Sci. Eng.* **1996**, 74, 178–179.
296. Rindfleisch, F.; DiNoia, T. P.; McHugh, M. A. *J. Phys. Chem.* **1996**, 100 (38), 15581.
297. Louie, B. M.; Carratt, G. M.; Soong, D. S. *J. Appl. Polym. Sci.* **1985**, 30 (10), 3985.
298. Cooper, A. L. and DeSimone, J. M. *Polym. Mater. Sci. Eng.* **1996**, 74, 262–263.
299. Hsiao, Y.-L.; Maury, E. E.; DeSimone, J. M.; Mawson, S.; Johnston, K. P. *Macromolecules* **1995**, 28 (24), 8159.
300. Qadir, M. A.; DeSimone, J. M.; van Herk, A. M.; German, A. L. *Macromolecules* **1998**, 31 (19), 6481.
301. Wang, Z.; Yang, Y. J.; Dong, Q. Z.; Hu, C. P. *J. Appl. Polym. Sci.* **2008**, 110 (1), 468.
302. POLYSTYRENE <http://www.societechimiquedefrance.fr/extras/Donnees/mater/ps/texps.htm>.
303. Odian, G. Radical Chain Polymerization. In *Principles of Polymerization, Fourth Edition*; John Wiley & Sons, Inc., 2004; pp 198–349.
304. Liu, J.; Han, B.; Liu, Z.; Wang, J.; Huo, Q. *J. Supercrit. Fluids* **2001**, 20 (2), 171.
305. Kagiya, T.; Machi, S.; Hagiwara, M.; Kise, S. Polymerization of ethylene by means of radical initiation using carbon dioxide as reaction medium. US3471463 A, October 7, 1969.
306. Ltd, R. and M. The Ethylene Technology Report 2016 - Research and Markets <https://www.researchandmarkets.com/reports/3643672/the-ethylene-technology-report-2016>.
307. Roscoe, H.-E. A. du texte; Schorlemmer, C. A. du texte. *A treatise on chemistry. Vol. 1 / by H. E. Roscoe, ... and C. Schorlemmer, ...*; Macmillan: London, 1879.
308. Priestley, J.; Johnson, J.; Adams, J.; John Adams Library (Boston Public Library) MB (BRL). *Experiments and observations relating to the various branches of natural philosophy: with a continuation of the observations on air*; London: Printed [sic] for J. Johnson, no. 72, St. Paul's Church-Yard, 1779.
309. Hofmann A. W. *Proc. Roy. Soc. London* **1866**, 15, 55–62.
310. Ethylene. *Wikipedia*; 2018.
311. Magnussen, P. *Chem. Ing. Tech.* **1981**, 53 (2), 116–116.
312. Lazonby, J. Ethene (Ethylene) <http://www.essentialchemicalindustry.org/chemicals/ethene.html>.
313. Ethylene Uses and Market Data <https://www.icis.com/>.
314. Pechmann, H. v. *Ber. Dtsch. Chem. Ges.* **1894**, 27 (2), 1888–1891.
315. Friedrich, M. E. P.; Marvel, C. S. *J. Am. Chem. Soc.* **1930**, 52, 376.

316. Fawcett, E. W. G.; Gibson, R. O.; Perrin, M. W.; Patton, J. G.; Williams, E. G. B. Patent, 471,590, 1937.
317. Demirors, M. In *100+ Years of Plastics. Leo Baekeland and Beyond*; ACS Symposium Series; American Chemical Society, 2011; Vol. 1080, pp 115–145.
318. Huang, Y. J. *Mater. Sci.* **1988**, *23*, 3648.
319. Brown, N. J. *Mater. Sci.* **1983**, *18*, 1405.
320. Fischer, E. W. L.; Lorenz, R. *Kolloid -Z. Polym.* **1963**, *189*, 197.
321. Kawak, T. *Macromol. Chem.* **1966**, *90*, 288.
322. Seguela, R. J. *Polym. Sci., Part B: Polym. Phys.* **2005**, *43* (14), 1729–1748.
323. Swan, P. R. J. *Polym. Sci.* **1962**, *56*, 409.
324. Antipov, E. M. A.; Samusenko, I. V.; Pelzbauer, Z. J. *Polym. Sci., Polym. Phys.* **1991**, *30*, 245.
325. Vonk, S. C. R.; Raynaers, H. *Polym Commun* **1990**, *31*, 190.
326. Li, D. S.; et al. *Polymer* **2003**, *44*, 5355.
327. Kennedy, M. A. *Macromolecules* **1995**, *28*, 1407.
328. Zhang, X. M. E.; Elkoun, S.; Ajji, A.; Huneault, M. A. J. *Plast. Film Sheeting* **2004**, *20* (1), 43.
329. Mattice, W. L.; Stehling, F. C. *Macromolecules* **1981**, *14*, 1479.
330. Hogan, J. P.; Banks, R. L. J. *Polym. Sci., Part A-1* **1970**, *8*, 2637.
331. McDaniel, M. P. In *Advances in Catalysis*; Gates, B. C., Knözinger, H., Eds.; Academic Press, 2010; Vol. 53, pp 123–606.
332. McDaniel Max P. Review of the Phillips Chromium Catalyst for Ethylene Polymerization. *Handb. Heterog. Catal.* **2008**, 3733–3792.
333. McDaniel Max P. Review of Phillips Chromium Catalyst for Ethylene Polymerization. *Handb. Transit. Met. Polym. Catal.* **2010**, 291–446.
334. Nowlin, T. E.; Mink, R. I.; Kissin, Y. V. In *Handbook of Transition Metal Polymerization Catalysts*; Hoff, R., Thers, R., Eds.; John Wiley & Sons, Inc., 2010; pp 131–155.
335. Böhm Ludwig L. The Ethylene Polymerization with Ziegler Catalysts: Fifty Years after the Discovery. *Angew. Chem. Int. Ed.* **2003**, *42* (41), 5010–5030.
336. Eisch, J. J. Fifty Years of Ziegler–Natta Polymerization: From Serendipity to Science. A Personal Account. *Organometallics* **2012**, *31* (14), 4917–4932.
337. *Polyolefins: 50 Years after Ziegler and Natta I*; Kaminsky, W., Ed.; Advances in Polymer Science; Springer Berlin Heidelberg: Berlin, Heidelberg, 2013; Vol. 257.
338. Kealy, T. J.; Pauson, P. L. *Nature* **1951**, *168* (4285), 1039.
339. Miller, S. A.; Tebboth, J. A.; Tremaine, J. F. J. *Chem. Soc. Resumed* **1952**, *0* (0), 632.
340. Wilkinson, G.; Rosenblum, M.; Whiting, M. C.; Woodward, R. B. *J. Am. Chem. Soc.* **1952**, *74* (8), 2125.
341. Long, W. P.; Breslow, D. S. J. *Am. Chem. Soc.* **1960**, *82*, 1953.
342. Natta, G.; Pino, P.; Mazzanti, G.; Giannini, U.; Montica, E.; Peralto, M. J. *Polym. Sci.* **1957**, *26*, 120.
343. Sinn, H.; Kaminsky, W. *Adv. Organomet. Chem.* **1980**, *18*, 99.
344. Sinn, H.; Kaminsky, W.; Vollmer, H. J.; Woldt, R. *Angew. Chem. Int. Ed. Engl.* **1980**, *19*, 390.
345. Herskovics-Korine, D.; Eisen, M. S. J. *Organomet. Chem.* **1995**, *503*, 307.
346. Johnson, L. K.; Killian, C. M.; Brookhart, M. S. J. *Am. Chem. Soc.* **1995**, *117*, 6414.
347. Small, B. L.; Brookhart, M. S.; Bennett, A. M. J. *Am. Chem. Soc.* **1998**, *120*, 4049.
348. Britovsek, G. J. P.; Gibson, V. C.; Kimberley, B. S.; Maddox, J.; McTavish, S. J.; Solan, G. A.; White, A. P.; Williams, D. *Chem. Commun.* **1998**, 849.
349. Younkin, T. R.; Connor, E. F.; Hendreson, J. I.; Friedrich, S. K.; Grubbs, R. H.; Bansleben, D. A. *Science* **2000**, *287*, 460.
350. Ihata, O.; Kayaki, Y.; Ikariya, T. *Macromolecules* **2005**, *38*, 6429–6434.
351. Liu, Z.; Torrent, M.; Morokuma, K. *Organometallics* **2002**, *21*, 1056–1071.
352. Darensbourg, D. J.; Yarbrough, J. C.; Ortiz, C.; Fang, C. C. J. *Am. Chem. Soc.* **2003**, *125*, 7586–7591.
353. Odian, G. *Principles of Polymerization*, 4th ed.; Wiley-Interscience: New York, 2004; p 275.
354. Jessup, R. S. J. *Chem. Phys.* **1948**, *16*, 661–664.
355. Cohen, N.; Benson, S. W. *Chem. Rev.* **1993**, *93*, 2419–2438.
356. Benson, S. W.; Cruickshank, F. R.; Golden, D. M.; Haugen, G. R.; O’Neal, H. E.; Rodgers, A. S.; Shaw, R.; Walsh, R. *Chem. Rev.* **1969**, *69*, 279–324.
357. Moha, V.; Cozzula, D.; Hölscher, M.; Leitner, W.; Müller, T. E. *ChemSusChem* **2016**, *9* (13), 1614–1622.

358. Shultz, C. S.; Ledford, J.; DeSimone, J. M.; Brookhart, M. *J. Am. Chem. Soc.* **2000**, *122* (27), 6351–6356.
359. Allegra G. *Makromol. Chem.* **1971**, *145* (1), 235–246.
360. Vela, J.; Lief, G. R.; Shen, Z.; Jordan, R. F. *Organometallics* **2007**, *26* (26), 6624–6635.
361. Soomro, S. S.; Cozzula, D.; Leitner, W.; Vogt, H.; Müller, T. E. *Polym. Chem.* **2014**, *5* (12), 3831–3837.

B. CHAPTER II. Ethylene Free Radical Polymerization in Supercritical CO₂.

Table of Contents

B.1. Abstract	110
B.2. Construction and Testing of the High-Pressure Reactor	110
B.2.1. Construction.....	110
B.2.2. Testing	112
B.2.2.1. Pressurizing with Ethylene	114
B.2.2.2. Pressurizing with CO₂.....	114
B.2.2.3. Pressurizing with a Mixture of Ethylene and CO₂.....	117
B.2.2.4. Average Increase of Pressure	119
B.3. Ethylene Free Radical Polymerization in scCO₂.....	119
B.3.1. Recent Work at LCPP: Ethylene Free Radical Polymerization under Mild Conditions by the Effect of Solvent	120
B.3.2. Ethylene Free Radical Polymerization in scCO₂ under Mild Conditions. 121	
B.3.2.1. Radical Initiators	122
B.3.2.2. AIBN-Initiated Reactions.....	124
B.3.2.3. Lauroyl Peroxide-Initiated Reactions.....	128
B.3.2.4. Benzoyl Peroxide-Initiated Reactions	134
B.4. Conclusion	142
B.5. References	144

B.1. Abstract

This chapter deals with ethylene free radical polymerization in supercritical CO₂ as a solvent or a reaction medium without any addition of organic solvent and under mild conditions (< 100°C, < 300 bar) with respect to conventional radical polymerization processes (1000-4000 bar). The polymerization reactions showed success using three different radical initiators. The effects of CO₂ pressure on the yield and the molar masses of the polyethylene produced have been investigated using the different initiators. The polyethylenes produced were analyzed thoroughly and compared in details to those produced by ethylene free radical polymerization in organic solvents. The construction and testing of the high-pressure reactor, in which the reactions were performed, have been explained in the first part of this chapter.

B.2. Construction and Testing of the High-Pressure Reactor

Before starting by the body of this chapter it is important to show in details the apparatus in which we have done our reactions, especially because it is not easy to have access to the conditions (supercritical conditions) that we need in our reactions. This part will explain the construction of the high-pressure reactor system and the tests done to study the pressure variation with respect to time, especially in the case of CO₂ gas which is used for the first time at LCPP under such high pressures.

B.2.1. Construction

First, our team put a general scheme for the apparatus that we will need in our manipulations (**Figure 1**, **Figure 2/a**). This apparatus is formed of a high-pressure reactor, which was ordered from "Parr Instrument Company", connected to a heating system (a circulating oil system, heating up to 200 °C) ordered from "Julabo" (**Figure 2/b**). In addition, two intermediate ballasts were constructed (ethylene and CO₂ ballasts) and connected from one side to the corresponding gas bottle and from the other side to a main ballast which is in its role connected to the reactor; all pieces are connected through high pressure resistant lines. The main ballast is also connected to a cooling/heating system (a circulating oil system; the temperature range of the used oil is from -60 °C till 80 °C) ordered from "Lauda" (**Figure 2/c**). This cooling system is needed to condense the gas in the main ballast in order to attain high pressures by isolating the

ballast and re-increasing the temperature (condensation process is summarized in a scheme in **Figure 3**). Other constituents include a pressure controller, a pressure and temperature detector for the reactor and the main ballast (**Figure 2/d**), manometers and safety valves for the reactor and for each ballast (safety valves are fixed at 344 bar for the reactor and the main ballast, and at 70 bar for the intermediate ballasts), and lines and valves that are able to hold out high pressures (**Figure 1**, **Figure 2/a**). The construction of this system took one month.

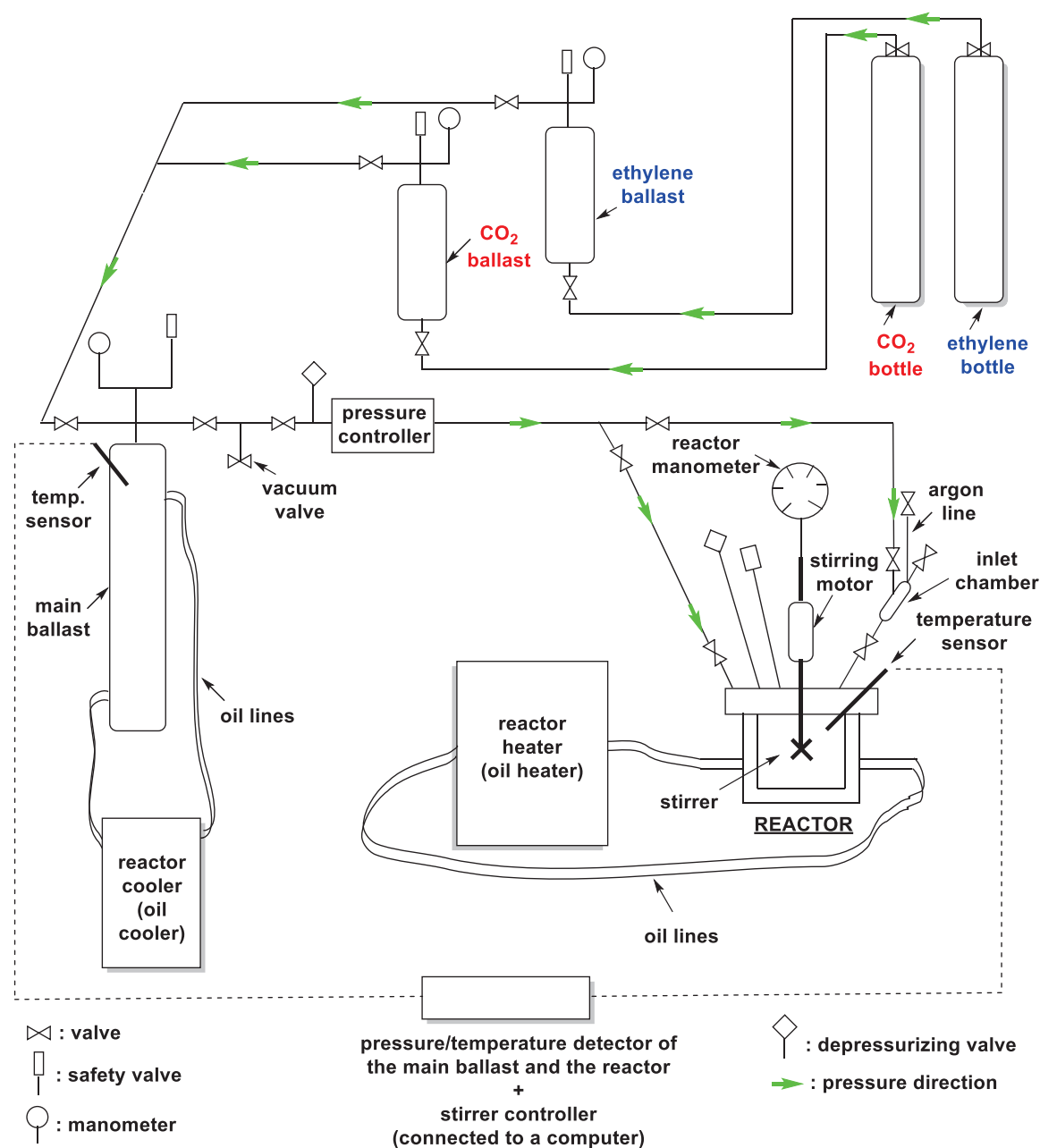


Figure 1. Schematic representation of the high-pressure reactor.

a)



b)



c)



d)



Figure 2. a) The constructed high-pressure reactor system; b) The reactor heater; c) The main ballast cooler; d) The pressure-temperature detector.

B.2.2. Testing

After constructing the reactor, we tested its performance to avoid any danger that could occur, especially because our reactions will be performed at pressures too much higher than the atmospheric pressure.

The tests were classified into two parts: tests in the main ballast and tests in the reactor. These tests concentrate on the variation of pressure of each gas (ethylene, CO_2 , and a mixture of both gases) with respect to temperature. The calculations were done either for one condensation of the gas in the main ballast or for a double condensation, where a double condensation is done to reach the target pressure which couldn't be attained by one condensation due to the limited pressure that the intermediate ballasts could hold out (maximum 70 bar). For simplicity: **a) One condensation:** It is done by

filling the intermediate ballast with 50 bar of the desired gas from its bottle, then pressurizing the main ballast from the intermediate one and cooling it (condensing) till -20 °C while keeping the valve between both ballasts opened. After that, this valve is closed and the main ballast is heated in order to achieve higher pressure (**Figure 3**); **b) Double condensation:** It is done by filling the intermediate ballast with 50 bar of the desired gas from its bottle, then pressurizing the main ballast from the intermediate one and cooling it (condensing) till -20 °C while keeping the valve between both ballasts opened. After that, this valve is closed and the intermediate ballast is re-filled to re-pressurize the main one while its temperature is still at -20 °C. By re-pressurizing the main one while its temperature is still at -20 °C. By re-pressurizing the main ballast the temperature will increase (temperature increases by increasing pressure), then the gas is re-condensed till reaching -20 °C. After that, the valve between the main and the intermediate ballasts is closed and the main ballast is heated in order to achieve higher pressure (**Figure 3**).

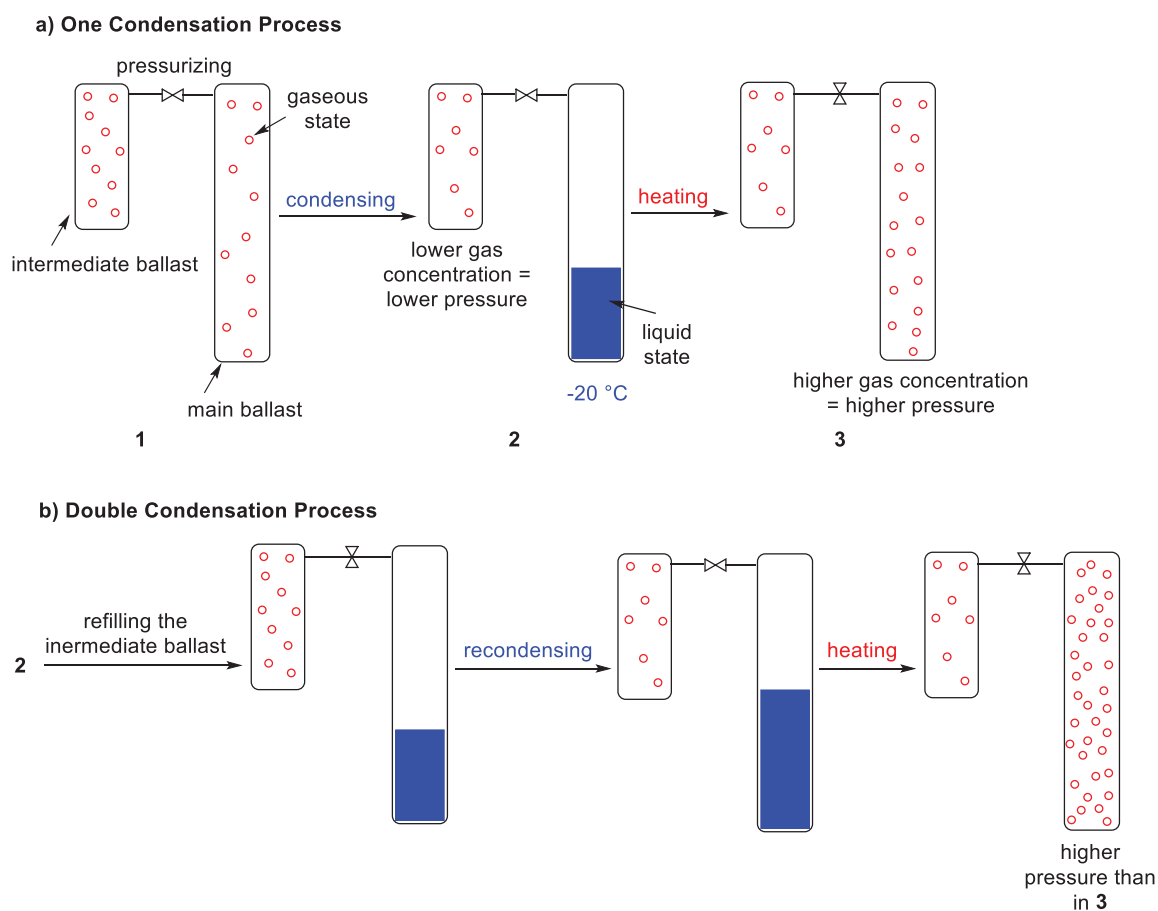


Figure 3. Schematic representation of the one and double condensation processes.

B.2.2.1. Pressurizing with Ethylene

We started a basic examination by pressurizing the main ballast and the reactor with ethylene, which has been already examined at LCPP group during the previous projects dealing with ethylene radical polymerization processes. We will just mention briefly a double check test for the main ballast since our team is familiar with the manipulation at high pressures of ethylene.

In the main ballast:

a) One Condensation:

- Time to reach -20 °C (-17 °C) (condensation): 1 h 5 min.
- Pressure in the main ballast at -17 °C: 27 bar.
- Time to reach 20 °C (heating): 35 min.
- Pressure in the main ballast at 20 °C: 47 bar.

b) Double Condensation:

- After carrying out the primary condensation then repressurizing the main ballast (after refilling the intermediate ballast by ethylene), the pressure reached 42 bar and temperature increased till -1 °C.
- Time to reach -20 °C (-17 °C) (condensation): 20 min.
- Pressure in the main ballast at -17 °C: 29 bar.
- Time to reach 20 °C (heating): 30 min.
- Pressure in the main ballast at 20 °C: 55 bar.
- Time to reach 60 °C (57 °C): 1 h.
- Pressure in the main ballast at 60 °C (57 °C): 92 bar.

Another method to go up to higher pressures of ethylene is by pressurizing the main ballast directly from the ethylene bottle: pressurizing by 42 bar and condensing at -20 °C give 200 bar at 20 °C.

B.2.2.2. Pressurizing with CO₂

Because dealing with CO₂ at high pressures is a new skill at LCPP, a detailed examination has been done to maintain safety during the manipulation.

In the main ballast:

a) One Condensation:

- Time to reach -20 °C (-17 °C) (condensation): 1 h 10 min.
- Pressure in the main ballast at -17 °C: 21 bar.
- Time to reach 20 °C (heating): 28 min.
- Pressure in the main ballast at 20 °C: 49 bar.
- Time to reach 60 °C (57 °C): 1 h 15 min.
- Pressure in the main ballast at 60 °C (57 °C): 63 bar.

Heating the ballast: the graph in **Figure 4** shows the variation of pressure with respect to temperature after a one condensation process in the main ballast.

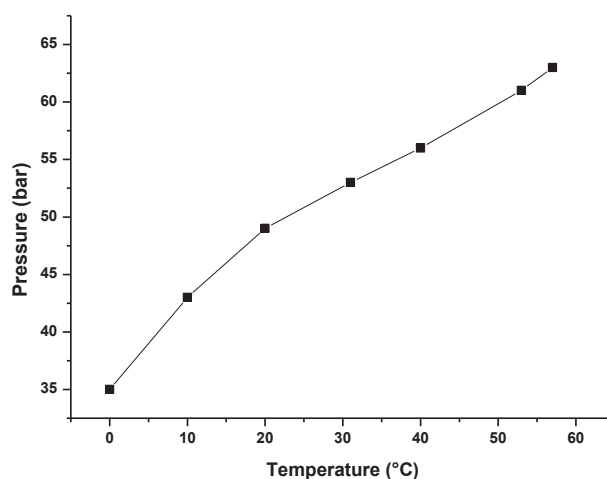


Figure 4. The variation of pressure of CO₂ as function of temperature after a one condensation process in the main ballast.

b) Double Condensation:

- After carrying out the primary condensation then repressurizing the main ballast (after refilling the intermediate ballast by CO₂), the pressure reached 29 bar and the temperature increased till 3 °C in the main ballast.
- Time to reach -20 °C (-17 °C) (condensation): 23 min.
- Pressure in the main ballast at -17 °C: 23 bar.
- Time to reach 20 °C (heating): 21 min.
- Pressure in the main ballast at 20 °C: 56 bar.
- Time to reach 60 °C (57 °C): 1 h.
- Pressure in the main ballast at 60 °C (57 °C): 95 bar.

Heating the ballast: the graph in **Figure 5** shows the variation of pressure with respect to

temperature after a double condensation in the main ballast.

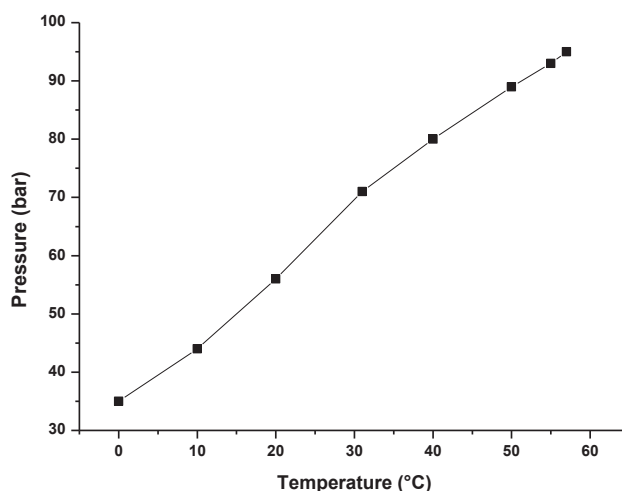


Figure 5. The variation of pressure of CO₂ as function of temperature after a double condensation process in the main ballast.

Another method to go up to higher pressures of CO₂ is by pressurizing the main ballast directly from the CO₂ bottle: pressurizing by 39 bar and condensing at -20 °C give 200 bar at 20 °C.

In the reactor:

After attaining 95 bar in the main ballast (pressure at 57 °C after a double condensation), we pressurized the reactor to test the variation of pressure in it with respect to temperature. The pressure attained primarily is 67 bar at a temperature of 27 °C, it increased by increasing the temperature till it reached 143 bar at 70 °C (**Figure 6**).

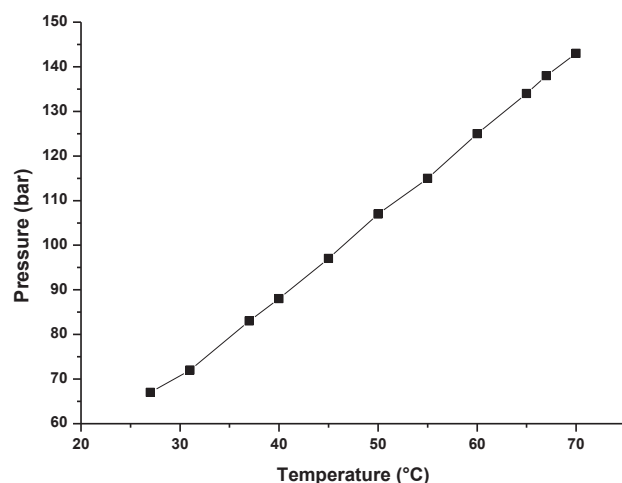


Figure 6. The variation of pressure of CO₂ as function of temperature in the reactor.

B.2.2.3. Pressurizing with a Mixture of Ethylene and CO₂

It was also important to measure the variation of pressure versus temperature for a mixture of ethylene and CO₂. In this case, both intermediate ballasts are filled to pressurize simultaneously the main ballast.

In the main ballast:

a) One Condensation:

- Time to reach -20 °C (-17 °C) (condensation): 1 h 30 min.
- Pressure in the main ballast at -17 °C: 27 bar.
- Time to reach 20 °C (heating): 24 min.
- Pressure in the main ballast at 20 °C: 62 bar.
- Time to reach 60 °C (57 °C): 57 min.
- Pressure in the main ballast at 60 °C (57 °C): 88 bar.

Heating the ballast: the graph in **Figure 7** shows the variation of pressure of ethylene/CO₂ mixture with respect to temperature after one condensation.

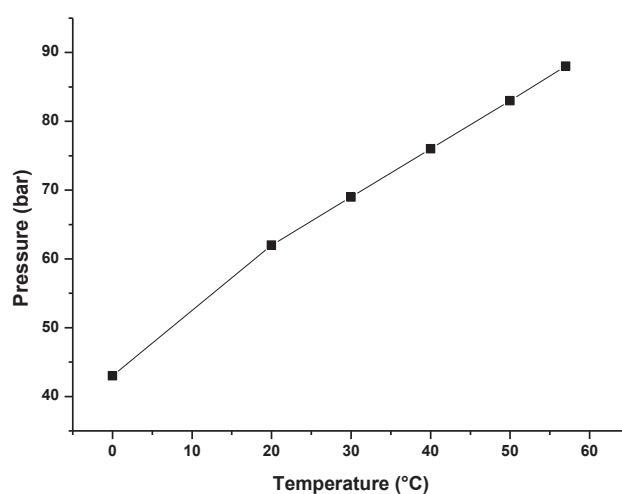


Figure 7. The variation of pressure of ethylene/CO₂ mixture as function of temperature after a one condensation process in the main ballast.

b) Double Condensation:

After carrying out the primary condensation then repressurizing the main ballast (after refilling the intermediate ballast), the pressure reached 42 bar and temperature increased till 1 °C.

- Time to reach -20 °C (-17 °C) (condensation): 20 min.

- Pressure in the main ballast at -17 °C: 30 bar.
- Time to reach 20 °C (heating): 35 min.
- Pressure in the main ballast at 20 °C: 72 bar.
- Time to reach 60 °C (57 °C): 1 h 11 min.
- Pressure in the main ballast at 60 °C (57 °C): 138 bar.

Heating the ballast: the graph in **Figure 8** shows the variation of pressure with respect to temperature after a double condensation.

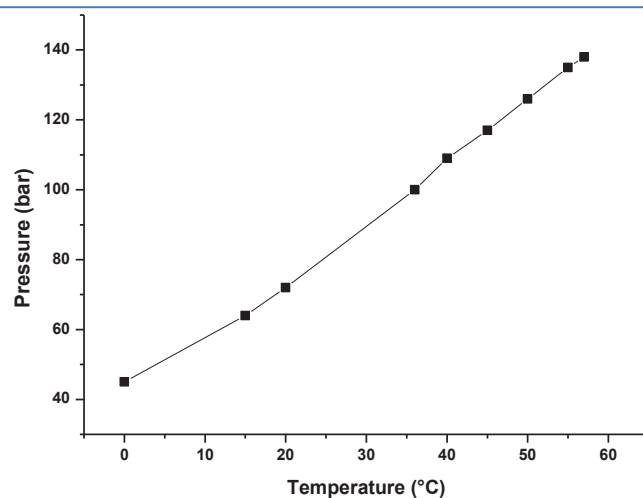


Figure 8. The variation of pressure as function of temperature after a double condensation process in the main ballast.

In the reactor:

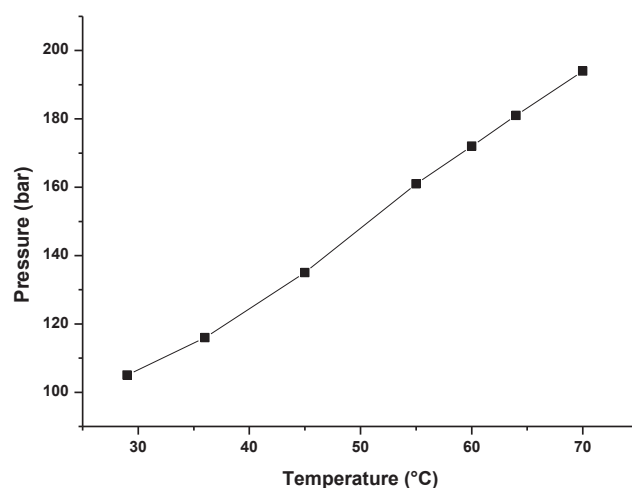


Figure 9. The variation of pressure as function of time in the reactor.

After attaining 138 bar in the main ballast (pressure at 57 °C after a double condensation), we pressurized the reactor to test the variation of pressure in it with

respect to temperature. The pressure attained primarily is 105 bar at a temperature of 29 °C, it increased by increasing the temperature till it reached a pressure of 194 bar at 70 °C (**Figure 9**).

B.2.2.4. Average Increase of Pressure

As a result, the average increase of pressure per 1 °C while pressurizing the main ballast (**Table 1**) and the reactor (**Table 2**) by CO₂ or ethylene/CO₂ are shown below:

Table 1. Average pressure increase per 1 °C in the main ballast.

Gas	Average pressure increase (bar/ 1 °C)
CO ₂ (one condensation)	0.5
CO ₂ (double condensation)	1.04
Ethylene + CO ₂ (one condensation)	0.8
Ethylene + CO ₂ (double condensation)	1.6

Table 2. Average pressure increase per 1 °C in the reactor.

Gas	Average pressure increase (bar/ 1 °C)
CO ₂ (double condensation)	1.8
Ethylene + CO ₂ (double condensation)	2.26

B.3. Ethylene Free Radical Polymerization in scCO₂

Carbon Dioxide is a renewable, non-toxic, and inexpensive C1 building block that can be used for many synthetic applications in chemistry.¹ Due to its abundance, as a byproduct of many chemical processes (such as the combustion of organic fuels, the aerobic metabolic processes of living organisms, the decay of organic materials, and the fermentation of sugars) and its need for harvesting and/or use to relieve its impact on the Earth's environment, it constitutes a prime target for the design of processes, either as a reactant or a reagent or a reaction medium.

The use of CO₂ as a sustainable polymerization medium constitutes a valuable starting point to new industrial processes for material production. A straightforward implementation of scCO₂ as a solvent was realized when polysiloxanes and fluoropolymers were identified as materials displaying high solubilities in CO₂ at easily

attainable temperatures ($T < 100\text{ }^{\circ}\text{C}$) and pressures ($P < 350\text{ bar}$).²

Free radical polymerization is one of the most utilized processes in polymer production. It is utilized in the production of a large fraction of polyolefins in the form of low density polyethylene (LDPE), it is also employed for most of the polar vinylic monomers including styrenics, acrylics, and vinyl esters. LDPE is a widely demanded polyolefin, and is currently produced *via* radical polymerization processes under harsh conditions ($T = 200\text{--}300\text{ }^{\circ}\text{C}$, $P = 1000\text{--}4000\text{ bar}$).^{3,4}

We find it important to introduce our work on ethylene free radical polymerization in scCO_2 under mild conditions starting by the recent work that has been done in our group on ethylene free radical polymerization under mild conditions by the effect of solvent.⁵⁻⁷

B.3.1. Recent Work at LCPP: Ethylene Free Radical Polymerization under Mild Conditions by the Effect of Solvent

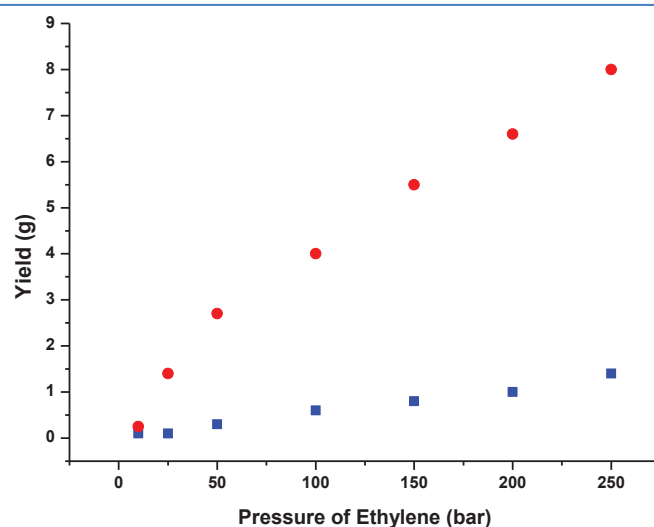


Figure 10. Pressure influence on ethylene radical polymerization: (blue) 50 mg of AIBN, 50 mL of toluene, 4 h at $70\text{ }^{\circ}\text{C}$ under ethylene pressure; (red) 50 mg of AIBN, 50 mL of THF, 4 h at $70\text{ }^{\circ}\text{C}$ under ethylene pressure.⁵

As aforementioned, free radical polymerization of ethylene is performed industrially under high pressure (1000-4000 bar) and high temperature (200-300 $^{\circ}\text{C}$) in bulk.^{3,4} Monteil et al. reported a radical polymerization of ethylene under mild conditions ($< 100\text{ }^{\circ}\text{C}$, $< 300\text{ bar}$) through the impact of solvent.⁵ The graph in **Figure 10** shows the variation of the mass of polyethylene produced as function of ethylene pressure in

tetrahydrofuran (THF) and toluene, where the activity in THF was really higher than that in toluene. All molar masses obtained are less than 3000 g/mol, which was attributed to transfer reactions to THF and evidenced by NMR spectroscopy. By screening a series of solvents under the same conditions mentioned in **Figure 10**, dimethylcarbonate (DMC) gave the highest molar mass for the produced polyethylene, with at 100 bar a M_n of 12000 g/mol and a yield of 1.6 g in 4 hours, using 50 mg of AIBN as initiator.⁷ At 200 bar of ethylene, under the same conditions, 2.8 g of polyethylene with a M_n = 16600 g/mol was produced.⁸

After this achievement, our team was looking for a greener alternative to the organic solvent with the maintenance of the advantage of polymerizing under mild conditions. The choice was CO₂ because of its various advantages as aforementioned (it is abundant, readily available, greener than organic solvents, etc.). Thus, we investigated thoroughly the free radical polymerization of ethylene in scCO₂ under mild conditions.

B.3.2. Ethylene Free Radical Polymerization in scCO₂ under Mild Conditions

Great efforts have been undertaken to use CO₂ as an alternative to conventional organic solvents.⁹⁻¹¹ Different goals and purposes have been achieved as mentioned previously, especially in the polymer field where CO₂ is now used as a multipurpose solvent, from impregnation of small molecules to washing of residual monomers or contaminants to polymerization medium for instance in fluorinated-monomer polymerizations.

Since ethylene is the most industrially relevant monomer, it appeared evident that investigating the use of CO₂ as a medium of ethylene radical polymerization would be of interest to the polymer chemist. We thus designed experiments using scCO₂ as the only solvent of polymerization, under mild conditions and using different initiators.

To the best of our knowledge, the only mention in the literature of the use of CO₂ as a polymerization medium in ethylene free radical polymerization processes was reported by Kagiya and coworkers in 1960s,¹² where they used 1.22 mmol (0.2 g) of azobisisobutyronitrile (AIBN) as an initiator, ethylene pressure of 392 bar (400 kg/cm²) at 55°C for 4 h. The yield obtained was 3 g, but they added 10 mL of 2-ethyl-hexyl adipate as an initiator diluent, therefore another organic solvent was required in their

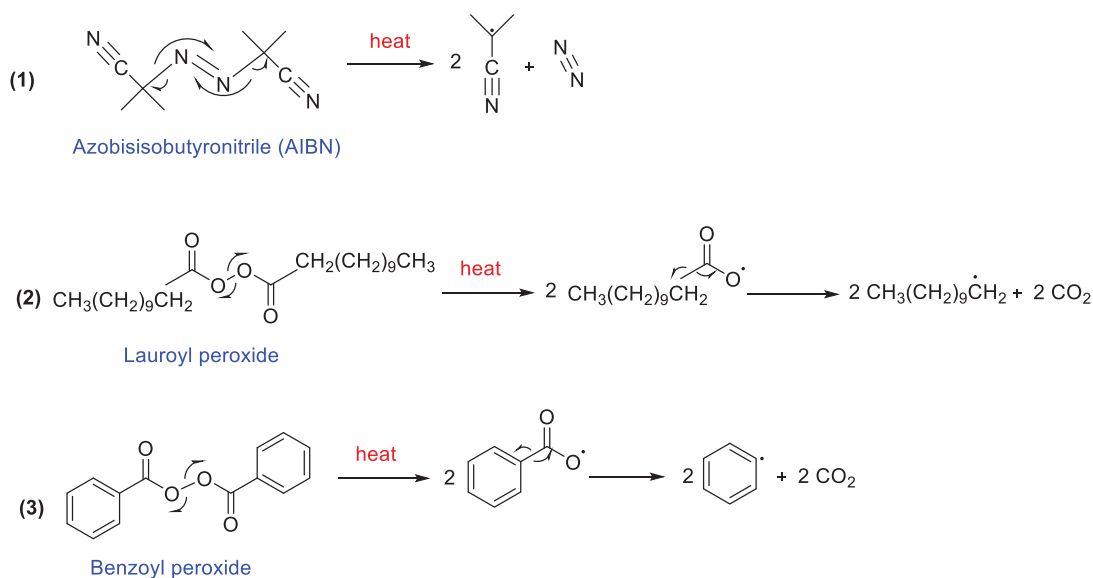
experiment.

In our work, we achieved the free radical polymerization of ethylene in CO₂ under mild conditions without the addition of any diluent other than scCO₂. Also, a screening of AIBN, lauroyl peroxide and benzoyl peroxide as initiators has been done to investigate the effect of the polymerization medium on the activity and the initiation process.

B.3.2.1. Radical Initiators

Three radical initiators were selected and evaluated in the polymerization of ethylene in CO₂. The thermal decompositions of the three initiators (AIBN, lauroyl peroxide, and benzoyl peroxide) are shown in **Scheme 1**. Reactions **(2)** and **(3)** show that the secondary decomposition of both peroxides produces CO₂, consequently, under high pressure of CO₂ this decomposition was anticipated not to be favorable. Thus, the production of the active phenyl and primary radicals that are produced from benzoyl peroxide and lauroyl peroxide respectively would decrease.

Scheme 1. Thermal decomposition of the radical initiators.



In order to have comparable rates of decompositions of the three initiators (**Table 3**), the reactions initiated by AIBN and lauroyl peroxide were done at 70 °C, while those initiated by benzoyl peroxide were done at 90 °C. In all cases, solubility of the initiating system was verified using a sapphire-windowed reactor (**Figure 11**), and solubilization was achieved when supercritical state was reached for the reaction mixture.

The process was done in CO₂ without any addition of organic solvent or diluent (**Scheme 2**). The variation of CO₂ pressure decides its state, above its critical point (the critical point of carbon dioxide occurs at $P=73$ bar and $T=31$ °C) CO₂ is in its supercritical state. Ethylene critical point occurs at $P=50$ bar and $T=9$ °C, thus it is in its supercritical state in all the reactions. Here, the mixture of the two gases (ethylene and CO₂) is always in its supercritical state because all reactions were done at pressures > 100 bar and temperatures > 50 °C.¹³

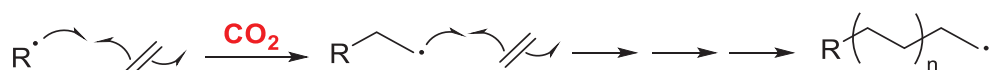
Table 3. Maximum rates of decomposition of the radical initiators.

Initiator	Temperature (°C)	Max. rate (s ⁻¹)
AIBN	70	$4 \cdot 10^{-5}$
Benzoyl peroxide	90	$1.7 \cdot 10^{-4}$
Lauroyl peroxide	70	$9.5 \cdot 10^{-5}$



Figure 11. Verification of the solubility of radical initiators using a sapphire-windowed reactor.

Scheme 2. Ethylene free radical polymerization in CO₂.



B.3.2.2. AIBN-Initiated Reactions.

Using AIBN as an initiator, the quantity of polyethylene (PE) produced increases as the CO₂ pressure increases (**Figure 12**). The yield increases from 0.3 g in the absence of CO₂ to 1 g under 80 bar of CO₂ added at 35 °C with the same concentration of ethylene (110 bar at 35 °C). Note that the total pressure at the reaction temperature (70 °C) varies from 180 to 280 bar under different CO₂ pressures, which means that the overall reaction mixture is always under supercritical conditions.¹³

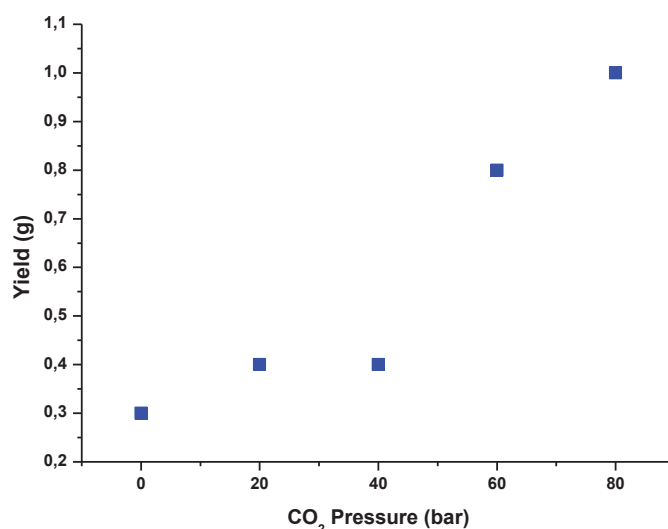


Figure 12. The variation of the yield of AIBN-initiated PE as function of CO₂ pressure.

Conditions: 0.3 mmol of AIBN, 110 bar of ethylene at 35 °C, CO₂ pressure is at 35 °C, reaction temperature: 70 °C, total pressure at the reaction temperature: 180-280 bar, each reaction lasted 3 h.

The molecular weight (Mw) of the PE produced increases as the CO₂ pressure increases. It increases from 16000 g/mol in the absence of CO₂ to 24000 g/mol under 80 bar of CO₂ added at 35 °C (**Figure 13**). The dispersity (Mw/Mn) of the polymers produced varies from 2.2 to 2.6. The melting point obtained by "Differential Scanning Calorimetry" (DSC) for all the PEs produced is close to 118 °C, which means that the PE produced is closer to MDPE than LDPE (melting point of LDPE are usually in the 105-115 °C range) (**Figure 14**).

In order to compare with the recent results achieved in our laboratory,⁷ an ethylene free radical polymerization reaction using dimethylcarbonate (DMC) as a solvent was done under the same conditions of that of the CO₂-mediated reactions, where the total pressure at the reaction temperature (70 °C) was 237 bar.

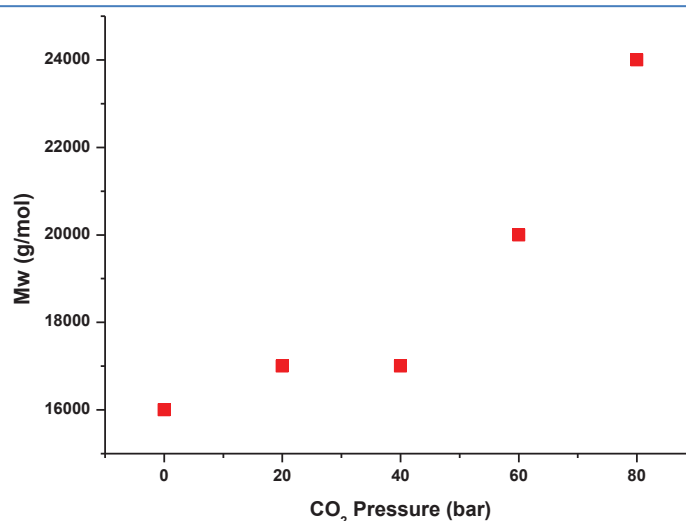


Figure 13. The variation of the molecular weight of the AIBN-initiated PE as function of CO₂ pressure. CO₂ pressure at 35 °C.

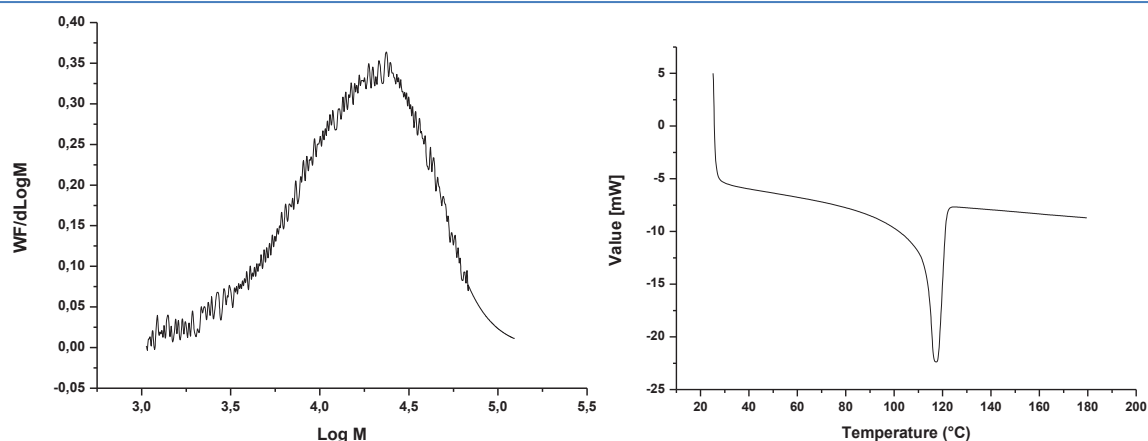


Figure 14. *To the left:* Molar mass distribution of the AIBN-initiated PE produced in CO₂ (80 bar CO₂ at 35 °C). *To the right:* DSC peak of the AIBN-initiated PE produced in CO₂ (80 bar at 35 °C).

Table 4 shows a comparison between the reaction done in 50 mL of DMC and that done under 80 bar of CO₂ added at 35 °C (the reaction with the highest activity in CO₂ using AIBN). The yield, molecular weight, and melting point of the PE produced from the polymerization reaction in DMC (0.8 g, 20000 g/mol, and 116 °C; **Figure 15**) are slightly lower than those of the PE produced in CO₂ (1 g, 24000 g/mol, and 118 °C). The dispersity of the PE produced in DMC (2.5) is higher than that of PE produced in CO₂ (2.2), thus ethylene polymerization in scCO₂ (80 bar at 35 °C) is slightly more active than that in DMC when initiated by AIBN, and produces PE of higher molar mass with narrower dispersity. The number of branches of the PE produced in CO₂ (5.56

branch/1000 C atoms) is slightly higher than that of the PE produced in DMC (5.18 branch/1000 C atoms).

Calculation of the number of branches:¹⁴

From ¹³C-NMR spectrum (**Figure 16**): (*I*= integration)

- I_a = Integration of the peak at 38.05 ppm= Integration of the peak corresponding to "^{br}B₄ + ^{br}B₅ + ^{br}B_n".
- I_b = Integration of the peak corresponding to any C atom of the PE backbone or branches; then ΣI_b = summation of all the integration of the peaks corresponding to C atoms of the PE.

Number of branches= $I_a/\Sigma I_b$.

Then: "number of branches per 1000 C atoms"= $I_a \times 1000/\Sigma I_b$.

Table 4. AIBN-initiated ethylene free radical polymerization in CO₂ (80 bar at 35 °C) versus that in DMC (50 mL).

	CO ₂ (80 bar)	DMC (50 mL)
Yield (g)	1	0.8
Mw of PE produced (g/mol)	24 000	20 000
Mw/Mn	2.2	2.6
Melting Point (°C)	118	116
Number of branches (per 1000 C atom)	5.56	5.18

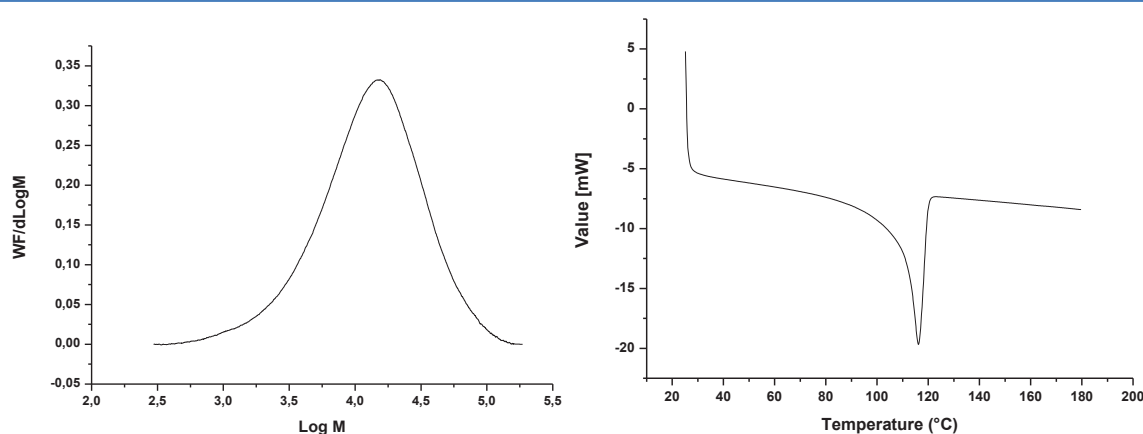


Figure 15. To the left: Molar mass distribution of the AIBN-initiated PE produced in DMC (50 mL). To the right: DSC peak of the AIBN-initiated PE produced in DMC (50 mL).

Moreover, the ¹H- and ¹³C-NMR spectra of both polymers are extremely similar; **Figure 16** represents the ¹H-NMR spectra and the aliphatic region of the ¹³C-NMR spectra for

both polymers.

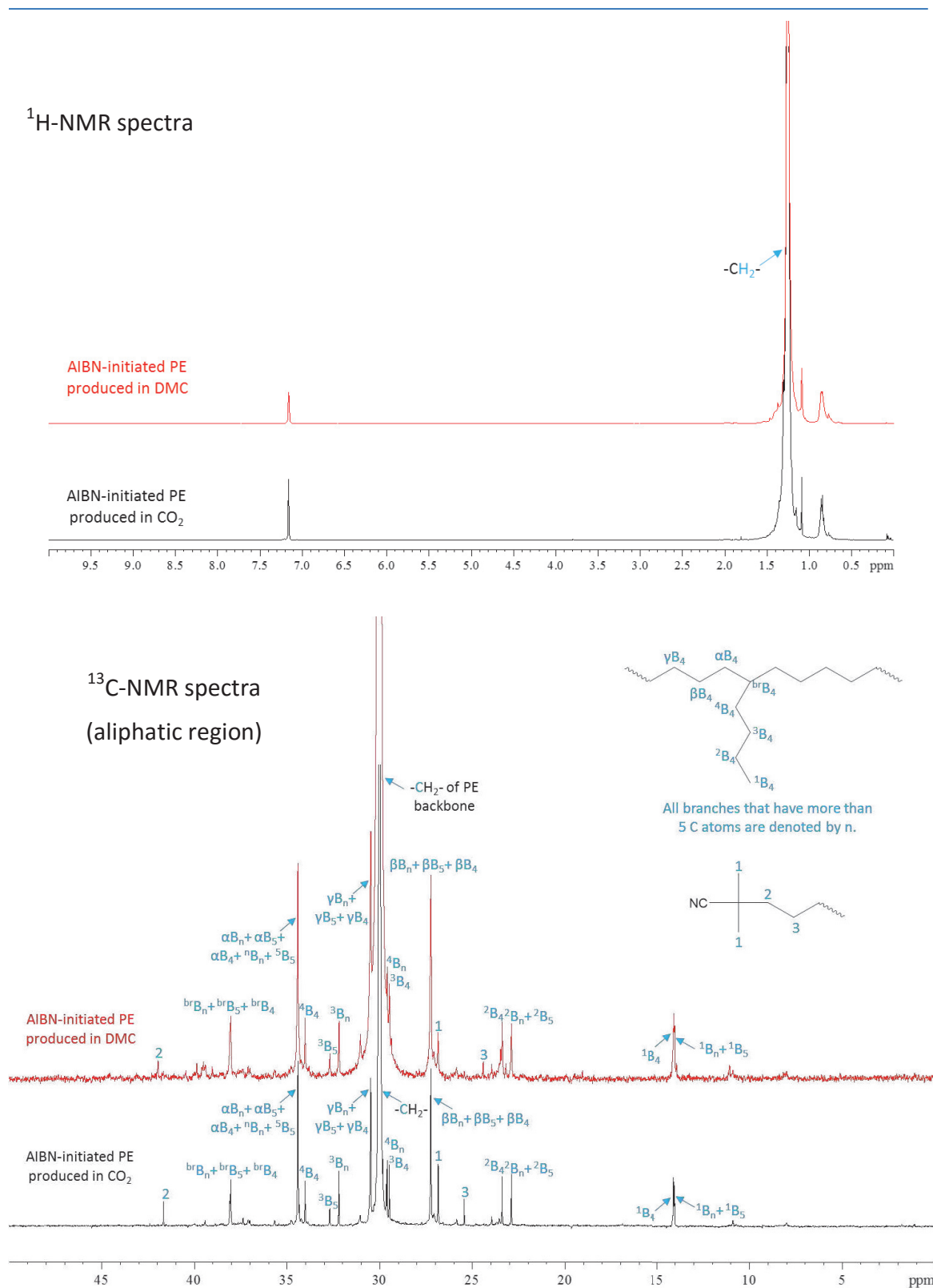


Figure 16. ¹H- and ¹³C-NMR spectra of the AIBN-initiated PE produced in CO₂ (80 bar at 35 °C) and in DMC (50 mL).

In the ^1H -NMR spectra, the peak corresponding to the protons of the methylene groups $-\text{CH}_2-$ appears at 1.26 ppm and that corresponding to the protons of the methyl chain-ends appears at 0.89 ppm; in the ^{13}C -NMR spectra, the peak corresponding to the carbon atoms of the methylene groups $-\text{CH}_2-$ appears at 30.0 ppm and that corresponding to the carbon atoms of the methyl chain-ends (and methyl branching-ends) appears at 14.1 ppm, the other peaks correspond to the carbon atoms of the different branches arising from the polymer backbone. CO_2 can therefore be considered a non-transferring solvent for the free radical polymerization of ethylene, which is a valuable feature considering the extreme reactivity of the primary polyethylenyl radical.

Figure 17 represents the infra-red spectrum of the PE produced in CO_2 (80 bar at 35 °C), the band corresponding to the PE backbone ($-\text{CH}_2-$) appears at 2840 cm^{-1} .

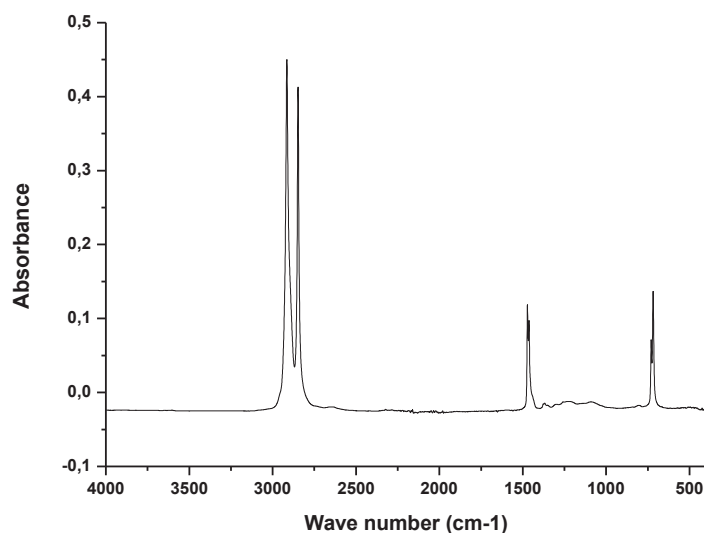


Figure 17. IR spectrum of the AIBN-initiated PE produced in CO_2 .

B.3.2.3. Lauroyl Peroxide-Initiated Reactions.

Using lauroyl peroxide as an initiator, the yield of PE produced increases strictly by the primary addition of CO_2 (20 bar at 35 °C) from 0.4 g in the absence of CO_2 to 1g in presence of CO_2 . However, by subsequently increasing the CO_2 pressure, the mass of PE produced decreases gradually to reach 0.45 g under 80 bar of CO_2 added at 35 °C (**Figure 18**). This decrease occurs due to the unfavorable secondary decomposition of lauroyl peroxide from the carboxylic radical to the primary $-\text{CH}_2\bullet$ radical in the presence of a high CO_2 concentration in the medium, since CO_2 is itself a by-product of the secondary

decomposition reaction (**Scheme 1-(2)**). Thus, the lauroyl peroxide carboxylic radical isn't successful in the initiation of ethylene polymerization or it is producing PE chains with very low molar masses that are soluble in methanol (precipitation solvent to remove the traces of initiator by-products).

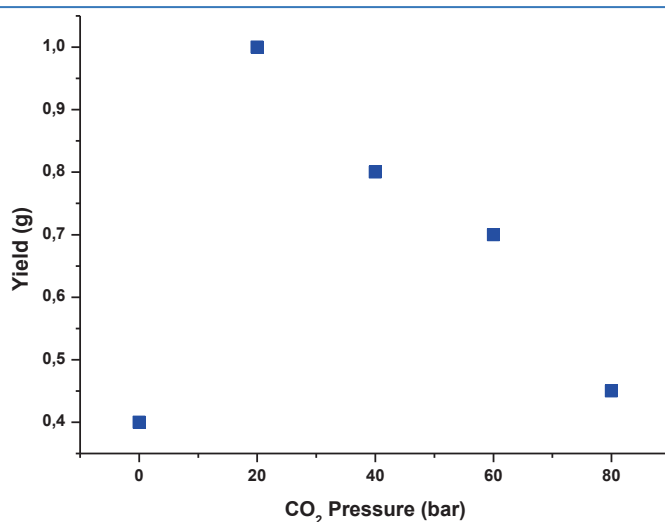
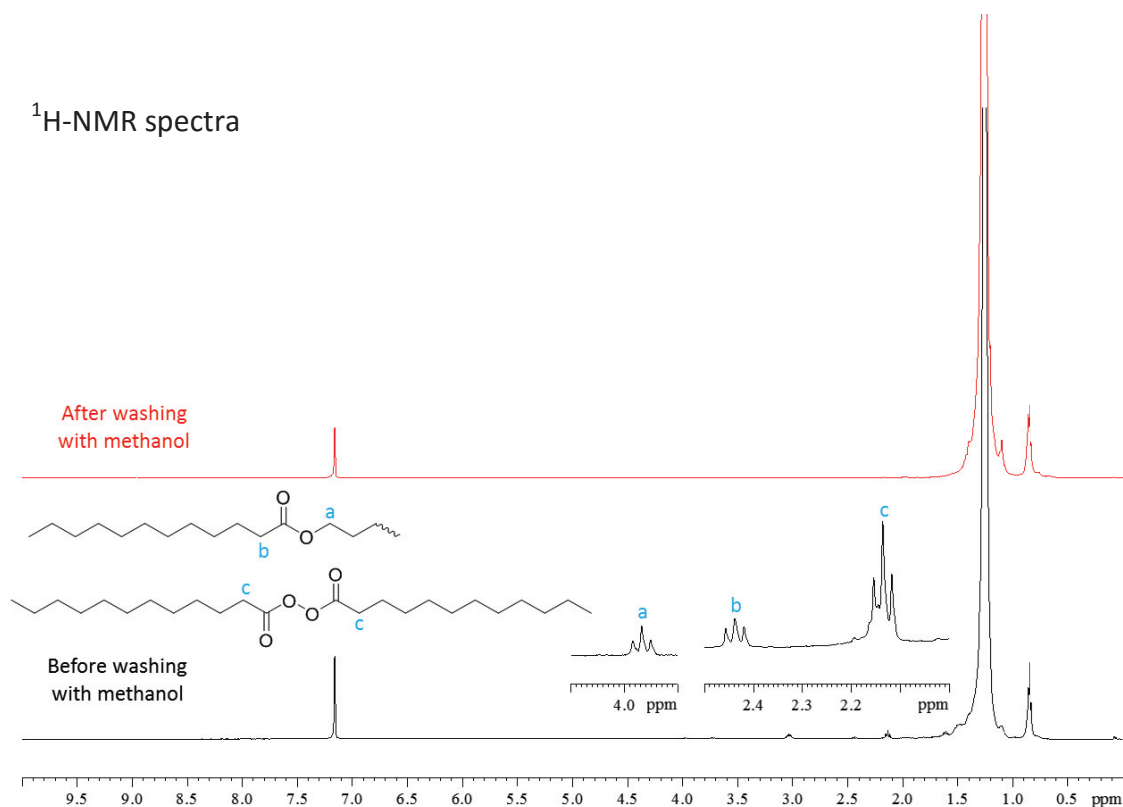


Figure 18. The variation of the yield of lauroyl peroxide-initiated PE as function of CO₂ pressure. Conditions: 0.3 mmol of lauroyl peroxide, 110 bar of ethylene at 35 °C, CO₂ pressure is at 35 °C, reaction temperature: 70 °C, total pressure at the reaction temperature: 180-280 bar, each reaction lasted 3 h.

¹H-NMR spectra



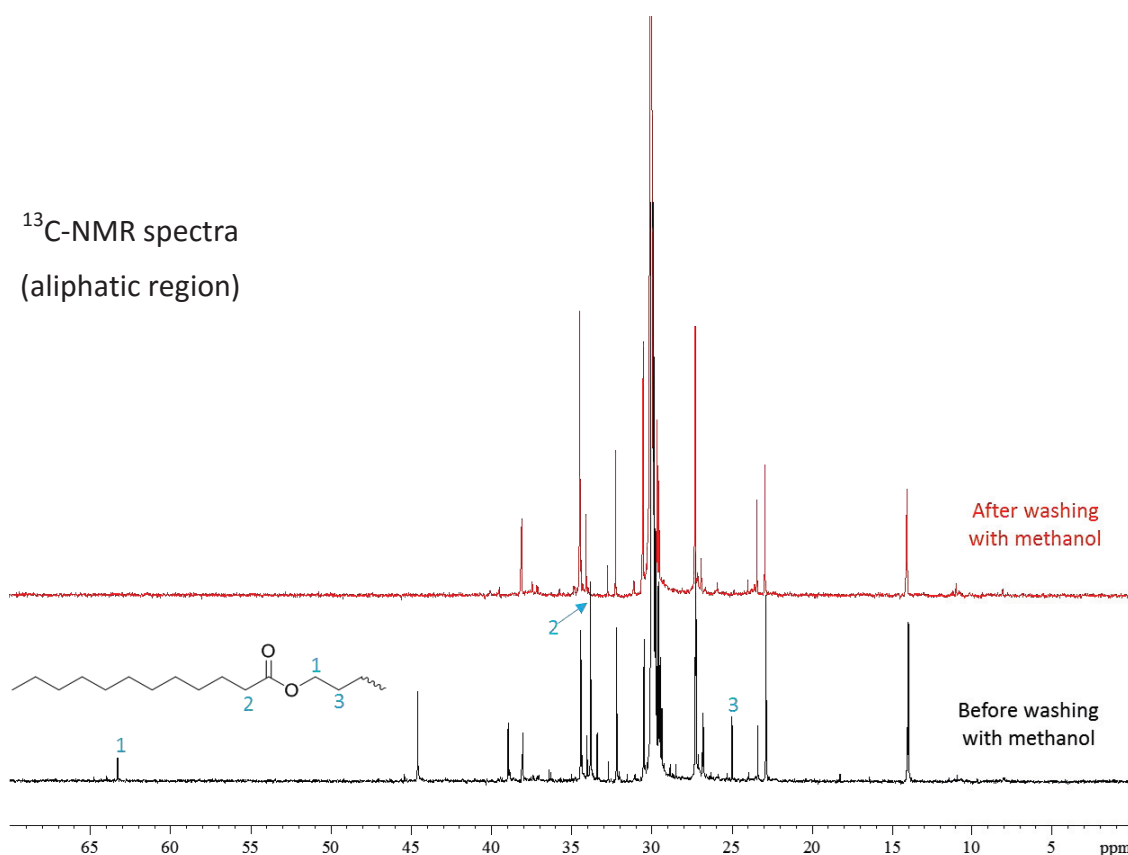


Figure 19. ¹H- and ¹³C-NMR spectra of the lauroyl peroxide-initiated PE produced in CO₂ (80 bar at 35 °C) before and after washing with methanol.

Indeed, as shown in the ¹H-NMR spectra in **Figure 19**, the peak (triplet) corresponding to the protons of the α carbon atom to the oxygen of the carboxyl group at 3.96 ppm and that corresponding to the α carbon atom to the quaternary carbon of the carboxyl group at 2.44 ppm, in addition to the peak (triplet) corresponding to the α carbon atom to the quaternary carbon of the carboxyl group of lauroyl peroxide at 2.13 ppm, disappear after washing with methanol.

Also, in the ¹³C-NMR spectra (**Figure 19**), the peaks corresponding to the α and β carbon atoms to the oxygen of the carboxyl group at 63.2 ppm and 25.0 ppm, respectively, in addition to that corresponding to the α carbon atom to the quaternary carbon of the carboxyl group at 33.8 ppm, disappear after washing with methanol. This also appears in the IR spectra by the disappearance of the bands corresponding to the C-O single and double bonds at 1150 cm⁻¹ and 1755 cm⁻¹, respectively, after washing (**Figure 20**). Therefore, the lauroyl peroxide carboxylic radical is producing PE chains with very low molar masses that are soluble in methanol.

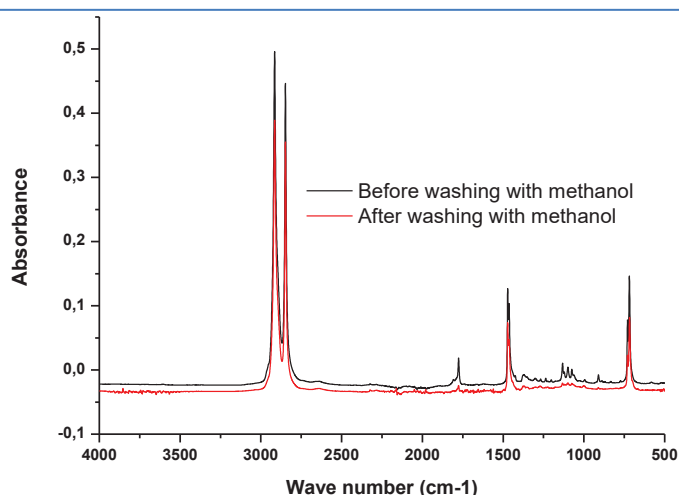


Figure 20. IR spectra of the lauroyl peroxide-initiated PE produced in CO₂ before and after washing with methanol.

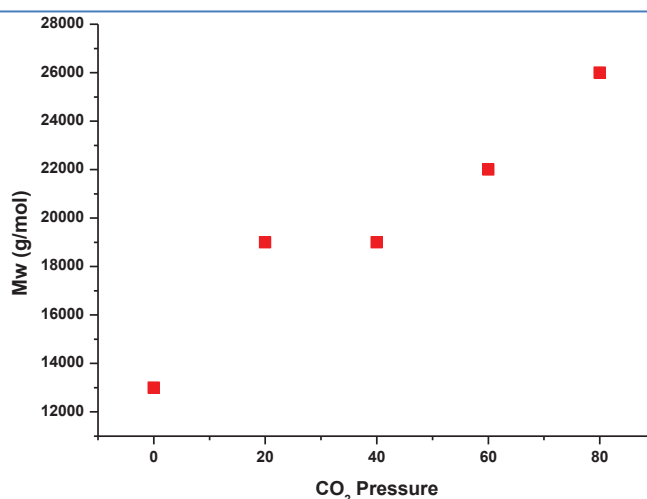


Figure 21. The variation of the molecular weight of the lauroyl peroxide-initiated PE as function of CO₂ pressure. CO₂ pressure at 35 °C.

The molecular weight of the PE produced increased with the increase of the CO₂ pressure, from 13000 g/mol in the absence of CO₂ to 26000 g/mol under a pressure of 80 bar of CO₂ added at 35 °C (**Figure 21**). The dispersity (Mw/Mn) of the polymers produced varies from 1.6 to 2.5 showing narrower distribution than that of the PE produced by AIBN-initiated reactions. The melting point obtained by DSC for all the PEs produced using lauroyl peroxide is 117 °C (**Figure 22**).

Table 5 represents a comparison between the PE produced in the CO₂-mediated reaction (under 20 bar at 35 °C; the most active lauroyl peroxide-initiated reaction) and that obtained from the reaction done in DMC (50 mL) under the same conditions (110 bar of ethylene at 35 °C, 70 °C, 3 h). The yield and molecular weight of the PE produced

from the polymerization reaction in DMC (2.2 g, 42000 g/mol (**Figure 23**)) are higher than those of the PE produced in CO₂ (1 g, 19000 g/mol), the melting point of the PE produced in DMC (118 °C; **Figure 23**) is slightly higher than that of PE produced in CO₂ (117 °C), and the dispersity of both PEs is 2.1. The number of branches of the PE produced in CO₂ (5.23 branch/1000 C atoms) is slightly lower than that of the PE produced in DMC (5.45 branch/1000 C atoms).

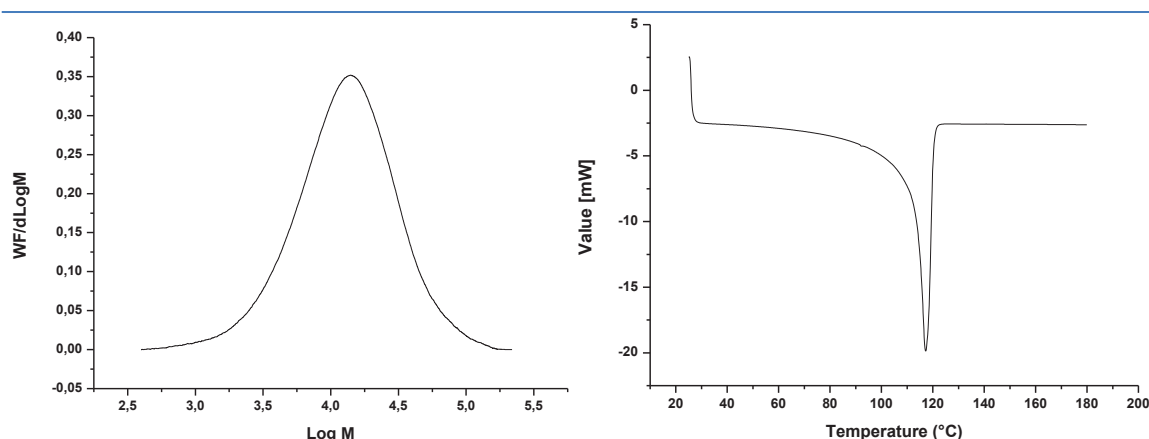


Figure 22. *To the left:* Molar mass distribution of the lauroyl peroxide-initiated PE produced in CO₂ (80 bar CO₂ at 35 °C). *To the right:* DSC peak of the lauroyl peroxide-initiated PE produced in CO₂ (80 bar at 35 °C).

Table 5. Lauroyl peroxide-initiated ethylene free radical polymerization in CO₂ (20 bar at 35 °C) versus that in DMC (50 mL).

	CO ₂ (20 bar)	DMC (50 mL)
Yield (g)	1	2.2
Mw (g/mol)	19 000	42 000
Mw/Mn	2.1	2.1
Melting Point (°C)	117	118
Number of branches (per 1000 C atom)	5.23	5.45

This higher activity is due to the higher solubility of lauroyl peroxide in DMC than in CO₂. Even then, synthesizing low-density polyethylene (LDPE) using an environmentally benign process free of organic solvents and direct access to dry PE (**Figure 24**) is still an important advantage of LDPE production *via* lauroyl peroxide as initiator in scCO₂.

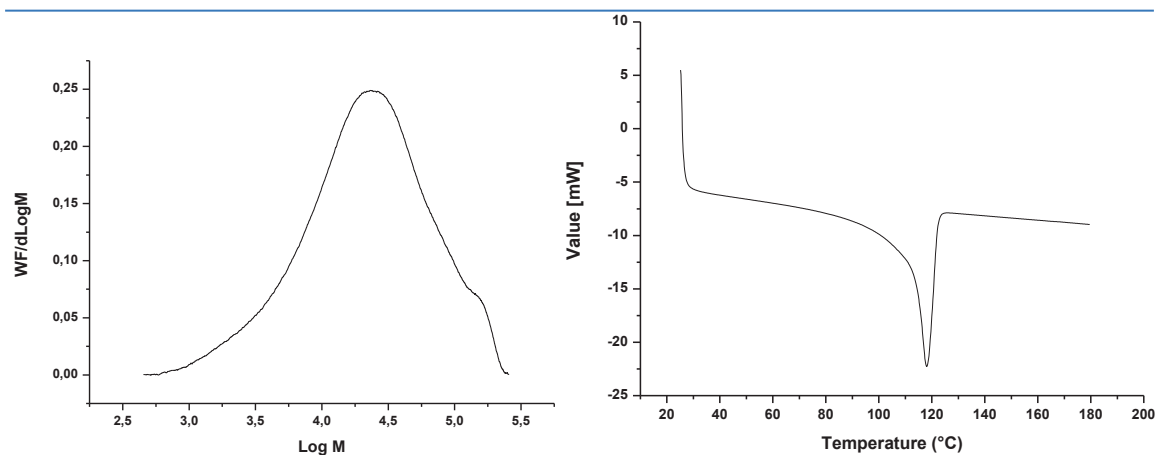
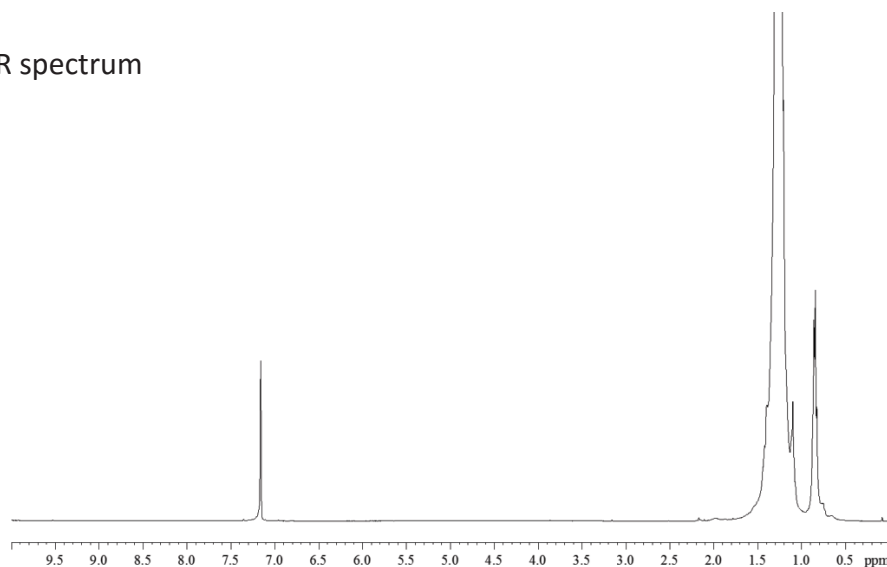


Figure 23. *To the left:* Molar mass distribution of the lauroyl peroxide-initiated PE produced in DMC (50 mL). *To the right:* DSC peak of the lauroyl peroxide-initiated PE produced in DMC (50 mL).



Figure 24. Dry PE produced by ethylene free radical polymerization in scCO₂.

¹H-NMR spectrum



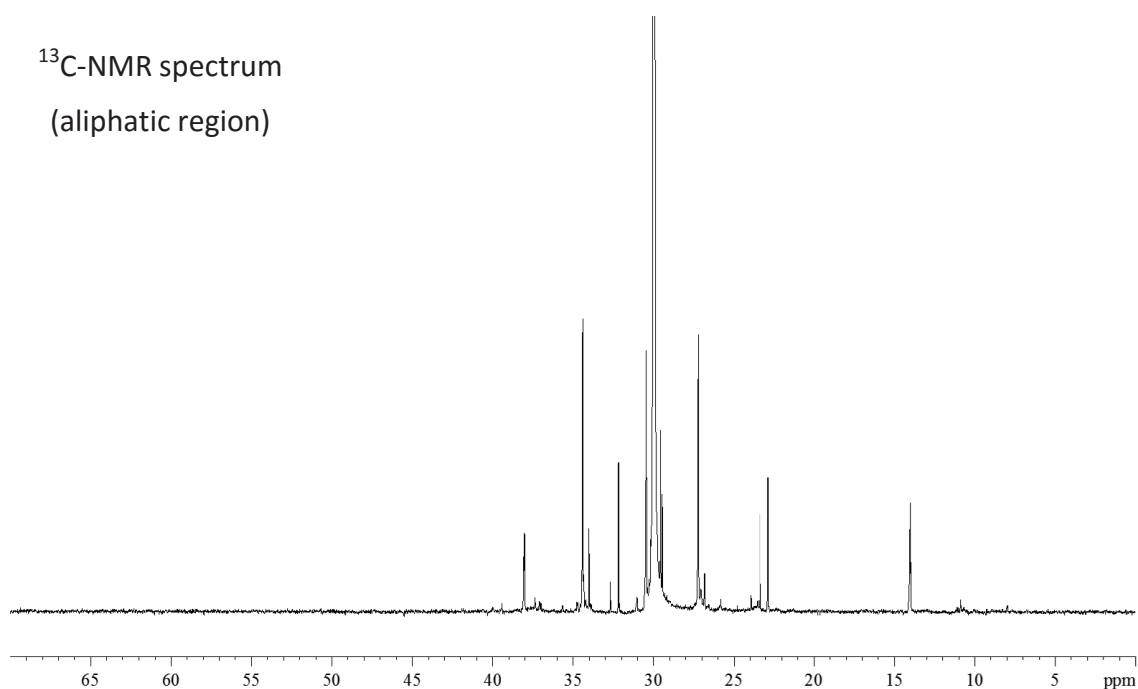


Figure 25. ^1H - and ^{13}C -NMR spectra of the lauroyl peroxide-initiated PE produced in DMC.

Also, the NMR ^1H - and ^{13}C -NMR spectra of the PE produced in DMC (**Figure 25**) are extremely similar to those of the the PE produced in CO_2 after washing with methanol.

B.3.2.4. Benzoyl Peroxide-Initiated Reactions

Using benzoyl peroxide as an initiator, the yield of PE produced increased strictly by the primary addition of CO_2 (20 bar at 45 °C) from 0.4 g in the absence of CO_2 to 1.2 g in presence of CO_2 , then by increasing the pressure of CO_2 the yield stayed constant at 1.2 g (**Figure 26**). This plateau obtained could be consistent with the potential ability of the carboxylic radical (produced by the primary decomposition of benzoyl peroxide) in initiating or terminating by recombination the ethylene polymerization in CO_2 . Moreover, the secondary decomposition of benzoyl peroxide into the phenyl radical is unfavorable in presence of CO_2 since it is a by-product of this decomposition reaction (**Scheme 1-(3)**).

The yield remains constant by increasing the CO_2 pressure, which could suggest a dual initiation process by both benzoyl-peroxide derived carboxylic radicals and phenyl radicals in ethylene polymerization in scCO_2 . To verify this assessment, ^1H and ^{13}C -NMR and infrared spectra of the PE produced by the benzoyl peroxide-initiated reactions

were realized, as well as SEC and DSC characterization.

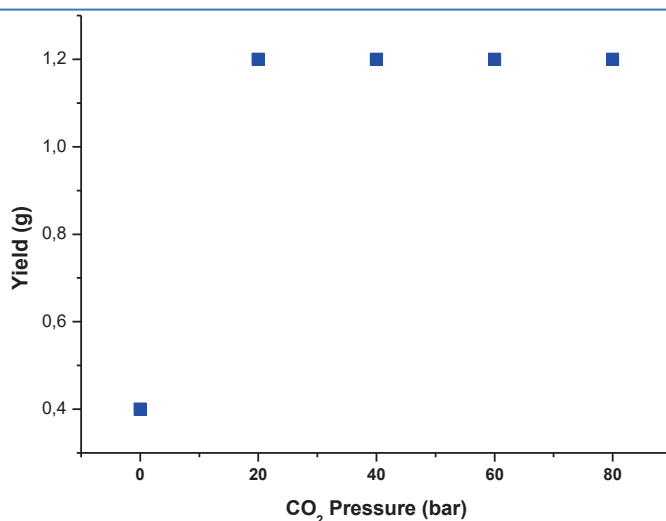
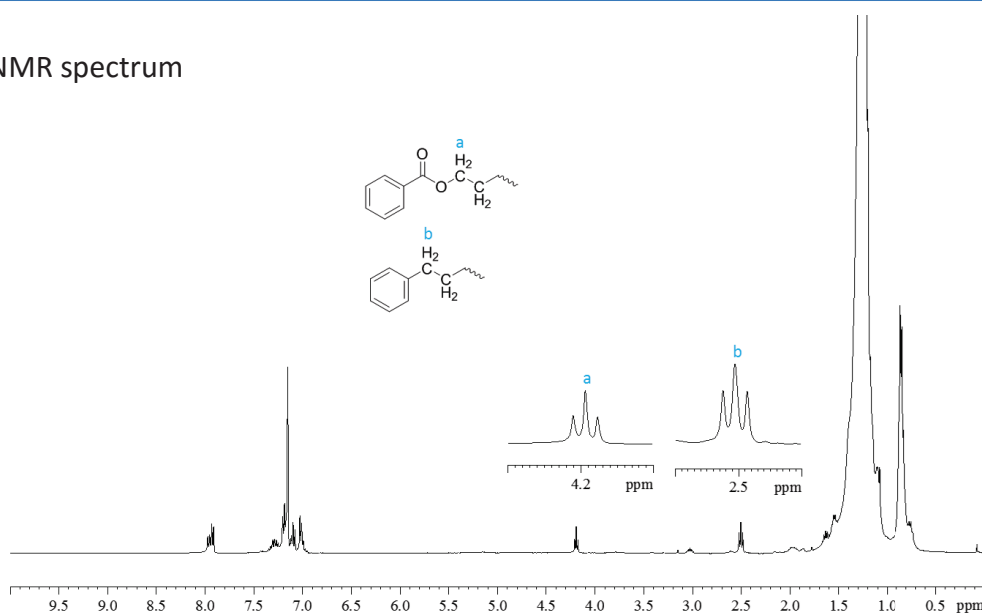


Figure 26. The variation of the yield of benzoyl peroxide-initiated PE as function of CO₂ pressure. Conditions: 0.3 mmol of benzoyl peroxide, 90 bar of ethylene at 45 °C, CO₂ pressure is at 45 °C, reaction temperature: 90 °C, total pressure at the reaction temperature: 180-280 bar, each reaction lasted 3 h.

In the ¹H-NMR spectrum of the benzoyl peroxide-initiated PE washed with methanol, two triplets appear at 2.5 ppm and 4.2 ppm corresponding to the protons on the α-carbon to the phenyl ring and that adjacent to the oxygen atom of the carboxyl group, respectively (**Figure 27**). In the ¹³C-NMR spectrum, the peaks corresponding to the α and β carbon atoms to the oxygen of the carboxyl group at 64.7 ppm and 31.5 ppm, respectively, appear even after washing with methanol, in addition to the peak corresponding to the quaternary carbon of the carboxyl group at 176.5 ppm (**Figure 27**).

¹H-NMR spectrum



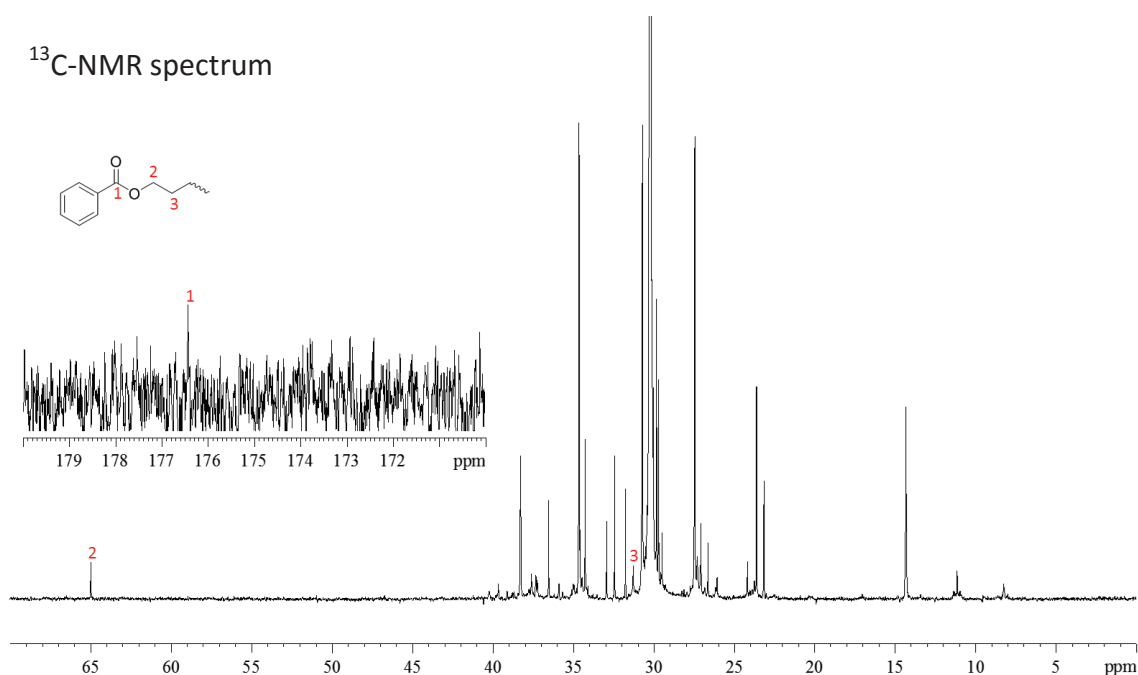


Figure 27. ¹H- and ¹³C-NMR spectra of the benzoyl peroxide-initiated PE produced in CO₂ (80 bar at 45 °C).

The initiation or termination *via* the carboxylic radical of benzoyl peroxide is also verified by the IR spectra, showing the C-O single bond band at 1272 cm⁻¹ and the C-O double bond band at 1724 cm⁻¹ (Figure 28).

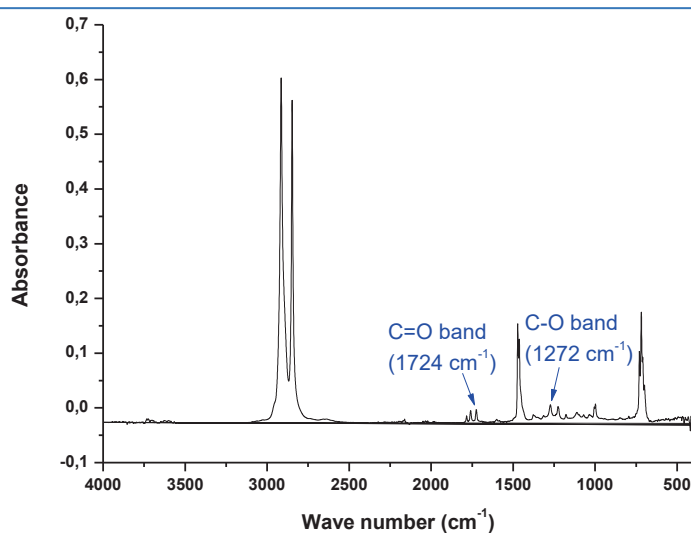


Figure 28. IR spectrum of the benzoyl peroxide-initiated PE produced in CO₂.

The molecular weight of the produced PE is 16000 g/mol in the absence of CO₂, then it decreases suddenly to 6000 g/mol by the primary addition of CO₂ (20 bar at 45°C), then it re-increased gradually with the increase of the CO₂ pressure till reaching 8000 g/mol at 80 bar of CO₂ added at 45°C (Figure 29).

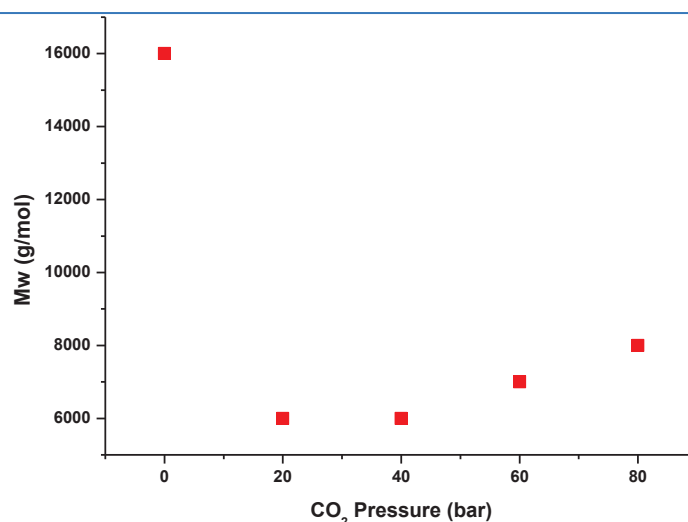
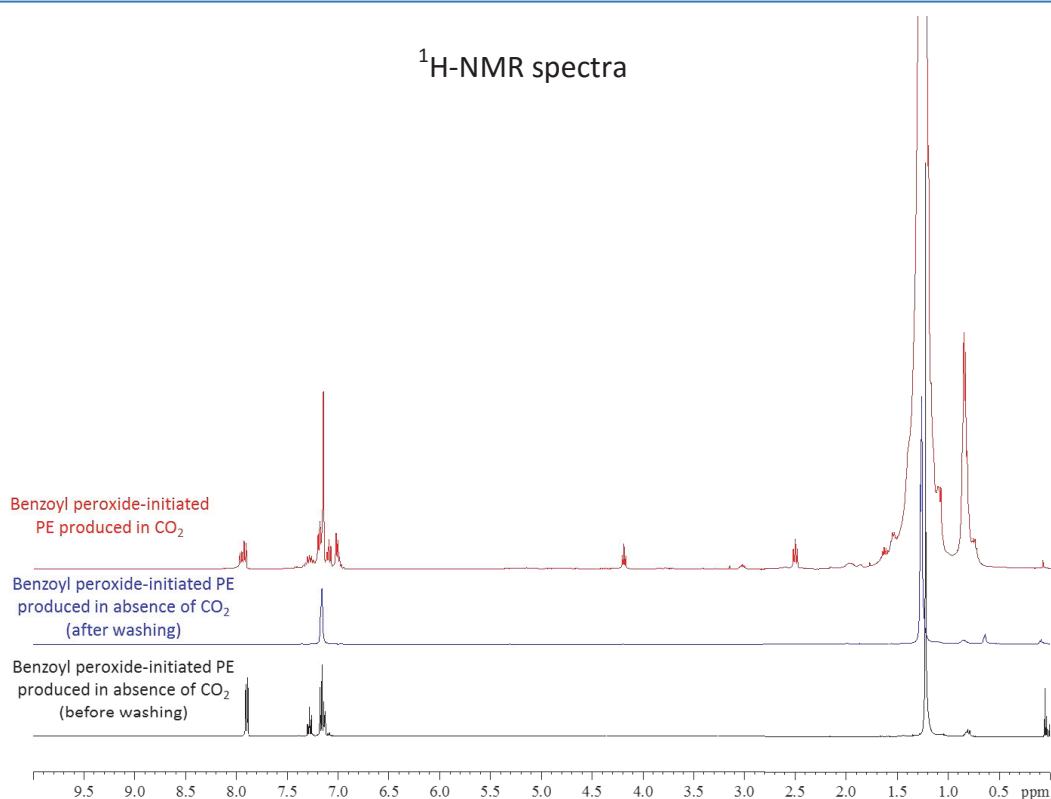


Figure 29. The variation of the molecular weight of the benzoyl peroxide-initiated PE as function of CO₂ pressure. CO₂ pressure at 45 °C.

This shows that more carboxylic radicals-phenyl radicals are generated and either initiating or terminating polyethylene chains. The flux and repartition of radicals (carboxyl and phenyl) and the efficiency of initiation thus strongly depends on the presence of CO₂ in the polymerization medium. In absence of CO₂ in the polymerization medium, neither phenyl nor carboxyl chain ends appear in the NMR spectra (**Figure 30**).



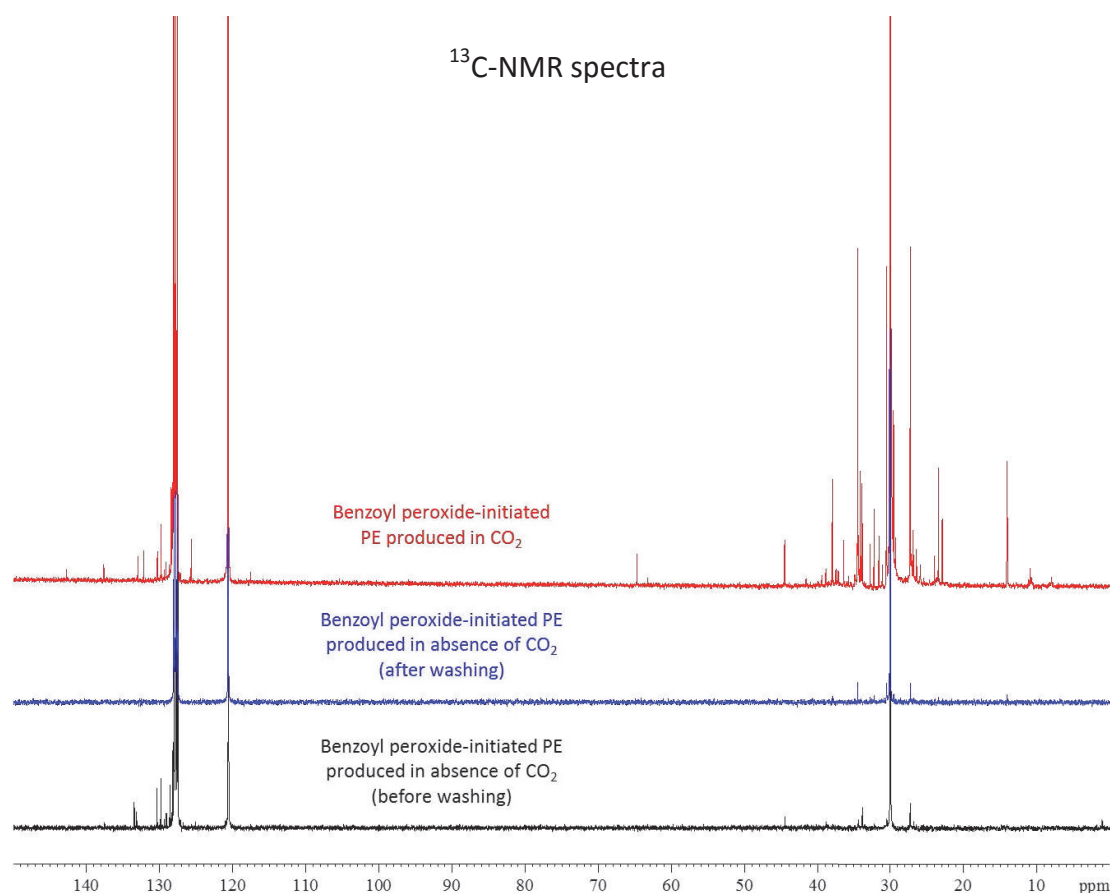


Figure 30. ^1H - and ^{13}C -NMR spectra of the benzoyl peroxide-initiated PE produced in presence and absence of CO_2 (before and after washing).

In absence of CO_2 pressure, neither phenyl nor carboxyl chain ends appear in the NMR spectra, but the peaks corresponding to the benzoyl peroxide appear obviously before washing with methanol (in the ^1H -NMR spectrum, the protons at the *ortho*, *para* and *meta* positions of the phenyl ring appear at 7.9 ppm, 7.3 ppm, and 7.1 ppm, respectively) and disappear after washing (**Figure 30**). This shows that in absence of solvent (CO_2 or an organic solvent) benzoyl peroxide is inefficient in initiating ethylene radical polymerization. Therefore, the PE obtained is initiated by other side reactions or radicals from impurities.

On the contrary, when CO_2 is present in the reaction mixture, benzoic ester moieties along phenyl chain-ends can be evidenced by NMR spectroscopy, signifying that carboxylic radicals are either efficiently initiating or terminating the polymerization of ethylene. The higher the CO_2 proportion in the supercritical mixture, the higher the concentration of benzoic ester chain-ends.

It is worth mentioning that the molar masses are increasing by increasing CO_2 pressure

(Figure 29). The dispersity (M_w/M_n) of the polymers produced varies from 1.6 to 2.2 showing narrower distribution than that of PEs produced by AIBN- and lauroyl peroxide-initiated reactions. The melting point obtained by DSC for all the PEs produced is 112 °C lower than that of the PEs produced by AIBN- and lauroyl peroxide-initiated reactions (Figure 31).

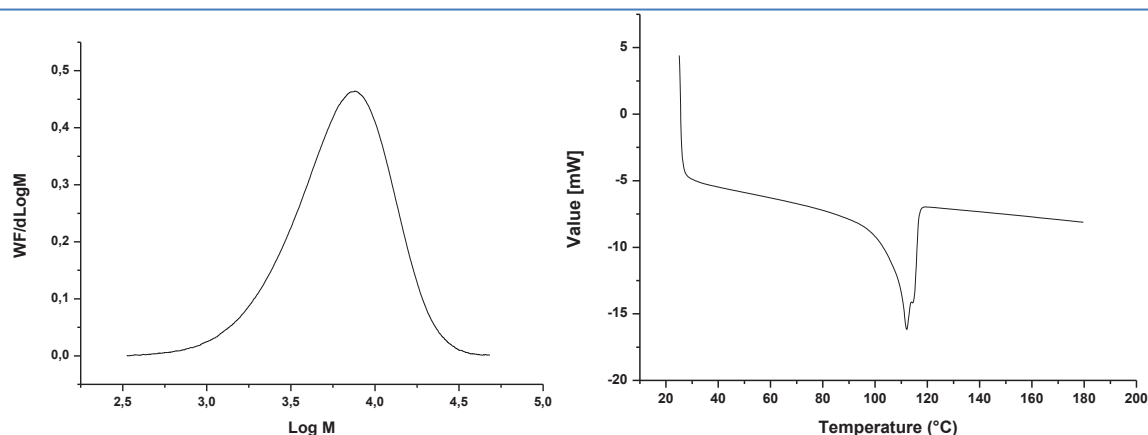


Figure 31. To the left: Molar mass distribution of the benzoyl peroxide-initiated PE produced in CO₂ (80 bar CO₂ at 45 °C). To the right: DSC peak of the benzoyl peroxide-initiated PE produced in CO₂ (80 bar at 45 °C).

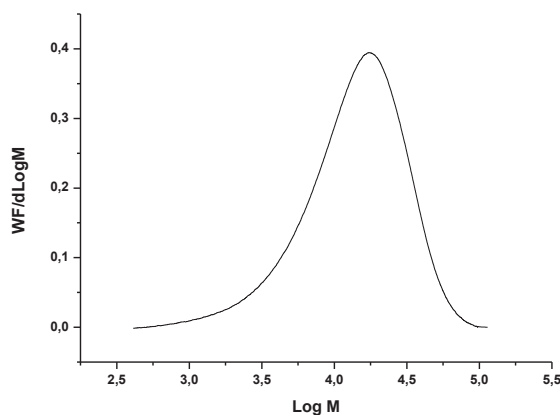


Figure 32. Molar mass distribution of the benzoyl peroxide-initiated PE produced in CO₂ (80 bar CO₂ at 35 °C) at 70 °C.

In order to produce higher molar masses of benzoyl peroxide-initiated PE, a reaction was performed at 70 °C (lower temperature) under a pressure of 80 bar of CO₂ and 110 bar of ethylene at 35 °C. This reaction yielded 0.7 g of PE in 3 h, with an M_w = 19000 g/mol and a dispersity equal to 1.9 (Figure 32). By decreasing the temperature the rate of decomposition of the initiator decreases, thus the concentration of radicals in the medium decreases and termination reactions consequently decrease so the molar masses of the polymer increase.

Table 6. Benzoyl peroxide-initiated ethylene free radical polymerization in CO₂ (80 bar at 45 °C) versus that in DMC (50 mL).

	CO ₂ (80 bar)	DMC (50 mL)
Yield (g)	1.2	2.4
Mw (g/mol)	8 000	19 000
Mw/Mn	1.6	2.0
Melting Point (°C)	112	118
Number of branches (per 1000 C atom)	6.51	6.45

Table 6 shows a comparison between the PE obtained from the polymerization reaction in CO₂ (under 80 bar at 45 °C) and that obtained from the reaction done in DMC (50mL) under the same conditions (the reaction was performed at 90 °C for 3 hours with 90 bar of ethylene were added at 45 °C). The yield, molecular weight, and melting point of the PE produced from the polymerization reaction performed in DMC (2.4 g, 19000 g/mol, 116 °C; **Figure 33**) are higher than those of the PE produced in CO₂ (1.2 g, 8000 g/mol, 112 °C); the dispersity of PE produced in CO₂ (1.6) is lower than that of PE produced in DMC (2.0). The number of branches of the PE produced in CO₂ (6.51 branch/1000 C atoms) is slightly higher than that of the PE produced in DMC (6.45 branch/1000 C atoms).

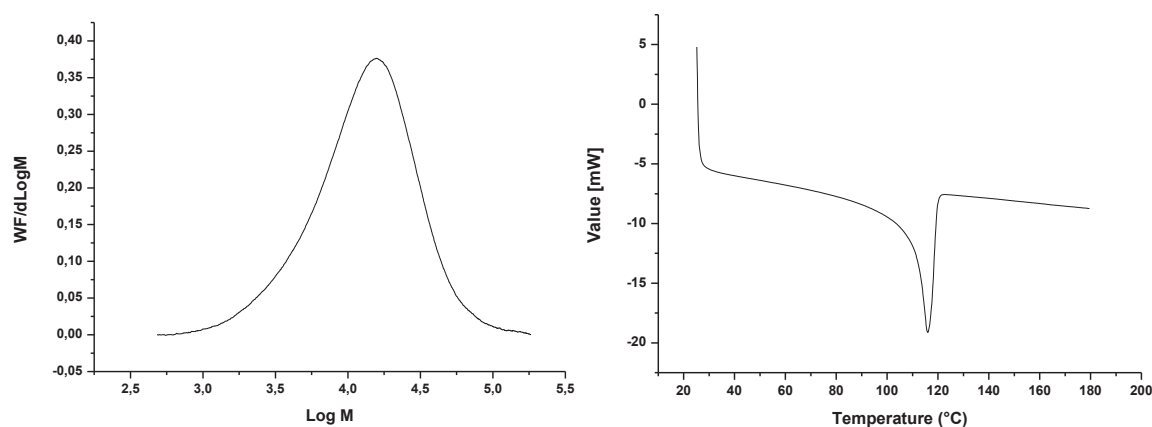


Figure 33. To the left: Molar mass distribution of the benzoyl peroxide-initiated PE produced in DMC. **To the right:** DSC peak of the benzoyl peroxide-initiated PE produced in DMC.

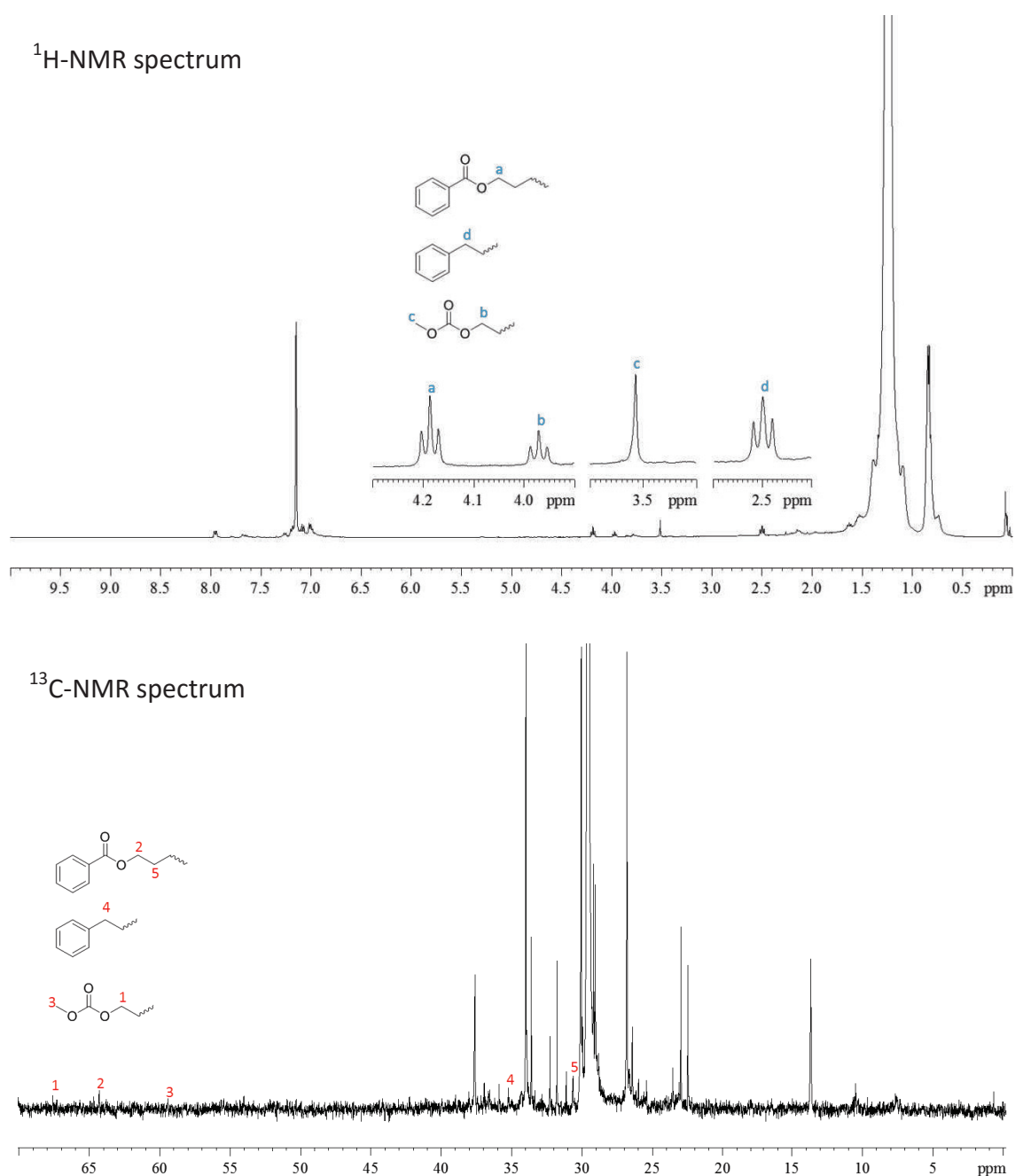


Figure 34. ¹H- and ¹³C-NMR spectra of the benzoyl peroxide-initiated PE produced in DMC.

This difference in activity is due to the higher solubility of benzoyl peroxide in DMC than in CO₂. Even though the activity in DMC is higher and there is a bit of initiation/termination by recombination with the benzoyl-peroxide derived carboxylic radical as evidenced by the NMR spectra (**Figure 34**), but there is also transfer to DMC, which in addition to its relative harmful effect as a volatile organic solvent, it is

producing a relatively complicated polymer structure as shown in the NMR spectra (**Figure 34**).

Therefore, only an ethylene radical polymerization in scCO_2 using benzoyl peroxide as an initiator leads to exclusively phenyl- and ester-functionalized PE chains, potentially post-modifiable.^{15,16}

B.4. Conclusion

Ethylene free radical polymerization in CO_2 harnessing a supercritical state for the reaction mixture without addition of any external organic solvent under mild conditions ($< 100^\circ\text{C}$ and < 300 bar) has been achieved to produce clean solvent-free LDPE.

Three different initiators were utilized, AIBN, lauroyl peroxide, and benzoyl peroxide, that possess a substantial solubility in scCO_2 , as verified using a sapphire-windowed reactor.

In the case of AIBN-initiated reactions, the yield and the molar mass of the PE produced increased with the increase of the CO_2 pressure. By comparison with the PE produced in a DMC (dimethylcarbonate)-mediated reaction, the yield and molar masses of the PE produced in the CO_2 -mediated reaction (80 bar at 35°C) were higher.

In lauroyl peroxide-initiated reactions, the yield increased strictly by the primary addition of CO_2 , then it decreased with the increase of the CO_2 pressure showing the negligible efficiency of the lauroyl peroxide carboxylic radical in initiating ethylene radical polymerization which is the favorable produced radical from the decomposition of lauroyl peroxide in presence of CO_2 . The yield and molar masses of the PE produced in a DMC-mediated reaction are higher than those of the PE produced in the CO_2 -mediated reactions. This higher activity is due to the higher solubility of lauroyl peroxide in DMC than in CO_2 . Even then, polymerizing LDPE using an environmentally benign process free of organic solvents with direct access to dry PE is still an important advantage of LDPE production *via* lauroyl peroxide as initiator in scCO_2 .

In benzoyl peroxide-initiated reactions, the yield increased strictly by the primary addition of CO_2 , then it stayed constant with the increase of the CO_2 pressure. This shows the efficiency of the benzoyl peroxide carboxylic radical in initiating ethylene

radical polymerization which is the favorably produced radical from the decomposition of benzoyl peroxide in presence of CO₂. The yield and molar masses of the PE produced in a DMC-mediated reaction are higher than those of the PE produced in the CO₂-mediated reactions. This higher activity is also due to the higher solubility of benzoyl peroxide in DMC than in CO₂.

More importantly, the initiation or termination of PE chains *via* the carboxylic radical produced by the primary decomposition of benzoyl peroxide is possible in the presence of CO₂, whereas in absence of CO₂, benzoyl peroxide seems to be inefficient in polymerizing ethylene. Using benzoyl peroxide, one can therefore obtain ester-functionalized LDPE in a very straightforward manner. Understanding the mechanisms of initiation and termination using this particular class of carboxy-radical precursors is currently the focus of attention in our research group.

B.5. References

1. Sakakura, T.; Choi, J.-C.; Yasuda, H. *Chem. Rev.* **2007**, *107* (6), 2365-2387.
2. McHugh, M.; Krukonis, V. *Supercritical Fluid Extraction: Principles and Practice*; Elsevier, 2013.
3. Doak, K. W. In *Encyclopedia of Polymer Science and Engineering*, 2nd ed.; Mark, H. F., Bikales, N. M., Overberger, C. G., Menges, G., Eds.; WileyInterscience: New York, 1985; Vol. 6, pp 386-428.
4. Aggarwal, S. L.; Sweeting, O. J. *Chem. Rev.* **1957**, *57*, 665-742.
5. Grau, E.; Broyer, J.-P.; Boisson, C.; Spitz, R.; Monteil, V. *Macromolecules* **2009**, *42*, 7279-7281.
6. Grau, E.; Broyer, J.-P.; Boisson, C.; Spitz, R.; Monteil, V. *Phys. Chem. Chem. Phys.* **2010**, *12* (37), 11665-11669.
7. Grau, E.; Broyer, J.-P.; Boisson, C.; Spitz, R.; Monteil, V. *Polym. Chem.* **2011**, *2* (10), 2328-2333.
8. Dommange, C.; D'Agosto, F.; Monteil, V. *Angew. Chem. Int. Ed.* **2014**, *53* (26), 6683-6686.
9. Hyatt, J. A. *J. Org. Chem.* **1984**, *49* (26), 5097-5101.
10. Morgenstern, D. A.; LeLacheur, R. M.; Morita, D. K.; Borkowsky, S. L.; Feng, S.; Brown, G. H.; Luan, L.; Gross, M. F.; Burk, M. J.; Tumas, W. Supercritical Carbon Dioxide as a Substitute Solvent for Chemical Synthesis and Catalysis. In *Green Chemistry*; ACS Symposium Series; American Chemical Society, 1996; Vol. 626, pp 132-151.
11. Ramsey, E.; Sun, Q.; Zhang, Z.; Zhang, C.; Gou, W. *J. Environ. Sci.* **2009**, *21* (6), 720-726.
12. kagiya, T.; Machi, S.; Hagiwara, M.; Kise, S. Polymerization of ethylene by means of radical initiation using carbon dioxide as reaction medium. US3471463 A, October 7, 1969.
13. Henderson, N.; Sacco, W. F.; Barufatti, N. E.; Ali, M. M. *Ind. Eng. Chem. Res.* **2010**, *49* (4), 1872-1882.
14. Galland, G. B.; de Souza, R. F.; Mauler, R. S.; Nunes, F. F. *Macromolecules* **1999**, *32* (5), 1620-1625.
15. Cheng, C.; Brookhart, M. *Angew. Chem. Int. Ed.* **2012**, *51* (37), 9422-9424.
16. Fischer, C.; Sparr, C. *Angew. Chem. Int. Ed.* **2018**, *57* (9), 2436-2440.

C. CHAPTER III. Triethylaluminum-Mediated Ethylene Radical Polymerization: From a Transfer Agent to a CO₂-Incorporating Agent.

Table of Contents

C.1. Abstract	147
C.2. Triethylaluminum-Mediated Ethylene Radical Polymerization: A Chain-Transfer Agent	147
C.2.1. Lewis Acid effect on the Ethylene Radical Polymerization	147
C.2.2. Controlling Agent versus Transfer Agent	148
C.2.3. Definition of a "Controlled Radical Polymerization"	149
C.2.4. Concept of "CRP"	150
C.2.5. Types of "CRP"	151
C.2.5.1. Reversible Termination Mechanism.....	151
C.2.5.2. Degenerative Chain Transfer Mechanism	152
C.2.6. Effect of TEA on the Ethylene Radical Polymerization	154
C.2.6.1. EPR Analysis: Interaction between TEA and Radicals	154
C.2.6.2. Conventional Ethylene Free Radical Polymerization (blank reaction) and "Aufbau" Reaction.....	156
C.2.6.3. Mn of Polyethylene versus [TEA]	158
C.2.6.4. Mn of Polyethylene versus Conversion	160
C.2.6.5. Variation of Mn as function of [AIBN]	170
C.2.6.6. Quenching the Polymerization Reaction by I ₂	172
C.3. Incorporation of CO ₂ in the Polyethylene Chain Using Triethylaluminum	174
C.3.1. Interaction of Triethylaluminum with CO ₂	174
C.3.2. Ethylene Radical Polymerization in scCO ₂ in the Presence of TEA	175
C.3.3. Hydrolysis of the CO ₂ -Functionalized Polyethylene	182

C.4.	Conclusion	185
C.5.	References	187

C.1. Abstract

This chapter consists of two sub-chapters. The first one deals with the utilization of triethylaluminum as a chain-transfer agent in ethylene radical polymerization. This function of triethylaluminum, which can interact with radicals, in addition to its capability to react with CO₂ form the basis for the second sub-chapter. The second sub-chapter deals with CO₂-incorporation within the polyethylene chains using triethylaluminum acting as a CO₂-incorporating agent in ethylene radical polymerization in scCO₂. Therefore, triethylaluminum acts as a power switch to go from the use of CO₂ as an inert polymerization medium to its activation to be able to use it as a functionalization agent in ethylene radical polymerization.

C.2. Triethylaluminum-Mediated Ethylene Radical Polymerization: A Chain-Transfer Agent

In this part, the role of triethylaluminum (TEA) as an irreversible chain-transfer agent in ethylene radical polymerization will be discussed thoroughly. However, since TEA is a Lewis acid we find it important to mention the effects of Lewis acids on the ethylene radical polymerization.

C.2.1. Lewis Acid Effect on the Ethylene Radical Polymerization

The effect of Lewis acids on the radical polymerizations of different monomers such as acrylates and acrylimides has been widely studied, especially their effect on the stereo control of the polymerization reaction.¹ But the effect of Lewis acids in the case of ethylene radical polymerization hasn't been studied extensively.

Lewis acids were used primarily in ethylene radical polymerization reactions by Clark et al., they concentrate on their role in increasing the activity of the polymerization through the activation of the ethylene double bond by coordination to the Lewis acid.²

An investigation of Lewis acids in ethylene radical polymerization has been conducted at C2P2 laboratory showing the effect of a list of Lewis acids (CuCl, CuCl₂, FeCl₂, FeCl₃, AlCl₃, and ScTf₃) on the polymerization in different solvents (toluene, THF, and diethyl carbonate (DEC)).³

In toluene almost all Lewis acids lead to a better activity (especially for CuCl and FeCl₃).

This is because toluene interaction with radical and ethylene is negligible (almost no solvent activation effect; a slight transfer to solvent is observed yielding toluyl chain-ends), then the addition of a Lewis acid could increase slightly the efficiency of the free radical polymerization of ethylene *via* an activation of the ethylene double bond as predicted by Clark.²

In THF, all the Lewis acids that were investigated decreased the efficiency of the polymerization. THF exhibits a high solvent-activation effect therefore these Lewis acids seem to disturb the activation by THF.

In DEC, all Lewis acids increased the yield. ScTf₃ and FeCl₃ led to the highest activity. Surprisingly the strong Lewis acid ScTf₃ was an activator only in DEC.

The rationalizations of these effects are not an easy task as Lewis acid and solvent play major roles in the free radical polymerization of ethylene. Clark calculations predict a drastic increase of the yield of polymerization by addition of Lewis acids. This is not the case here and it is mostly due to Clark hypothesis of a gaseous polymerization in which no interaction occurs between ethylene and solvent.²

Monteil et al. at C2P2 continued their investigation towards the study of metal alkyls. A series of metal alkyls has been studied, ZnMe₂ and AlEt₃ (TEA) were the only activating agents of the polymerization. In the case of longer alkyl chains the activity drastically decreases.³

Also, for ZnEt₂ and TEA, the molar masses decreased and the dispersities became extremely narrow. A possible explanation is that this narrowing with considerable decrease of Mn could be due to a control of molar mass by these metal alkyls.

From these premises we started our investigations of the effect of TEA on the ethylene radical polymerization, where we conclude that TEA is acting as a chain-transfer agent but not as a controlling agent.

At this stage, it is crucial to explicit the differences between a chain-transfer agent and a controlling agent.

C.2.2. Controlling Agent versus Transfer Agent

We found it important to differentiate these two terms which are usually used in

controlled radical polymerization processes indicating the same reagent, but that actually convey different meanings. The following definitions explain the differences between a controlling agent, which is a **reversible chain-transfer agent**, and a chain-transfer agent, which is an **irreversible chain-transfer agent**.

Controlling agent: is a compound used in a "controlled radical polymerization" which is a chain polymerization propagated by radicals that are deactivated **reversibly** through a reaction with the **controlling agent**, bringing them into an "active-dormant" equilibrium. This results in a controlled increase of the chain length of polymers versus time.

Chain-transfer agent: Compound able to react with a chain propagated by radicals **irreversibly**, in this reaction the original chain carrier is deactivated and a new chain carrier is generated.

Moreover, a third mode of action of such agents lead to a third term which is a **radical trap**.

Radical trap: Compound able to react with a chain propagated by radicals **irreversibly** without any production of new chain carrier (radical); it is an irreversible terminating agent.

And since we are concerned with controlled radical polymerization processes, it is clearer to summarize general concepts and mention types of controlled radical polymerizations in a brief explanation.

C.2.3. Definition of a "Controlled Radical Polymerization"

IUPAC recommended the term "reversible-deactivation radical polymerization" (RDRP) for a controlled radical polymerization process. IUPAC definition is: RDRP is a chain polymerization, propagated by radicals that are deactivated reversibly, bringing them into active-dormant equilibria of which there might be more than one.⁴

In another simpler way, we could say: a controlled radical polymerization (CRP) is a chain polymerization in which the chain carriers are radicals (alike free radical polymerization), but in the presence of a controlling agent to limit termination by decreasing the concentration of the active species (radicals) in the medium through a reversible-deactivation radical process (*only in the case reversible-termination*

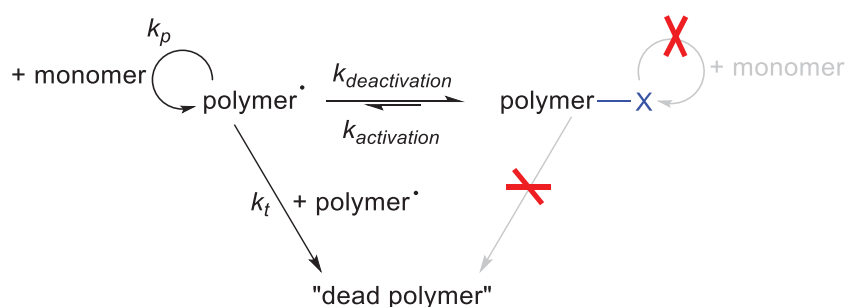
mechanism).

C.2.4. Concept of "CRP"

Chain-growth polymerization has been successfully performed for many decades through conventional free radical polymerization for a wide range of vinylic monomers. This polymerization technique generates many important polymers and the wide range of available molar mass distributions gives rise to important physical properties such as toughness (long chains) with improved processability (shorter chains). While this technique is useful for a number of applications starting from a wide variety of monomers, several applications benefit from using more precisely controlled polymers, particularly when block copolymers are involved.

In conventional radical polymerization, the component steps in the process are chain initiation, chain propagation, chain termination, and sometimes also chain transfer. The process is a classical chain reaction using a radical as a chain carrier. The lifetime of an individual radical is very short and equal to the period of chain growth for that chain, the termination step involves the mutual destruction of two chain carriers, and the distribution of molar masses of the resulting polymers is rather broad.

Scheme 1. General mechanism of a controlled radical polymerization.



Since the early 1980s, it has been found that certain additives are able to react reversibly with radicals (chain carriers). Because the reaction is reversible, the period of chain growth of an individual propagating chain may be extended to the duration of the experiment (**Scheme 1**). However, for most of the time, chains are in a dormant state, unable to participate in chain propagation or termination. Thus, polymerization conditions can be chosen such that the majority of chains are living, most of these are in a dormant form, and at any given instant only a small fraction are active chains capable of chain growth. As long as the interconversion of active and dormant forms is rapid

compared to propagation, all chains are able to grow at the same rate.

If the initiating species are fully consumed prior to any appreciable chain growth, all chains grow at the same rate and the distribution of molar masses of the products can be much narrower than in the conventional radical polymerization. This controlled radical polymerization has attracted a great deal of interest.

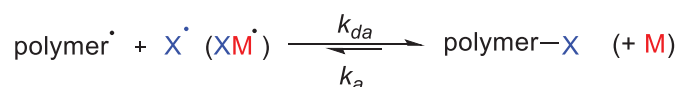
C.2.5. Types of "CRP"

Depending on their mechanisms, the different types of CRP are classified into two families, the "reversible termination mechanism" and the "degenerative chain transfer mechanism".

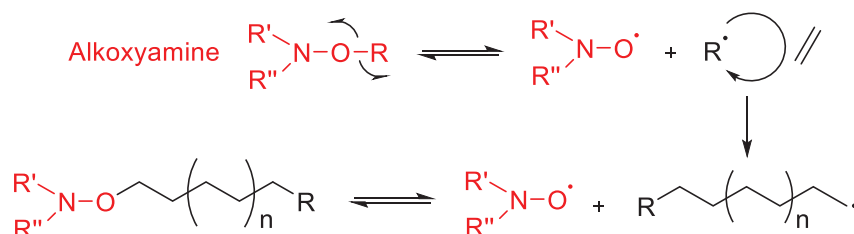
C.2.5.1. Reversible Termination Mechanism

Scheme 2. a) General reversible termination mechanism; b) NMP general mechanism; c) ATRP general mechanism.

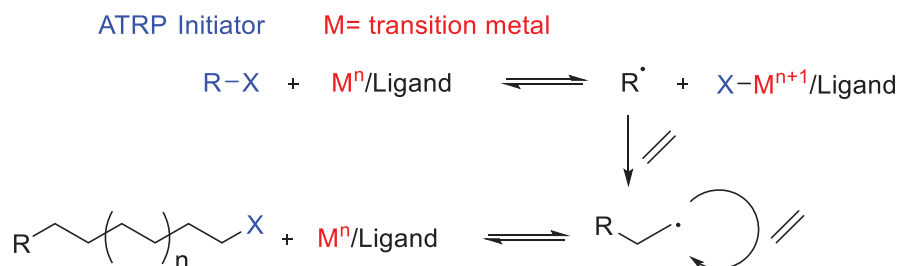
a) General Reversible Termination Mechanism



b) Nitroxide-Mediated Radical Polymerization (NMP) [Ethylene monomer]



c) Atom Transfer Radical Polymerization (ATRP) [Ethylene monomer]



In the reversible termination mechanism, "polymer[•]" is deactivated by a reversible termination reaction with X[•] (or XM[•]) (**Scheme 2/a**). Prominent examples are the

nitroxide-mediated polymerization "NMP" (X= nitroxyl group, **Scheme 2/b**),⁵ first reported by Georges et al. in 1993,⁶ and the atom transfer radical polymerization "ATRP" (X = e. g., Cl, Br and M = transition-metal complex, **Scheme 2/c**),⁷ first reported independently by Matyjaszewski et al.⁸ and Sawamoto et al.⁹ in 1995.

Reversible termination systems are based on the persistent-radical effect (PRE):¹⁰ in contrast to "polymer•", the persistent radical X^\bullet (or XM^\bullet) does not undergo irreversible self-termination. This leads to an accumulation of X^\bullet and thus an increased probability for "polymer•" to reversibly react with X^\bullet rather than irreversibly with another "polymer•".

In ethylene radical polymerization, the processes involving a reversible termination mechanism (NMP and ATRP) are not considered effective. This is due to the less activated ethylene monomer which leads to a polyethylenyl primary radical that is not stabilized well, hindering the release of active species. The equilibrium between the activated state and the dormant state is thus strongly shifted towards the dormant one. As a consequence, controlled polymerization of ethylene does not proceed effectively in these systems.

C.2.5.2. Degenerative Chain Transfer Mechanism

In degenerative transfer, "polymer•" is deactivated by the transfer of X^\bullet from another polymer-X (**Scheme 3/a**). More generally, this process is a reversible chain transfer. However, in order to emphasize that transfer occurs between two chemically (almost) identical polymer chains, the process was termed degenerative.¹¹ Prominent examples are the reversible addition-fragmentation chain-transfer (RAFT, with X= e. g., thiocarbonylthio group, **Scheme 3/b**) polymerization,¹² first reported by Rizzardo et al. in 1998,¹³ the iodine-transfer polymerization (ITP, with X= I, **Scheme 3/c**),¹⁴ first reported by Matyjaszewski et al. in 1995,¹⁵ and the tellurium-mediated radical polymerization (TERP, with X= TeR, **Scheme 3/d**), first reported by Yamago et al. in 2002.¹⁶

In this context, the RAFT process is termed after the unique mechanism of consecutive addition and fragmentation, leading to a fairly stable intermediate radical. In contrast, for ITP and TERP, the iodine atom and the tellurium group, respectively, are directly

transferred from one chain to the other.

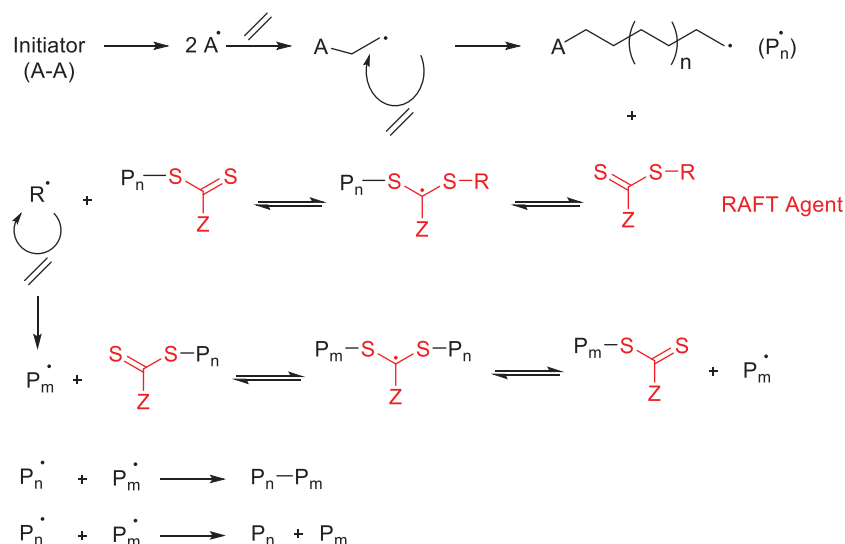
In ethylene radical polymerization, the processes involving a degenerative chain-transfer mechanism (RAFT polymerization, ITP, and TERP) are considered effective. In RAFT polymerization, there is an intermediate tertiary radical between two equilibria (**Scheme 3/b**), the equilibria are shifted from the thiocarbonylthio radical by deactivating it through a radical destabilizing group (for example, Z= OEt). Thus the transfer of the polyethylene chains on the thiocarbonylthio group is favored.¹⁷

Scheme 3. a) General degenerative chain-transfer mechanism; b) RAFT polymerization general mechanism; c) ITP general mechanism; d) TERP general mechanism.

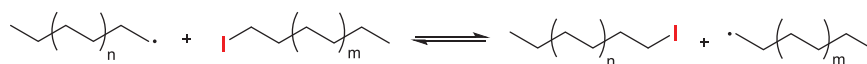
a) Genral Degenerative Chain-Transfer Mechanism



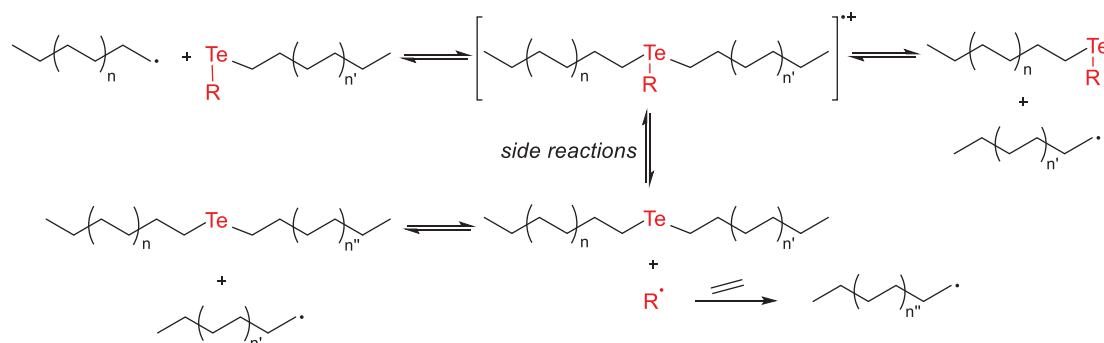
b) Reversible Addition-Fragmentation Chain-Transfer Polymerization (RAFT Polymerization)
[Ethylene monomer]



c) Iodine-Transfer Polymerization (ITP) [*Ethylene monomer*]



d) Organotellurium-Mediated Radical Polymerization (TERP) [Ethylene monomer]



In the case of ITP and TERP, there is a direct transfer of the iodine and the tellurium compound, respectively, without any intermediate (**Scheme 3/c,d**). Thus a fair equilibrium occurs allowing the controlled polymerization of monomers such as ethylene.¹⁸

After this explanation, it is concluded that in the case of **ethylene radical polymerization**, the agents utilized in the processes of reversible termination mechanism act as "radical traps" because their action mode satisfies the definition of a radical trap, they deactivate the chain carriers irreversibly without production of any new one (**Scheme 2**). While those utilized in the processes of degenerative chain transfer mechanism act as "controlling agents", they are capable of directing a reversible deactivation process.

To simplify this conclusion, **Figure 1** represents the classification of the agents depending on the mechanism which they satisfy.

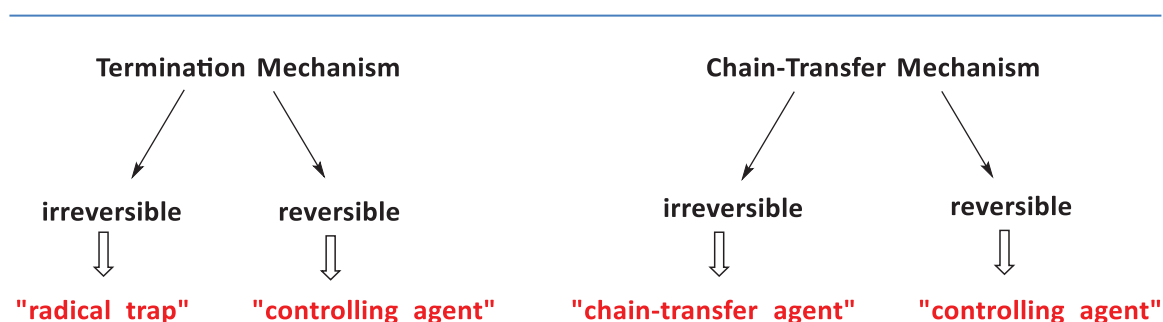


Figure 1. Classification of the agents in radical polymerization processes depending on their mode of action.

After this introduction, the discussion of our work about the effect of TEA on the ethylene radical polymerization could be more obvious and simpler.

C.2.6. Effect of TEA on the Ethylene Radical Polymerization

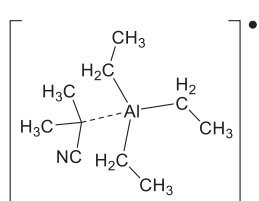
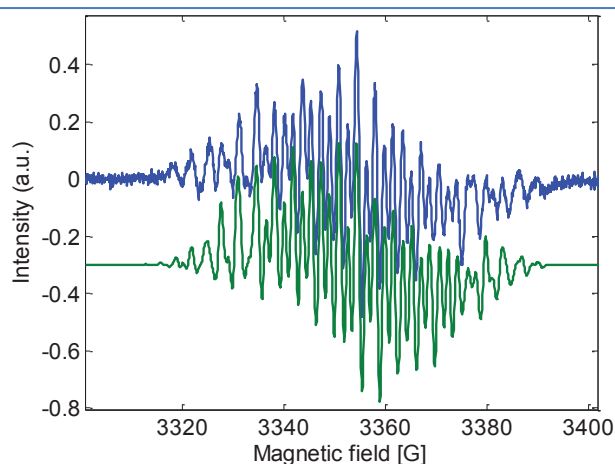
The main reason that encouraged our team to study the effect of TEA on ethylene radical polymerization is the proof of the interaction between TEA and radicals obtained by electron paramagnetic resonance "EPR" (electron spin resonance "ESR").

C.2.6.1. EPR Analysis: Interaction between TEA and Radicals

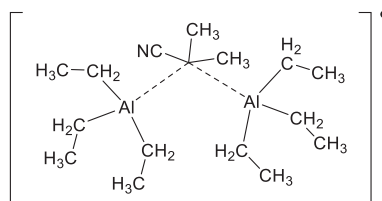
Electron paramagnetic resonance (EPR) or electron spin resonance (ESR) spectroscopy is a method for studying materials with unpaired electrons. The basic concepts of EPR

are analogous to those of nuclear magnetic resonance (NMR), but it is electron spins that are excited instead of the spins of atomic nuclei.

The EPR analysis has been done to check the interaction between TEA and radicals. The simulation of a mixture of AIBN radical initiator with TEA (**Figure 2**) allows to distinguish two major species after resolving most of the hyperfine couplings (**Figure 2**). The experimental spectrum obtained is similar to the simulated one showing that there is an interaction between TEA and radicals (**Figure 2**).



Simulation: 60 %



40 %

Figure 2. EPR analysis of a mixture of AIBN and TEA. (experimental, simulated)

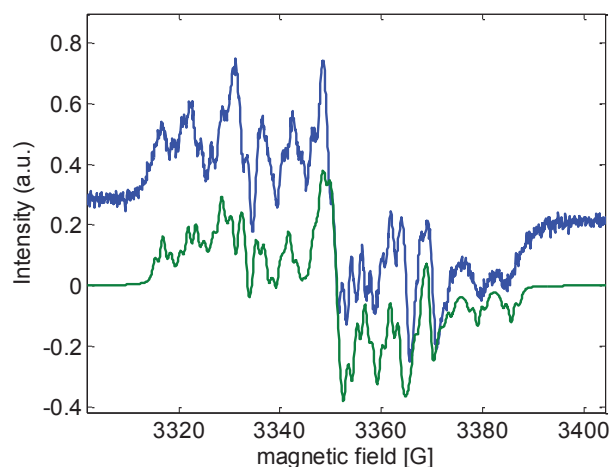


Figure 3. EPR analysis of trapping the TEA molecule by TEMPO. (experimental, simulated)

To verify the interaction of TEA with radicals, an EPR analysis of a mixture of TEA with TEMPO ((2,2,6,6-tetramethylpiperidin-1-yl)oxyl), which is a stable radical used as a radical marker in EPR, has been realized. The EPR simulation of trapping of TEMPO by the TEA molecule showed a 65 % rate of trapping. The experimental spectrum obtained is similar to the simulated one (**Figure 3**).

An important step before starting the investigation of the effect of TEA on the ethylene radical polymerization was to run a blank reaction with full characterization in order to compare all experiments to this reference. In addition an Aufbau reaction has been done to insure that TEA alone couldn't produce polyethylene chains under mild conditions.

C.2.6.2. Conventional Ethylene Free Radical Polymerization (blank reaction) and "Aufbau" Reaction

A blank free radical polymerization (FRP) has been done using heptane as a solvent, where heptane was chosen because it is a solvent with negligible transfer, and under the same conditions at which the reactions in presence of TEA will be carried out: 0.6 mmol (100 mg) of AIBN, 50 mL of heptane, 200 bars of ethylene at 90 °C; AIBN is the radical initiator used (azobisisobutyronitrile). Heptane is indeed compatible with the use of aluminum alkyls to the contrary of solvents generally used for the FRP of ethylene (such as DMC, DEC, and THF).

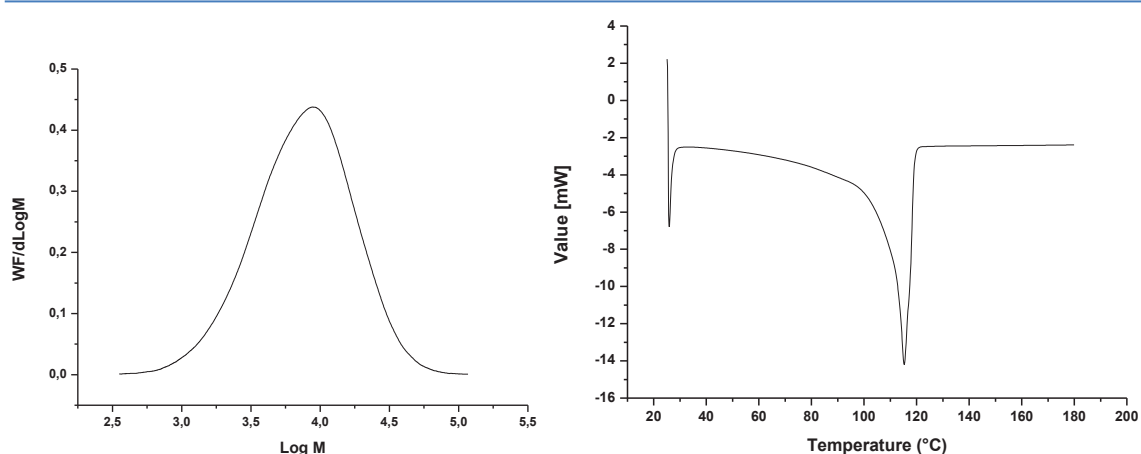


Figure 4. *To the left:* Molar mass distribution obtained by HT-SEC for the PE produced from the conventional FRP in heptane; *to the right:* DSC peak of the PE obtained from the conventional FRP in heptane.

A three-hour reaction produced 6.2 g of polyethylene (PE) with $M_n = 5060$ g/mol, a

dispersity of 2.01, and a melting point equal to 115 °C. **Figure 4** represents the molar mass distribution peak obtained from high temperature size exclusion chromatography (HT-SEC) in addition to the differential scanning calorimetry (DSC) peak from which the melting point is obtained.

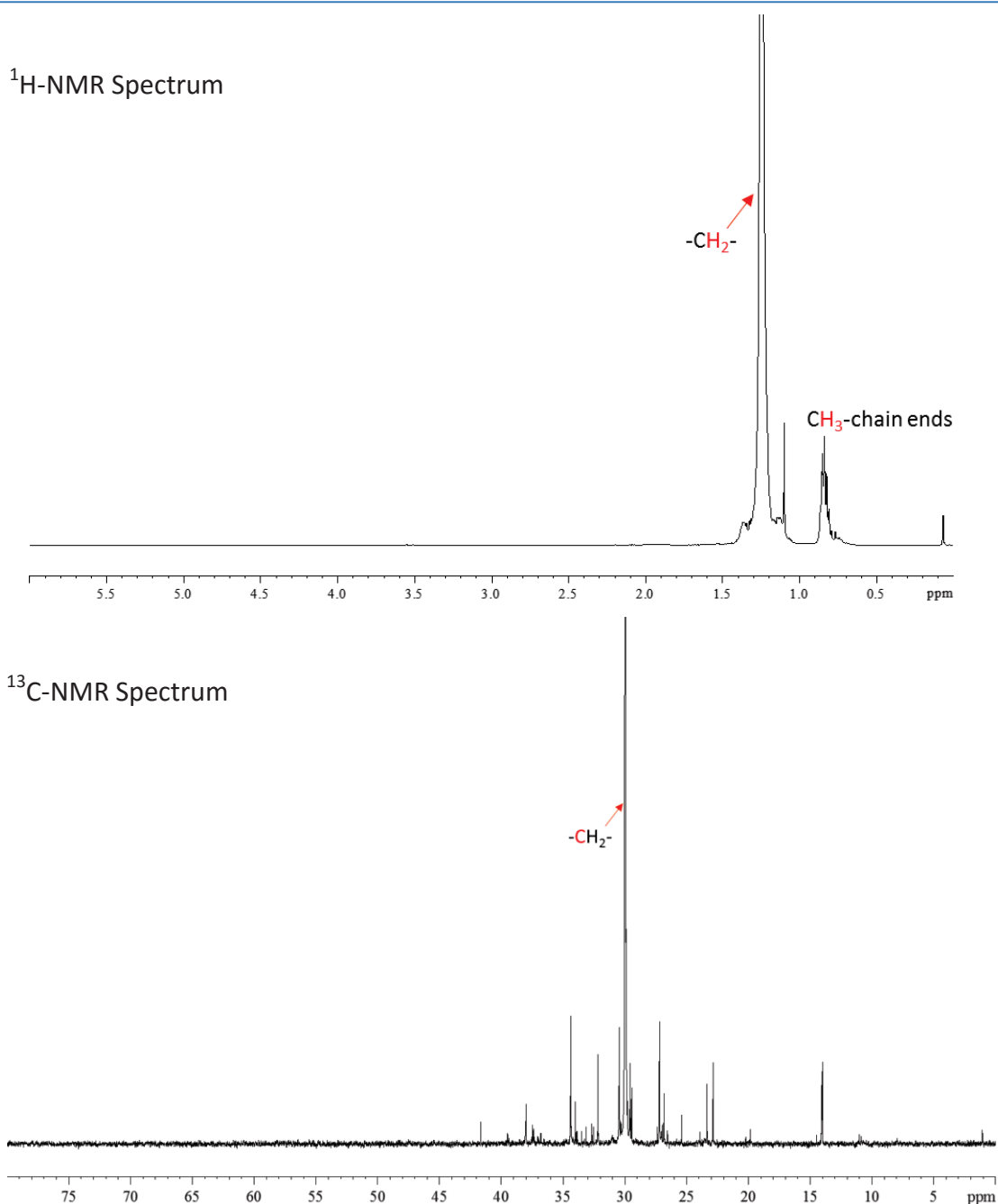


Figure 5. ¹H- and ¹³C-NMR spectra of the PE produced from the conventional FRP in heptane.

Figure 5 shows the proton and carbon NMR spectra, in the ¹H-NMR spectrum the peak corresponding to the protons on the carbon atoms of the PE backbone appears at 1.26 ppm, and that corresponding to the terminal CH₃ appears at 0.87 ppm. In the ¹³C-NMR

spectrum the peak corresponding to the carbon atoms of the PE main chain appears at 30 ppm, and the other peaks correspond to the carbon atoms of the different branches of the polymer; it is a low-density polyethylene (produced from a radical process).

An "Aufbau" reaction (a reaction discovered by Ziegler about the insertion of ethylene into an aluminum alkyl compound to produce ethylene oligomers¹⁹) has been also done to insure that TEA couldn't produce PE alone especially under such mild conditions (P= 200 bar and T= 90 °C), where it produced just few mgs (200 mg) of ethylene oligomers (200 g/mol).

After this rapid study, we started the investigation of the effect of the concentration of TEA on the molar mass and the dispersity of the PE produced in order to optimize the amount of TEA that should be added.

The AIBN/TEA/heptane mixture was prepared in a Schlenk before introducing it into the reactor through a cannula. The desired amount of AIBN was added, and the Schlenk was dried under vacuum for 10 min. Then, under argon atmosphere, 50 mL of dry heptane and the desired amount of TEA were added into the Schlenk. The AIBN/TEA/heptane solution was stirred for 10 min, a pale yellow solution is obtained (the darkness of the solution increases by increasing the amount of TEA). AIBN become soluble in heptane in presence of TEA.

C.2.6.3. Mn of Polyethylene versus [TEA]

Table 1. The effect of [TEA] on the molar mass and the dispersity of the PE produced.

Run ^a	Number of eq. of TEA ^b	Mn ^c (g/mol)	Mw/Mn ^c	Melting Point ^d (°C)
1	0	5100	2.01	115
2	2.5	2700	2.4	112
3	5	600	1.1	90
4	10	500	1.07	80

^a: polymerizations are performed during 3 hours with 0.6 mmol (100 mg) of AIBN at 90 °C in 50 mL of heptane under 200 bars of ethylene pressure; ^b: with respect to 0.6 mmol of AIBN; ^c: determined by HT-SEC; ^d: determined by DSC.

As it is shown in **Table 1** and **Figure 6**, the molar masses decrease by increasing the amount of TEA, in addition to extremely narrowed dispersities obtained in the case of 5 eq. and 10 eq. (with respect to [AIBN]) of TEA (≈ 1.1) (**Table 1**; **Figure 7**). From these results, we preferred to add 5 eq. of TEA in the upcoming reactions in order to achieve narrow molar mass distributions.

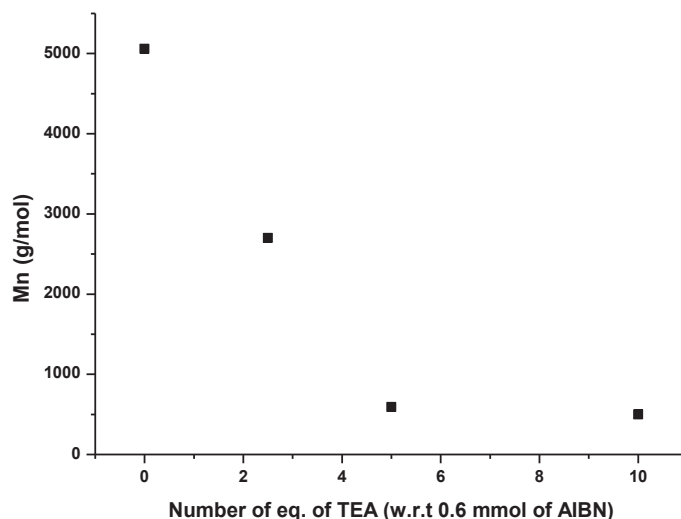


Figure 6. The variation of M_n as function of [TEA].

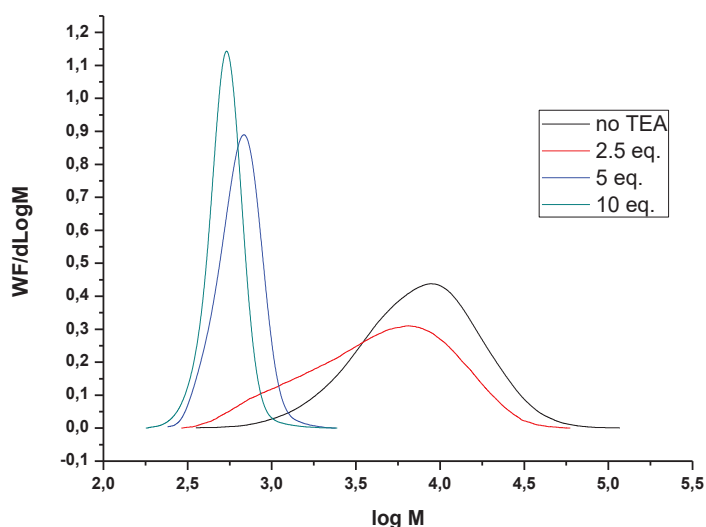
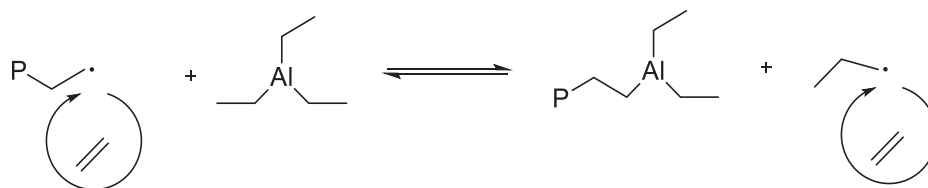


Figure 7. Molar mass distributions obtained by HT-SEC for the PE produced in presence of different [TEA] in the polymerization reactions.

Depending on the obtained data (the lower molar masses and the narrower dispersities compared to the ethylene free radical polymerization), our primary hypothesis was that TEA could act as a controlling agent in the ethylene radical polymerization *via* a degenerative transfer mechanism, which means that it could be a reversible chain-transfer agent (**Error! Not a valid bookmark self-reference.**).

Scheme 4. Proposed mechanism of a possible control of ethylene radical polymerization by TEA.

To verify this primary assumption, it was necessary to study the variation of the molar mass as function of conversion in which a linear increase in the molar mass of PE should be obtained and it must be close to the theoretical calculations to insure that there is a controlled polymerization or what would be a reversible chain-transfer mechanism in that case. This rule is essential to the main concepts of a controlled radical polymerization: *"The number of polymer chains produced must be virtually equal to the number of the controlling agent molecules"*.

C.2.6.4. Mn of Polyethylene versus Conversion

A series of reactions has been performed with 0.6 mmol (100 mg) of AIBN and 5 eq. of TEA at 90 °C in 50 mL of heptane under 200 bars of ethylene. The variable parameter was time in order to check the variation in conversion, and thus study the variation of the molar mass of the polyethylene produced with respect to conversion (**Table 2**).

Table 2. The variation of conversion and Mn of PE as function of time.

Run ^a	Reaction Time (h)	Conversion (g)	Mn ^b (g/mol)	Mw/Mn ^b	Melting Point ^c (°C)
5	1	2	550	1.06	88
6	2	2.35	560	1.07	84
7	3	2.85	590	1.1	90
8	4	3.15	630	1.08	92
9	6	3.8	640	1.1	95
10	8	3.9	620	1.08	92

^a: polymerizations are performed with 0.6 mmol (100 mg) of AIBN and 5 eq. of TEA at 90 °C in 50 mL of heptane under 200 bars of ethylene pressure; ^b: determined by HT-SEC; ^c: determined by DSC.

As it is shown in **Figure 8**, conversion increases as time increases. This increase could be a minor evidence of the occurrence of a controlled polymerization but is not, especially since after 6 h the conversion rate decreases slightly, which could be an evidence that the increase in conversion is just due to the consumption of active radicals (propagation is proceeding) and not because of a reversible living polymerization.

On the other hand, the increase in molar masses, even if it was a slight increase (from 550 g/mol till 640 g/mol), with the narrowed dispersities (≈ 1.1) (**Table 2, Figure 9**) tell us that there is a high possibility of TEA behaving as an irreversible chain-transfer agent.

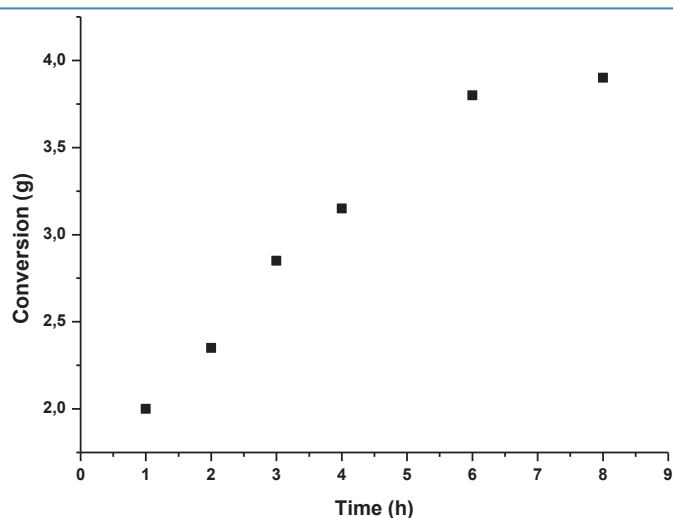


Figure 8. The variation of conversion in presence of TEA as function of time.

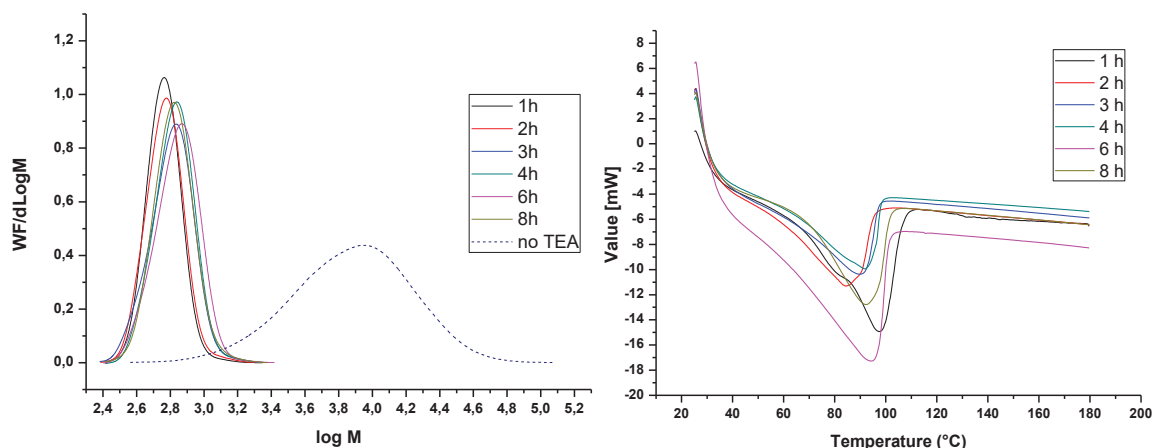


Figure 9. To the left: Molar mass distributions obtained by HT-SEC for the PEs produced in the reactions in Table 2; to the right: DSC peaks of the PEs obtained from the reactions in Table 2.

In order to clear up this doubt we studied the variation of the molar mass of PE as function of conversion. We should observe a linear increase in molar masses that must

be virtually equal to the theoretical calculations. In these calculations it is considered that a perfectly controlled reaction occurred: *"The number of polymer chains produced is exactly equal to the number of the controlling agent molecules"*.

The theoretical calculation in the case of TEA can be a bit difficult because it is different from the case with other controlling agents. For example, in RAFT polymerization, each molecule of the RAFT agent control the growth of one chain, while in the case of TEA there is a possibility of the control of one, two, or three chains per TEA molecule (**Figure 10**).

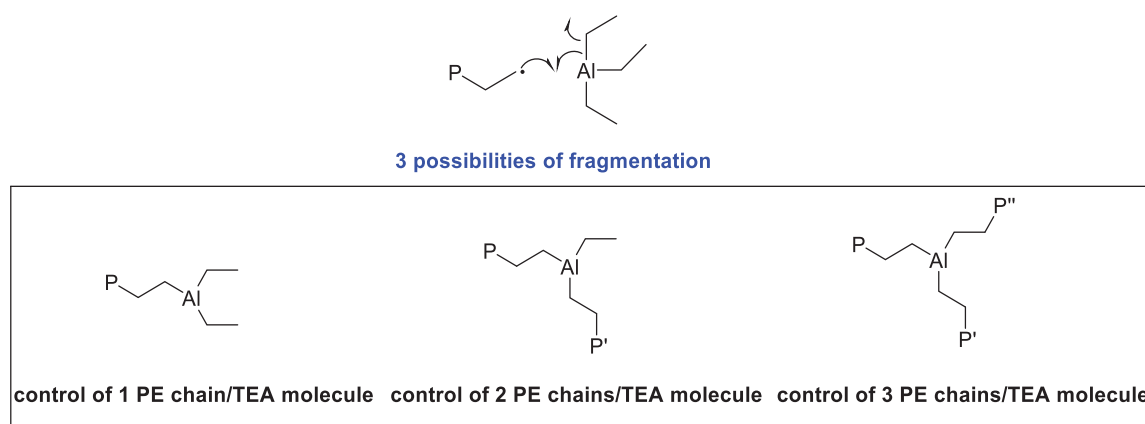
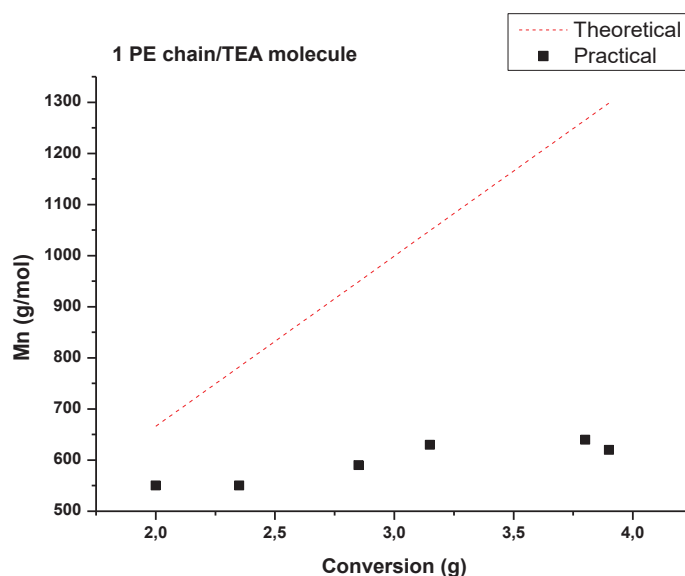


Figure 10. The possible number of PE chains that could be controlled per one TEA molecule.

The plot of the three possibilities has been done in order to compare each of these theoretical calculations with the obtained results.



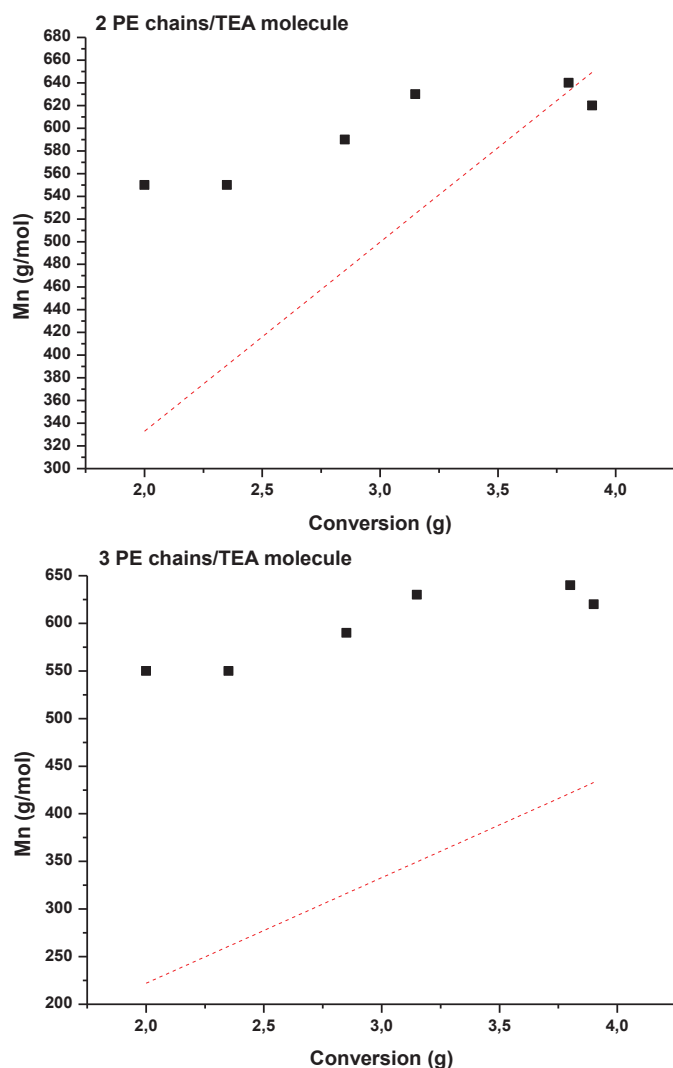


Figure 11. The variation of the molar mass of the PEs produced in presence of TEA with respect to conversion.

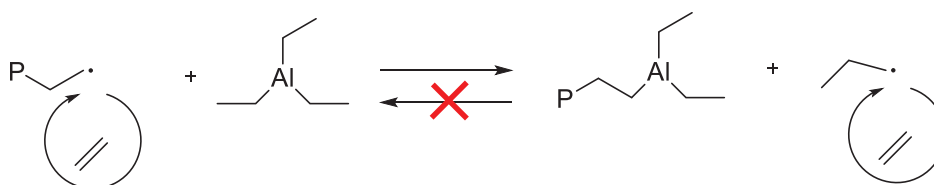
The theoretical calculations follow the equations:

1. 1 PE chain/TEA molecule: $Mn_{theo} = m_{PE \text{ produced}} / n_{PE \text{ chains}} = m_{PE \text{ produced}} / n_{TEA}$
2. 2 PE chains/TEA molecule: $Mn_{theo} = m_{PE \text{ produced}} / n_{PE \text{ chains}} = m_{PE \text{ produced}} / 2n_{TEA}$
3. 3 PE chains/TEA molecule: $Mn_{theo} = m_{PE \text{ produced}} / n_{PE \text{ chains}} = m_{PE \text{ produced}} / 3n_{TEA}$

It was obvious from these plots that the real (practical) increase of the molar mass of PE versus conversion is far from the theoretical one in all of the cases (1, 2, and 3 chains/TEA molecule) (**Figure 11**). This shows that the number of chains produced is really different from the number of molecules of TEA, thus TEA is not acting as a controlling agent (reversible chain-transfer agent), and therefore there is no reversible reaction occurring similar to the degenerative chain-transfer mechanism. Instead, TEA is

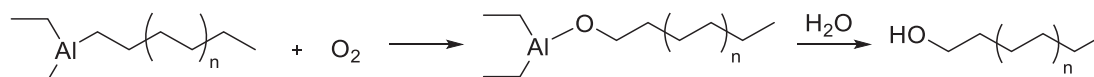
acting as a "chain-transfer agent" (irreversible chain-transfer agent) which explains the lower molar masses and the narrower dispersities of the PEs produced in its presence compared to those of the PE produced in conventional FRP. Also, TEA couldn't be just a radical trap because it follows a chain-transfer mechanism by deactivating a chain carrier and producing a new one (**Scheme 5**). **Scheme 5** represents a correction for our primary proposition of the controlled ethylene radical polymerization mechanism by TEA (**Scheme 4**) showing an irreversible reaction that follows behavior of an irreversible chain-transfer mechanism (**Figure 1**).

Scheme 5. Proposed mechanism for the function of TEA as a chain-transfer agent in ethylene radical polymerization.



The function of TEA as a chain-transfer agent was also proved by NMR analyses. As it is known that TEA is unstable in air, so that the PE chain-end is readily oxidized when the polymer is exposed to air (oxygen) according to the "Ziegler-Alfol process",²⁰ then a PE terminated by an -OH group is obtained (**Scheme 6**). This appears clear in the ¹H- and ¹³C-NMR spectra of the PE produced. The ¹H-NMR spectrum shows a triplet at 3.41 ppm corresponding to the protons on the α-carbon to the OH group. And this α-carbon appears at 62.8 ppm in the ¹³C-NMR spectrum; the other peaks in the ¹³C-NMR spectrum correspond to the carbon atoms of the different branches (**Figure 12**).

Scheme 6. Ziegler-Alfol process.



In the series of reactions that have been done, the molar masses of the PEs produced were too low (< 1000 g/mol) not only because of the presence of a chain-transfer agent, but also because of the high concentration of the radical initiator "AIBN" (100 mg). This high concentration of radicals increases the rate of termination in the polymerization process.

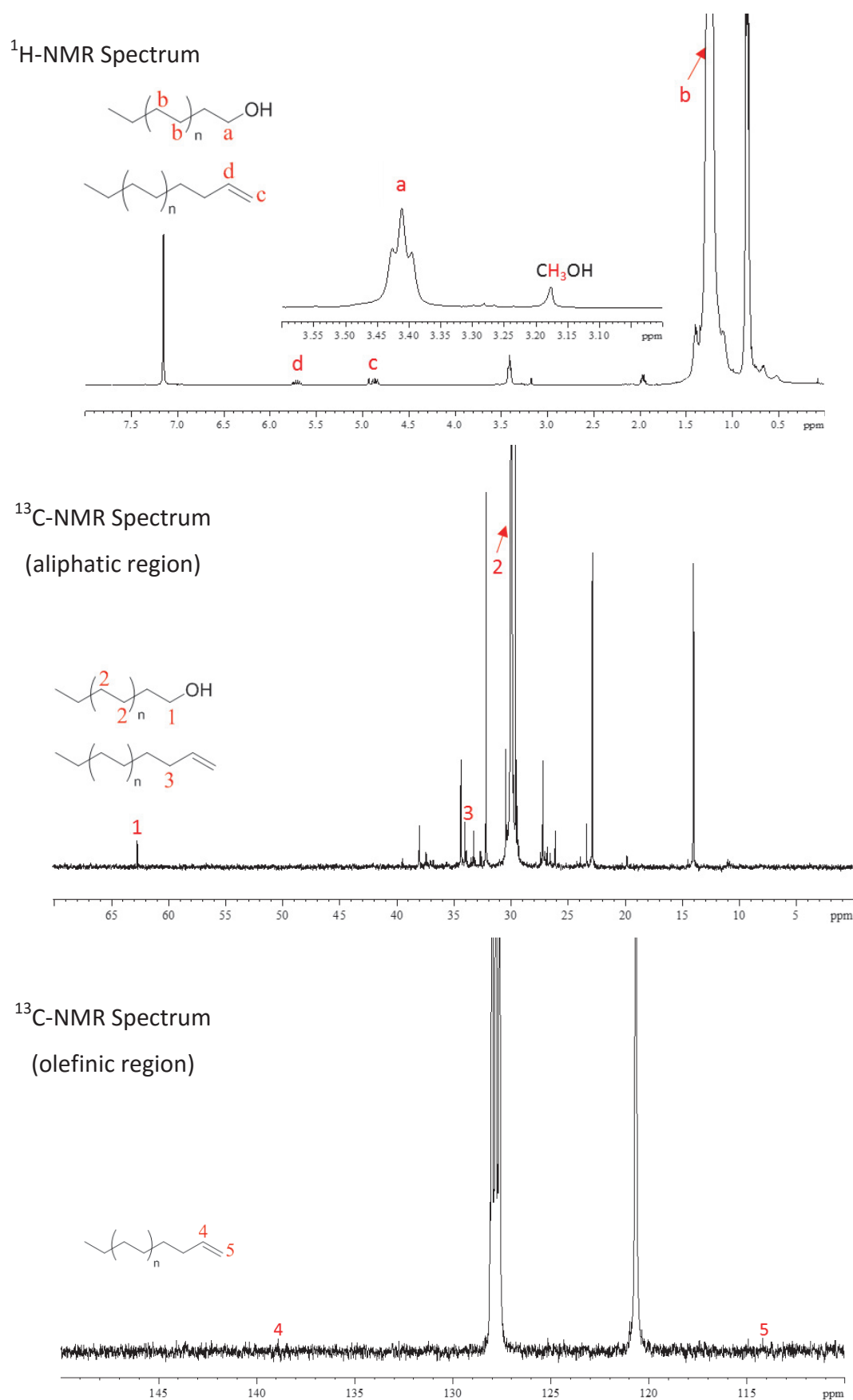
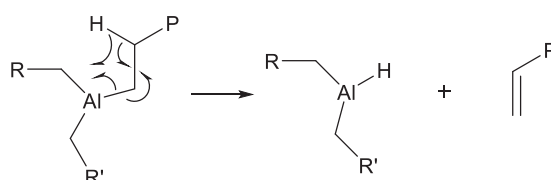


Figure 12. ¹H- and ¹³C-NMR spectra of the PE produced in presence of TEA.

The termination could occur either by combination or by disproportion. The vinyl chain-ends that appear in the NMR spectra originate either from the disproportionation termination reaction or from the H-transfer to aluminum (**Scheme 7**).

Scheme 7. H-transfer to aluminum.



P: polyethylene chain
R, R': H or alkyl

Thus we repeated our studies of the effect of TEA on the radical polymerization of ethylene with lower concentration of AIBN (30 mg) to verify our new hypothesis.

- Effect of TEA on ethylene radical polymerization in presence of lower concentration of AIBN (0.18 mmol):

Table 3. The variation of conversion and Mn of PE produced from a 0.18 mmol of AIBN-initiated reactions as function of time.

Run ^a	Reaction Time (h)	Conversion (g)	Mn ^b (g/mol)	Mw/Mn ^b	Melting Point ^c (°C)
11	1	0.7	5300	1.8	117
12	2	0.9	5400	1.7	118
13	3	1.2	5800	1.7	117
14	4	1.3	6100	1.7	117
15	6	1.4	5800	1.7	117
16	8	1.5	6600	1.7	117
17	24	1.6	6900	1.6	118
18 ^d	3	3.45	5600	2.2	116

^a: polymerizations are performed with 0.18 mmol (30 mg) of AIBN and 5 eq. of TEA at 90 °C in 50 mL of heptane under 200 bars of ethylene pressure; ^b: determined by HT-SEC; ^c: determined by DSC; ^d: no TEA added (conventional free radical polymerization).

A series of reactions was performed with 0.18 mmol (30 mg) of AIBN and 5 eq. of TEA

at 90 °C in 50 mL of heptane under 200 bars of ethylene. Similar to the previous series, the variable parameter was time in order to check the variation in conversion and thus study the variation of the molar masses of the polyethylenes produced with respect to conversion (**Table 3**).

For comparison, a conventional FRP reaction has been done under the same conditions (Run 18/**Table 3**). In 3 h, 3.45 g of PE was produced with $M_n = 5600$ g/mol, $M_w/M_n = 2.2$, and a melting point of 116 °C.

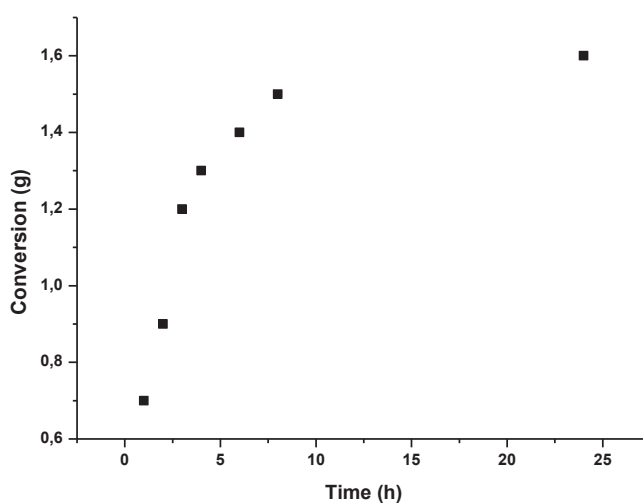


Figure 13. The variation of conversion of PE produced in presence of TEA as function of time. ($[AIBN] = 0.18$ mmol)

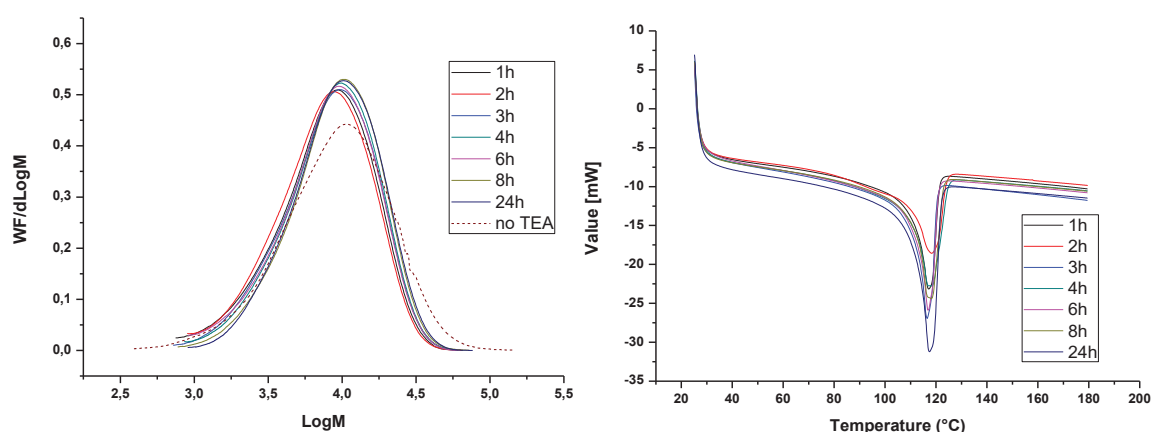


Figure 14. *To the left:* Molar mass distributions obtained by HT-SEC for the PEs produced in the reactions in "Table 3"; *to the right:* DSC peaks of the PEs obtained from the reactions in "Table 3".

Similar to the series of reactions in which 0.6 mmol of AIBN was added, as displayed in **Figure 13**, conversion increases as time increases. This increase is quite important at the early stages but slows down rapidly. After 8 h the conversion rate decreases again,

which confirms that the increase in conversion is due to the consumption of active radicals (propagation is proceeding) and not because of a reversible living polymerization.

The increase in molar masses (from 5300 g/mol till 6900 g/mol), with relatively narrow dispersities (≈ 1.7) (**Figure 14**) is again an indication of TEA behaving as an irreversible chain-transfer agent.

Similar to the previous series, we studied the variation of the PE molar masses as function of conversion. Again we should have a linear increase in molar masses, virtually equal to the theoretical calculations to insure that there is control.

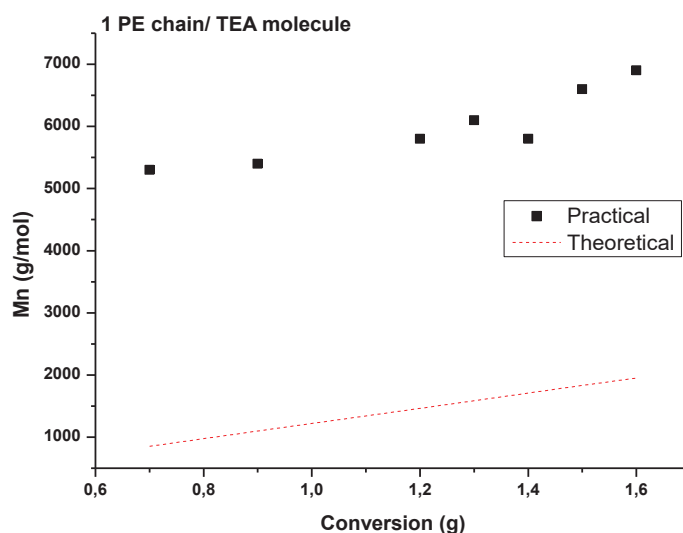


Figure 15. The variation of the molar mass of the PE produced in presence of TEA with respect to conversion. ($[AIBN] = 0.18 \text{ mmol}$)

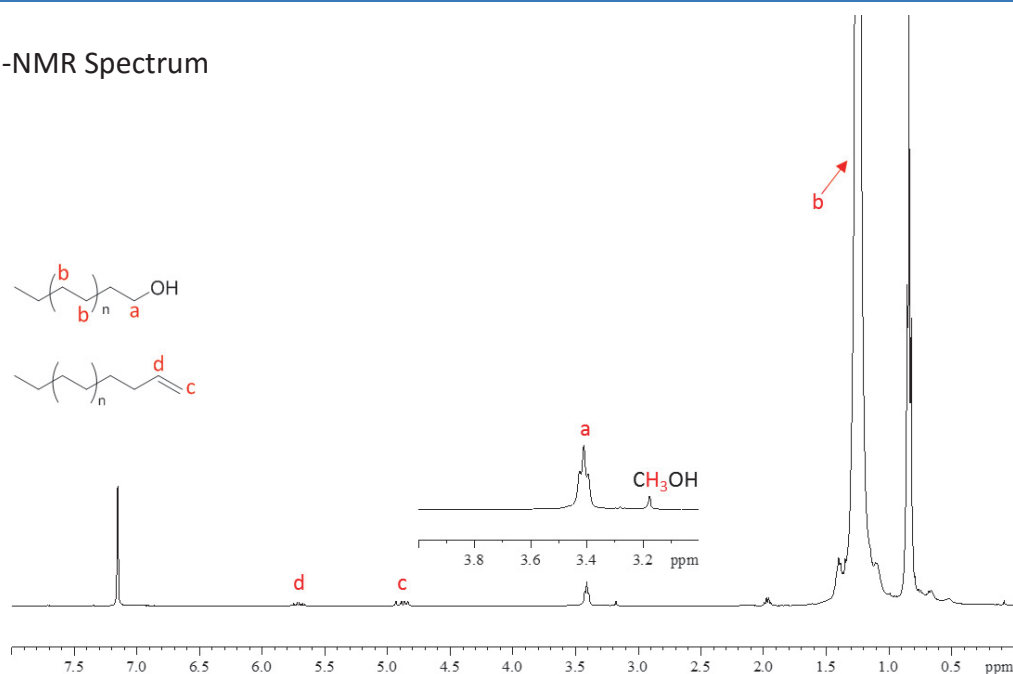
It was obvious from the plot of M_n versus conversion (in the case of the control of 1 PE chain per TEA molecule) that there is no control, since there is a large difference between the calculated molar masses (in the case where each TEA molecule is responsible for the growth of one PE chain) and the measured ones (**Figure 15**). It is thus unnecessary to plot the other two cases (2 or 3 PE chains/TEA molecule) in which the difference between the practical and theoretical results would be even bigger (the theoretical molar masses will be even smaller than those calculated in the case of 1 PE chain/TEA molecule).

This study yielded the same conclusion as the previous one, that the number of chains produced is extremely different from the number of molecules of TEA, thus TEA is not

acting as a controlling agent (reversible chain-transfer agent), and therefore there is no reversible reaction following the degenerative chain-transfer mechanism. Instead, TEA is acting as an irreversible chain-transfer agent.

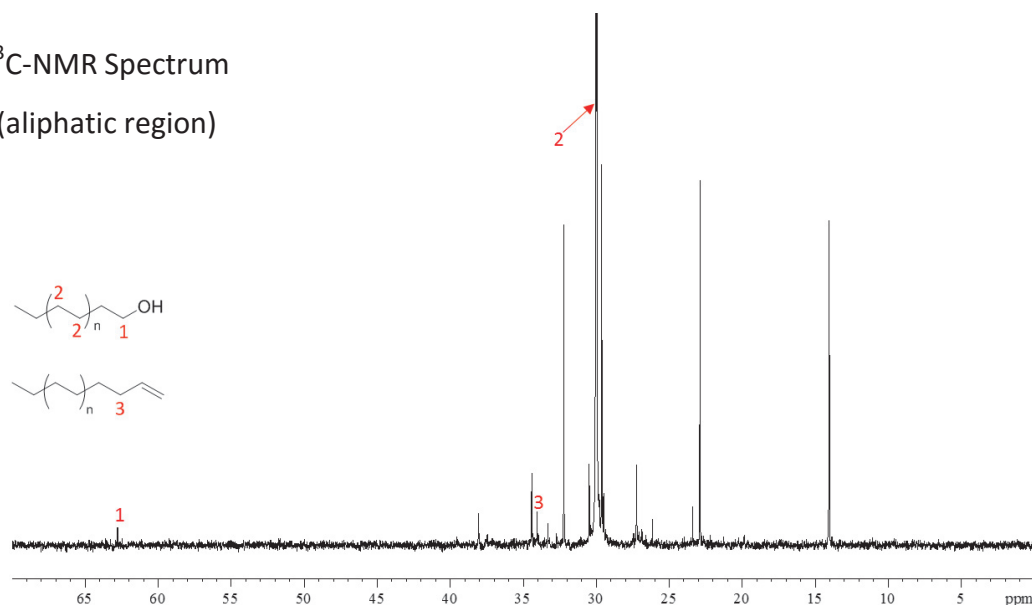
In the same manner, since C-Al bond reacts in the presence of O₂, the PE chain-end is readily oxidized when the polymer is exposed to air, and a PE terminated by an -OH group is obtained (**Scheme 6**). This is evidenced in the ¹H- and ¹³C-NMR spectra, the ¹H-NMR spectrum shows a triplet at 3.40 ppm corresponding to the protons on the α-carbon to the OH group, and this α-carbon appears at 62.9 ppm in the ¹³C-NMR spectrum (**Figure 16**).

¹H-NMR Spectrum



¹³C-NMR Spectrum

(aliphatic region)



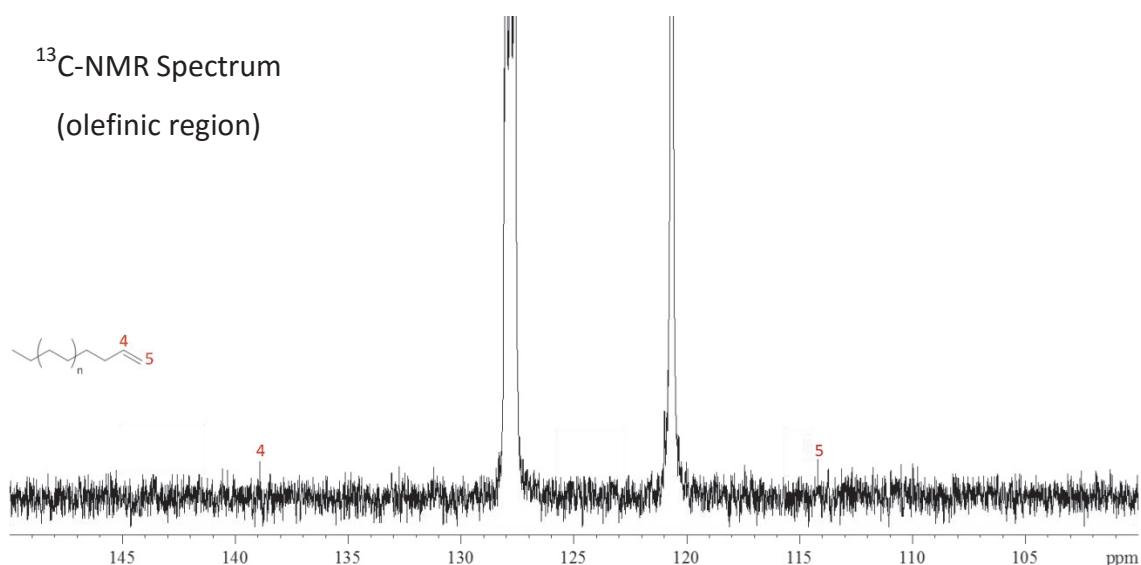


Figure 16. ¹H- and ¹³C-NMR spectra of the PE produced in presence of TEA. ([AIBN] = 0.18 mmol)

Because of the difference between the molar masses of the PEs obtained in the first series ([AIBN] = 0.6 mmol) and the second one ([AIBN] = 0.18 mmol), we checked the variation of M_n versus the concentration of AIBN.

C.2.6.5. Variation of M_n as function of [AIBN]

Table 4. The variation of M_n with respect to [AIBN].^a

[AIBN] mmol	[TEA] ^b	Conversion (g)	M_n^c (g/mol)	M_w/M_n^c	Melting Point ^d (°C)
0	6 mmol	0.2	200	1.02	-
0.18 (30 mg)	5 eq	1.2	5800	1.7	117
0.32 (60 mg)	5 eq	1.4	650	1.5	92
0.45 (80 mg)	5 eq	2.1	600	1.09	90
0.6 (100 mg)	5 eq	2.85	590	1.1	90

^a: polymerizations are performed during 3 hours at 90 °C in 50 mL of heptane under 200 bars of ethylene pressure; ^b: number of equivalent with respect to [AIBN]; ^c: determined by HT-SEC; ^d: determined by DSC.

As it is shown in **Table 4** and **Figure 17**, the PE molar masses decrease by increasing the concentration of the radical initiator AIBN, which is logical because by increasing the concentration of the radical initiator, the concentration of active species (radicals) increases in the medium, and thus the rates of transfer and termination increase which

will lead to lower molar masses of the PE chains.

The relatively higher molar masses obtained in the case of 30 mg of AIBN, which are similar to that of the PE produced in conventional radical polymerization, might indicate that a high enough radical concentration is needed to react with a fivefold ratio of TEA and enable it to take part in the polymerization. Otherwise, conventional radical polymerization takes place before any participation of the transfer agent.

The obtained PEs are of narrowed dispersities (**Table 4; Figure 17**), this is due to the effect of TEA as a chain-transfer agent. The melting point varies according to the PE molar masses (**Table 4; Figure 18**).

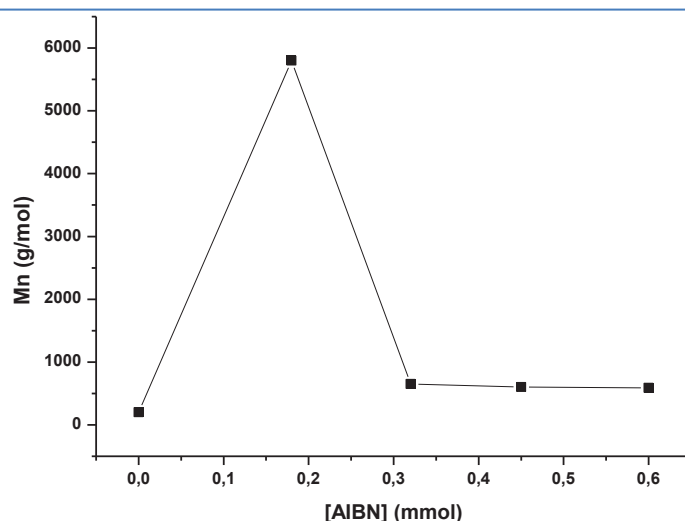


Figure 17. Variation of Mn as function of [AIBN].

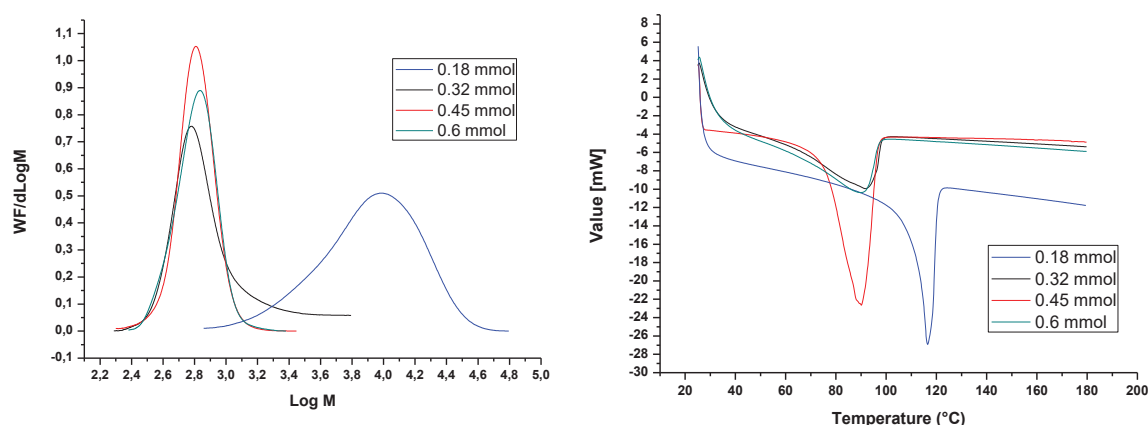


Figure 18. *To the left:* Molar mass distributions obtained by HT-SEC for the PEs produced in the reactions initiated by different [AIBN]; *to the right:* DSC peaks of the PEs obtained from the reactions initiated by varying [AIBN].

After this investigation, we added a proof for the occurrence of PE chains still connected to aluminum. We harnessed the reactivity of the C-Al bond by quenching the

reaction with iodine (I_2) to get PE bearing a C-I moiety as chain-end; in other words, an I-functionalized PE. This quenching forms a definite proof that TEA is a chain-transfer agent in ethylene radical polymerization. It could be used in the synthesis of block copolymers in further iodine-mediated radical processes (ethylene/co-monomer blocks), or further functionalizations to achieve a wide variety of end-functionalized PEs.

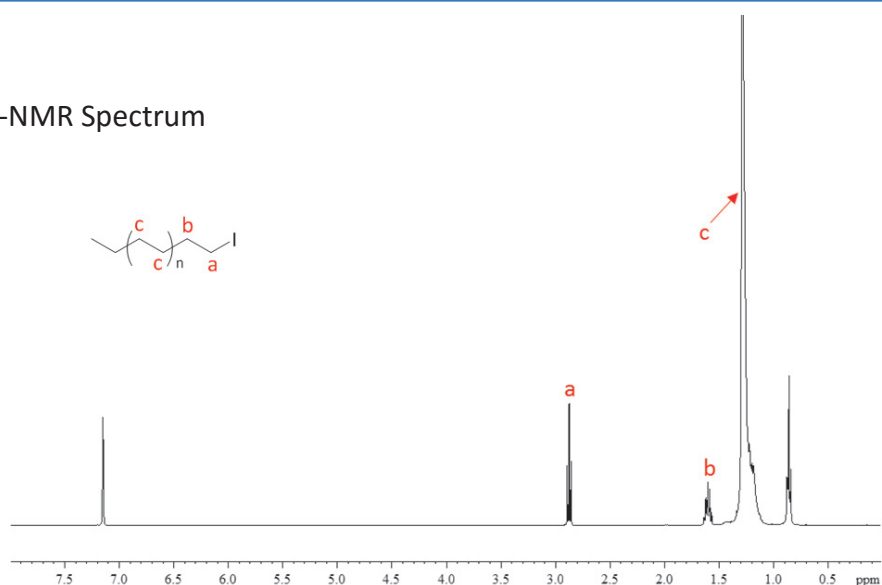
C.2.6.6. Quenching the Polymerization Reaction by I_2

A reaction has been performed with 0.6 mmol (100 mg) of AIBN and 5 eq. of TEA at 90 °C in 50 mL of heptane under 200 bars of ethylene pressure; the reaction lasted 3 hours. It was quenched by 2 eq. of iodine (with respect to TEA). The NMR analyses of the produced PE evidence the I-C bond at the chain ends. In the 1H -NMR spectrum (**Figure 19**), a triplet appears at 2.95 ppm corresponding to the protons on the α -carbon to "I" (CH_2-I). This C atom appears at 4.9 ppm in the ^{13}C -NMR spectrum (**Figure 19**). The total percentage of the I-terminated PE chains was equal to 87 %, therefore most of the PE chains were attached to Al.

The molar mass distribution is shown in **Figure 20**, where the molar mass of the PE produced is 500 g/mol with a dispersity of 1.17.

Therefore, The TEA-mediated ethylene radical polymerization reaction constitutes a valuable alternative to Aufbau reaction, where it produces short PE chains that are functionalizable. In addition, this process could be used in synthesis of ethylene/co-monomer block copolymers.

1H -NMR Spectrum



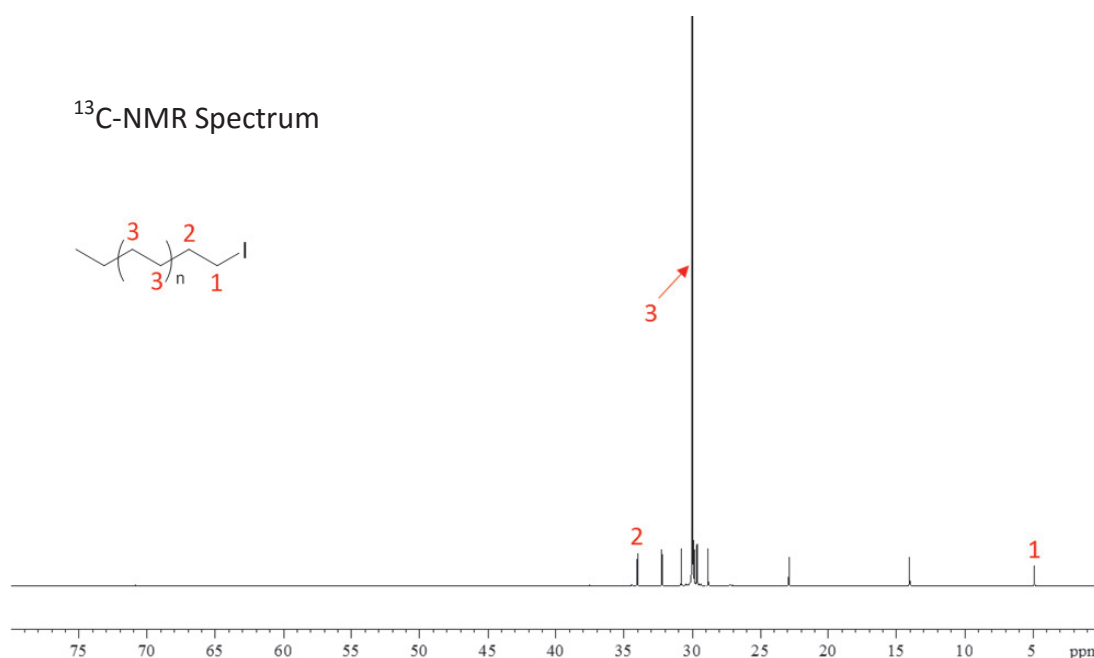


Figure 19. ^1H - and ^{13}C -NMR spectra of the I-chain ended PE.

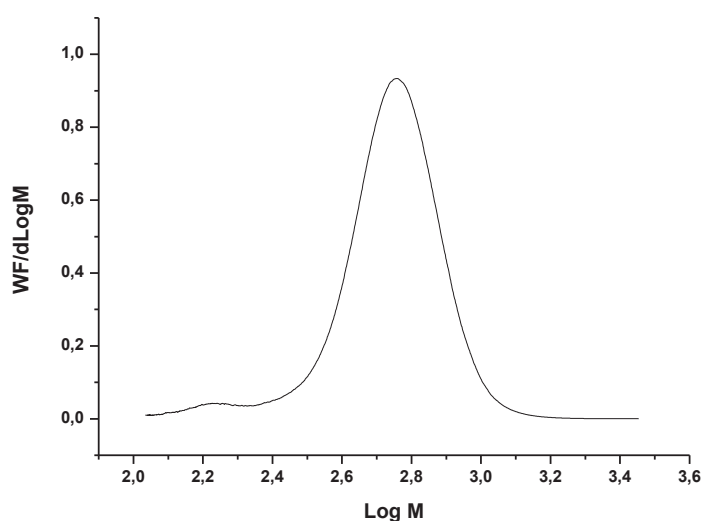


Figure 20. Molar mass distribution obtained by HT-SEC for the I-chain ended PE.

From all what have been investigated it is concluded that TEA is acting as a chain-transfer agent in ethylene radical polymerization. This role which proves the interaction of TEA with polyethylenyl radicals opened our eyes on exploiting this Lewis acid in breaking the inertness of CO₂ in ethylene radical polymerization and incorporating it in the PE chains. Thus moving from the activation of CO₂ as a polymerization medium to its activation as a functionalization agent in ethylene free radical polymerization using TEA.

C.3. Incorporation of CO₂ in the Polyethylene Chain Using Triethylaluminum

Although a wide variety of chemical reactions that incorporate CO₂ are known today,^{21,22} many more can be envisioned. Thus, there is a continuing requirement to develop new chemistries based on the CO₂ molecule, particularly in the polymer field. There is no reports published about the incorporation of CO₂ in polyethylene chains, and since CO₂ is inert in ethylene free radical polymerization (chapter II) we tried to find a very reactive additive to force the incorporation of CO₂ in the PE chain.

After we unveiled the interaction between TEA and radicals, we realized that this interaction in addition to the interaction of TEA with CO₂ (which has been proved in the literature, see section "C.3.1") could be harnessed to allow for CO₂-incorporation within the PE chains. This work opens a route to new LDPE-type polyethylene bearing CO₂-derived motifs to alter the polarity of PE, to ease its compatibilization with fillers for instance, while retaining its intrinsic mechanical and chemical properties.

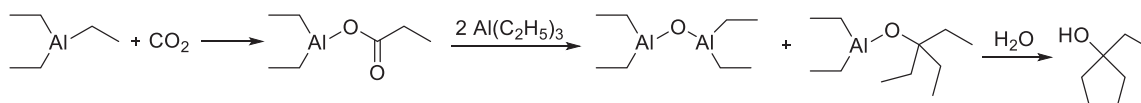
Before starting the discussion of our work in this section it is important to mention the reports that investigated the interaction of TEA with CO₂ in the literature.

C.3.1. Interaction of Triethylaluminum with CO₂

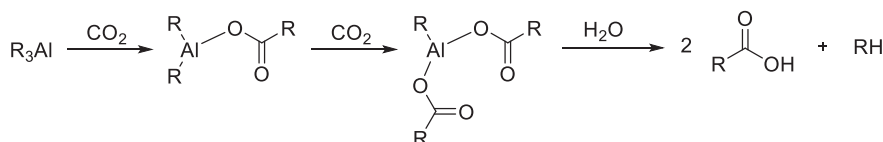
There are few old reports including the interaction between metal alkyls and CO₂.

Scheme 8. Reactions of trialkylaluminum with CO₂.

a) Weidlein work



b) Tolstikov work



In 1969, Weidlein reported that triethylaluminum reacts with CO₂ to produce an alcohol (**Scheme 8**). Primarily a carboxylated aluminum compound is formed, then by a reaction with two TEA molecules a dimer with an oxygen bridge is produced plus an oxygenated aluminum compound. The last step was the addition of H₂O to produce a

tertiary alcohol.²³

In 1974, Tolstikov et al. reported the production of a carboxylic acid from the reaction of aluminum trialkyls with CO₂, where some polyunsaturated carboxylic acids were synthesized and the scheme for the carboxylation of aluminum trialkyls was refined (**Scheme 8**).²⁴

C.3.2. Ethylene Radical Polymerization in scCO₂ in the Presence of TEA

Even though carbon dioxide is considered an important sustainable solvent in different polymerization processes and a successful co-monomer in some copolymerization processes (mainly with epoxides), its use as a co-monomer together with olefins, especially with ethylene, is still considered an impossible task. Here we tried to bypass the thermodynamic and kinetic obstacles (described at the end of chapter I) by incorporating carbon dioxide in the polyethylene chain produced in a radical process *via* triethylaluminum, hoping for a breakthrough in the way towards copolymerization of ethylene with carbon dioxide.

Although there is no reported work in literature about incorporation of CO₂ in polyethylene, this idea originated in our team after the success in utilizing CO₂ as a polymerization medium in ethylene free radical polymerization (chapter II). We looked for strategies to break the inertness of CO₂ to incorporate it within the PE chains through a specific additive. This additive must possess a capability of interacting with both polyethylenyl radicals and CO₂. From what has been shown in the first part of this chapter about the role of TEA as a chain-transfer agent in ethylene radical polymerization in addition to its capability of interacting with CO₂ (part C.3.1), we deduced that the suitable additive could be TEA. Thus, we thought of utilizing TEA as an agent that could incorporate CO₂ within the polyethylene chains in an ethylene radical polymerization process as a logical suite to its use as an inert polymerization medium.

Azobisisobutyronitrile (AIBN) has been used as a radical initiator with 5 eq. of TEA, and heptane as a solvent. The reaction was conducted in a 160 mL reactor pressurized using a 1:1 mixture of ethylene and CO₂ (250 bars at 70°C). In 3 hours, 2.85 g of polymer was produced.

The SEC analysis of the polymer produced gave a molar mass equal to 1500 g/mol with

a dispersity of 2.7, and the melting point of the polymer is 120 °C obtained by DSC (Figure 21).

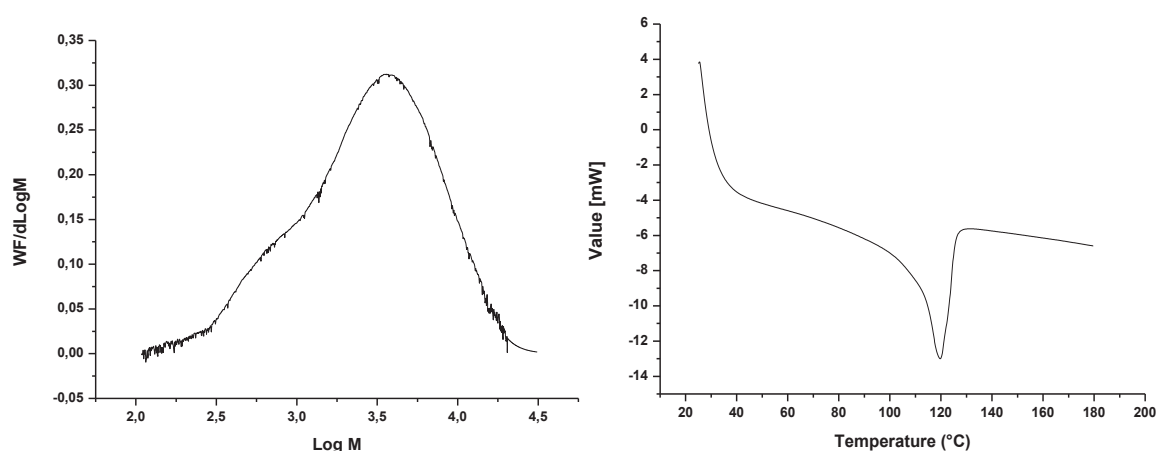
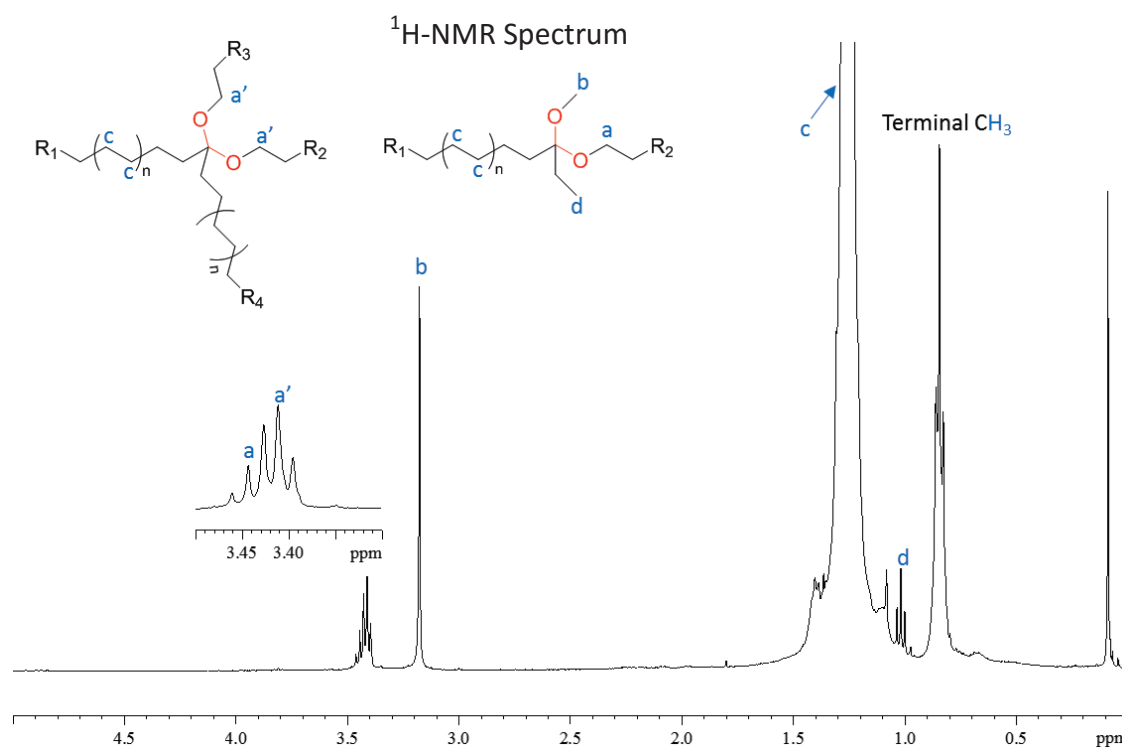


Figure 21. *To the left:* Molar mass distribution obtained by HT-SEC for the CO₂-functionalized PE; *to the right:* DSC peak of the CO₂-functionalized PE.

The incorporation of CO₂ in the polyethylene chain is proved by carrying out different analyses of the polymer produced, mainly nuclear magnetic resonance (NMR).

Depending on the NMR analysis, we proposed the incorporation of CO₂ in the PE chain as a ketal. The ¹H and ¹³C-NMR spectra verify the formation of a ketal.



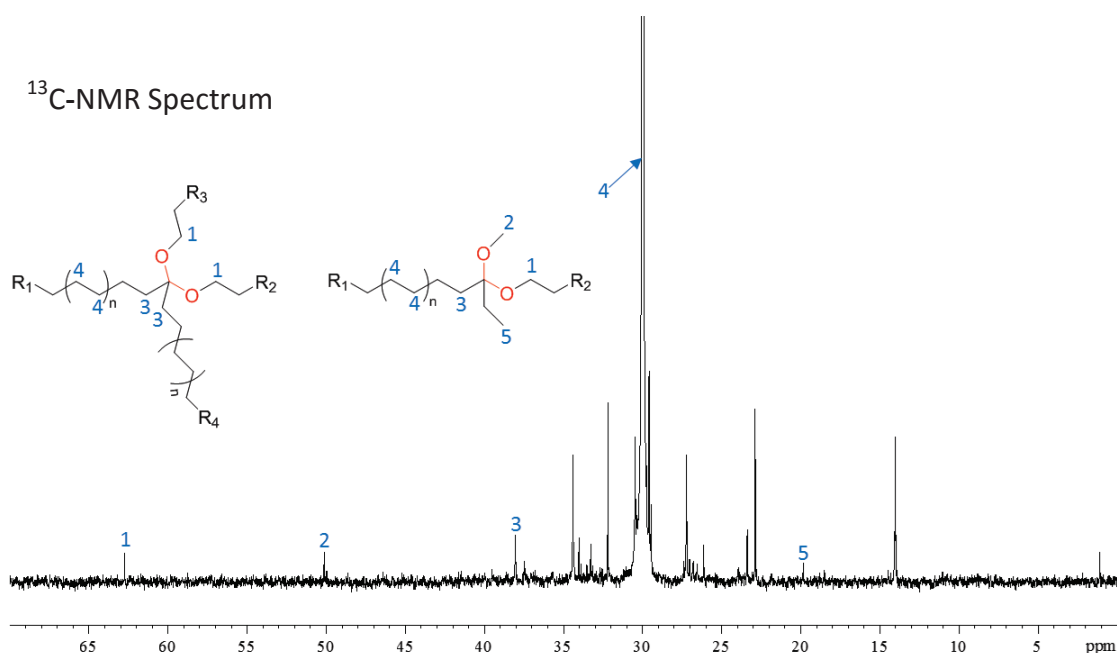


Figure 22. ¹H- and ¹³C-NMR spectra of the CO₂-functionalized PE.

First, in the ¹H-NMR spectrum, a doublet of triplet (resembling a quintet) appears at 3.4 ppm corresponding to the protons on the α-C to the oxygen atoms of the ketal group (**Figure 22**); a singlet appears at 3.15 ppm corresponding to the protons of the methyl group connected to the oxygen of the ketal group, the high intensity of this peak could be due to the formation of other types of methylated ketal-functionalized PE chains; and a triplet that corresponds to the protons of the CH₃ of the ethyl group connected to the quaternary carbon of the ketal functional group appears at 1.02 (**Figure 22**). The peak that corresponds to the protons of the PE main chain appears at 1.26 ppm, and a triplet at 0.88 ppm represents the protons of the terminal CH₃ (methyl chain-end and branching-end).

Next, in the ¹³C-NMR spectrum, the peak corresponding to the α-C atoms to the O of the ketal group appears at 62.5 ppm, and that corresponding to the α-C atoms to the quaternary C appears at 38.5 ppm (**Figure 22**). The peak at 50.0 ppm corresponds to the carbon of the methyl group α to O of the ketal group. The peak at 30.0 ppm represents the C atoms of the polymer backbone and the other peaks corresponds to the branches in the polyethylene chain, it is indeed a low density polyethylene (produced by a radical process). Note that there no peak in the carbonyl region, which indicates that there is no carbonyl carbon within the polymer.

In IR analysis, the band corresponding to the main chain of the PE appears in the IR

spectrum at 2840 cm^{-1} , and a C-O band appears at 1080 cm^{-1} which is the C-O of the ketal (**Figure 23**). In addition there is a band at 1560 cm^{-1} , this band could correspond to a C=O of some aluminum carboxylates.

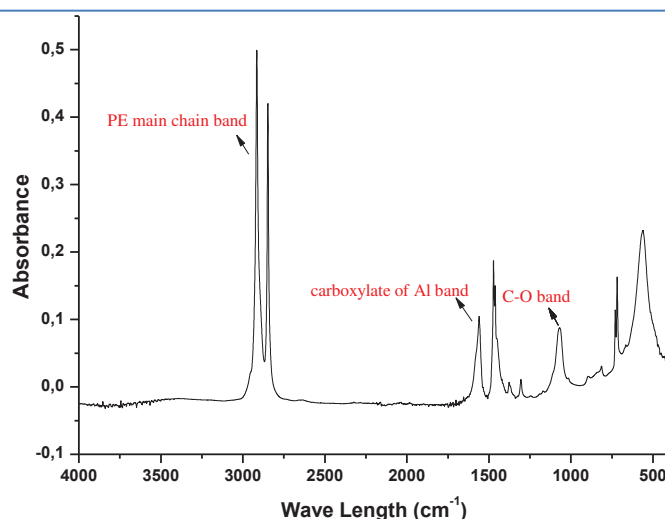


Figure 23. Infrared spectrum of the CO₂-functionalized PE.

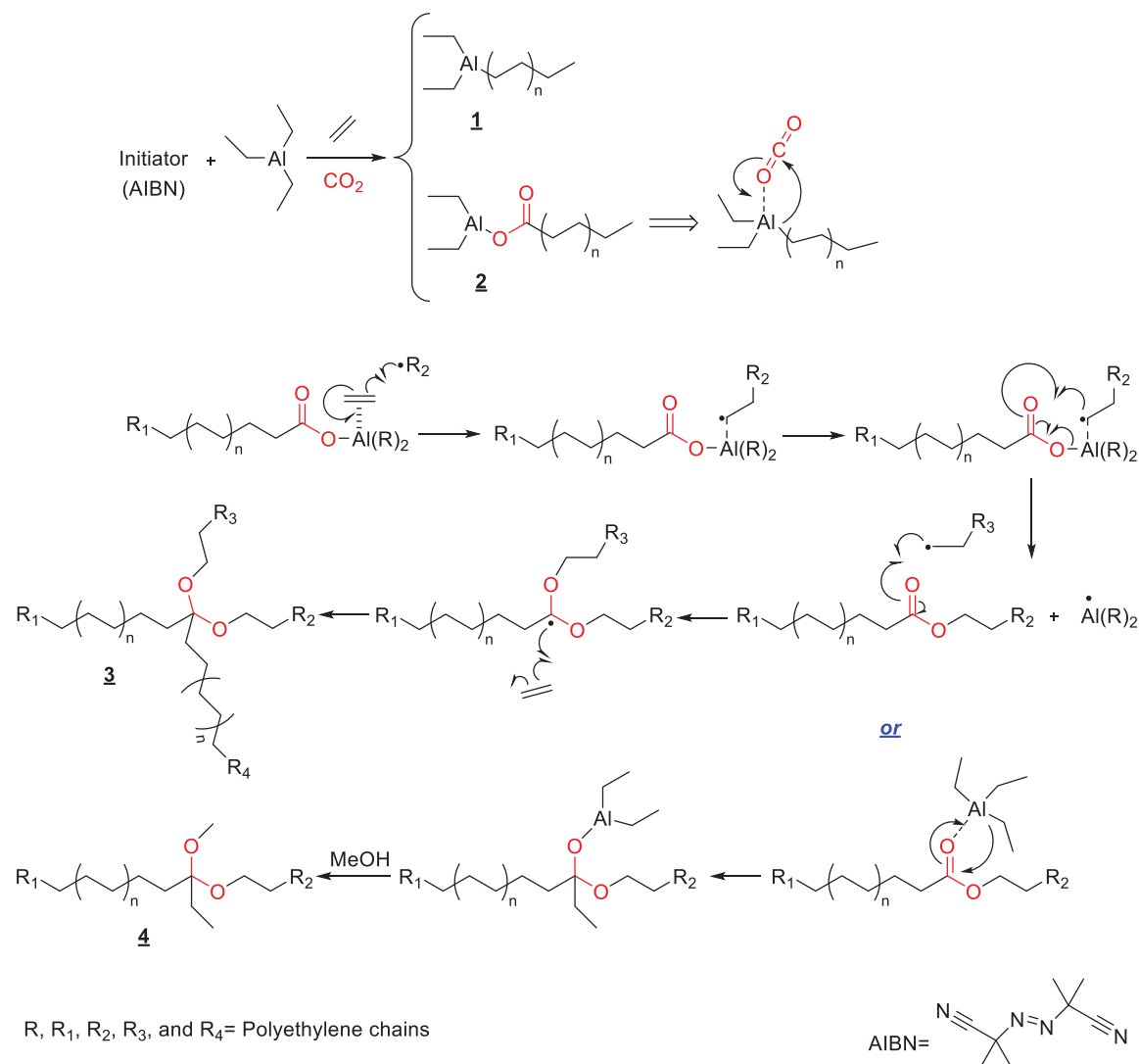
Relying on the characterizations that have been done, we proposed that CO₂ is incorporated as a ketal group in the polyethylene chain, the proposed mechanism is shown in **Scheme 9**.

Primarily, two types of chains could be attached to the aluminum center, either a simple polyethylene chain coordinated directly to aluminum (**1**; **Scheme 9**) or a polyethylene chain connected to aluminum by a COO bridge (**2**; **Scheme 9**) which is more favored due to the oxophilicity of Al. The path towards the ketal formation starts by the Lewis base-Lewis acid interaction between an ethylene molecule and Al of **2**. Then the *pi* bond of ethylene is cleaved *via* a radical process utilizing a radical source (a radical initiator or a propagating chain) which is favored because of the formation of a secondary radical. In the third step, an intramolecular radical process occurs which leads to the break of the Al-O bond and incorporation of the CO₂ molecule in the propagating polyethylene chain as an ester functional group. Here, two mechanisms could lead to the ketal formation, a radical mechanism or a coordination-insertion mechanism. In the radical one, the C=O bond is cleaved by the formation of a sigma bond between the oxygen and a radical source, a tertiary radical is produced which starts polymerizing ethylene, thus the polyethylene functionalized by a ketal group is synthesized. In the coordination-insertion mechanism, the oxygen of the C=O is coordinated to the Al and

either a long PE chain or an ethyl group on aluminum migrates to carbon, therefore a ketal-functionalized polyethylene is formed. This functional group is methylated by washing the polymer with methanol.

Scheme 9. Proposed mechanism of the incorporation of CO₂ in the PE chain.

CO₂ Incorporation Mechanism (Formation of Ketal)



In order to verify the mechanism that we proposed (passing from an ester to a ketal), we depend on an ester model compound, decyl decanoate, which is similar in its structure to a PE functionalized by an ester group. **Figure 24** shows the different ¹H- and ¹³C-NMR spectra. First, the ¹H-NMR spectrum of decyl decanoate shows mainly two triplets at 2.15 ppm and 3.95 ppm corresponding to the protons at the α carbons to the C=O and the O of the ester functional group, respectively; the ¹³C-NMR spectrum shows mainly two peaks at 64.4 ppm and 172.6 ppm corresponding to the α-C to the O of the

ester group and to the quaternary carbon of the ester group, respectively.

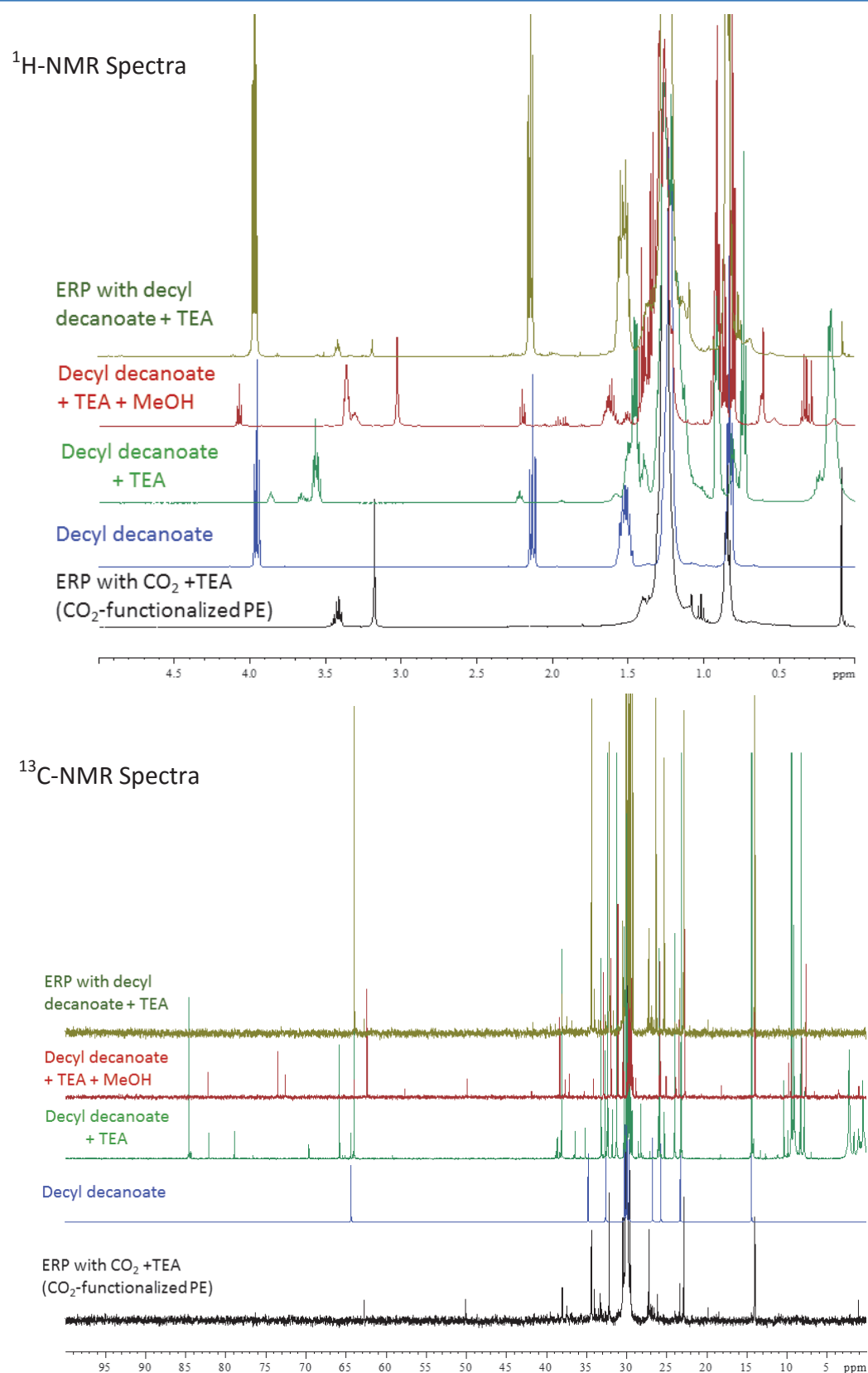


Figure 24. Comparison of the NMR spectra of the CO₂-functionalized PE with the spectra of different model reactions.

Then, the analysis of a mixture of decyl decanoate and TEA gave extremely different spectra from those of decyl decanoate. In the ^1H -NMR spectrum the triplets at 2.15 ppm and 3.95 ppm corresponding to the protons at the α carbons to the C=O and the O of the ester group disappeared and a multiplet appeared at 3.57 ppm similar to what has been obtained in the ethylene radical polymerization (ERP) in presence of CO_2 and TEA with a limited difference in chemical shift. This shows that the ester group is transformed into a group to be considered as an analogue to a ketal. The ^{13}C -NMR spectrum also insures this by the disappearance of the peak corresponding to the ester quaternary carbon at 172.6 ppm and the appearance of different types of C atoms attached to oxygen atoms, between them a peak at 62.5 ppm (exactly the same chemical shift of the α -C to the O of the ketal obtained in the CO_2 -functionalized PE spectrum) (**Figure 24**).

By addition of methanol to the decyl decanoate/TEA mixture, the ^1H -NMR spectrum shows the regeneration of an ester (two triplets at 2.2 ppm and 4.05 ppm corresponding to the protons at the α carbons to the C=O and the O of the ester group, respectively). Also, a multiplet appears at 3.37 ppm which is almost at the same chemical shift as that of the doublet of triplet obtained in the spectrum of the CO_2 -functionalized PE. The ^{13}C -NMR spectrum shows also different types of C atoms attached to oxygen atoms, between them a peak at 62.5 ppm (exactly the same chemical shift of the α -C to the O of the ketal obtained in the CO_2 -functionalized PE spectrum) (**Figure 24**).

Finally, an ethylene radical polymerization reaction (ERP) has been done in presence of TEA and decyl decanoate without any CO_2 to check the change that could happen and compare the NMR spectra with those of the polymer produced under the same conditions but by exchanging the decyl decanoate with CO_2 which is the CO_2 -functionalized PE. The ^1H -NMR spectrum of the polymer produced in this reaction was similar to that of decyl decanoate but a triplet at 3.41 ppm (exactly the same chemical shift of the protons at the α -C to the O of the ketal obtained in the CO_2 -functionalized PE spectrum) appeared, thus a new product that resembles what is obtained in presence of CO_2 is produced. This is also evidenced in the ^{13}C -NMR spectrum in which a peak appears at 62.5 ppm (exactly the same chemical shift of the α -C to the O of the ketal obtained in the CO_2 -functionalized PE spectrum) (**Figure 24**).

Therefore, the suggested mechanism (**Scheme 9**) which shows the passage through an

ester functionalization towards the formation of a ketal seems to be an acceptable one. This mechanism is still considered a proposition which could be modified, however, it forms a base for understanding the way of incorporation of CO₂ in the PE chain through using TEA.

C.3.3. Hydrolysis of the CO₂-Functionalized Polyethylene

To insure the incorporation of CO₂ in the polyethylene chain, a hydrolysis reaction of the polymer produced has been done to check the cut of the chain. This reaction was done using a diluted solution of hydrochloric acid (HCl) in excess of H₂O at 60 °C.

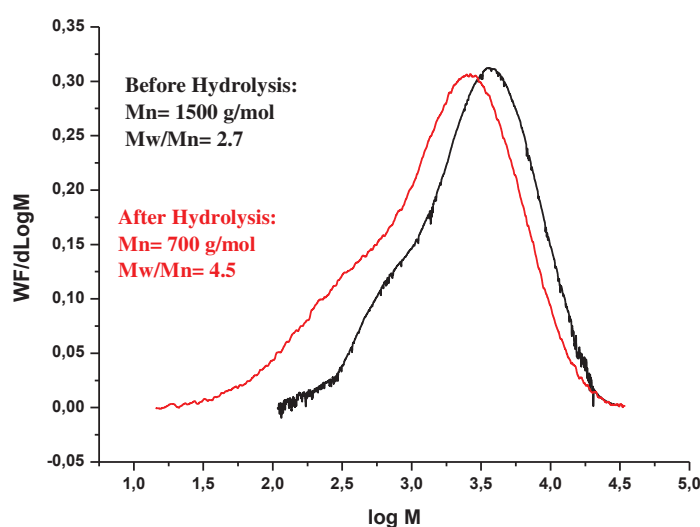


Figure 25. Molar mass distributions obtained by HT-SEC for the CO₂-functionalized PE before and after hydrolysis.

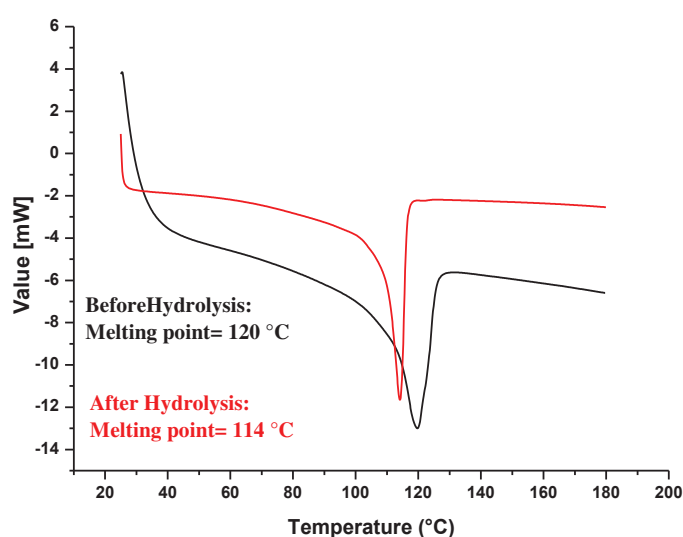
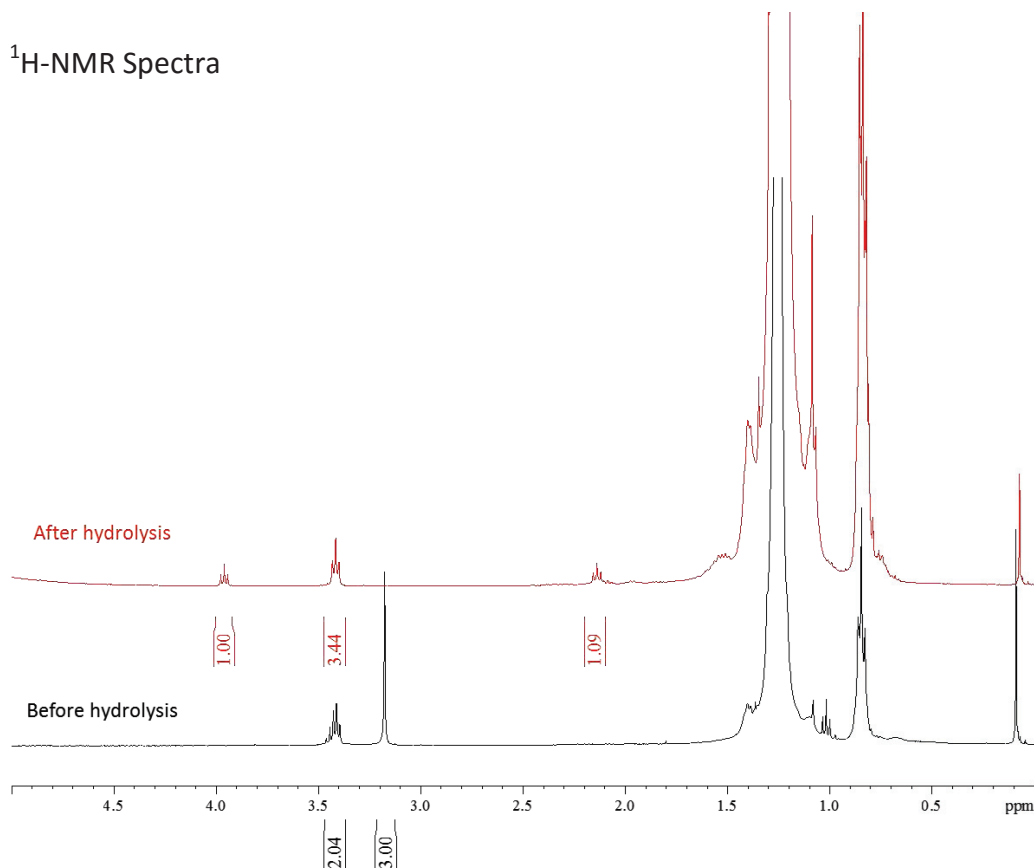


Figure 26. DSC peaks of the CO₂-functionalized PE before and after hydrolysis.

The results obtained confirmed the incorporation of CO₂ in the PE chains. The decrease

in the molar mass of the polymer after hydrolysis form an evidence for this incorporation. The M_n of the polymer was equal to 1500 g/mol before hydrolysis with a dispersity of 2.7, it decreases to 700 g/mol after hydrolysis with a dispersity of 4.5 (**Figure 25**). This decrease proves that the chains are cut at a specific functional group within the chains. Also, the DSC analysis shows a decrease in the melting point of the polymer from 120 °C before hydrolysis to 114 °C after hydrolysis (**Figure 26**), representing an additional evidence for the cutting of the polymer chains.

In the NMR analysis, the superimposed ^1H -NMR spectra of the polymer before and after hydrolysis show obvious difference (**Figure 27**). After hydrolysis, the doublet of triplet at 3.4 ppm, which corresponds to the protons at the α -C atoms to the O of the ketal group (according to our proposition), disappeared and three triplets appeared at 3.95 ppm, 3.4 ppm, and 2.13 ppm (**Figure 27**). The two triplets at 2.13 ppm and 3.95 ppm (with equal integration) fit exactly with the triplets of decyl decanoate (which correspond to the protons at the α carbons to the C=O and the O of the ester group) (**Figure 24**), showing that a formation of an ester occurred. The triplet at 3.4 ppm corresponds to the protons at the α carbon to OH.



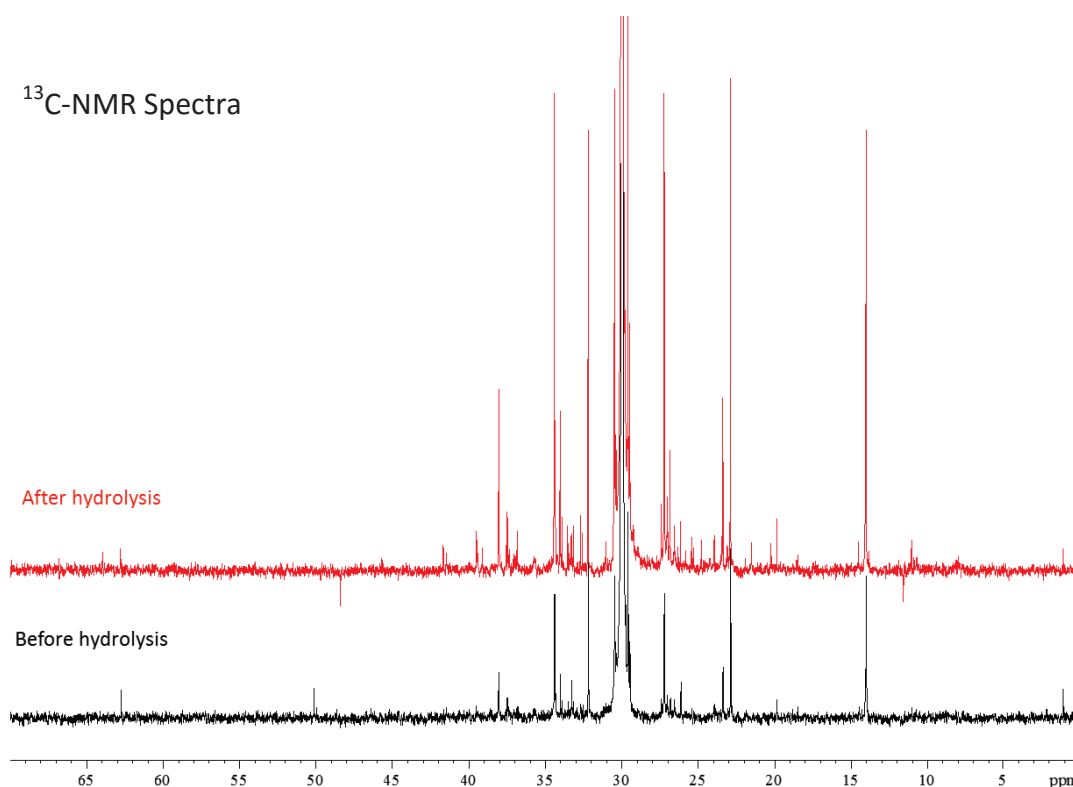
^{13}C -NMR Spectra

Figure 27. ^1H - and ^{13}C -NMR spectra of the CO_2 -functionalized PE before and after hydrolysis.

In the ^{13}C -NMR spectrum, the peaks corresponding to the α -C atoms to the O of the ester group and the OH appear at 63.5 ppm and 62.5 ppm, respectively (**Figure 27**).

The IR spectrum shows a C=O band at 1630 cm^{-1} and a C-O band at 1180 cm^{-1} corresponding to the ester group. Also a broad OH band appears at 3340 cm^{-1} from alcohol (**Figure 28**).

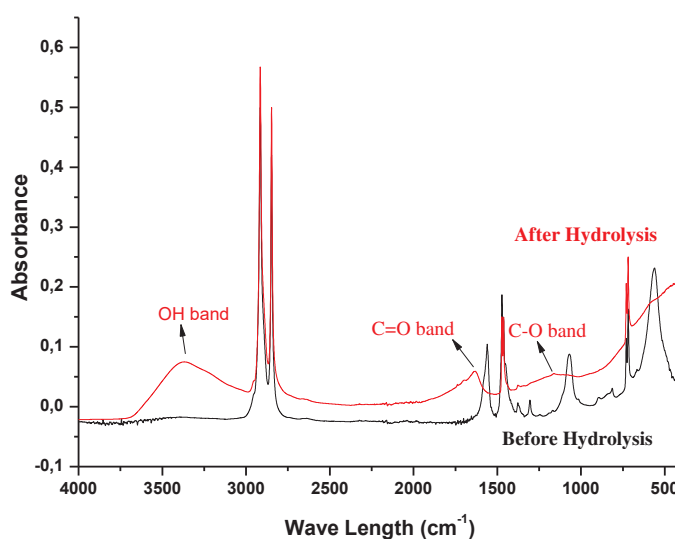
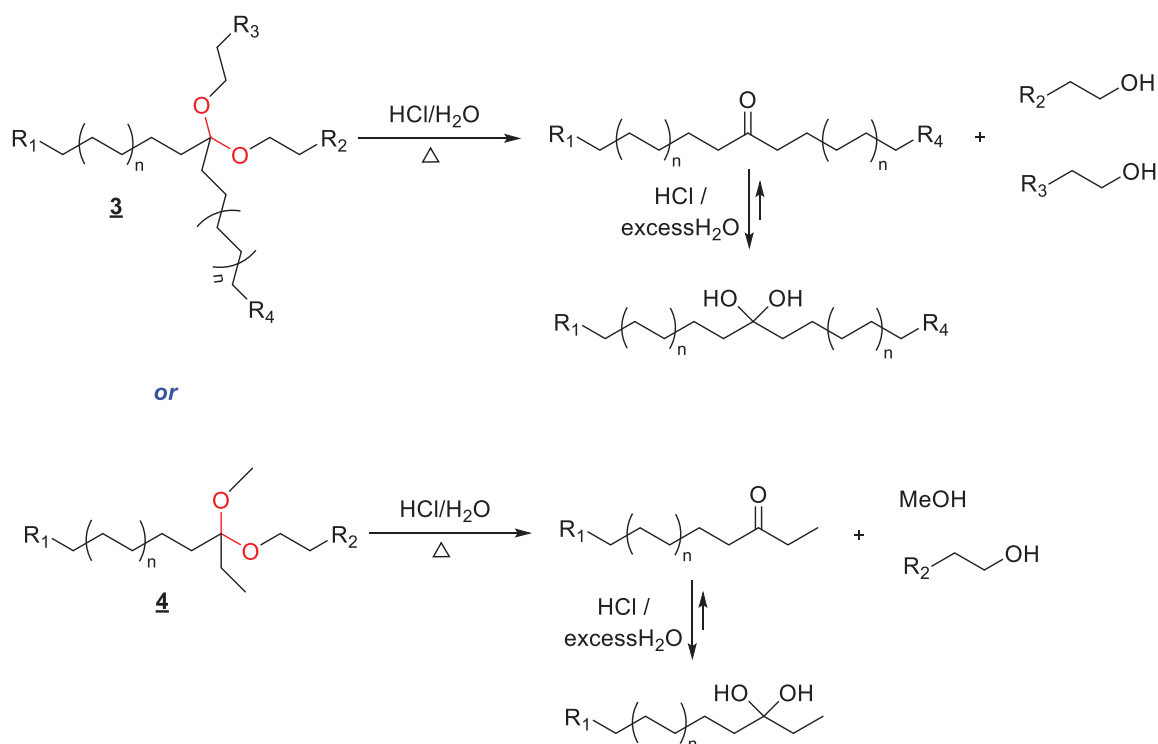


Figure 28. Infrared spectra of the CO_2 -functionalized PE before and after hydrolysis.

The logic question that should be asked here is: How are the ester and the alcohol produced? The ketal hydrolysis produces ketone and alcohol (**Scheme 10**). Even though the hydration of ketone is not favored (geminal diol is rather not stable in specific conditions), in presence of excess of H_2O it is favored (**Scheme 10**).

The production of an ester in this hydrolysis reaction is surprising. This production needs further investigation to understand the route from which an ester is produced.

Scheme 10. Proposed mechanism of the hydrolysis of the CO_2 -functionalized PE.



C.4. Conclusion

This chapter consists of two subchapters. In the first one, the effect of triethylaluminum on ethylene radical polymerization has been investigated. This study showed that triethylaluminum is acting as an irreversible chain transfer agent in ethylene radical polymerization. This achievement represents an activated Aufbau reaction through the enhancement of this process by using triethylaluminum in an ethylene radical polymerization process. It could form the basic step for the synthesis of ethylene-comonomer block copolymers *via* AlEt_3 -mediated radical processes.

The interaction of triethylaluminum with radicals, which is reported in the first

subchapter, added to the reactivity of triethylaluminum with CO_2 , which has been reported early in the literature, form the basis of the idea to utilize triethylaluminum as a functionalizing agent which incorporates CO_2 within polyethylene chains in an ethylene radical polymerization process. This achievement has been putatively explained in the second subchapter. This strategy showcases the potential of triethylaluminum in breaking the CO_2 symmetry and incorporating it within growing polymeric chains.

Relying on NMR analysis, our primary proposition about the incorporation of CO_2 within the polyethylene chains is that CO_2 is incorporated in the form of a ketal.

This incorporation was asserted through a hydrolysis reaction that has been done for the polymer produced in which the molar mass of the polymer decreased from 1500 g/mol before hydrolysis to 700 g/mol after hydrolysis. Thus the polymer was cut at a specific functional group within the polyethylene chain which is the ketal, therefore a CO_2 -functionalized polyethylene is produced.

This work opens a route to new LDPE-type polyethylenes bearing CO_2 -derived motifs to alter the polarity of the PE, to help its compatibilization with fillers for instance, while retaining its intrinsic mechanical and chemical properties.

C.5. References

1. Noble, B. B.; Coote, M. L. Chapter Four - Mechanistic Perspectives on Stereocontrol in Lewis Acid-Mediated Radical Polymerization: Lessons from Small-Molecule Synthesis. In *Advances in Physical Organic Chemistry*; Williams, I. H., Williams, N. H., Eds.; Academic Press, 2015; Vol. 49, pp 189–258.
2. Horn, A. H. C.; Clark, T. J. *Am. Chem. Soc.* **2003**, *125* (9), 2809–2816.
3. Grau, E. Polymerization of Ethylene: From Free Radical Homopolymerization to Hybrid Radical/Catalytic Copolymerization. PhD Thesis, Université Claude Bernard-Lyon I, 2010.
4. Jenkins, A. D.; Jones, R. G.; Moad, G. Terminology for Reversible-Deactivation Radical Polymerization Previously Called “Controlled” Radical or “Living” Radical Polymerization (IUPAC Recommendations 2010). *Pure Appl. Chem.* **2009**, *82* (2).
5. Nicolas, J.; Guillaneuf, Y.; Lefay, C.; Bertin, D.; Gimes, D.; Charleux, B. *Prog. Polym. Sci.* **2013**, *38*, 63–235.
6. Georges, M. K.; Veregin, R. P. N.; Kazmaier, P. M.; Hamer, G. K. *Macromolecules* **1993**, *26*, 2987–2988.
7. Matyjaszewski, K. *Macromolecules* **2012**, *45*, 4015–4039.
8. Wang, J.-S.; Matyjaszewski, K. *J. Am. Chem. Soc.* **1995**, *117*, 5614–5615.
9. Kato, M.; Kamigaito, M.; Sawamoto, M.; Higashimura, T. *Macromolecules* **1995**, *28*, 1721–1723.
10. Fischer, H. *Chem. Rev.* **2001**, *101*, 3581–3610.
11. Matyjaszewski, K.; Gaynor, S.; Greszta, D.; Mardare, D.; Shigemoto, T. *J. Phys. Org. Chem.* **1995**, *8*, 306–315.
12. Moad, G.; Rizzardo, E.; Thang, S. H. *Aust. J. Chem.* **2012**, *65*, 985–1076.
13. Chiefari, J.; Chong, Y. K.; Ercole, F.; Krstina, J.; Je_ery, J.; Le, T. P. T.; Mayadunne, R. T. A.; Meijs, G. F.; Moad, C. L.; Moad, G.; Rizzardo, E.; Thang, S. H. *Macromolecules* **1998**, *31*, 5559–5562.
14. Lacroix-Desmazes, P.; Tonnar, J. In *Polymer Science: A Comprehensive Reference*; Matyjaszewski, K., Müller, M., Eds.; Elsevier: Amsterdam, 2012; pp 159–180.
15. Gaynor, S. G.; Wang, J.-S.; Matyjaszewski, K. *Macromolecules* **1995**, *28*, 8051–8056.
16. Yamago, S.; Iida, K.; Yoshida, J. *J. Am. Chem. Soc.* **2002**, *124* (12), 2874–2875.
17. Dommanget, C.; D’Agosto, F.; Monteil, V. *Angew. Chem. Int. Ed.* **2014**, *53* (26), 6683–6686.
18. Nakamura, Y.; Ebeling, B.; Wolpers, A.; Monteil, V.; D’Agosto, F.; Yamago, S. *Angew. Chem.* **2018**, *130* (1), 311–315.
19. Ziegler, K. *Angew. Chem.* **1952**, *64* (12), 323–329.
20. Ziegler process - Wikipedia https://en.wikipedia.org/wiki/Ziegler_process#cite_ref-1.
21. Aresta, M.; Dibenedetto, A. *Dalton Trans.* **2007**, *28*, 2975–2992.
22. *Carbon Dioxide Recovery and Utilization*; Aresta, M., Ed.; Springer Netherlands: Dordrecht, 2003.
23. J. Weidlein *Angew. Chem.* **1969**, *81*, 947.
24. Yur’ev, V. P.; Kuchin, A. V.; Tolstikov, G. A. *Bull. Acad. Sci. USSR Div. Chem. Sci.* **1974**, *23* (4), 817.

**D. CHAPTER IV. Iron-Catalyzed Ethylene-Isoprene Copolymerization:
From a Chain Shuttling Process towards a CO₂-Activated Process.**

Table of Contents

D.2. Abstract	191
D.3. Chain Shuttling Copolymerization	191
D.3.1. Definition	191
D.3.2. Concept	191
D.3.3. Literature Review	192
D.4. Iron Complexes	194
D.4.1. Oxidation States of Iron	194
D.4.2. Iron Complexes in Ethylene Polymerization	195
D.4.3. Iron Complexes in Isoprene Polymerization	200
D.5. Ethylene-Isoprene Copolymerization	202
D.6. Ethylene-Isoprene Chain Shuttling Copolymerization <i>via</i> Fe-Al-Fe Transmetallation Reactions	206
D.6.1. Catalysts A and B in Homo-polymerizations	207
D.6.1.1. Ethylene Homo-polymerization Using Catalyst A	207
D.6.1.2. Isoprene Homo-polymerization Using Catalyst B.....	210
D.6.2. Catalysts A and B in Ethylene-Isoprene Copolymerization	213
D.6.2.1. Ethylene-Isoprene Copolymerization Test Using Catalyst A.....	213
D.6.2.2. Ethylene-Isoprene Copolymerization Test Using Catalyst B.....	216
D.6.3. Ethylene-Isoprene Chain Shuttling Copolymerization	217
D.6.3.1. Random Copolymerization	218
D.6.3.2. Block Copolymerization	226

D.7. Homo-Polymerizations of Ethylene and Isoprene in scCO₂.....	236
D.7.1. Iron-Catalyzed Ethylene Polymerization in scCO₂.....	236
D.7.2. Iron-Catalyzed Isoprene Polymerization in scCO₂.....	238
D.8. Conclusion	241
D.9. References	242

D.2. Abstract

This chapter presents the section of this thesis dedicated to catalytic polymerization. We begin by testing iron complexes in conventional catalytic polymerizations of ethylene and isoprene with the intention to implement these catalysts in CO₂-mediated processes. But our investigation continued from these initial tests since ethylene-isoprene chain shuttling copolymerization was envisioned. This process that can conveniently yield copolymers proved extremely promising in the case of iron. Random and block copolymers using two different iron complexes, one is responsible for ethylene polymerization and the other for isoprene polymerization, have been produced *via* transmetallation reactions between the two catalysts mediated by triethylaluminum as a chain shuttling agent. Eventually, this achievement was followed by testing of iron-catalyzed ethylene and isoprene polymerizations in scCO₂ media.

The introduction first includes the definition, concept, and a brief literature review of chain shuttling copolymerization; then a narrow literature review about iron complexes presenting mainly the complexes which polymerize ethylene and isoprene; finally, a review on ethylene-isoprene copolymerization is presented in details.

D.3. Chain Shuttling Copolymerization

D.3.1. Definition

Chain shuttling copolymerization (CSC) is a dual-catalyst method for producing block copolymers with alternating or variable chemical nature, architecture or tacticity, either from the same monomer or from several co-monomers. The desired effect is the production of hybrid polymers that bear the properties of both polymer segments.

D.3.2. Concept

The first instance of CSC use has been reported by Arriola and co-workers at Dow Chemical Company in 2006.¹ They defined chain shuttling as the exchange of a growing polymer chain between catalyst sites, such that portions of a single polymer macromolecule are synthesized by at least two different catalysts. Likewise, a chain shuttling agent (CSA) is a transmetallating agent such as a metal alkyl complex that facilitates this transfer. This approach can thus be used to prepare block copolymers by

using a mixture of catalysts of different abilities for copolymerization or of different selectivities, namely stereoselectivity. Under the right conditions, efficient chain shuttling produces a linear multiblock copolymer that features alternating hard and soft blocks.¹ One key to forming differentiated block copolymers *via* chain shuttling is finding a monomer or combination of monomers that, on the basis of their arrangement in the polymer chain, can give rise to both hard and soft materials. **Figure 1** summarizes the general concept of CSC.

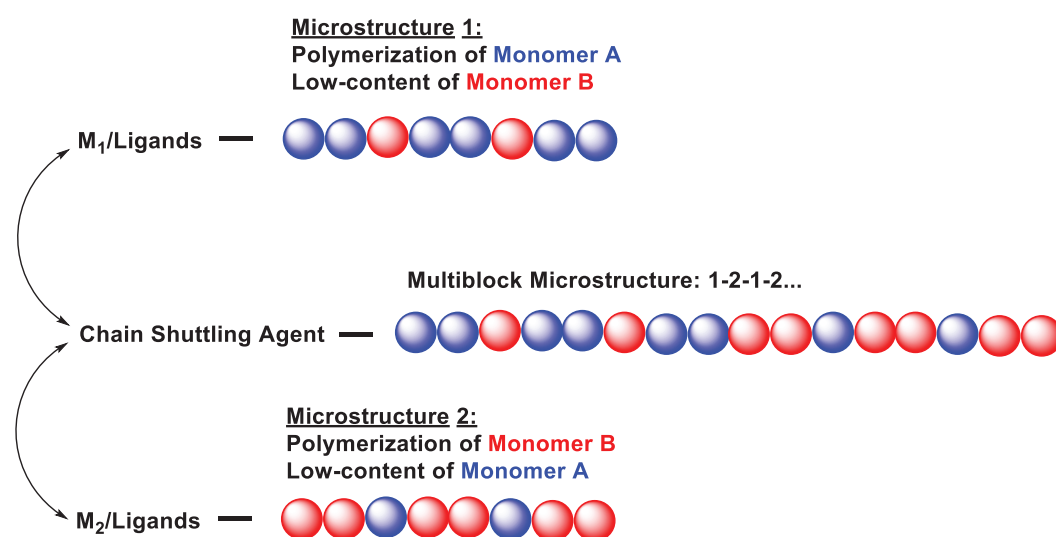


Figure 1. General concept of chain shuttling copolymerization.

D.3.3. Literature Review

Arriola et al. synthesized multiblock ethylene/1-octene copolymers with sequential crystallizable (low 1-octene content) and non-crystallizable (low ethylene content) statistical copolymer segments *via* a CSC. Such an original microstructure results from the simultaneous presence in the reactive medium of chains growing on two different catalysts and of a chain transfer or "chain shuttling agent" (CSA).¹

Pyridylamide Hf (1) and bis(phenoxyimine) Zr (2) (**Figure 2**) complexes combined with ZnEt_2 as CSA have been selected for this purpose using high-throughput experiments. The co-monomers reactivity ratios are different for the two catalysts, leading to ethylene-rich and 1-octene-rich segments respectively. The chains are able to grow in a sequential way on the two different catalysts *via* transfer to the CSA. These copolymers synthesized by chain shuttling are composed of crystallizable ethylene/1-octene blocks with low 1-octene content and high melting temperature (hard blocks), and amorphous

ethylene/1-octene blocks with high 1-octene content and low glass transition temperature (soft blocks). Compared to statistical ethylene/1-octene copolymers, the new architecture leads to higher crystallization temperatures and rates, higher melting temperatures, and a better organized crystalline morphology, together with lower glass transition temperatures.²⁻⁴

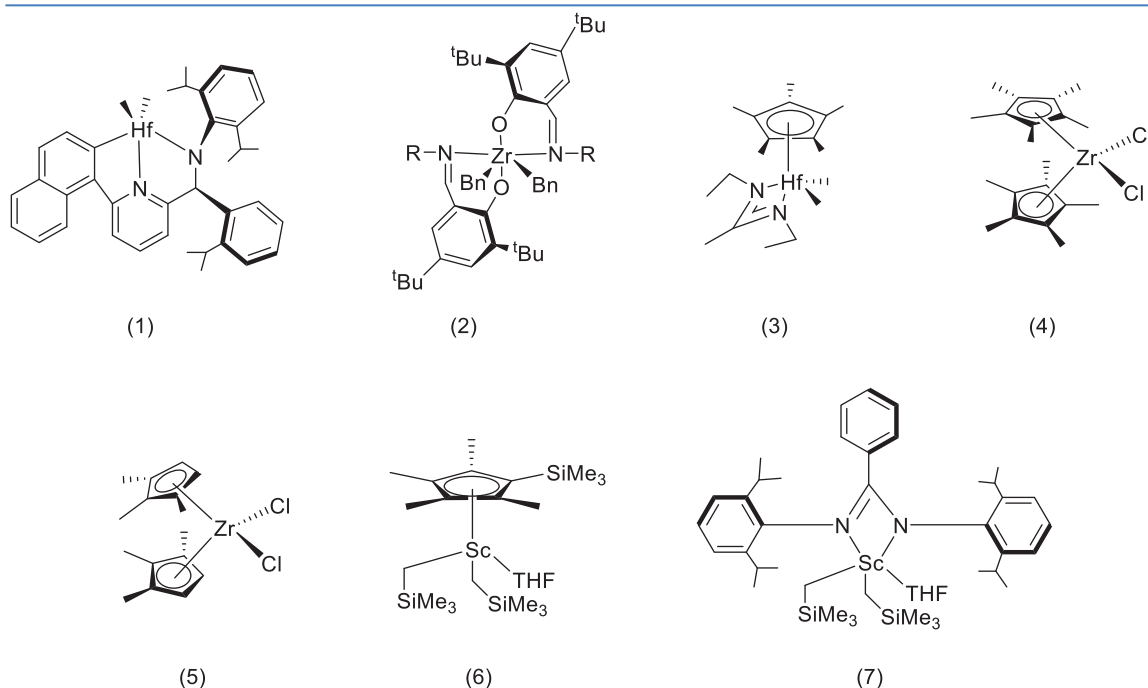


Figure 2. Precatalysts for chain shuttling copolymerizations.

Ethylene/1-hexene CSC was further reported by Sita et al. using (3) (**Figure 2**) in combination with two different co-catalysts, the borate $[\text{PhNHMe}_2][\text{B}(\text{C}_6\text{F}_5)_4]$ and the borane $\text{B}(\text{C}_6\text{F}_5)_3$ and ZnEt_2 as a CSA.⁵ Rytter et al. also advanced a possible ethylene/1-hexene CSC using (4) and (5) (**Figure 2**) combined to MAO in order to explain the presence of ethylene rich and 1-hexene rich blocks in the microstructure of the formed copolymers.⁶

The scandium based precatalysts (6) and (7) (**Figure 2**) were further used by Hou et al. for the styrene-isoprene CSC in combination with Al^iBu_3 as a CSA.⁷ This chain shuttling process induces this particular microstructure, as catalyst (6) when used alone is known to copolymerize efficiently isoprene and styrene, leading to a mixture of 1,4- and 3,4-polyisoprene microstructure.⁸

Isoprene polymerization to produce stereoselective polyisoprenes was also an area of investigation, Hou and coworkers were able to produce isospecific 3,4-polymerization of

isoprene by cationic rare earth metal alkyl species.⁹ Regioselective isoprene chain shuttling polymerization was reported by Cui and coworkers using a combination of a 1,4-regulating pyridylmethylene fluorenyl scandium complex and the 3,4-regulating lutetium analogue.¹⁰ Zinck and coworkers also reported recently an isoprene chain shuttling polymerization between *cis* and *trans* regulating catalysts.¹¹

Ethylene chain shuttling polymerization was achieved using α -diimine Ni(II) bromide and *ansa*-ethylenebis(1- η 5-indenyl)Zr chloride complexes. The nickel catalyst produces branched polyethylene blocks, while the zirconocene leads to linear polyethylene blocks.¹²

CSC processes have been studied extensively in a chemical review from Zinck et al.²

Since our work relies on iron complexes, it is essential to include the importance of these complexes and their applications, mainly in ethylene and isoprene polymerizations.

D.4. Iron Complexes

Iron is the most abundant and least expensive of the transition metals, and the level of interest in studying its organometallic chemistry has been, and continues to be, truly staggering due to the versatility, easy access to various oxidation states and numerous applications of iron catalysis.

The organometallic chemistry of iron has been frequently reviewed by Kerber between 1984 and 1992.¹³ And an extensive review of the applications of organoiron complexes to organic synthesis appeared in 1991.¹⁴ In 2006, Paley followed a ligand-based classification of iron complexes in his report, depending upon the hapticity of ligands.¹⁵ More recently, Bauer and Knölker published a review in iron catalysis studying extensively the applications of iron complexes in different domains of chemistry mainly in organic chemistry.¹⁶ Also, in 2016, Füstner reported a review about iron catalysis in organic synthesis.¹⁷

D.4.1. Oxidation States of Iron

Generally, the oxidation state shows the ability of an atom to oxidize (to lose electrons) or to reduce (to gain electrons). It is related to the number of electrons which

an atom loses, gains, or appears to use when bonding with another atom in a compound. It's a difference between the number of electrons of the same atom in a compound, as compared with the number of electrons in an atom of the element. However, nowadays this formalism seems to be questioned by the advent of redox-active or non-innocent ligands that effectively participate in the relative oxidation state of the active metal in complexes.

Iron has an electronic configuration of $[\text{Ar}]4s^23d^6$. The most common oxidation states for iron are +2 and +3. Moreover, the oxidation states +6, 0, -1 and -2 are of importance. In air, most iron(II) compounds are readily oxidized to their iron(III) analogs, which represent the most stable and widespread iron species. For iron(II) complexes a coordination number of six with an octahedral ligand sphere is preferred. Iron(III) can coordinate three to eight ligands and often exhibits an octahedral coordination. Iron(III) generally is a harder Lewis acid than iron(II) and thus binds to hard Lewis bases. Iron(0) mostly coordinates five or six ligands with trigonal bipyramidal and octahedral geometry. Iron(-II) is tetrahedrally coordinated. Iron in low oxidation states is the most interesting for organometallic chemistry and in particular for iron-catalyzed reactions because they can form more reactive complexes than their iron(II) and iron(III) counterparts. Therefore, iron(0) and iron(-II) compounds are favored for iron catalysis involving coupling reactions for instance. Iron carbonyl complexes are of special interest due to their high stability with an iron(0) center capable of coordinating complex organic ligands, which represents the basis for organoiron chemistry. Also, the oxidation states +4 and +5 occur, Fe(IV) and Fe(V) complexes are known as excellent oxidation promoters (iron oxo species).

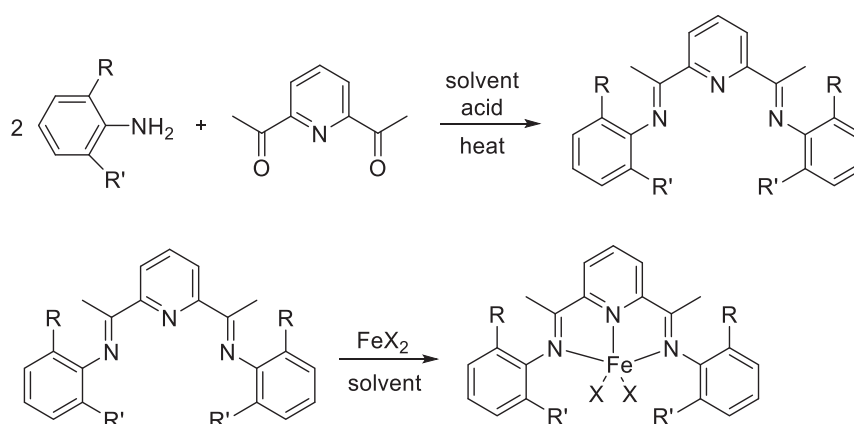
D.4.2. Iron Complexes in Ethylene Polymerization

Polymerization and polycondensation reactions play an important role in the chemical industry and are the basis for a billion-dollar market. Thus, the search for new efficient, selective, environmentally benign, and low cost catalysts has been permanently on the agenda of industrial and academic research. Iron perfectly abides all of these principles and was thus extensively investigated. Important contributions have been reported at the end of the 1990s with work on iron-catalyzed conventional alkene polymerizations by Brookhart^{18,19} and Gibson,²⁰ Further achievements in this field until 2004 have been

documented by Bolm and co-workers.²¹ Bianchini et al. and Giambastiani et al. summarized the developments in olefin polymerization catalyzed by iron and other late transition metals in 2006 and 2010, respectively.^{22,23} Bis(imino)pyridine complexes of iron and other metals and their performance in olefin polymerization have been the subject of reviews and book chapters by Gibson, Redshaw, and Solan in 2007²⁴ and 2010²⁵ and Li and Gomes in 2011.²⁶ A recent review on iron NHC complex catalysis also includes a chapter on polymerization reactions.²⁷ Redshaw and coworkers summarized recent developments in the field of iron complexes as catalysts for the oligomerization and polymerization of ethylene in a perspective article.²⁸ The development of non-bis(imino)pyridine ligands for the iron-catalyzed oligomerization of ethylene has been summarized recently by Olivier-Bourbigou and coworkers.²⁹

Because of this large number of reviews available on this subject, the reader is referred to those for a comprehensive coverage. In the following section selected examples are presented.

Scheme 1. Synthesis of bis(imino)pyridine iron(II) complexes.

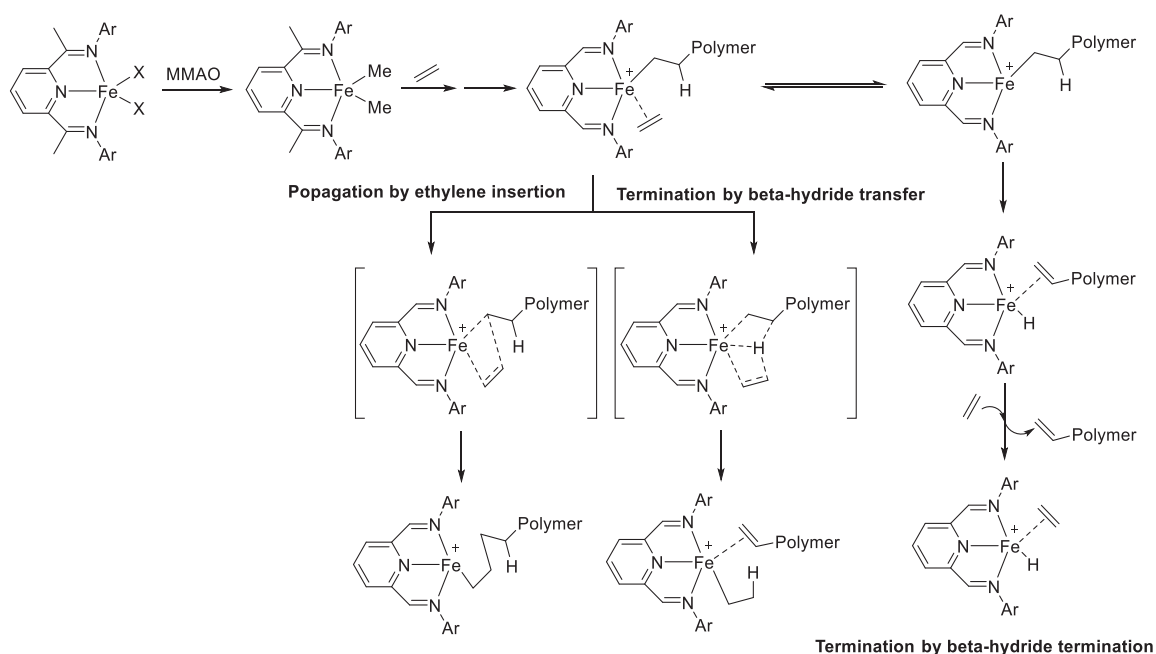


The groups of Brookhart^{18,19} and Gibson²⁰ were the pioneers of iron-catalyzed ethylene polymerization using complexes with tridentate ligands. They have investigated the catalytic potential of iron(II) and cobalt(II) complexes with tridentate pyridine bisimine ligands. They found that especially the iron(II) system can produce high-density polyethylene in good yields when bulky ortho-substituted aryl groups are attached to the imine nitrogens. The new catalysts have polymerization activities comparable to, or even higher than, those of metallocenes under similar conditions. They exhibit further great potential for controlling polymer properties by external parameters such as

pressure and temperature. **Scheme 1** shows the general procedure of synthesizing these iron complexes.

Directly after this achievement, Ziegler and his coworkers reported the mechanistic aspects of this successful polymerization. **Scheme 2** shows the mechanism of the ethylene polymerization catalyzed by the bis(imino)pyridine iron(II) complex, where they predict ethylene capture by the cationic iron(II) alkyl complex to be rate determining for both termination and propagation steps.³⁰

Scheme 2. Mechanism of ethylene polymerization catalyzed by iron(II)-bisimino pyridine complexes.



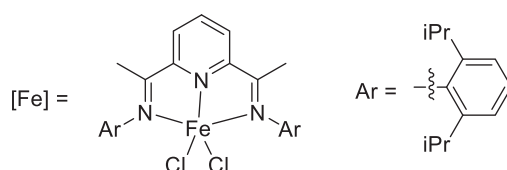
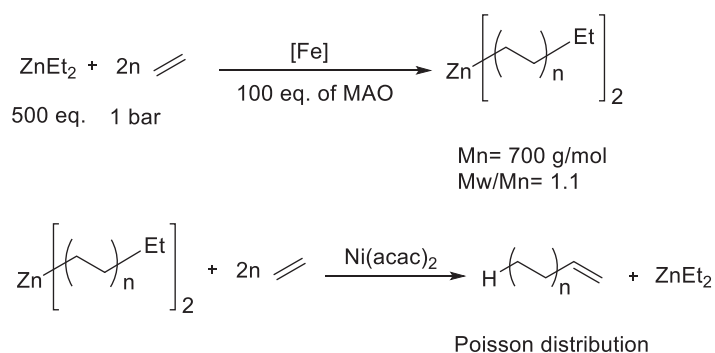
An efficient polyethylene chain growth on zinc catalyzed by a bis(imino)pyridine iron/methylaluminoxane (MAO) catalyst system has been examined by Gibson et al.^{31,32} A fast and reversible exchange of the growing polymer chains between the zinc and the iron centers has been observed. A Poisson distribution of linear alkanes was obtained. Alternatively, displacement of the polymer chains from $\text{Zn}(\text{polymer})_2$ by a nickel catalyzed transmetallation reaction led to linear α -olefins (**Error! Not a valid bookmark self-reference.**).

Chirik and co-workers described cationic bis(imino)pyridine iron(II) alkyl complexes to catalyze olefin polymerization efficiently even without addition of MAO (**Scheme 4**).³³ This procedure provided polyethylene with a higher molar mass and lower dispersity

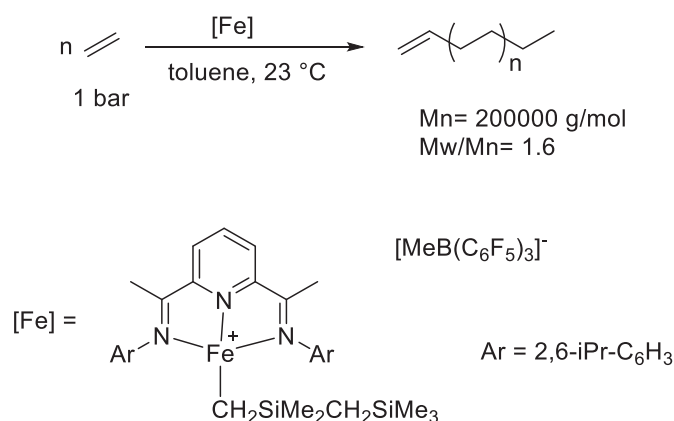
than conventional MAO-activated catalysts.

Herrmann and co-workers synthesized and tested a series of bis(imino)pyridine and monoiminoacetyl iron(II) complexes as catalysts for the oligomerization and polymerization of ethylene and propylene in the presence of modified methylaluminoxane (MMAO).³⁴ With increasing bulk of the *ortho*-position of the N-aryl ring, an increase in molecular weight of the polymers was observed.

Scheme 3. Polyethylene chain growth on zinc catalyzed by a bis(imino)pyridine iron/MAO system. "Adapted with permission from (Bauer, I.; Knölker, H.-J. *Chem. Rev.* **2015**, *115* (9), 3170-3387.). Copyright (2015) American Chemical Society."



Scheme 4. Olefin polymerization by cationic bis(imino)pyridine iron(II) alkyl complexes. "Adapted with permission from (Bauer, I.; Knölker, H.-J. *Chem. Rev.* **2015**, *115* (9), 3170-3387.). Copyright (2015) American Chemical Society."



Very active nonbis(imino)pyridine iron complexes for the oligomerization of ethylene have been reported by Small et al.^{35,36} High product purities of 1-hexene and 1-octene have been achieved. The highest TON of about 2.5×10^6 mol of ethylene/mol of Fe was

reported for a NNP tridentate α -diimino-(phosphine)iron complex (**Figure 3/(1)**). Activities in the range 10^4 - 10^6 g/(mol h atm) for nonbis(imino)pyridine iron complexes remain below the original values obtained for bis(imino)pyridine systems [10^8 g/(mol h atm)] by Brookhart et al.^{18,19}

Erker and co-workers prepared cobalt and iron bis(iminoethyl)pyridine complexes with pendent alkenyl groups which functioned in combination with MAO as Ziegler-Natta catalysts for ethylene polymerization (**Figure 3/(2)**).³⁷ The iron complexes were more active than the cobalt catalysts and gave mixtures of linear polyethylene and low molecular weight oligoethylenes.

Several 2,8-bis(arylimino)-5,6,7,8-tetrahydroquinoline iron complexes have been synthesized by Redshaw, Hu, Sun, and co-workers (*example: Figure 3/(3)*).³⁸ After treatment with MAO or MMAO they showed high activity in the polymerization of ethylene at 50 °C.

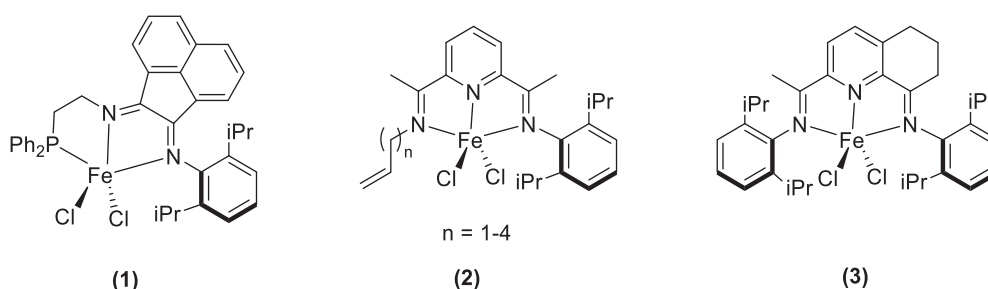


Figure 3. Some iron complexes used in ethylene oligomerization and polymerization.

Recently, Huang and co-workers have described the synthesis of a series of phosphine-iminoquinoline PNN iron complexes that are highly active for ethylene polymerization, producing linear, low molar mass polyethylene. Among them, the iron complexes with the iPr_2P groups enable the formation of polyethylene with narrow dispersity. In addition, they demonstrated that using a sterically less bulky and electronically deficient iron complex allows for efficient copolymerization of ethylene with 1-octene.³⁹

Propylene polymerization is also successful using iron complexes. In 2015, Nozaki and co-workers reported a series of iron complexes bearing a bis(imino)pyridine ligand successful in homopolymerization of propylene. The alkyl substituents attached to the aryl group on the imine nitrogen atoms significantly affected the catalytic activity and molecular weight of the obtained polypropylenes. Copolymerization of propylene and

various allyl comonomers catalyzed by iron/bis(imino)pyridine was also investigated.⁴⁰

D.4.3. Iron Complexes in Isoprene and 1,3-Diene Polymerization

As aforementioned, iron can adopt different oxidation states, from $-II$ to $+VI$. Low-valent iron complexes are capable of catalyzing a variety of reactions, including cross-coupling, cycloisomerization, and cycloaddition reactions.⁴¹⁻⁴³ The electron-rich nature of low-valent iron allows for π -activation of bound alkenes, mainly 1,3-dienes. The large number of stable oxidation states of iron allows for many possible reactions.

Ligation of iron with carefully selected redox-active ligands can channel reactivity into selective pathways. Iminopyridine-ligated low-valent iron catalysts have been developed to facilitate selective 1,4-hydrovinylation, hydroboration, hydrosilylation, and polymerization of 1,3-dienes.⁴⁴⁻⁴⁶

Natural rubber is perhaps the most-familiar natural polymer. It occurs in nature in the sap of tropical trees such as *Hevea brasiliensis* or *Gutta percha*, it is composed largely of the same repeating unit as polymerized isoprene. Natural rubber is produced in quantities of over 10 million tons per year, and non-natural polyisoprene (synthetic rubber) is produced in even greater quantities.⁴⁷ Polymerization of isoprene can potentially result in several different microstructures (**Figure 4**). The double bond resulting from 1,4-insertion can be either *cis* or *trans*, and 1,4-insertion must compete with 1,2- or 3,4-insertion pathways. Natural rubber derived from *Hevea brasiliensis* contains $> 99.9\%$ *cis*-1,4-polyisoprene, while *Gutta-percha* rubber is $> 99.9\%$ *trans*-1,4-polyisoprene. Synthetically produced polyisoprene is typically a mixture of *cis*- and *trans*-1,4-polyisoprene, often with significant quantities of 1,2- or 3,4-insertion observed. This lack of stereocontrol in synthetic polyisoprene means that natural rubber has high-performance mechanical properties superior to the synthetic version.⁴⁸

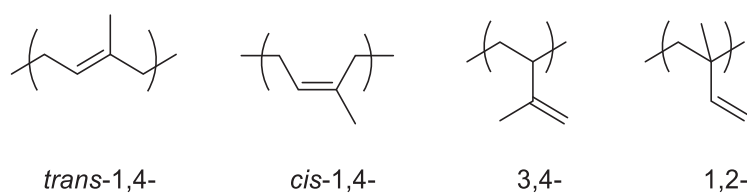


Figure 4. Different microstructures of polyisoprene.

Iron-catalyzed polymerization is well-known for ethylene,¹⁸⁻²⁰ but polymerization of

1,3-dienes is considerably less explored, and selective. Building on their experience with other diene functionalization reactions, Ritter et al. chose iminopyridines as appropriate ligands for diene polymerization.⁴⁹ Bisiminopyridines have been used as ligands for iron-catalyzed olefin polymerization;¹⁸⁻²⁰ iminopyridines should retain the redox-active behavior of bisiminopyridines while leaving an additional coordination site open to facilitate binding of dienes rather than olefins. They identified ferrous complexes **1** and **2** (**Figure 5**) as suitable catalysts. In combination with an alkylating reagent (trialkylaluminum) and a dealkylating reagent ($\text{Ph}_3\text{C}^+\text{B}(\text{C}_6\text{F}_5)_4^-$), these complexes catalyzed efficient polymerization of isoprene in an aprotic solvent, leading to polymer molar masses $>10^5$ g/mol and with $>99:1$ selectivity for double bond geometry (*trans* for complex **1**, *cis* for complex **2**). Selectivity for 1,4-addition over 3,4-addition was lower, ranging from 2:1 to 12:1. Interestingly, these complexes also polymerize butadiene and bio-available β -myrcene and β -farnesene.

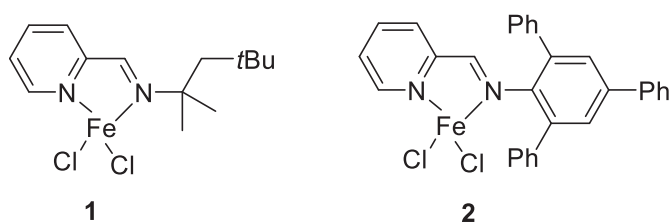
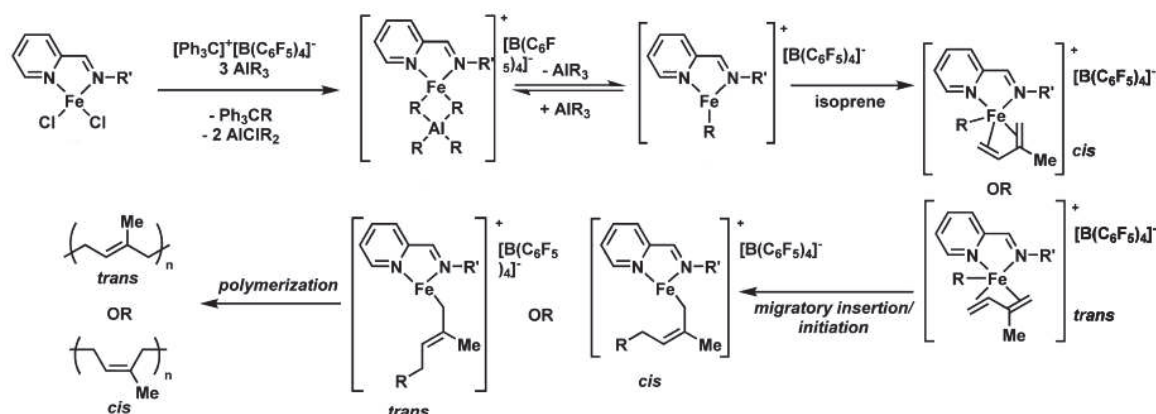


Figure 5. Ferrous complexes used in isoprene polymerization.

Scheme 5. Potential mechanism for the stereoselective iron-catalyzed polymerization of isoprene. "Adapted with permission from (McNeill, E.; Ritter, T. *Acc. Chem. Res.* 2015, 48 (8), 2330-2343.). Copyright (2015) American Chemical Society."



The proposed mechanism by Ritter et al. for the iron-catalyzed polymerization of isoprene is given in **Scheme 5**.⁴⁸ Initial reaction of the iron dichloride complex with 3 eq. of AlR_3 and 1 eq. of $\text{Ph}_3\text{C}^+\text{B}(\text{C}_6\text{F}_5)_4^-$ gives mixed iron-aluminum species. Reversible

dissociation of AlR_3 gives a coordinatively unsaturated iron alkyl complex. Coordination of isoprene in either the *cis*- or *trans*- configurations, followed by migratory insertion, gives either *cis*- or *trans*-olefin incorporation into the growing polymer chain; note that also a σ - π rearrangement *via* an allyl-coordinated Fe complex decides whether a *cis*- or a *trans*- olefin incorporation will occur. Further coordination of monomer, and migratory insertion elongates the chain. The factors responsible for control over *cis* versus *trans* selectivity are not clear for them at this point, especially given the similarity of the ligands involved.

In the the same vein, DFT calculations have been conducted by Luo and co-workers for the regioselective polymerization of isoprene and 3-methyl-pentadiene, catalyzed by a bipyridiene-ligated cationic iron complex.⁵⁰

After presenting iron-catalyzed ethylene and isoprene polymerizations, we will end the introduction of this chapter by a review about ethylene-isoprene copolymerizations.

D.5. Ethylene-Isoprene Copolymerization

Isoprene is one of the most common conjugated dienes, it has attracted much attention from both academic and industrial researchers because of its different polymerization modes, such as 3,4-, *cis*-1,4-, or *trans*-1,4-selectivity, caused by the methyl substituent on the conjugated diene and its *cis*-/*trans*-1,4-selective homo-polyisoprenes serving as alternatives for natural rubber.

A wide range of organometallic catalysts, especially of the organo-rare earth metal catalysts, have been reported for the regio- and stereoselective homo-polymerization of isoprene.⁵¹⁻⁶⁸ However, the low strength and low stiffness of homo-polyisoprenes, and their tendency of becoming soft and sticky by increasing temperature limited their extensive application in industry. The copolymerization of isoprene with ethylene is supposed to be an effective method to improve the properties of the homo-polyisoprenes and afford different high-performance copolymer materials with high tear strength and tensile strength, high impact resistance, and good rubber compatibility for many industrial applications.

Further post-functionalization of the remaining C-C double bonds in such copolymers can introduce the polar groups or reactive sites in the copolymers backbone, affording

new functionalized copolymers with improved properties including solubility and dyeing. In view of the completely different reactivity characteristics of these two types of monomers for a given catalyst, the copolymerization of isoprene with ethylene is rather challenging. Although different studies have been devoted to this subject for many years, only few catalysts were reported to be active for the copolymerization of isoprene with ethylene.⁶⁹⁻⁷⁶

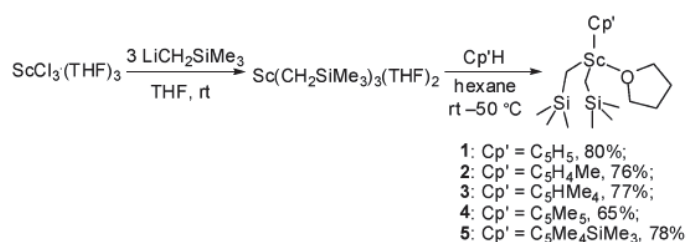
One of the primary reports in the copolymerization of ethylene and isoprene is the one done by Suminoe in 1963, Suminoe has copolymerized ethylene and isoprene using a triethylaluminium titanium tetrachloride catalyst.⁶⁹ In 1972, another type of methods for producing ethylene-isoprene block copolymers has been reported. This method involves an indirect copolymerization of ethylene and isoprene through a selective catalytic hydrogenation of 1,4-butadiene-1,4-isoprene copolymer.⁷⁰

A brief description on the copolymerization of isoprene with ethylene by a neutral neodymocene allyl catalyst has been mentioned by Carpentier et al. in a report dealing with stereocontrolled styrene-isoprene copolymerization and styrene-ethylene-isoprene terpolymerization.⁷¹

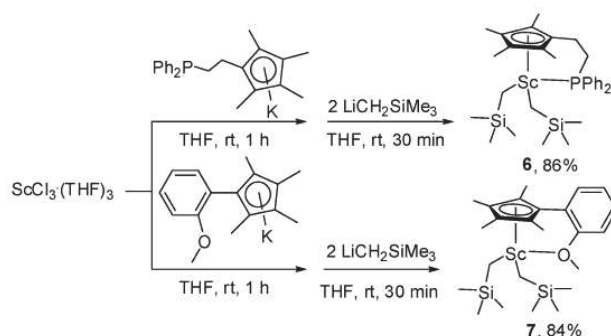
Scheme 6. (a) Synthesis of half-sandwich scandium dialkyl complexes bearing mono(cyclopentadienyl) ligands. (b) Synthesis of half-sandwich scandium dialkyl complexes bearing cyclopentadienyl ligands with a phosphine or ether side arm.

"Adapted with permission from (Li, X.; Nishiura, M.; Hu, L.; Mori, K.; Hou, Z. *J. Am. Chem. Soc.* 2009, 131 (38), 13870–13882.). Copyright (2009) American Chemical Society."

(a)



(b)



Then, in 2009, Hou and co-workers⁷² published an alternating and random copolymerization of ethylene and isoprene catalyzed by cationic half-sandwich scandium alkyls. All the dialkyl complexes that they synthesized (**1-7**/ **Scheme 6**) were active for the polymerization of isoprene and the copolymerization of isoprene with ethylene, with the activity and selectivity being significantly dependent on the ancillary ligands, to produce a new family of polymer materials with different microstructures and compositions.

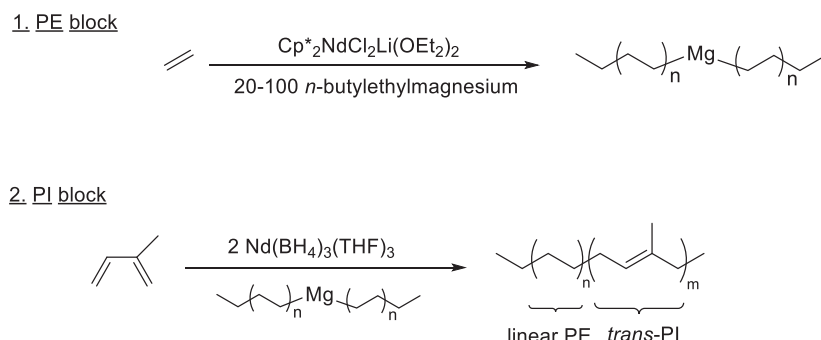
In the homopolymerization of isoprene, the less sterically demanding complexes **1** and **2** yielded high *cis*-1,4 selectivity ($\geq 95\%$), while the ether side arm containing complex **7** produced *trans*-1,4-polyisoprene (60-79%) as a major product. In the case of the more sterically demanding complexes **3-5**, the production of 3,4-polyisoprene (51-65%) was favored.

In the isoprene/ethylene copolymerization, complexes **1** and **2** afforded the random copolymers with high isoprene contents (85-92 mol %) and predominant *cis*-1,4-microstructures ($\geq 90\%$), thus constituting the first example of *cis*-1,4-selective isoprene/ethylene copolymerization. In contrast, the isoprene/ethylene copolymerization by **3**, **4**, **6**, and **7** gave almost perfect alternating isoprene-ethylene copolymers.⁷²

In 2010, Proto et al. reported an ethylene/isoprene copolymerization catalyzed by titanium complexes containing a tetradentate [OSSO]-type bis(phenolato) ligand and methylaluminoxane with good activity. The copolymer microstructure varied by changing the ratio between the monomers feed in the copolymerization, affording copolymers with IP content $\geq 60\%$.⁷³

Then, in 2012, Visseaux et al. prepared block copolymers comprising a sequence of linear polyethylene segments connected to *trans*-polyisoprene by means of *in situ* generated neodymium based catalysts. Two different catalytic systems were used consecutively, each of them being specific to a type of monomer. Ethylene was first polymerized by catalyzed chain growth with a Nd/Mg catalyst, affording bis(polyethylenyl)Mg, which was subsequently reacted with an equimolar amount of neodymium trisborohydride in the presence of isoprene as second monomer (**Scheme 7**).⁷⁴

Scheme 7. Synthesis of (polyethylene)-*b*-(*trans*-polyisoprene) by a two-step procedure.^a "Adapted with permission from (Chenal, T.; Visseaux, M. *Macromolecules* 2012, 45 (14), 5718–5727.). Copyright (2012) American Chemical Society."



^a The Mg(PE)₂ is represented with two PE of same length for simplicity.

In 2015, Li et al. reported cationic half-sandwich fluorenyl scandium catalysts that exhibit high activities and selectivities in the isoprene homo-polymerization and afford the random or almost alternating isoprene/ethylene copolymerization with different comonomer incorporation. In the isoprene polymerization, the presence of a small amount of Al*i*Bu₃ could promote the activity and selectivity, affording high molecular weight polyisoprene containing mainly *cis*-1,4-isoprene units and a small amount of 3,4-isoprene units. In the copolymerization, the complexes/activator/Al*i*Bu₃ ternary system showed completely different control on the comonomer incorporation and distribution in the copolymer being significantly dependent on the substituents at the fluorenyl ligands, producing random or almost alternating ethylene/isoprene copolymers with different microstructures and compositions.⁷⁵

The residual C-C double bonds of the 1,4-isoprene units of the resulting isoprene/ethylene copolymers could be selectively epoxidized by *meta*-chloroperoxybenzoic acid for preparing high performance polymers. Such functionalization could improve the solubility, dyeing, acidity and surface properties of these copolymer materials.⁷⁵

Recently, in 2017, DFT studies on isoprene/ethylene copolymerization catalyzed by cationic scandium complexes bearing different ancillary ligands have been reported by Luo et al.⁷⁶

After what has been introduced, here we start the discussion of our achievement in ethylene-isoprene chain shuttling copolymerization *via* Fe₁-Al-Fe₂ transmetallation

reactions. This work has been realized while testing the iron complexes in conventional polymerizations to go further towards their implementation in CO₂-mediated polymerizations. We then continued this study of the Fe-catalyzed chain shuttling copolymerization process which showed promising results.

D.6. Ethylene-Isoprene Chain Shuttling Copolymerization via Fe-Al-Fe Transmetallation Reactions

As aforementioned, chain shuttling copolymerization (CSC) is a dual catalyst process in which each catalyst is responsible of the polymerization of one monomer. Here, two iron complexes have been synthesized, a bisiminopyridine iron(II) complex "catalyst **A**" (**Figure 6**), which is known as an active catalyst in polymerizing ethylene, and an iminopyridine iron(II) complex "catalyst **B**" (**Figure 6**), which is known as an active catalyst in polymerizing isoprene.^{49,77}

Even though there are other more active iron catalysts in polymerizing ethylene, catalyst **A** was selected due to its relatively less hindrance around the Fe center which facilitates more the occurrence of the transmetallation reactions. Catalyst **B** is synthesized using a bidentate ligand instead of the tridentate one used in the synthesis of catalyst **A**. By decreasing the steric hindrance around the metal center the coordination of isoprene become feasible.

The two complexes were synthesized depending on the procedure mentioned in the literature (see experimental part).

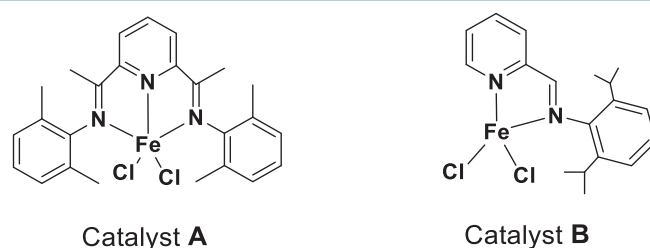


Figure 6. Iron(II) complexes responsible of polymerizing ethylene (catalyst **A) and isoprene (catalyst **B**).**

Catalyst **A** (2,6-diacetylpyridinebis(2,6-dimethylanil))FeCl₂ and catalyst **B** (2-pyridinecarboxaldehyde(2,6-diisopropylanil))FeCl₂ combined to AlEt₃ as chain shuttling agent (CSA) have been selected for copolymerizing ethylene and isoprene through a chain shuttling process. On paper, the co-monomers reactivity ratios should be different

for the two catalysts, leading to ethylene-rich and isoprene-rich segments respectively. The chains are able to grow in a sequential way on the two different catalysts *via* transfer to the CSA (**Figure 7**).

We tested catalysts **A** and **B** in the homo-polymerization of ethylene and isoprene, respectively. These tests were conducted first to insure the efficiency of the catalysts and their selectivity toward a specific monomer insertion; second, to analyze the polymers produced for comparison with the polymers that will be produced from the chain shuttling processes.

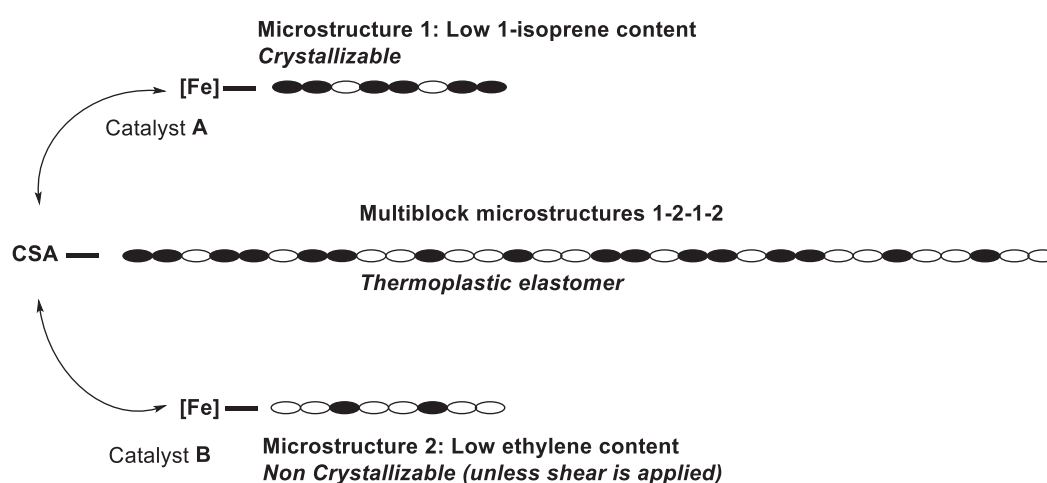


Figure 7. Ethylene-isoprene chain shuttling copolymerization *via* Fe-Al-Fe transmetallation reactions.

D.6.1. Catalysts A and B in Homo-polymerizations

D.6.1.1. Ethylene Homo-polymerization Using Catalyst A

Catalyst **A** has been tested in an ethylene polymerization reaction with tritylBARf (trityl tetra(pentafluorophenyl)borate; $\text{Ph}_3\text{C}^+ \text{B}(\text{C}_6\text{F}_5)_4^-$) as a dealkylating agent (1 equiv.) and AlEt_3 (27 equiv.) as an alkylating agent (co-catalyst), it shows high activity with 6500 g of PE/(g of catalyst.h). The PE is produced from a chain transfer polymerization reaction between catalyst **A** and the co-catalyst AlEt_3 ; the reaction is done in a 1 L reactor under 7 bar of ethylene at 70 °C.

From the NMR analysis (**Figure 8**), it has been determined that three types of chain-terminated PE are produced. The first type is the CH_3 -terminated PE which forms 72 % of the PE produced. The second is the vinyl-terminated PE which is formed because of the

β -H transfer side reactions that occurs usually in olefins polymerizations done by coordination catalysis; this type represents 17 % of the produced polymer. The third is the HO-terminated PE which is formed by the oxidation of the Al-C bond (Al from AlEt_3 which acts here as a chain-transfer agent (co-catalyst)) when the polymer is exposed to air.⁷⁸ This type represents 11 % of the produced PE (**Scheme 8**).

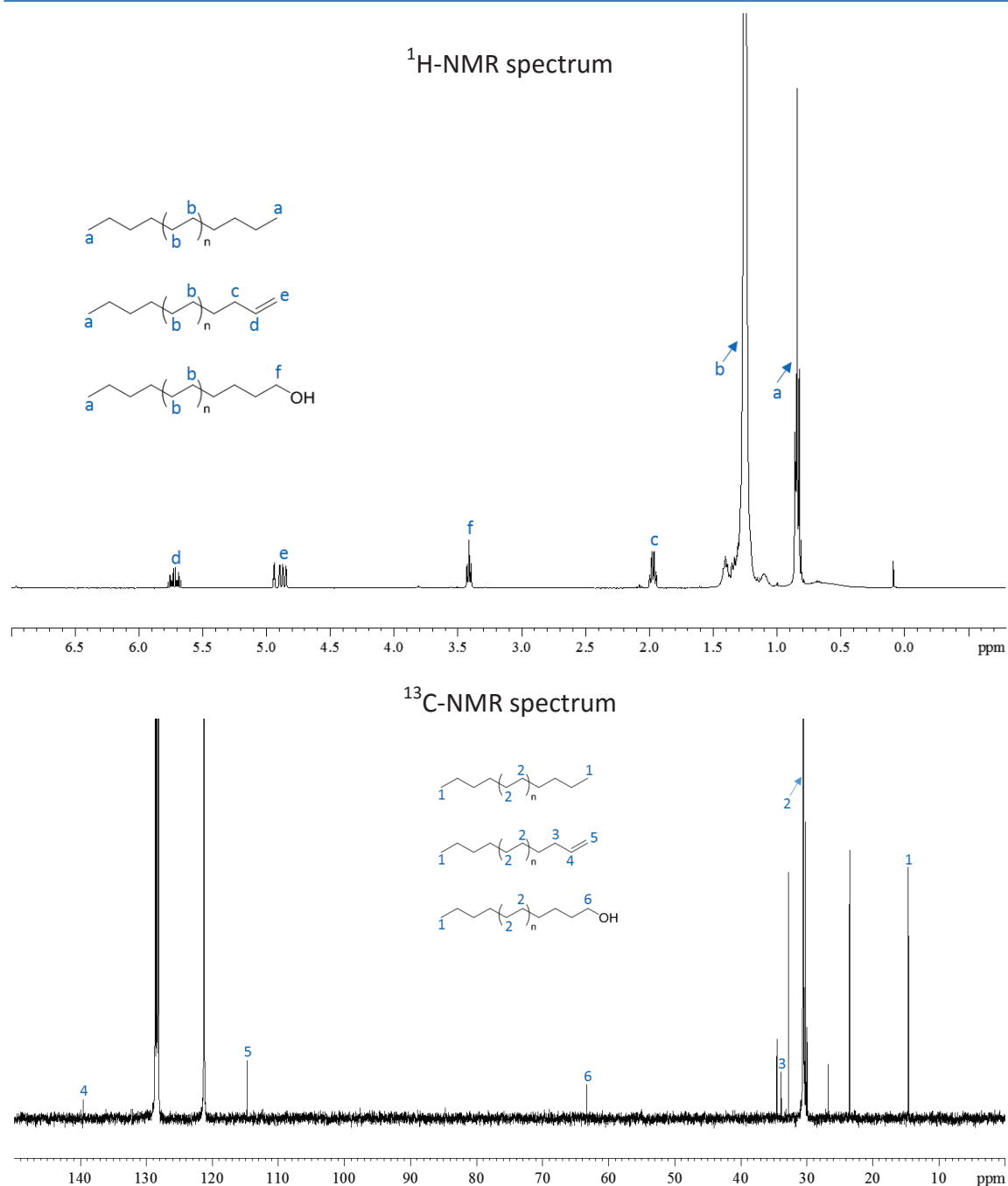


Figure 8. ^1H - and ^{13}C -NMR spectra of the homo-PE produced by catalyst A.

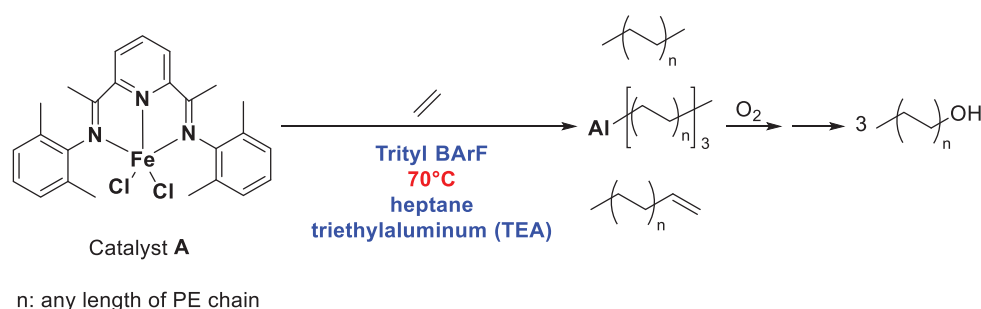
The other end of all the chains is $-\text{CH}_3$ because the AlEt_3 is the alkylating agent, thus the primary insertion in this polymerization is done by the ethyl group (Fe-ethyl), or it

could be done by a hydrogen atom (Fe-H from β -H elimination) which will also produce a $-\text{CH}_3$; therefore all the chains are terminated at least on one side by a $-\text{CH}_3$ group.

The percentages of each class of PE is calculated from the integrations of the peaks in the ^1H -NMR spectrum (**Figure 8**) according to the following equations: (I = integration)

1. % CH_3 -terminated PE = $(I_a/3)/[(I_a/3)+(I_e/2)+(I_f/2)]$.
2. % Vinyl-terminated PE = $(I_e/2)/[(I_a/3)+(I_e/2)+(I_f/2)]$.
3. % OH-terminated PE = $(I_f/2)/[(I_a/3)+(I_e/2)+(I_f/2)]$.

Scheme 8. Homo-polymerization of ethylene using catalyst A.



The three types of termination appear obviously in the NMR spectra. First, in the ^1H -NMR spectrum, the peak which corresponds to the protons of the carbon atoms of the PE backbone appears at 1.26 ppm. The triplet at 0.88 ppm corresponds to the protons of the terminal- CH_3 . The multiplets at 5.7 ppm and 4.9 ppm correspond to the protons of the $-\text{CH}$ and $-\text{CH}_2$ of the vinyl group, respectively; in addition, the quartet at 2.0 ppm corresponds to the protons of the α -C to the vinyl group. Also, a triplet at 3.4 ppm corresponds to the protons of the α -C to the $-\text{OH}$ group (**Figure 8**).

Second, the ^{13}C -NMR spectrum displays all the peaks that are consistent with the existence of these three types of chain-terminated PE. The peak that corresponds to the carbon atoms of the PE backbone appears at 30.0 ppm. The peak at 14.7 ppm corresponds to the terminal- CH_3 , and the peak at 23.6 ppm corresponds to the α -C to the terminal- CH_3 . The peaks at 139.7 ppm and 115.0 ppm correspond to the $-\text{CH}$ and $-\text{CH}_2$ of the vinyl group, respectively; in addition, the peak at 34.0 ppm corresponds to the α -C to the vinyl group. Also, a peak at 63.4 ppm corresponds to the α -C to the $-\text{OH}$ group (**Figure 8**).

The PE produced has a low M_n (700 g/mol) of a narrow dispersity equal to 1.3 (**Figure**

9). This is due to the relatively limited steric hindrance around the Fe center where the imino groups of the tridentate ligand are *ortho*-substituted by the smallest alkyl group (methyl). It has been proved in the literature that decreasing the steric hindrance around the metal center in ethylene polymerization leads to the preference of transfer reactions over propagation; for example, more space around the center leads to easier β -H transfer.^{18,79}

The melting point of the PE produced is 130 °C with a crystallinity of 66 % (obtained by Differential Scanning Calorimetry "DSC") (Figure 9).

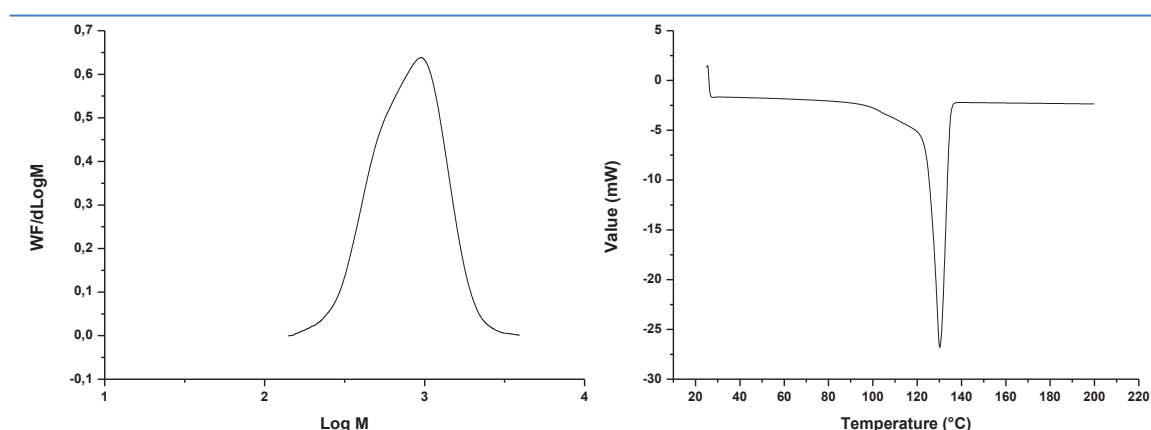
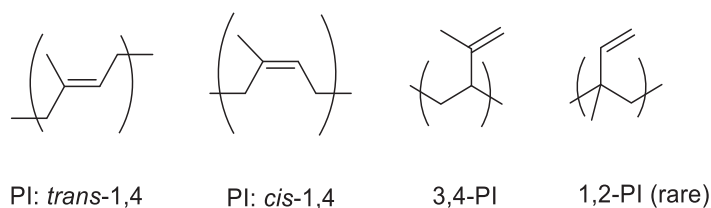


Figure 9. To the left: The molar mass distribution of the homo-PE produced by catalyst A. To the right: DSC peak of the homo-PE produced by catalyst A.

D.6.1.2. Isoprene Homo-polymerization Using Catalyst B

Generally, the homopolymerization of isoprene can yield polyisoprenes with various microstructures which show different chemical, physical, and mechanical properties (Scheme 9). *cis*-1,4-Polyisoprene is a major component of natural rubber and acts as an excellent elastomer, whereas *trans*-1,4-polyisoprene and 3,4-polyisoprene are crystalline polymers. 1,2-Polyisoprene is usually not available in coordination polymerization because of the steric reason.⁸⁰⁻⁸²

Scheme 9. Polyisoprene microstructures.

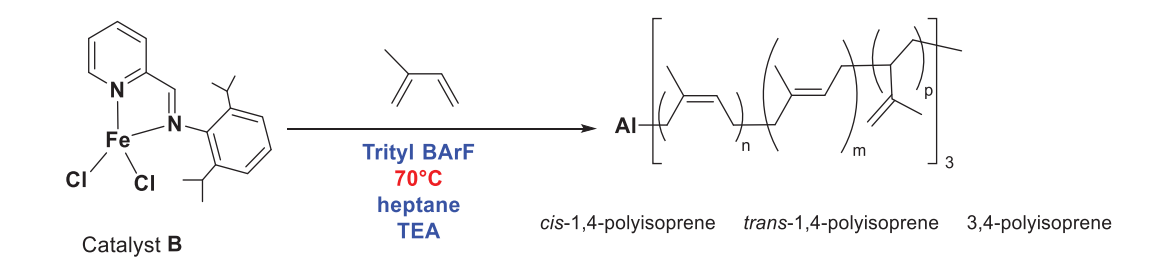


Catalyst **B** has been tested in an isoprene polymerization reaction with tritylBARf (trityl

tetra(pentafluorophenyl)borate; $\text{Ph}_3\text{C}^+ \text{B}(\text{C}_6\text{F}_5)_4^-$) as a dealkylating agent and AlEt_3 as an alkylating agent (co-catalyst), it shows high activity with a conversion > 90 %. This high yield is due to the bidentate nature of the ligand which allows an easy coordination of the isoprene molecule, as aforementioned.

Scheme 10 shows the transfer of polyisoprene chains between the iron and aluminum centers. Polyisoprene (PI) is produced from this chain transfer polymerization reaction between catalyst **B** and AlEt_3 (27 equivalent), with 1 equiv. of trityl BARf and 2000 equiv. of isoprene were added. The reaction was conducted at room temperature.

Scheme 10. Homo-polymerization of isoprene using catalyst B.



The imine moiety of iminopyridine ligand is not able to control the stereoselectivity of isoprene insertion on the active iron complex. From ^1H -NMR and ^{13}C -NMR (**Figure 10**), the poly-isoprene is produced as a mixture of *trans*-1,4-polyisoprene (21.8 %), *cis*-1,4-polyisoprene (39.5 %), and 3,4-polyisoprene (38.7 %).

The isomer contents of polyisoprene were determined from the ^1H - and ^{13}C -NMR spectra according to the following formulas: (I = integration)

From ^1H -NMR:

1. Mol 1,4-PI % = $[I_c / (I_c + 0.5I_g)] \times 100$.
2. Mol 3,4-PI % = $[0.5I_g / (I_c + 0.5I_g)] \times 100$.

From ^{13}C -NMR:

1. Mol *trans*-1,4-PI % = $[I_3 / (I_3 + I_7 + I_{12})] \times 100$.
2. Mol *cis*-1,4-PI % = $[I_7 / (I_3 + I_7 + I_{12})] \times 100$.
3. Mol *trans*-1,4-PI % = $[I_{12} / (I_3 + I_7 + I_{12})] \times 100$.

The ^1H -NMR spectrum shows all the peaks that correspond to the protons of the 1,4-PI (*cis*- and *trans*-) and 3,4-PI; this is depicted in **Figure 10**. Also, the ^{13}C -NMR spectrum displays all the peaks that correspond to the carbon atoms of the 1,4-PI (*cis*- and *trans*-)

and 3,4-PI; both aliphatic and olefinic regions of the ^{13}C -NMR spectrum are represented in **Figure 10**.

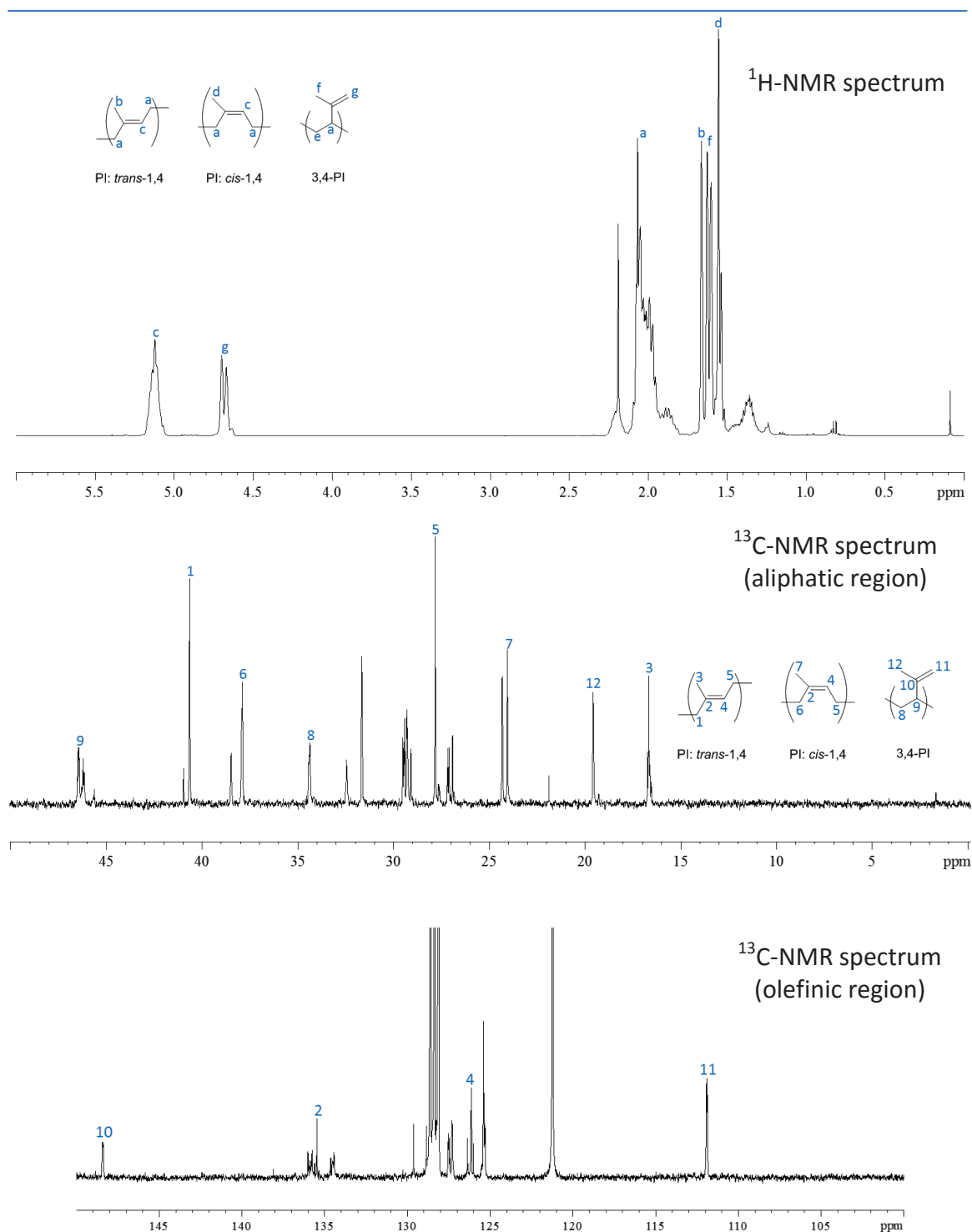


Figure 10. ^1H - and ^{13}C -NMR spectra of the homo-PI produced by catalyst B.

The PI produced has a $M_n = 29\,000$ g/mol with a dispersity of 3.2 (**Figure 11**). From DSC, the glass transition (T_g) of the PI produced is at -39°C (**Figure 11**).

It was also valuable to test the efficiency of each of the catalysts **A** and **B** in the copolymerization of ethylene and isoprene.

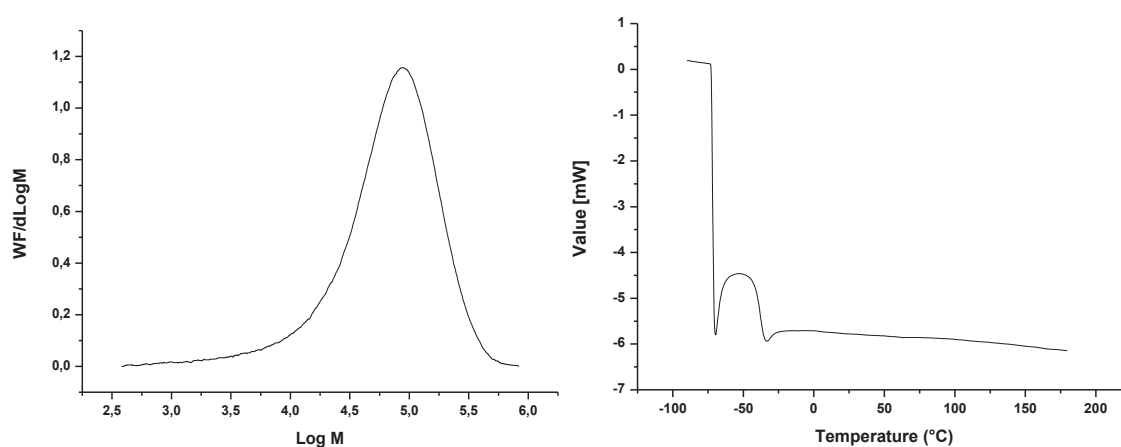


Figure 11. *To the left:* The molar mass distribution of the homo-PI produced by catalyst **B**. *To the right:* DSC peak of the homo-PI produced by catalyst **B**.

D.6.2. Catalysts **A** and **B** in Ethylene-Isoprene Copolymerization

Even though it is known that catalyst **A** family (iron complexes bearing bis(imino)pyridine ligands) is mainly active in ethylene polymerization and that of catalyst **B** (iron complexes bearing iminopyridine ligands) is active in dienes polymerizations, it is important to check the activity of each catalyst in ethylene-isoprene copolymerization process before starting by our trials on chain shuttling copolymerization process.

D.6.2.1. Ethylene-Isoprene Copolymerization Test Using Catalyst **A**

Catalyst **A** is used as a precatalyst for this reaction in combination with trityl BARF as a de-alkylating agent and AlEt_3 as a co-catalyst. Two reactions have been done (**Table 1**) to check the effect of the concentration of isoprene on the activity of the catalyst. The reactions were done in a 1 L reactor under a 7 bar of ethylene pressure at 70 °C.

As it is shown in **Table 1**, the catalyst activity decreases by increasing the concentration of isoprene in the medium, in which the consumption of ethylene decreased by 3 times (from 64 300 equiv. till 17 300 equiv.) and the mass of the polymer produced deceased (from 59 g till 25 g) when the amount of isoprene added is doubled (from 2500 equiv. till 5100 equiv.). This shows primarily that catalyst **A** is more effective in polymerizing ethylene.

Table 1. Testing ethylene-isoprene copolymerization using catalyst A.

	A : Trityl BArF (equiv.)	AlEt₃ (equiv.)	Isoprene^a (equiv.)	Ethylene^b (equiv.)	Time (min)	T (°C)	m (g)
entry 1	1:1	34	2500	64 300	30	70	59
entry 2	1:1	34	5100	17 300	30	70	25

^a : number of equivalents of isoprene added with respect to catalyst A.

^b : number of equivalents of ethylene consumed with respect to catalyst A.

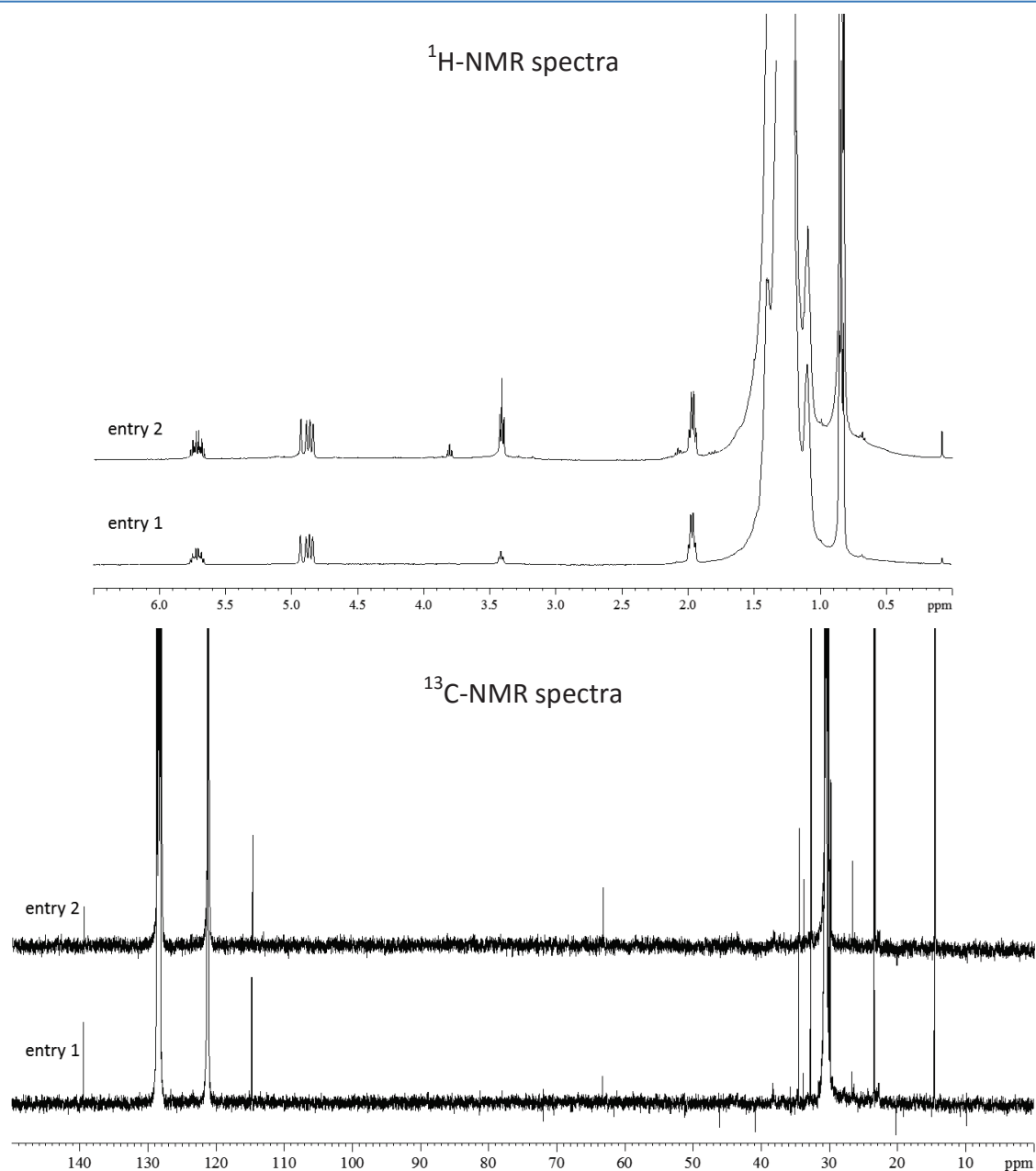


Figure 12. ¹H- and ¹³C-NMR spectra of the polymer produced by catalyst A in presence of ethylene and isoprene.

Then, it was determined from ¹H- and ¹³C-NMR spectra of the polymers produced in

entries 1 and 2 that catalyst **A** is not able to copolymerize ethylene and isoprene since no isoprene derived-motif appears in the NMR spectra (**Figure 12**), and thus no isoprene insertion. The ^1H -NMR and ^{13}C -NMR spectra (**Figure 12**) are identical to those of the homo-PE produced by catalyst **A** (**Figure 8**), showing the three types of terminated-PE (CH_3 -terminated PE, vinyl-terminated PE, and HO-terminated PE). Thus, catalyst **A** is not efficient in copolymerizing ethylene and isoprene, only homo-PEs are produced.

The PE produced in entry 1 possesses the three types of terminated-PE with the following percentages: CH_3 -terminated PE= 81.8 %, vinyl-terminated PE= 14.2 %, and HO-terminated PE= 4 %; the PE produced in entry 2 has this percentages: CH_3 -terminated PE= 84.5 %, vinyl-terminated PE= 9 %, and HO-terminated PE= 6.5 %. These percentages show that the vinyl-terminated PE percentage decreases by increasing the amount of isoprene in the medium, thus β -H elimination is less favored in presence of isoprene. Even if isoprene cannot be inserted it seems to be able to coordinate to the metal center and thus hinder the β -H transfer process.

The SEC analysis shows the formation of two populations of PE in each of the two reactions. One is of low molar mass, which is in the same range as that of the PE produced from the homo-polymerization of ethylene using catalyst **A**. The second is of relatively high molar mass, which is produced because of the less favored β -H elimination in presence of isoprene and thus possibility of formation of longer chains.

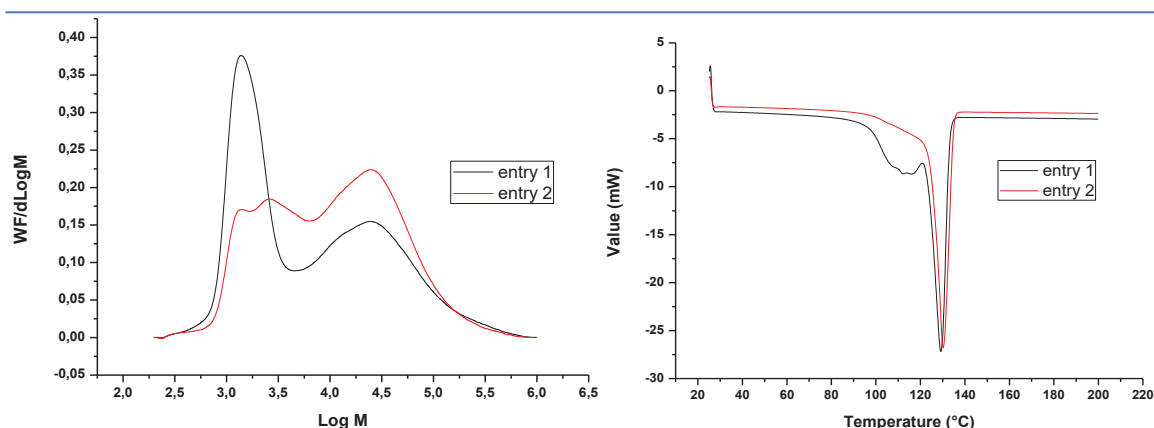


Figure 13. *To the left:* The molar mass distributions of the polymers produced by catalyst **A** in presence of ethylene and isoprene. *To the right:* DSC peaks of these polymers.

The molar masses of the two populations of the PE produced in entry 1 are: 17 700 g/mol with a dispersity of 3.2, and 1400 g/mol with a dispersity of 1.2. That of the PE

produced in entry 2 are: 19 900 g/mol with a dispersity of 2.4, and 1700 g/mol with a dispersity of 1.4 (**Figure 13**). The melting points of the polymers produced in entries 1 and 2 are 129 °C and 130 °C, respectively (**Figure 13**).

D.6.2.2. Ethylene-Isoprene Copolymerization Test Using Catalyst B

Catalyst **B** is used as a precatalyst for this reaction in combination with trityl BARF as a de-alkylating agent and AlEt_3 as a co-catalyst. A reaction has been done in a 1 L reactor which was charged with a mixture of a 1:1 ratio of catalyst **B** : trityl BARF, 34 equiv. of AlEt_3 , and 2500 equiv. of isoprene. The reactor was pressurized by 7 bar of ethylene at 70 °C; no consumption of ethylene was observed which shows that catalyst **B** is not active in copolymerizing ethylene and isoprene.

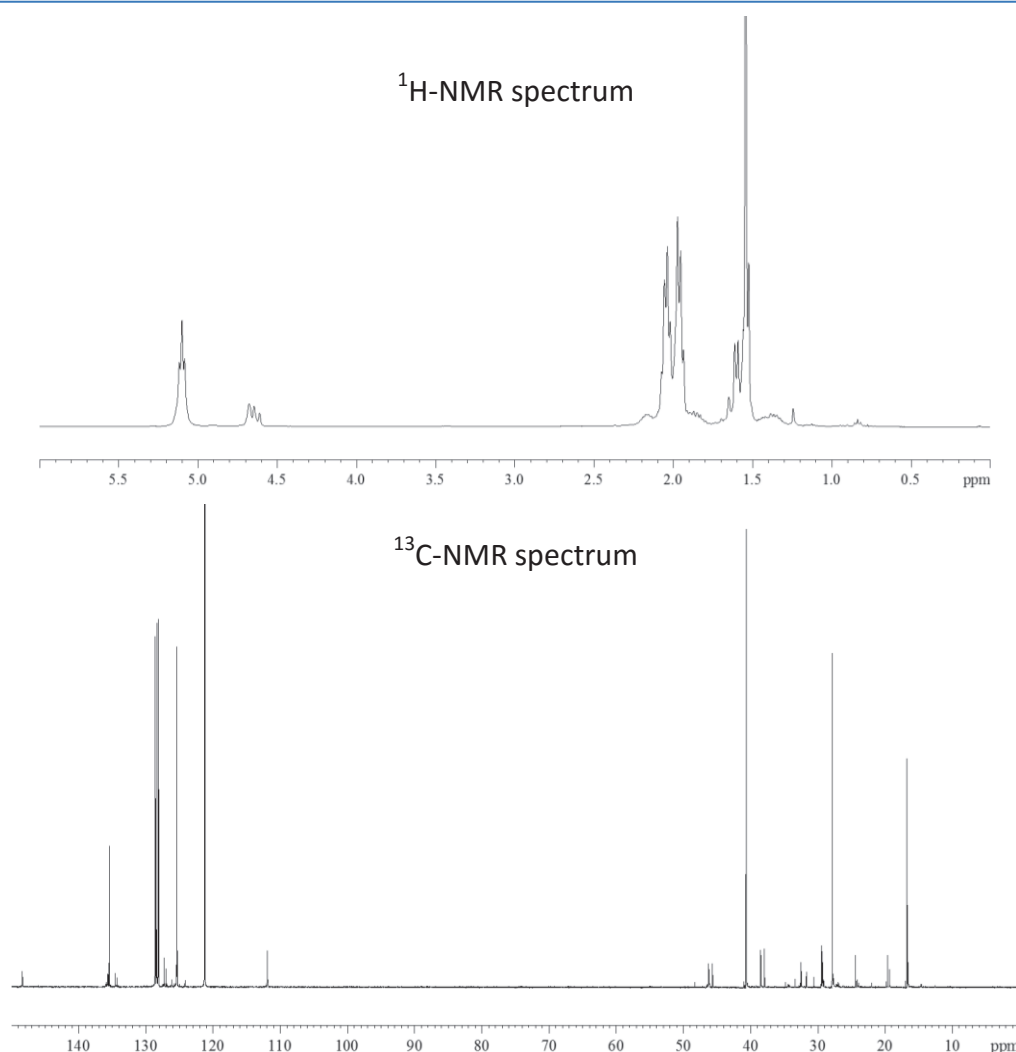


Figure 14. ^1H - and ^{13}C -NMR spectra of the polymer produced by catalyst B in presence of ethylene and isoprene.

To quantitatively assess this conclusion, NMR analyses have been done. The ^1H - and ^{13}C -NMR spectra of the product produced show that it is a homo-polyisoprene (**Figure 14**), all the peaks fit exactly with the peaks in the spectra of the homo-PI produced by catalyst **B** (**Figure 10**). Thus catalyst **B** is also not active in copolymerizing ethylene and isoprene. In addition, the presence of ethylene lead to an increase in the selectivity of catalyst **B** towards 1,4-insertion of isoprene.

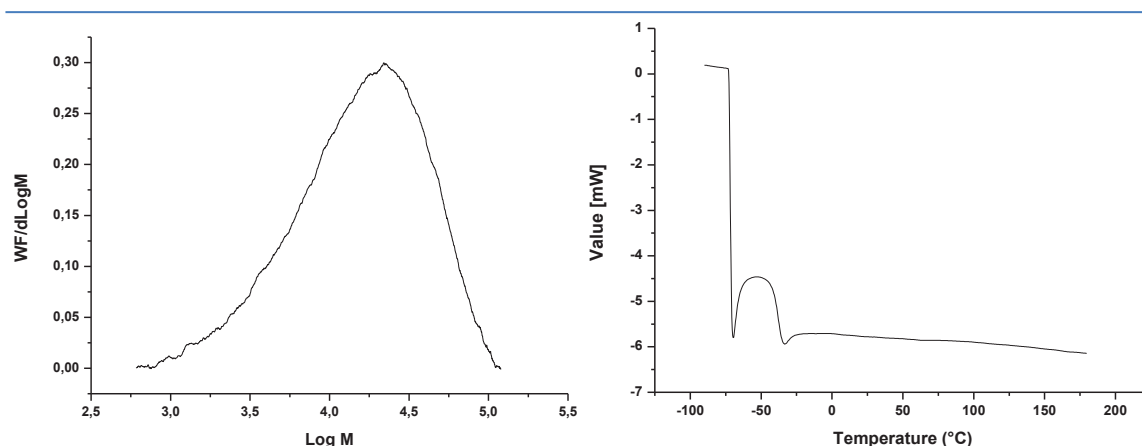


Figure 15. *To the left:* The molar mass distribution of the polymer produced by catalyst **B** in presence of ethylene and isoprene. *To the right:* DSC peak of this polymer.

The yield of isoprene polymerization is 55 %, which is lower than that of the homo-polymerization of isoprene using catalyst **B** (90 %). In addition, the SEC analysis of the polymer produced showed a molar mass of 10 500 g/mol with a dispersity of 2.3 (**Figure 15**). This molar mass is lower than that of the PI obtained from the homo-polymerization of isoprene using catalyst **B** (29 000 g/mol). Thus the presence of ethylene decreases the activity of catalyst **B** in polymerizing isoprene. The T_g of the polymer produced is at -39°C (similar to that of the homo-PI produced by catalyst **B** in absence of ethylene) (**Figure 15**).

After evaluating the exclusive activity of each catalyst for a specific monomer polymerization (catalyst **A** is only active in polymerizing ethylene; catalyst **B** is only active in polymerizing isoprene), we envisioned that a chain shuttling process could be the solution to copolymerize ethylene and isoprene using these (bis)iminopyridine-based catalysts.

D.6.3. Ethylene-Isoprene Chain Shuttling Copolymerization

Ethylene-isoprene copolymers are elastomers that could have a major role in synthesis

of rubber materials, such as car tires. The industrial importance of such copolymers forces researchers to find more sustainable and cheaper methods in their production. This goal could be achieved by using iron catalysis in the production of these copolymers.

In this process, each of the catalysts **A** and **B** will homo-polymerize by inserting its corresponding monomer, and the copolymerization will take place on the chain shuttling agent AlEt_3 *via* transmetallation reactions. Triethylaluminum is a common transfer agent for both catalysts, thus the transfer of both polyethylenyl and polyisoprenyl moieties will take place on the same center (Al). This transfer will lead to the copolymerization of both PE and PI chains either randomly or as blocks, according to the applied procedure.

D.6.3.1. Random Copolymerization

In this process, both catalysts A and B were added simultaneously into the reaction system. Several reactions have been done to assure the reproducibility of our results and to vary the percentage of polyisoprene incorporation. Three main reactions are summarized in **Table 2**. These reactions were done in a 1 L reactor under different ethylene pressures at 70 °C.

Table 2. Chain shuttling random copolymerization reactions between catalyst A, catalyst B, and triethylaluminum.

	A : B^a (equiv.)	AlEt₃^b (equiv.)	Isoprene^c (equiv.)	Ethylene^d (equiv.)	Time (min)	T (°C)	m (g)
entry 3	1:1	23	4000	60 200	50	70	70
entry 4	1:5	13	4000	24 400	50	70	45
entry 5	1:5	13	4000	12 600	50	70	30

^a : trityl BArF : catalyst is 1:1.

^b : number of equivalents with respect to both catalysts **A** and **B**.

^c : number of equivalents of isoprene added with respect to catalyst **B**.

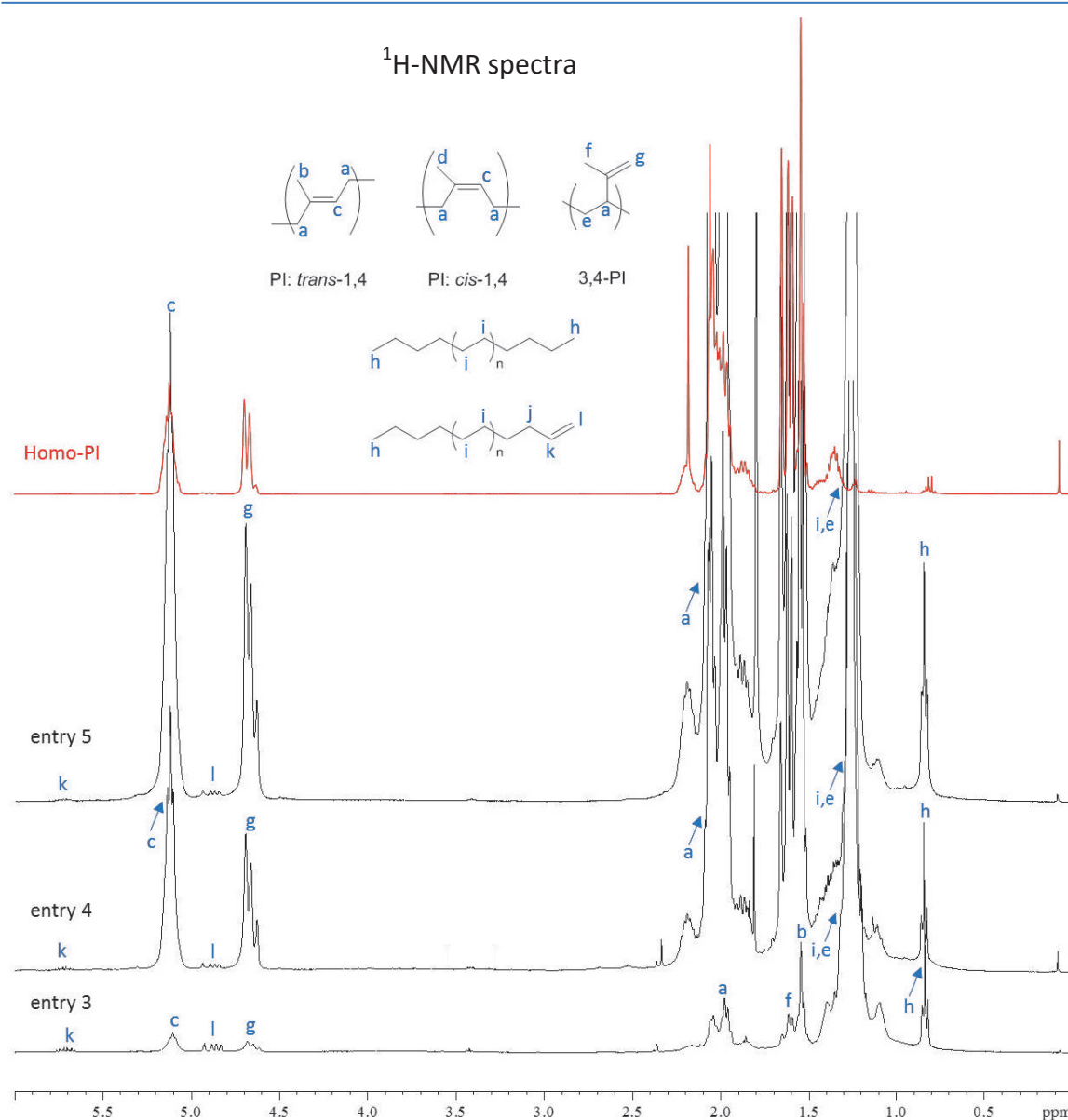
^d : number of equivalents of ethylene consumed with respect to catalyst **A**.

The NMR analyses of the polymers obtained in all the entries show that either isoprene-ethylene copolymers or mixtures of polymers are produced. In entry 3, the isoprene content in the copolymer produced was low (1.8 %) as it was determined from ¹H-NMR spectrum, the isoprene was polymerized as 1,4-*trans*-PI with very limited

amount of 3,4-PI (**Table 3**). It was also assured by the ^{13}C -NMR spectrum that PI is incorporated majorly as 1,4-*trans*-PI (**Figure 16**).

Table 3. Molar percentages of incorporated polyisoprene in the random copolymers.

	Total PI Percentage (%)	1,4- <i>cis</i> units (%)	1,4- <i>trans</i> units (%)	3,4 units (%)
entry 3	1.8	-	99.2	0.8
entry 4	32.8	12.0	72.4	15.6
entry 5	36.8	15.0	64.9	20.1



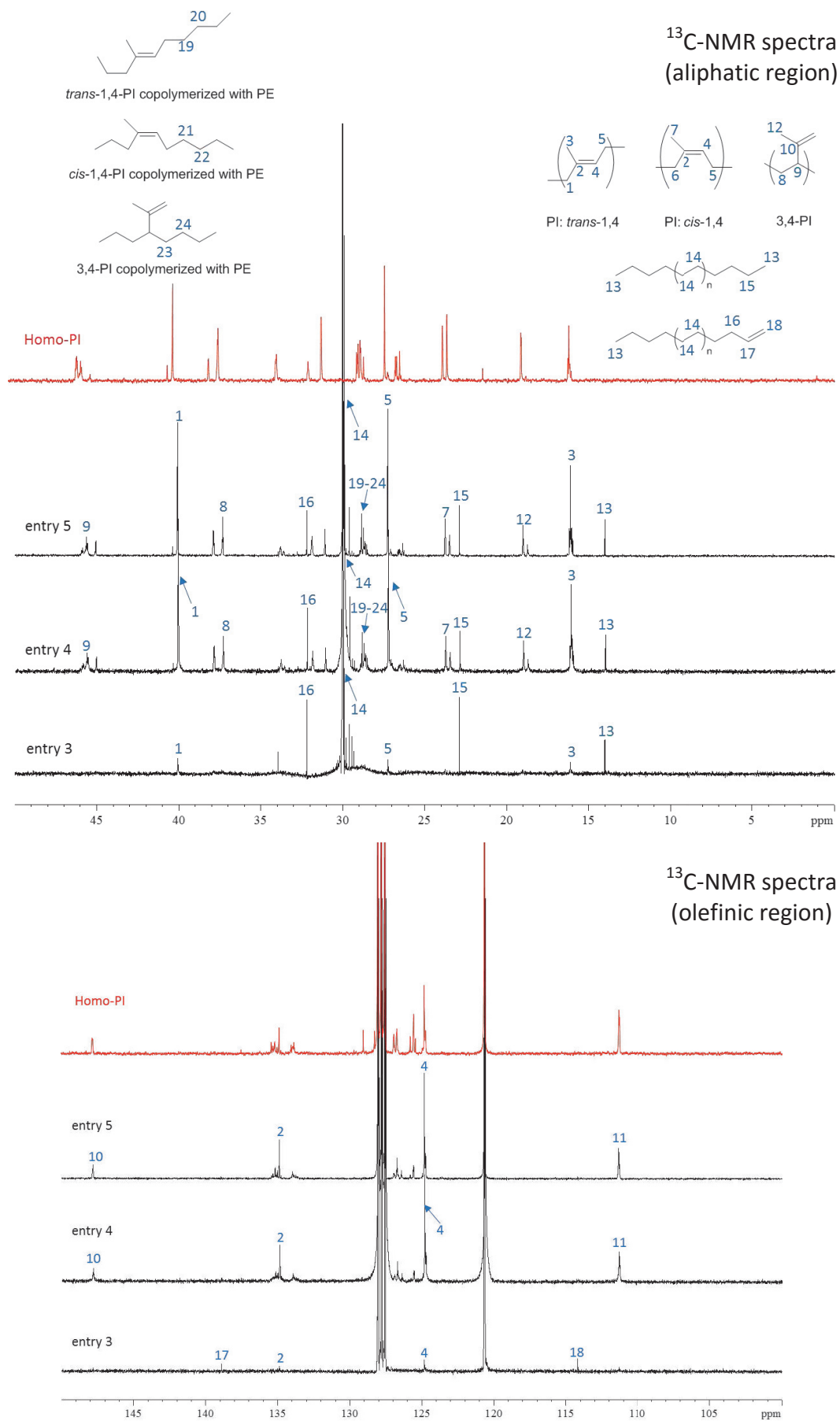


Figure 16. ^1H - and ^{13}C -NMR spectra of the ethylene-isoprene random copolymers.

The TOF of catalyst **A** in polymerizing ethylene is more than that of catalyst **B** in polymerizing isoprene, this what led to the consumption of very high amount of ethylene (60 200 equiv.) with respect to that of isoprene. The yield of isoprene polymerization was only 12.3 %. Note that this reaction was done under a pressure of 8 bar of ethylene.

In order to increase isoprene incorporation in the copolymer, entries 4 and 5 were performed. Axiomatically, increasing the amount of catalyst **B** with respect to that of catalyst **A** must occur, this was done in both entries 4 and 5; the ratio used was 1:5 (**Table 2**).

In entry 4, 24 400 equiv. of ethylene were consumed in 50 min, which is about half of the amount consumed in entry 3. From ^1H - and ^{13}C -NMR (**Figure 16**), it was obvious that the incorporation of isoprene increases much more than that in entry 3, where the percentage of isoprene incorporated reaches 32.8 % including 12 % of 1,4-*cis* units, 72.4 % of 1,4-*trans* units, and 15.6 % of 3,4 units (**Table 3**); the isoprene polymerization yield is 40.5 %. This reaction also took place under a pressure of 8 bar of ethylene.

Decreasing the ethylene pressure under which the copolymerization reaction is taking place is one of the key steps to produce a copolymer with higher isoprene content. Entry 5 was done under a pressure of 2 bar of ethylene; 12 600 equivalents of ethylene were consumed in 50 minutes, which is about half of what is consumed in entry 4. Depending on ^1H and ^{13}C NMR spectra (**Figure 16**), the amount of isoprene incorporated is higher than that in entry 4, where the percentage of PI incorporated is 36.8 % including 15 % of 1,4-*cis* units, 64.9 % of 1,4-*trans* units, and 20.1 % of 3,4 units (**Table 3**); the yield of isoprene polymerization is 54.2 %.

Figure 16 shows the ^1H - and ^{13}C -NMR spectra of the random copolymers produced with the assignment of all the corresponding protons and carbon atoms in addition to the superimposition of these spectra with the homo-PI spectrum to show the new peaks that arise after copolymerization. The total PI content in the copolymer is determined from ^1H -NMR spectrum according to the following equation (I = integration): Mol PI % = $[(I_c + 0.5I_g)/(I_c + 0.5I_g + 0.25(I_{i,e}-I_g))] \times 100$; whereas the PI isomer contents are calculated according to the equations mentioned in part D.6.1.2.

As shown in **Table 3** the percentage of 1,4-*trans* units decreases by increasing the incorporation of isoprene, while that of 1,4-*cis* units and 3,4 units increase. Thus by increasing the total polyisoprene content and decreasing that of ethylene; catalyst **B** become less selective towards the incorporation of PI as discrete 1,4-*trans* unit in the copolymer.

Figure 17 represents the HSQC (heteronuclear single quantum correlation) spectrum of the copolymer produced in entry 5, showing mainly the J1 (HC) correlation between the protons and the carbon atoms of the random copolymer in addition to the J2 (HCC) correlations. Some of these correlations are assigned in the spectrum. The correlation *a*-(19,21,23) shows the alternance between the isoprene and ethylene units.

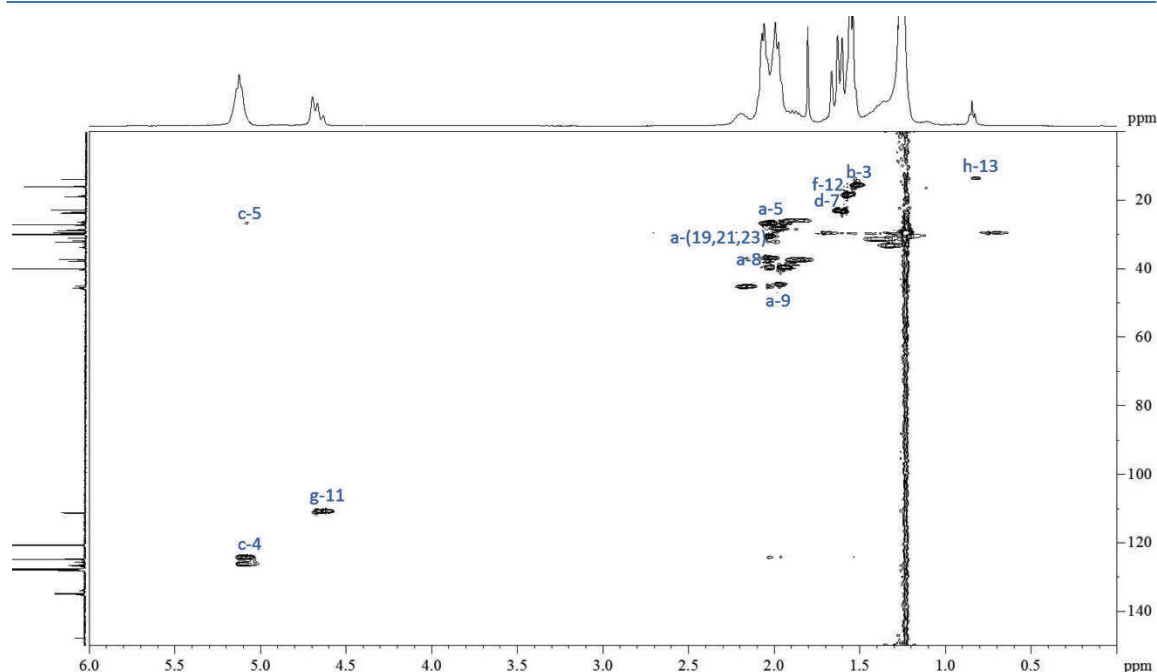


Figure 17. HSQC spectrum of the ethylene-isoprene random copolymer produced in entry 5.

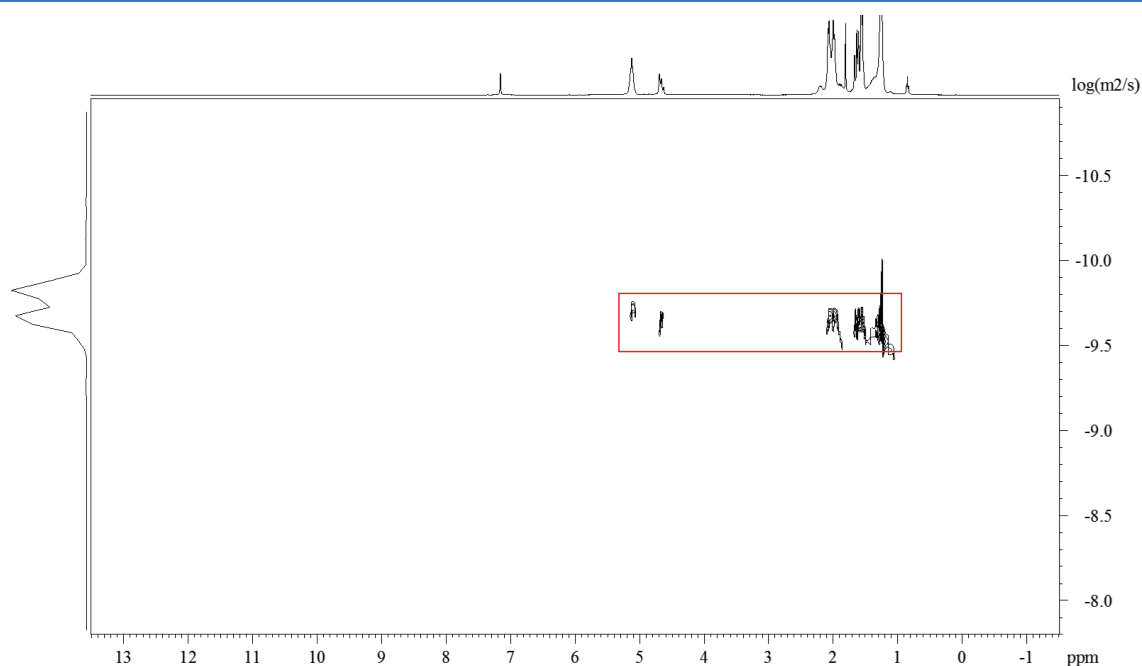
At this stage, one could say that the obtained polymer could be just a mixture of the two homo-polymers (PE and PI), so to prove that what is produced is a copolymer we did DOSY NMR analysis (diffusion ordered spectroscopy). This spectroscopic analysis seeks to separate the NMR signals of different species according to their diffusion coefficient, thus we did this analysis for the random copolymer, the two homo-polymers, and a mixture of the two homo-polymers.

As it is shown in **Table 4**, the diffusion coefficient of the random copolymer produced

in entry 5 (the copolymer with the highest percentage of incorporated PI) is $2 \times 10^{-10} \text{ m}^2/\text{s}$ which is different from those of the mixture of the homo-polymers ($4 \times 10^{-11} \text{ m}^2/\text{s}$ and $3.5 \times 10^{-10} \text{ m}^2/\text{s}$). The diffusion coefficient of the copolymer is the same on both peaks at 1.26 ppm (which corresponds to the methylene protons of PE) and at 5.11 ppm (which corresponds the vinyl H of 1,4 unit), thus what is obtained is a copolymer and not a mixture of two homo-polymers.

Table 4. Diffusion coefficients obtained from DOSY NMR.

	Diffusion coefficient (m^2/s)	
	5.11 ppm (vinyl H of 1,4-PI)	1.26 ppm (methylene protons)
Homo-polyethylene	-	3.5×10^{-10}
Homo-polyisoprene	4×10^{-11}	-
Mixture of the two homo-polymers	4×10^{-11}	3.5×10^{-10}
Random copolymer (entry 5)	2×10^{-10}	2×10^{-10} 1.5×10^{-10}



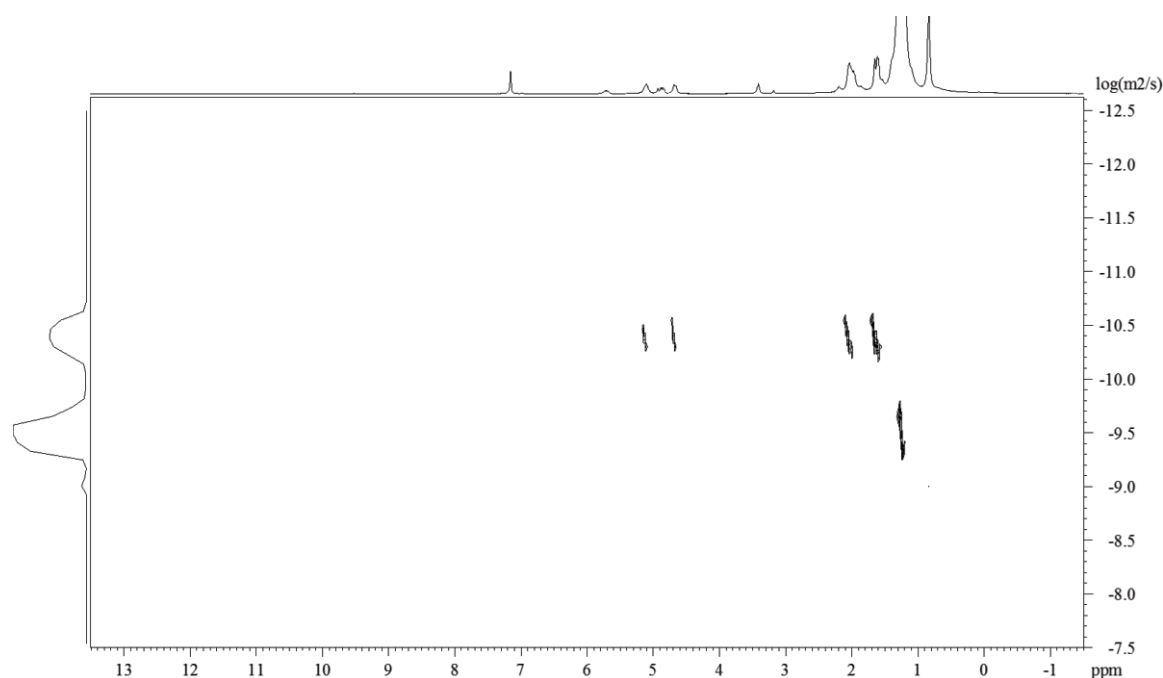


Figure 18. DOSY-NMR spectra of the random copolymer produced in entry 5 (*up*) and the mixture of homo-polymers (*down*).

In addition to the copolymer, the DOSY spectrum shows the presence of a homo-PE of a diffusion coefficient 1.5×10^{-10} , this coefficient is different from that of the PE produced in the homo-polymerization process because of the difference in molar masses. The presence of homo-PE is normal because of the higher activity of catalyst **A** with respect to catalyst **B**. **Figure 18** represents the DOSY-NMR spectrum of the copolymer and the spectrum of the mixture of the two homo-polymers.

From SEC, the molar mass distribution of the copolymers produced in entries 3, 4 and 5 show double peak distributions, one peak corresponds to the ethylene-isoprene random copolymer and the other corresponds to the homo-PE, where the presence of this homo-polymer also appeared in the DOSY-NMR. **Figure 19-(a)** shows the full distributions, but these distributions are not true since it is a combination of two types of polymers, we present it just to show the relative content of homo-PE and random copolymer in the mixture.

The molar mass distributions of the copolymer portions are presented in **Figure 19-(b)**. The M_n of the copolymer produced in entry 3 is 18 300 g/mol with a dispersity of 1.4; that of the copolymer produced in entry 4 is 27 000 g/mol with a dispersity of 1.7; and that of the copolymer produced in entry 5 is 69 800 with a dispersity of 2.7. The molar masses of the homo-PE produced in entries 3, 4 and 5 are 1700 g/mol with a dispersity

equal to 1.18, 1200 g/mol with a dispersity equal to 1.1, and 700 g/mol with a dispersity of 1.4, respectively.

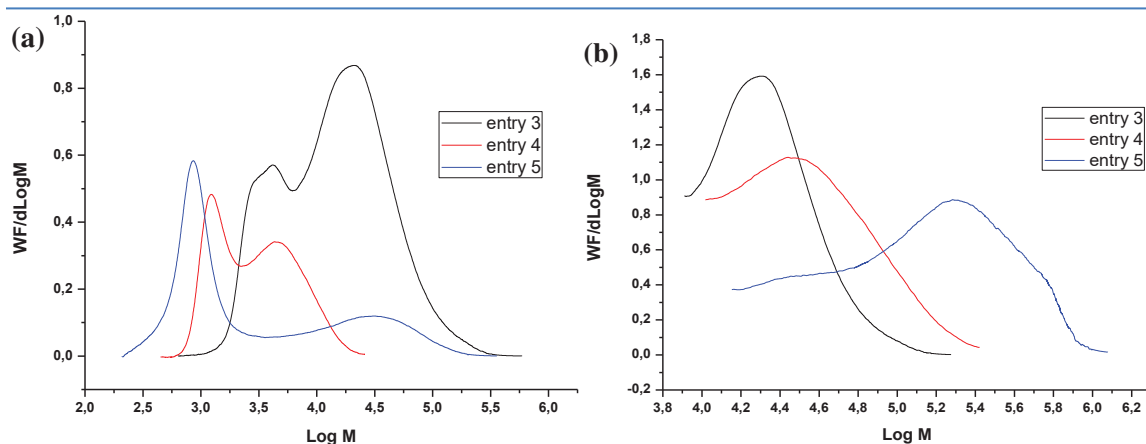


Figure 19. (a) Molar mass distribution of the random copolymers with the homo-PE; (b) Molar mass distributions of the random copolymers portions.

From DSC, the melting point of the obtained copolymers in entries 3, 4, and 5 are 133 °C, 126 °C, and 127 °C, respectively (**Figure 20**). The T_g of the polymer produced in entry 3 didn't appear in its DSC (which is conducted at a temperature range from -90 °C till 180 °C) since the incorporation of isoprene in the polymer is very low and thus the polymer thermal properties are similar to those of PE, therefore the T_g is around -100 °C. The T_g of the polymer produced in entry 4 is equal to 34 °C and that of the polymer produced in entry 5 is equal to -39 °C. Such difference in T_g could occur in random copolymers mainly due to the uncontrolled (different) arrangement of the polymer units which will lead to different microstructure of the copolymer and thus different glass transitions.

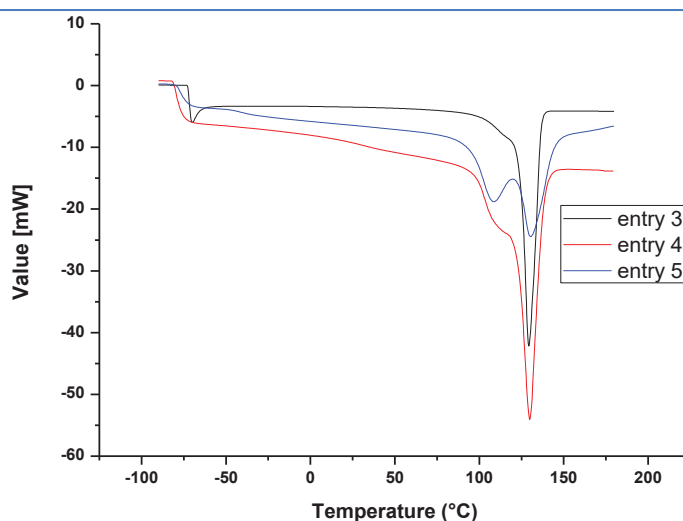


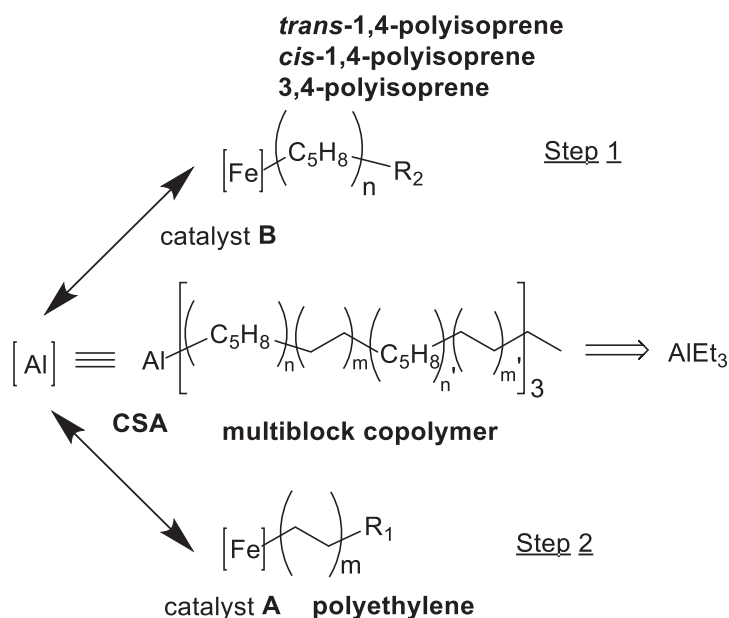
Figure 20. DSC peaks of the random copolymers.

D.6.3.2. Block Copolymerization

Following the achievement of the iron-catalyzed chain shuttling random copolymerization of ethylene and isoprene, we aimed at the production of block copolymers *via* this process.

In order to obtain ethylene-isoprene block copolymers we changed the procedure applied previously in the chain shuttling random copolymerization process. Here, a two-step procedure is applied, step 1 forms the homo-polymerization of isoprene using catalyst **B** and step 2 forms the copolymerization process. In the previous part, the random copolymer is produced by the addition of both catalysts **A** and **B** simultaneously into the reaction medium. While in this part, the two catalysts are added sequentially, catalyst **B** system (catalyst **B**, trityl BArF, and AlEt_3) with isoprene are added first to promote the production of polyisoprene (PI) chains. After a specific time, catalyst **A** system is added into the reaction medium which is then pressurized by ethylene. In this step, the polyethylene chains are produced by catalyst **A**, the activation of the precatalyst **A** (Fe-Cl) is achieved by alkylation exclusively *via* Al(PI)_3 systems without further addition of AlEt_3 . **Scheme 11** summarizes this process.

Scheme 11. Ethylene-isoprene chain shuttling block copolymerization.



In order to insure the reproducibility of our results and to check the variation of the percentage of polyisoprene incorporation, different reactions have been realized. **Table 5** summarizes the main reactions.

Entries 6 and 7 were done in a 1 L reactor, while entry 8 was done in a 0.5 L glass reactor from which a sample of the homo-PI produced in the first step could be taken.

Table 5. Chain shuttling block copolymerization reactions between catalyst A, catalyst B, and triethylaluminum.

	A:B ^a	TEA ^b (equiv.)	Isoprene ^c (equiv.)	Ethylene ^d (equiv.)	Time (hr) step 1	Time (min) step 2	T (°C)	m (g)
entry 6	1:1	23	4000	36 000	2	9	70	58
entry 7	1:2	17	4000	24 000	5	35	70	44
entry 8	1:2	17	4000	21500	5	120	70	29

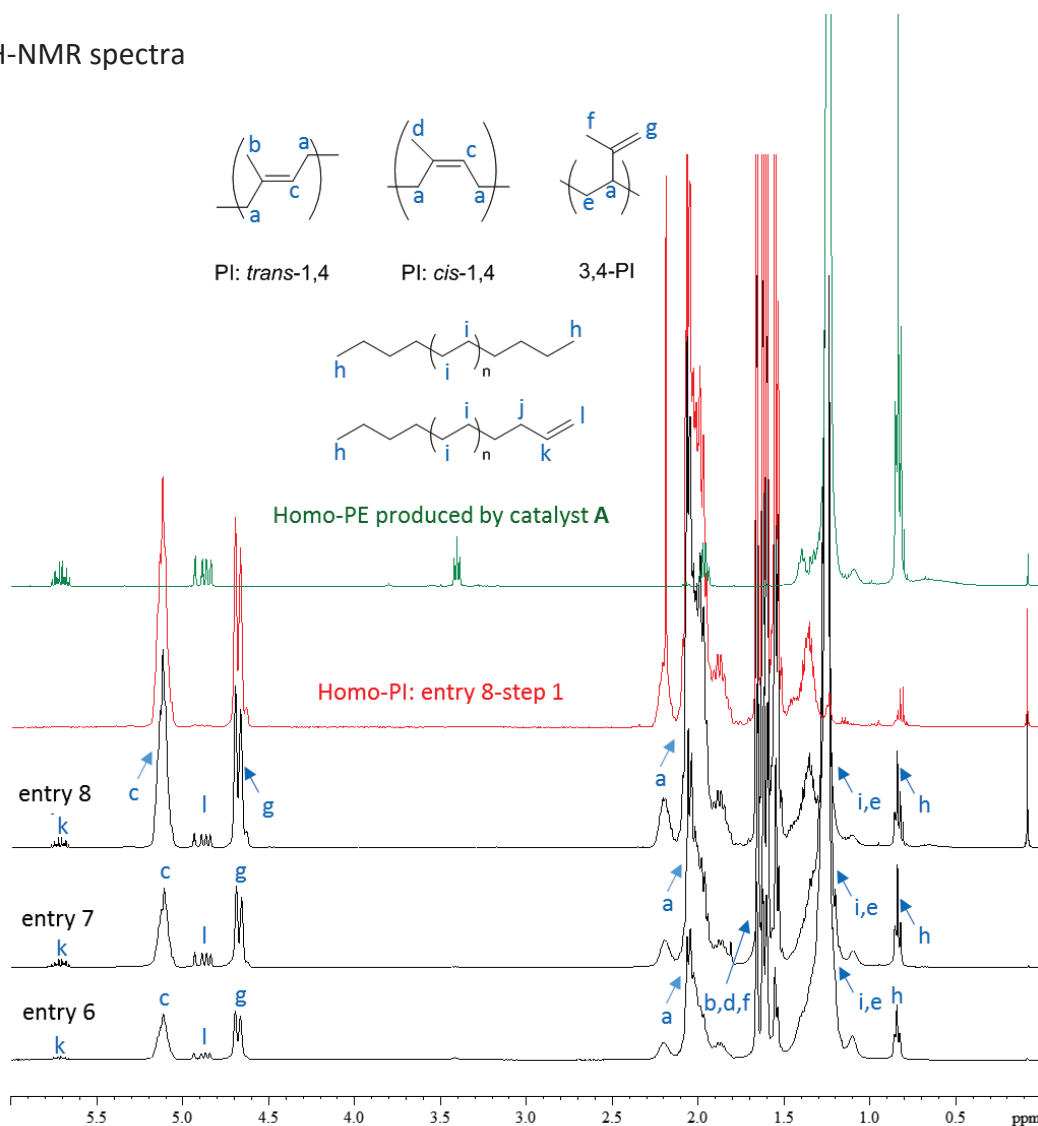
^a: Trityl BARF : Catalyst is 1:1.

^b: number of equivalents with respect to both catalysts A and B.

^c: number of equivalents of isoprene added with respect to catalyst B.

^d: number of equivalents of ethylene consumed with respect to catalyst A.

¹H-NMR spectra



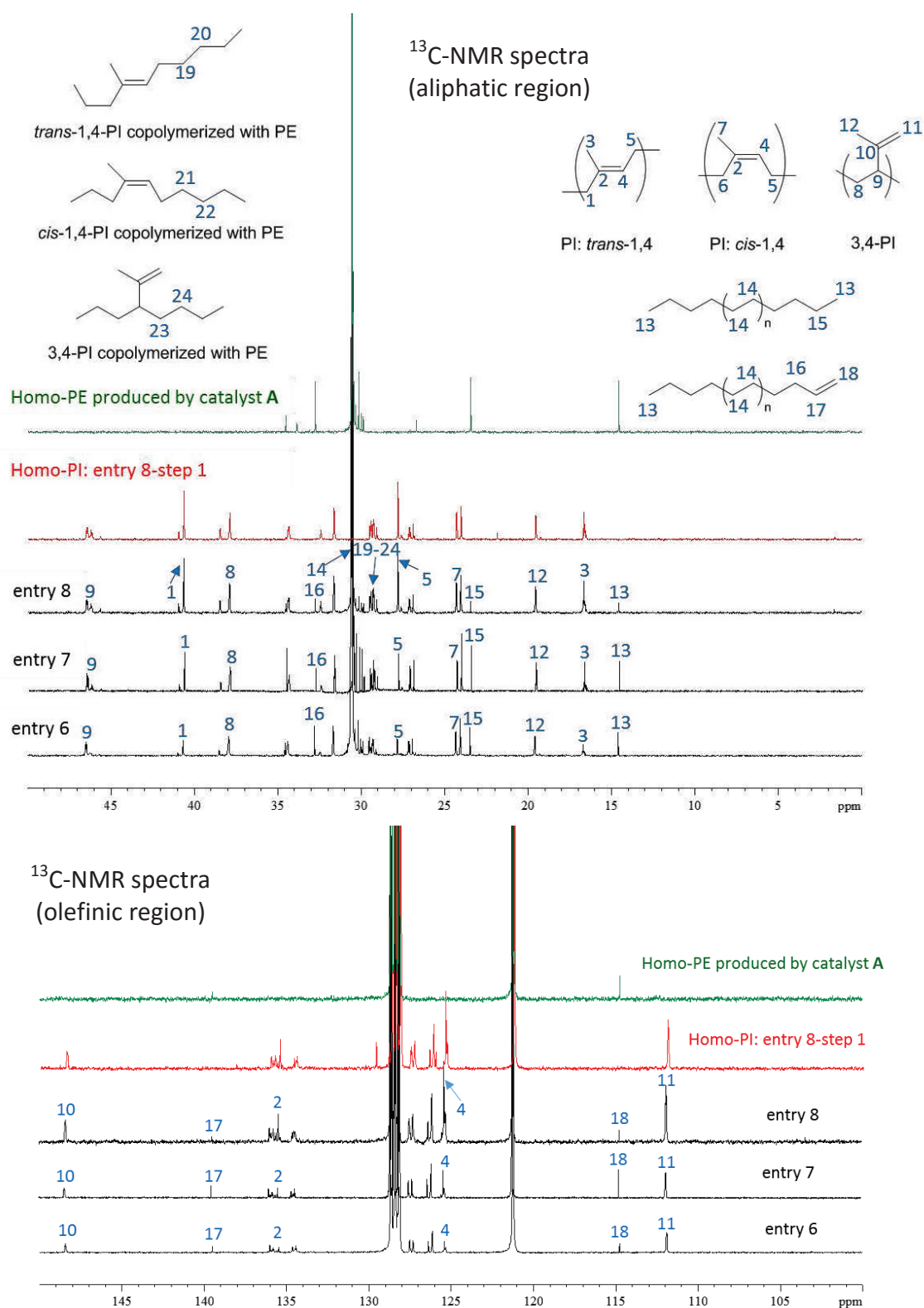


Figure 21. ¹H- and ¹³C-NMR spectra of the ethylene-isoprene block copolymers.

The NMR analyses show that the product produced is a copolymer (**Figure 21**). In entry 6, a 1:1 ratio of the two catalysts was used, step 1 lasted 2 h, then the copolymerization step (step 2) lasted just 9 minutes due to the high activity of catalyst **A** (the system was

pressurized by 7 bar of ethylene). The percentage of the polyisoprene incorporated was 7.4 % with a 42.2 % of 1,4- *cis* units, 22.4 % of 1,4- *trans* units, and 35.4 % of 3,4 units as it has been calculated from the ^1H - and ^{13}C -NMR spectra.

In order to increase the percentage of the PI incorporated in the copolymer, we doubled the amount of catalyst **B** and increased the time of step 1 (isoprene polymerization step); the second step proceeded under a pressure of 2 bar of ethylene (entry 7). As it was expected, the percentage of the PI incorporated increased till 15.5 % with a 41.1 % of 1,4-*cis* units, 25.1 % of 1,4-*trans* units, and 33.8 % of 3,4 units. Also, the reaction shows relatively lower activity in ethylene polymerization mainly due to the lower pressure of ethylene at which the reaction has been performed. We kept the second reaction step running for longer time (35 minutes).

Then, to check the difference in the microstructure of polyisoprene between step 1 and 2 (between the homo-polyisoprene and the polyisoprene blocks in the copolymer) we performed entry 8 in a 0.5 L reactor from which a sample of the homo-PI produced in step 1 could be withdrawn. In addition, we expected an increase in the incorporation of polyisoprene in the copolymer due to the lower concentration of ethylene in step 2 ($P_{\text{ethylene}} = 2$ bar but in a smaller reactor, a glass reactor that could resist pressure up to 3 bar) and the longer copolymerization time that could be achieved.

The total percentage of PI in the copolymer obtained was 45.7 % with a 35.2 % of 1,4-*cis* units, 35.9 % of 1,4-*trans* units, and 28.9 % of 3,4 units. By comparison with the percentages obtained in the homo-polymerization of isoprene in step 1 (40.7 % of 1,4-*cis* units, 21.3 % of 1,4-*trans* units, and 38 % of 3,4 units), the percentages of 1,4-*cis* units and 3,4 units decrease after the incorporation of PI in the copolymer, and that of the 1,4-*trans* units increases.

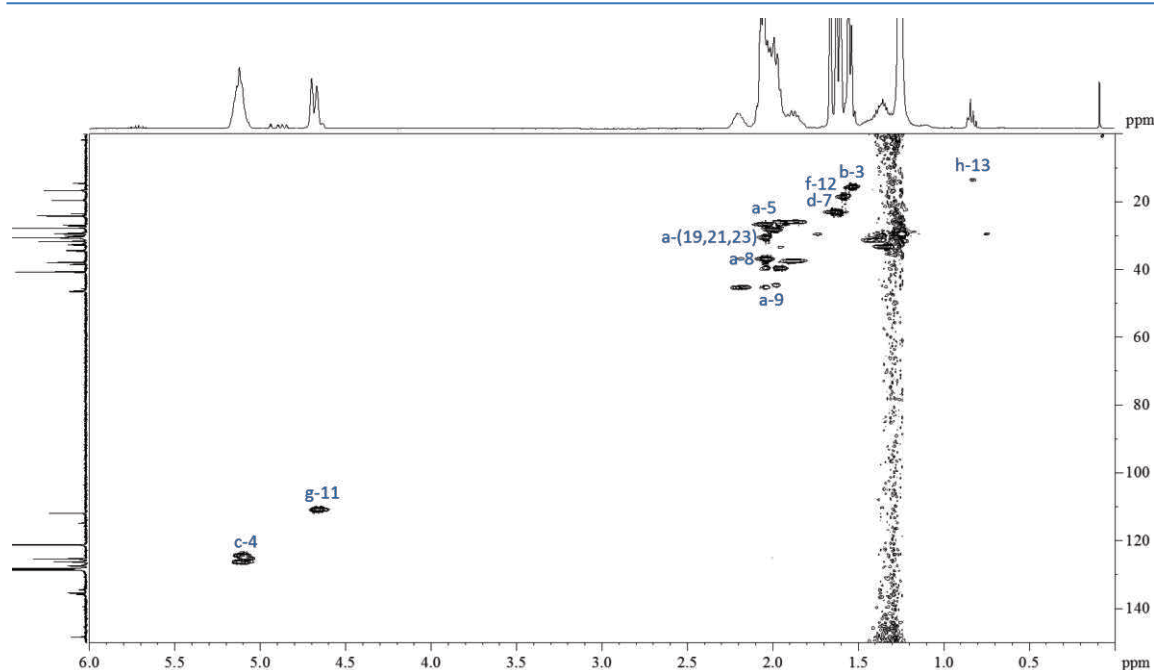
In addition, as it is shown in **Table 6**, as the percentage of PI incorporation in the copolymer increases the percentages of 1,4-*cis* and 3,4 units decrease and that of the 1,4-*trans* units increases.

Figure 21 represents also the superimposition of the homo-PI produced in step 1 and the copolymer produced in step 2 of entry 8, in addition to the homo-PE produced by catalyst **A**. All the peaks in the ^1H - and ^{13}C -NMR are assigned in **Figure 21**.

Table 6. Molar percentages of incorporated polyisoprene in the block copolymers.

	Total PI Percentage (%)	1,4- <i>cis</i> units (%)	1,4- <i>trans</i> units (%)	3,4 units (%)
entry 6	7.4	42.2	22.4	35.4
entry 7	15.5	41.1	25.1	33.8
entry 8	45.7	35.2	35.9	28.9

The HSQC spectrum of the block copolymer produced in entry 8 (in which the highest percentage of PI incorporation is achieved) is represented in **Figure 22** where the different correlations are assigned. The correlation *a*-(19,21,23) shows the alternance between the isoprene and ethylene units. Also, HMBC (Heteronuclear Multiple Bond Correlation) experiment has been done (**Figure 23**). HMBC gives correlations between carbons and protons that are separated by two, three, and, sometimes in conjugated systems, four bonds; direct one-bond correlations are suppressed. The correlations *a*-(19-24) and *c*-(19-24) show also the alternance between the isoprene and ethylene units.

**Figure 22. HSQC spectrum of the ethylene-isoprene block copolymer produced in entry 8.**

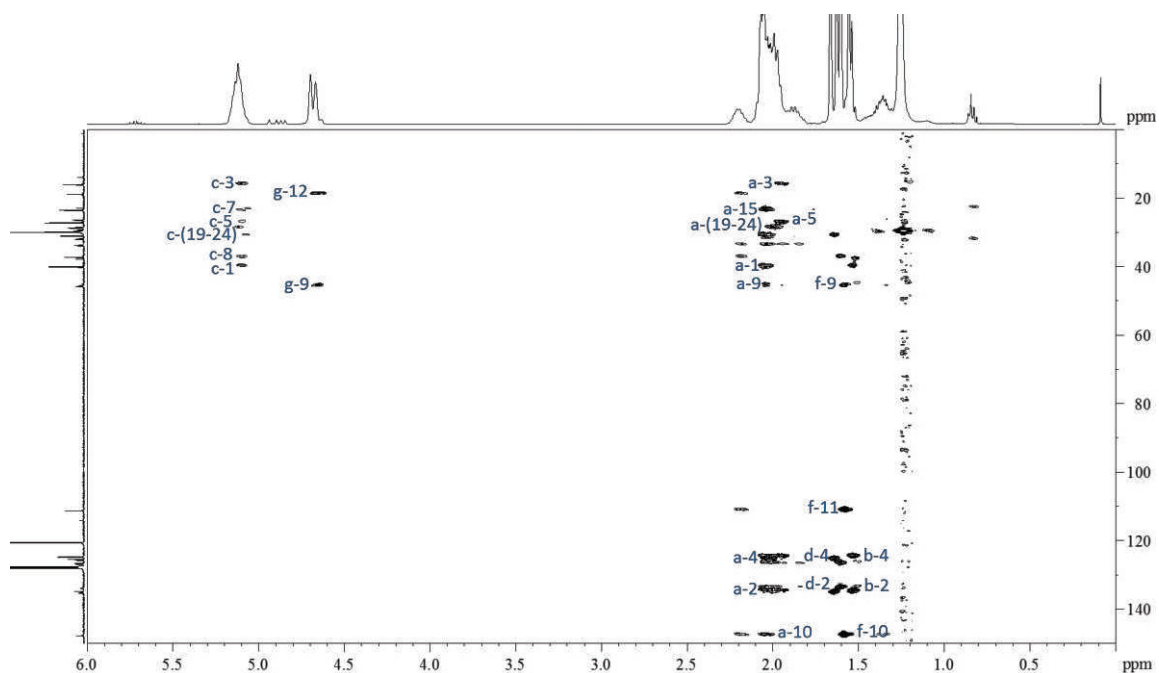


Figure 23. HMBC spectrum of the ethylene-isoprene block copolymer produced in entry 8.

In addition, DOSY NMR was performed to assure that a copolymer is produced and not a mixture of the two homo-polymers (PE and PI). Similar to what have been done with the random copolymer, we did this analysis for the block copolymer, the two homo-polymers, and a mixture of the two homo-polymers.

As it is shown in **Table 7**, the diffusion coefficient of the block copolymer produced in entry 7 ($1.05 \times 10^{-10} \text{ m}^2/\text{s}$), which is done under the same conditions as entry 5 (in random copolymerization), is different from those of the mixture of the homo-polymers ($4 \times 10^{-11} \text{ m}^2/\text{s}$ and $3.5 \times 10^{-10} \text{ m}^2/\text{s}$). The diffusion coefficient of the copolymer is the same on both peaks at 1.26 ppm (which corresponds to the methylene protons of PE) and at 5.11 ppm (which corresponds the vinyl H of 1,4 units), thus what is obtained is a copolymer and not a mixture of two homo-polymers.

Also, the DOSY NMR shows the difference in the diffusion coefficients between the random copolymer (2×10^{-10}) and the block copolymer (1.05×10^{-10}) which are produced under the same conditions (entries 5 and 7). **Figure 24** represents the DOSY NMR spectrum of the copolymer produced in entry 7.

Table 7. Diffusion coefficients obtained from DOSY NMR.

	Diffusion coefficient (m^2/s)	
	5.11 ppm (vinyl H of 1,4-polyisoprene)	1.26 ppm (methylene protons)
Homo-polyethylene	-	3.5×10^{-10}
Homo-polyisoprene	4×10^{-11}	-
Mixture of the two homo-polymers	4×10^{-11}	3.5×10^{-10}
Random copolymer (entry 5)	2×10^{-10}	2×10^{-10} 1.5×10^{-10}
Block copolymer (entry 7)	1.05×10^{-10}	1.05×10^{-10} 3.55×10^{-10} 4.07×10^{-11}

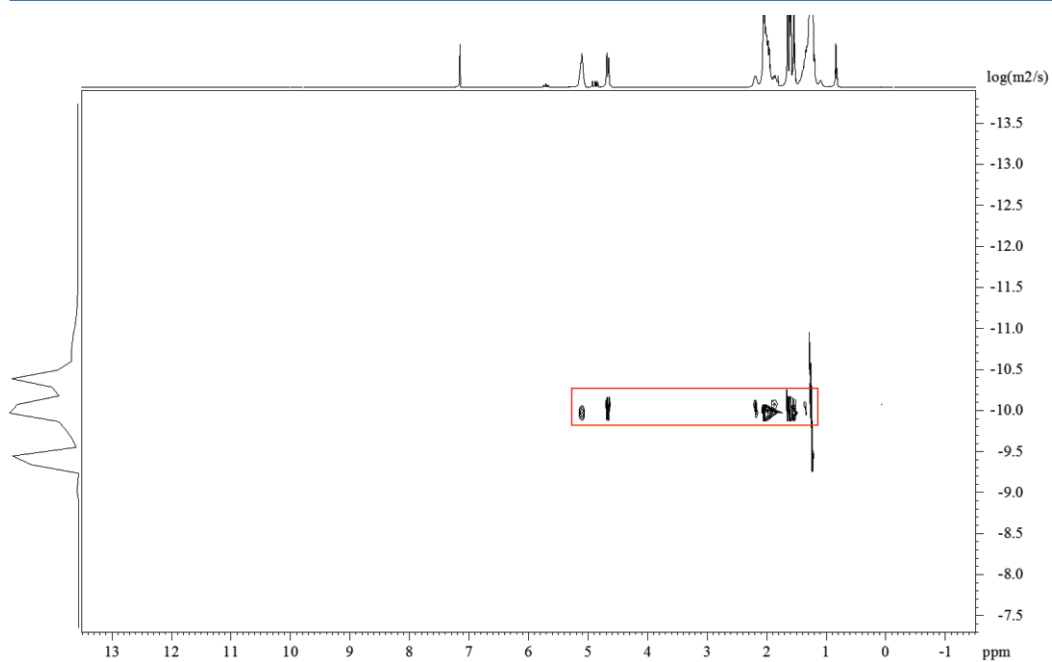
**Figure 24. DOSY-NMR spectrum of the block copolymer produced in entry 7.**

Figure 25 shows the DOSY-NMR spectra of the homo-PI produced in entry 8-step 1 and the copolymer produced in entry 8-step 2. The diffusion coefficient of the homo-PI is 1.45×10^{-11} while that of the copolymer is 2.36×10^{-11} (at 5.11 ppm and 1.26 ppm). The spectrum that corresponds to the copolymer shows also at 1.26 ppm different diffusion coefficients corresponding to homo-PE chains of different lengths; the diffusion coefficients are: 1.49×10^{-11} , 2.87×10^{-11} , and 3.33×10^{-11} .

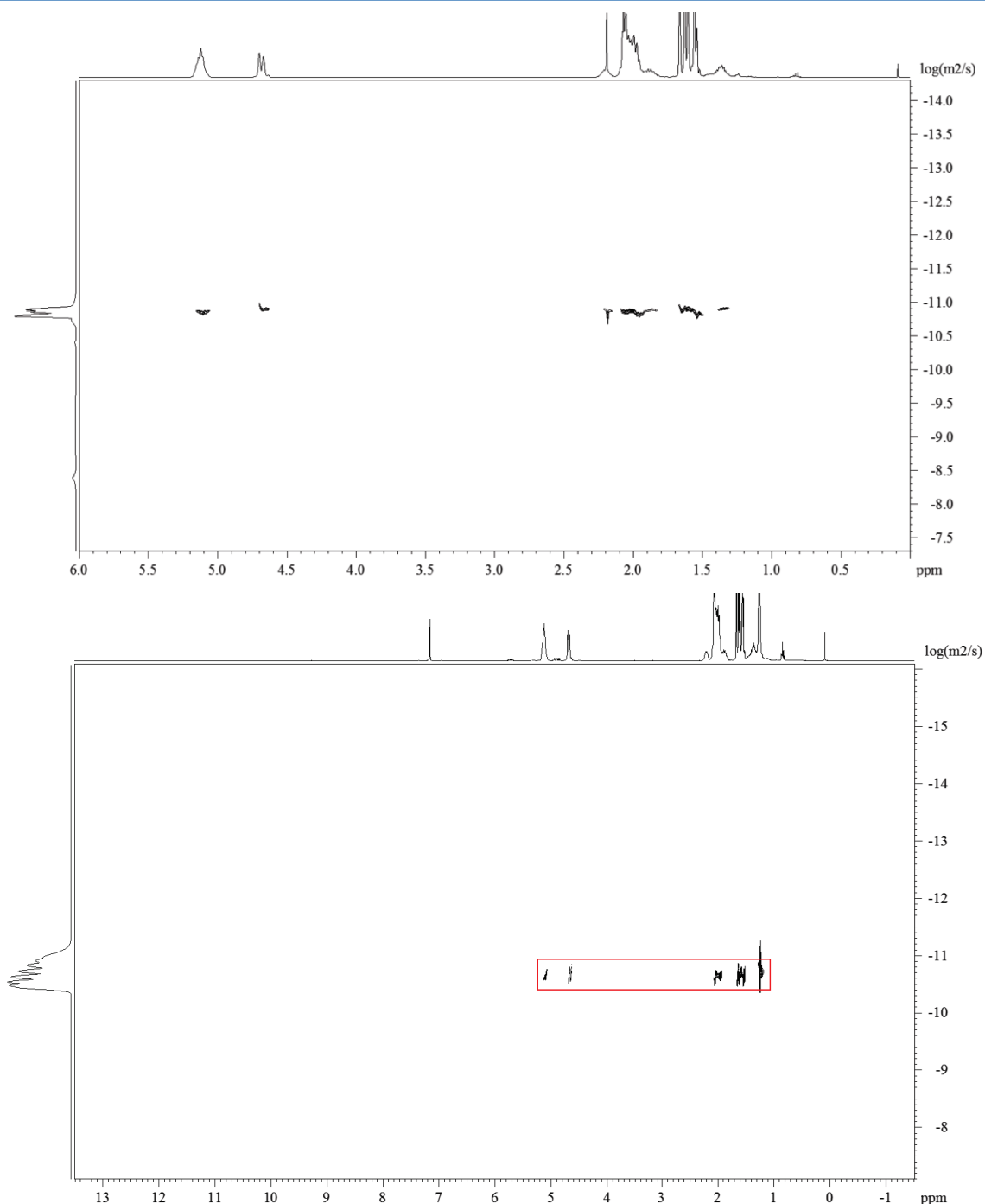


Figure 25. DOSY-NMR spectra of the homo-PI produced in entry 8-step 1 (*up*) and the block copolymer produced in entry 8-step 2 (*down*).

The molar mass distributions of the copolymers produced in entries 7 and 8 show bimodal mass distributions, one population corresponds to the ethylene-isoprene block copolymer and the other corresponds to the homo-PE. The presence of this homo-polymer also appeared in the DOSY-NMR. **Figure 26-(a)** displays the full distributions. This homo-polymerization of ethylene cannot be entirely suppressed since β -H transfer takes place and re-initiate new PE oligomers.

The molar mass distributions of the copolymer fractions are presented in **Figure 26-(b)** (removal of homo-PE signal contamination is applied for clarity). The M_n of the copolymer produced in entry 7 is 42 900 g/mol with a dispersity of 4.2; that of the copolymer produced in entry 8 is 38 100 g/mol with a dispersity of 4.7. The molar masses of the homo-PE produced in entries 7 and 8 are 900 g/mol with a dispersity equal to 1.3 and 1200 g/mol with a dispersity equal to 1.17, respectively.

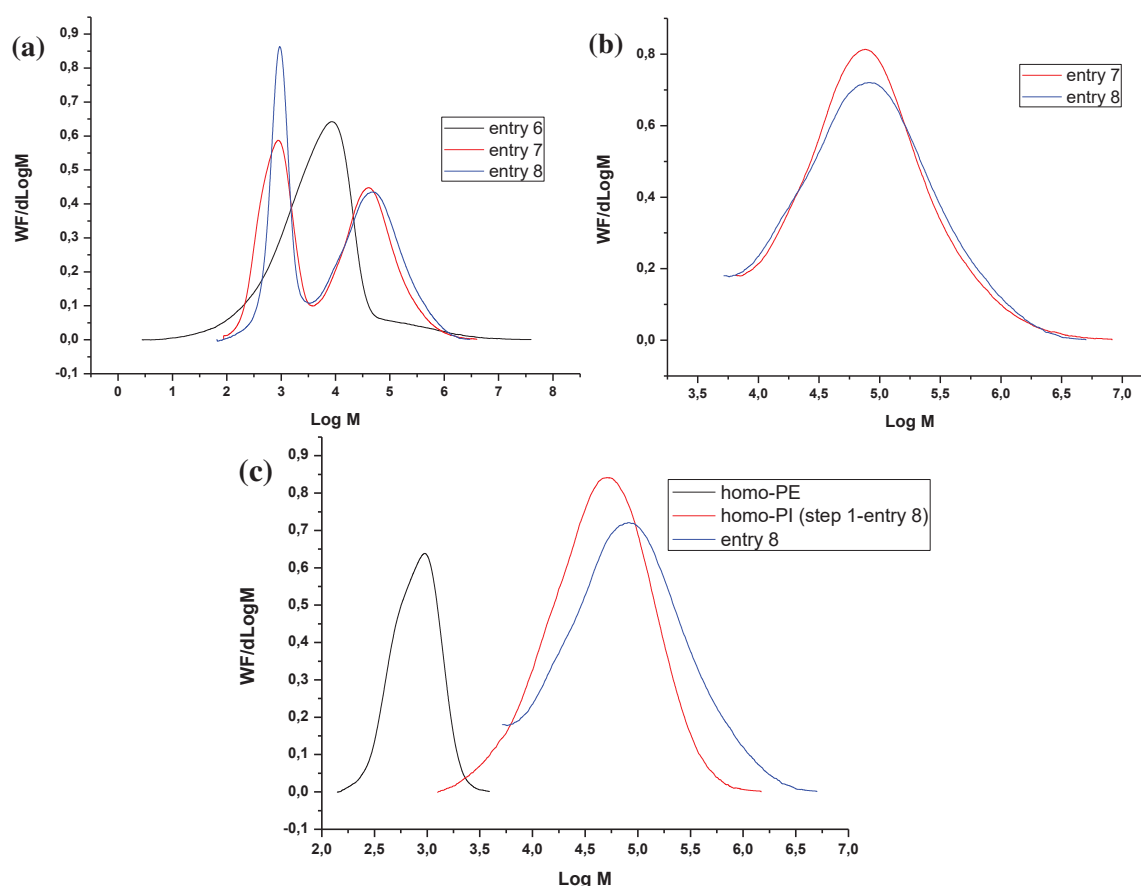


Figure 26. (a) Molar mass distribution of the block copolymers obtained from HT-SEC showing the existence of homo-PE; (b) Molar mass distribution of the block copolymers portions; (c) superimposition of the MWDs of the block copolymer produced in entry 8, the homo-PI produced in entry 8-step 1, and the homo-PE.

The molar mass distribution of the copolymer produced in entry 6 shows a uniform peak due to the low incorporation of PI where the SEC read both the copolymer and the homo-PE as a uniform peak (**Figure 26-(a)**); $M_n = 4100$ g/mol with a dispersity of 2.3.

Also, the superimposition of the molar mass distribution of the block copolymer produced in entry 8 with that of the homo-PI produced in entry 8-step 1 and that of the homo-PE is presented in **Figure 26-(c)**, showing the higher molar mass of the block copolymer with respect to that of the homo-PI. The molar mass of the homo-PI is equal to 23 300 g/mol with a dispersity of 3.2, while that of the block copolymer is equal to 38 100 with a dispersity of 4.7.

From DSC, The melting points of the block copolymers produced in entries 6, 7, and 8 are 130 °C, 131 °C, and 135 °C, respectively (**Figure 27**). The T_g of the PI produced in entry 8-step 1 is -46 °C (**Figure 27**). The T_g of the polymer produced in entry 6 didn't appear in its DSC (which is conducted at a temperature range from -90 °C till 180 °C) since the incorporation of isoprene in the polymer is low and thus the polymer thermal properties are similar to those of PE, therefore the T_g is around -100 °C. The T_g of the polymer produced in entry 7 is equal to -43 °C and that of the polymer produced in entry 8 is equal to -45 °C. Thus, the DSC of both copolymers produced in entries 7 and 8 show glass transitions similar to that of homo-PI (-46 °C) and a fusion behavior similar to that of PE (130-135 °C), therefore these block copolymers combine the thermal properties of both homo-polymers.

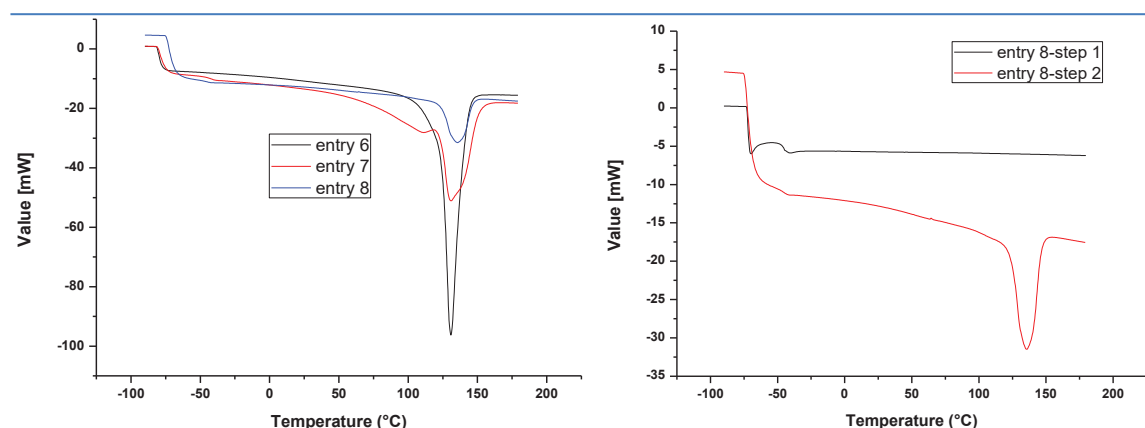


Figure 27. To the left: DSC peaks of the block copolymers. To the right: DSC peaks of the PI produced in entry 8-step 1 and the block copolymer produced in step 2.

Therefore, ethylene-isoprene chain shuttling random and block copolymerizations *via*

Fe-Al-Fe transmetallation reactions have been achieved. This success open the door for more sustainable and cheap production of such elastomers which could have several applications in tire manufacturing for instance.

D.7. Homo-Polymerizations of Ethylene and Isoprene in scCO_2

After what have been achieved from its utilization in ethylene radical polymerization processes, we tried to utilize CO_2 in catalytic polymerizations of ethylene and isoprene using the family of iron catalysts used in ethylene-isoprene chain shuttling copolymerization. In these reactions the role of CO_2 could be **1)** a neutral solvent (in which it could be used as an alternative to organic solvents), **2)** a deactivating solvent (in which it could act as a poison of the iron catalysts), **3)** a functionalization agent in ethylene or isoprene polymerization reactions through its activation by iron catalysts, **4)** a chain-end functionalization agent of PE or PI through its interaction with AlEt_3 (AlEt_3 is acting as a cocatalyst in these reactions), or **5)** a comonomer in ethylene or isoprene polymerization reactions (far goal).

D.7.1. Iron-Catalyzed Ethylene Polymerization in scCO_2

A primary test was done for iron-catalyzed ethylene polymerization in scCO_2 using catalyst **A** showed a negligible activity, thus we look for another iron catalyst from the same family which is more active than catalyst **A**.

As aforementioned, it has been proved that by increasing the steric hindrance around the Fe metal center the activity of the catalyst increases. Thus we chose the (2,6-diacetylpyridinebis(2,6-diisopropylanil)) FeCl_2 "catalyst **C**" (**Figure 28**) to test it in ethylene polymerization in scCO_2 .

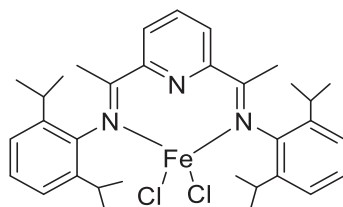


Figure 28. (2,6-diacetylpyridinebis(2,6-diisopropylanil)) FeCl_2 "catalyst **C**".

The polymerization reaction was done in the high-pressure reactor (160 mL reactor) under a pressure of 2 bar of ethylene and 100 bar of CO_2 at 70 °C. The catalyst (10 mg)

was dissolved in a co-solvent (5 mL of toluene) with tritylBARF (1 equiv.) and TEA (50 equiv.). In 1 hour, 0.3 g of polyethylene was produced which shows acceptable activity of the catalyst (the concentration of ethylene was only 2 bars in a 0.16 L reactor).

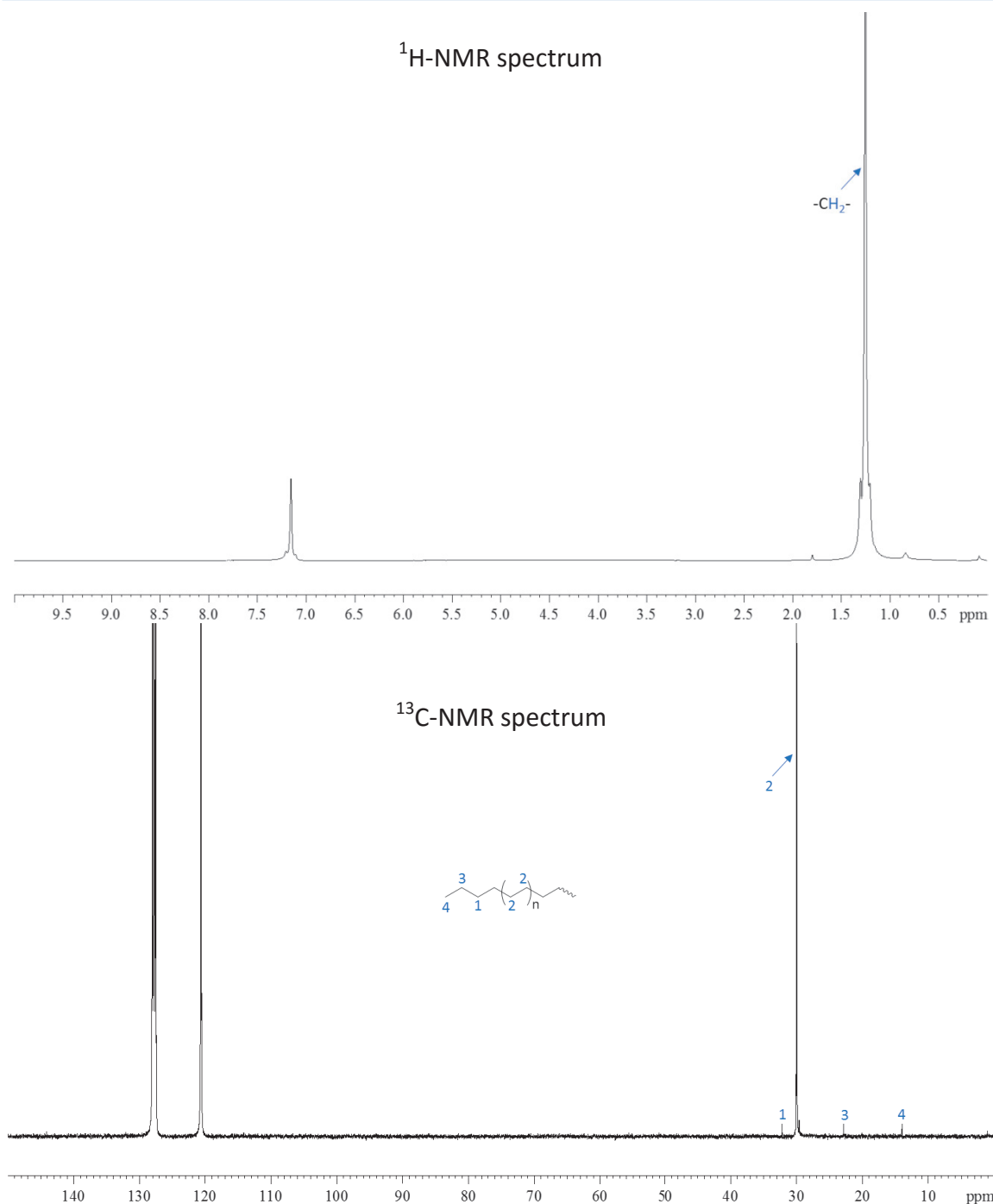


Figure 29. ^1H - and ^{13}C -NMR spectra of the polyethylene produced from the iron-catalyzed ethylene polymerization in scCO_2 .

The ^1H - and ^{13}C -NMR spectra of the polyethylene produced show that it is almost linear (**Figure 29**). The role of CO_2 in this reaction was only a polymerization medium

(neutral solvent) with no incorporation in the polymer chains, this incorporation is kinetically not favored as it has been explained in chapter I. But interestingly, the polymerization took place, suggesting that many ethylene insertions occurred before quenching by CO₂, which is prevalent when early transition metals such as Ti are used. End-chain characterization was difficult in this case however since the molar masses of the corresponding PE are too high.

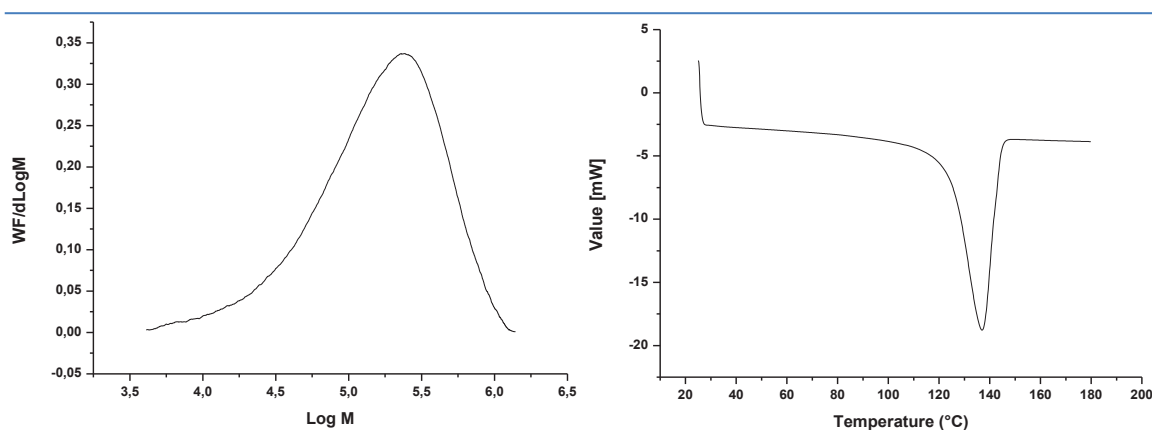


Figure 30. *To the left:* The molar mass distribution of the polyethylene produced by catalyst **C** in scCO₂. *To the right:* DSC peak of this polymer.

The SEC analysis of the polyethylene produced showed a $M_n = 95\,000$ g/mol with a dispersity of 2.8, which shows also that it is a HDPE (**Figure 30**). Catalyst **C** has been studied thoroughly in conventional ethylene polymerization processes (in organic solvents), it produces also polyethylene of high molar mass; for example, Williams et al. obtained from catalyst **C** a polyethylene of $M_n = 64\,000$ g/mol and dispersity = 9.5.⁸³

The DSC gave a melting point of 137 °C for the polymer produced (**Figure 30**).

Another catalyst producing PE of lower molar masses than those of the PE produced by catalyst **C** and exhibiting high enough activity (higher than that of catalyst **A**) must be tested.

D.7.2. Iron-Catalyzed Isoprene Polymerization in scCO₂

The polymerization of isoprene in scCO₂ using catalyst **B** was tested successfully. The polymerization reaction was done in the high-pressure reactor under a 100-bar pressure of CO₂ at room temperature. The catalyst (10 mg) was dissolved in a co-solvent (5 mL of toluene) with tritylBARF (1 equiv.) and TEA (50 equiv.); 10 mL of isoprene was added. In 2

hours, polyisoprene was produced with an approximate yield of about 15 %. This could be improved by increasing the reaction time.

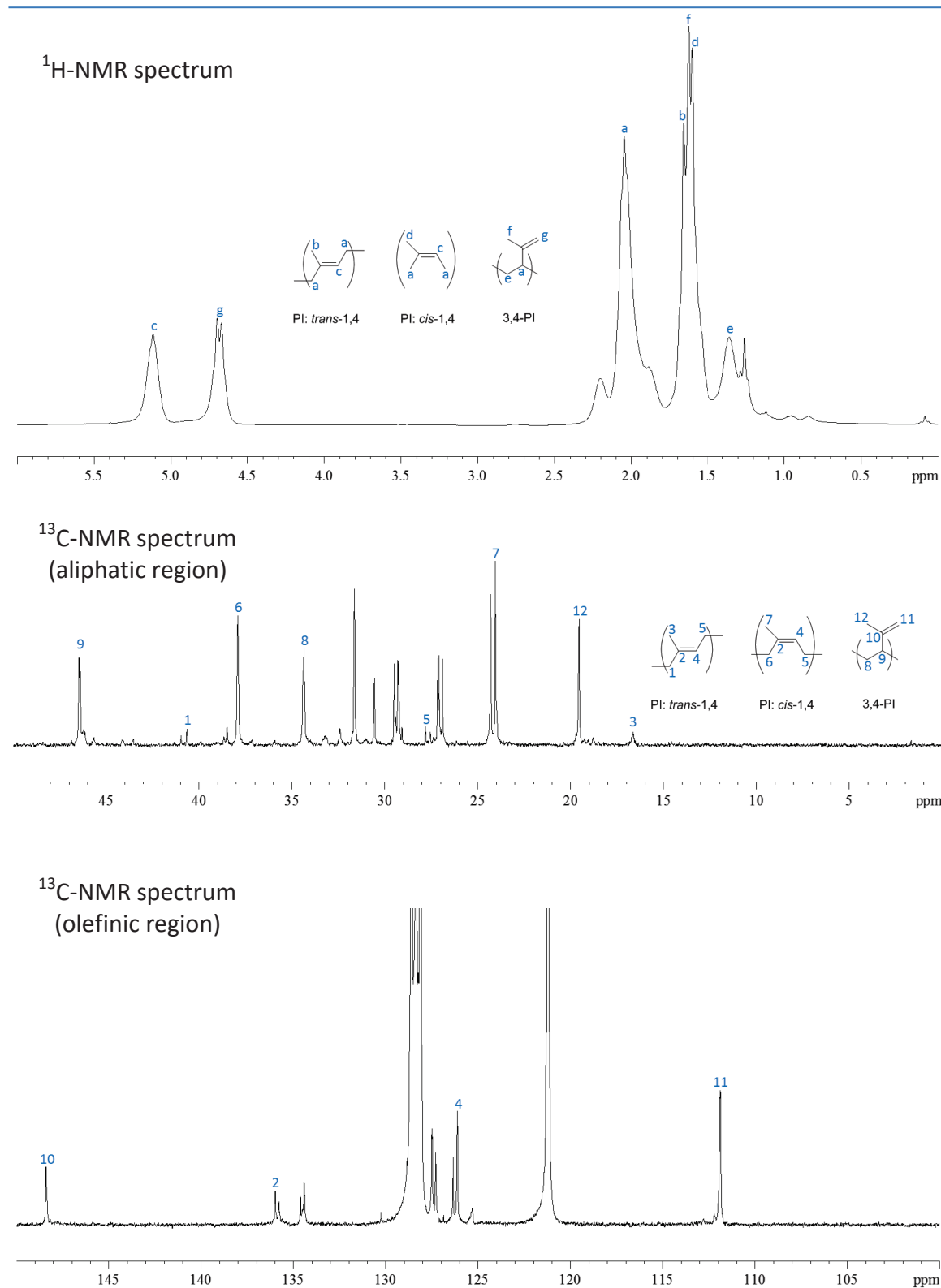


Figure 31. ¹H- and ¹³C-NMR spectra of the polyisoprene produced by catalyst B in scCO₂.

The ^1H - and ^{13}C -NMR spectra show the production of polyisoprene in its different microstructures with the following percentages: 8.2 % of *trans*-1,4-PI, 48.1 % of *cis*-1,4-PI, and 43.7 % of 3,4-PI. The composition of the polyisoprene produced in CO_2 is different from that of the polyisoprene produced in a conventional polymerization (in toluene) by its lower *trans*-1,4-PI percentage and higher *cis*-1,4-PI and 3,4-PI percentages (percentages in conventional polymerization: *trans*-1,4-PI= 21.8 %, *cis*-1,4-PI= 39.5 %, and 3,4-PI= 38.7 %).

The SEC analysis gave a molar mass of 37 300 g/mol with a dispersity of 3.3 for the polyisoprene produced (**Figure 32**). This M_n is slightly higher than that of the polyisoprene produced in the conventional polymerization (29 000 g/mol) with almost the same dispersity (3.2).

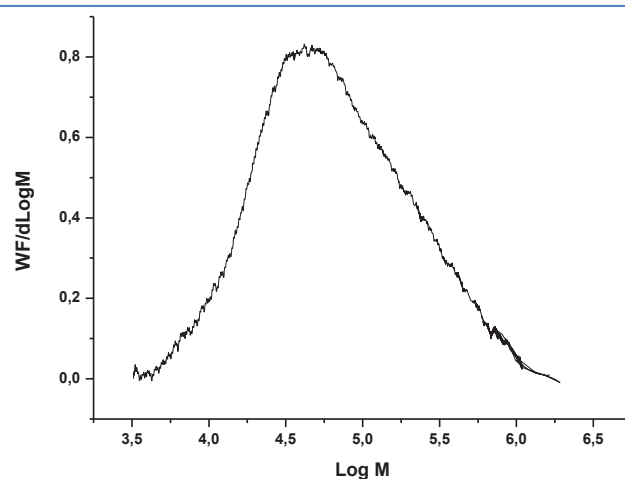


Figure 32. Molar mass distribution of the polyisoprene produced by catalyst B in scCO_2 .

Therefore, it is possible to polymerize ethylene and isoprene in scCO_2 as an alternative to organic solvents, CO_2 act as a neutral solvent in these catalytic polymerizations. Developments of these strategies benefiting from the relative reactivities of Fe-C bonds towards either insertion of CO_2 or of an olefin/diene, seemingly in favor of the latter, could rejuvenate the use of Fe catalysis to make valuable polymers and copolymers in scCO_2 , limiting the use of organic solvents.

Further investigations will be done on iron-catalyzed polymerizations of olefins in scCO_2 to improve the yields and understand the mechanisms of deactivation. In addition, the studies will continue towards adjusting the sterics and electronics of Fe complexes to modulate CO_2 -insertion kinetics and hope for an incorporation within the

polymer chains using these catalytic processes.

D.8. Conclusion

This chapter is comprised of two parts. In the first part, the copolymerization of ethylene and isoprene *via* an iron-catalyzed chain shuttling polymerization process has been investigated thoroughly. In this method, a dual-catalyst process was applied in order to synthesize ethylene-isoprene copolymers using two iron complexes, each one is exclusively active in the polymerization of a specific monomer. By varying the procedure, either a random or a block copolymer was produced. The produced copolymers were analyzed extensively by NMR analysis, 1D (^1H - and ^{13}C -NMR) and 2D (HSQC, HMBC, and DOSY), to assure the synthesis of the copolymers and study their microstructure.

The second part represents tests in polymerizing ethylene and isoprene in scCO_2 using their corresponding dedicated iron catalysts. These tests showed a primary success, which will form the basis for exchanging petro-based organic solvents with CO_2 in iron-catalyzed olefin polymerizations, with the agenda of end-functionalizing the produced polymers.

This work requires further investigations in order to achieve activities comparable to those in the conventional iron-catalyzed polymerization. They probably require fine tuning of the catalysts' sterics and electronics to improve polymerization over termination if increased yield is targeted or enhance reactivity with respect to CO_2 if functionalization is preferred.

D.9. References

- Arriola, D. J.; Carnahan, E. M.; Hustad, P. D.; Kuhlman, R. L.; Wenzel, T. T. *Science* **2006**, *312*, 714-718.
- Valente, A.; Mortreux, A.; Visseaux, M.; Zinck, P. *Chem. Rev.* **2013**, *113*, 3836-3857.
- Wang, H. P.; Khariwala, D. U.; Cheung, W.; Chum, S. P.; Hiltner, A.; Baer, E. *Macromolecules* **2007**, *40*, 2852-2862.
- Khariwala, D. U.; Taha, A.; Chum, S. P.; Hiltner, A.; Baer, E. *Polymer* **2008**, *49*, 1365-1375.
- Wei, J.; Zhang, W.; Wickham, R.; Sita, L. R. *Angew. Chem., Int. Ed.* **2010**, *49*, 9140-9144.
- Bruaseth, I.; Rytter, E. *Macromolecules* **2003**, *36*, 3026-3034.
- Pan, L.; Zhang, K.; Nishiura, M.; Hou, Z. *Angew. Chem.* **2011**, *50*, 12012-12016.
- Zhang, H.; Luo, Y.; Hou, Z. *Macromolecules* **2008**, *41*, 1064-1066.
- Zhang, L.; Luo, Y.; Hou, Z. *J. Am. Chem. Soc.* **2005**, *127*, 14562-14563.
- Liu, B.; Cui, D. *Macromolecules* **2016**, *49*, 6226-6231.
- Phuphuak, Y.; Bonnet, F.; Stoclet, G.; Bria, M.; Zinck, P. *Chem. Commun.* **2017**, *53* (38), 5330-5333.
- Xiao, A.; Wang, L.; Liu, Q.; Yu, H.; Wang, J.; Huo, J.; Tan, Q.; Ding, J.; Ding, W.; Amin, A. M. *Macromolecules* **2009**, *42*, 1834-1837.
- Kerber, R. C. *J. Organomet. Chem.* **1992**, *422* (1-3), 209-299.
- Fatiadi, A. J. *J. Res. Natl. Inst. Stand. Technol.* **1991**, *96* (1), 1-113.
- Paley, R. S. Iron: Organometallic Chemistry. In *Encyclopedia of Inorganic and Bioinorganic Chemistry*; John Wiley & Sons, Ltd, 2011.
- Bauer, I.; Knölker, H.-J. *Chem. Rev.* **2015**, *115* (9), 3170-3387.
- Fürstner, A. *ACS Cent. Sci.* **2016**, *2* (11), 778-789.
- Small, B. L.; Brookhart, M.; Bennett, A. M. *J. Am. Chem. Soc.* **1998**, *120* (16), 4049-4050.
- Small, B. L.; Brookhart, M. *J. Am. Chem. Soc.* **1998**, *120* (28), 7143-7144.
- Britovsek, G. J. P.; Gibson, V. C.; McTavish, S. J.; Solan, G. A.; White, A. J. P.; Williams, D. J.; Britovsek, G. J. P.; Kimberley, B. S.; Maddox, P. J. *Chem. Commun.* **1998**, *0* (7), 849-850.
- Bolm, C.; Legros, J.; Le Paih, J.; Zani, L. *Chem. Rev.* **2004**, *104*, 6217.
- Bianchini, C.; Giambastiani, G.; Rios, I. G.; Mantovani, G.; Meli, A.; Segarra, A. M. *Coord. Chem. Rev.* **2006**, *250*, 1391.
- Bianchini, C.; Giambastiani, G.; Luconi, L.; Meli, A. *Coord. Chem. Rev.* **2010**, *254*, 431.
- Gibson, V. C.; Redshaw, C.; Solan, G. A. *Chem. Rev.* **2007**, *107*, 1745.
- Gibson, V. C.; Solan, G. A. In *Catalysis without Precious Metals*; Bullock, R. M., Ed.; Wiley-VCH: Weinheim, Germany, 2010; p 111.
- Li, L.; Gomes, P. T. In *Olefin Upgrading Catalysis by Nitrogen-based Metal Complexes II*; Campora, J., Giambastiani, G., Eds.; Springer: Dordrecht, Netherlands, 2011; Vol. 36, p 77.
- Bézier, D.; Sortais, J.-B.; Darcel, C. *Adv. Synth. Catal.* **2013**, *355*, 19.
- Zhang, W.; Sun, W.-H.; Redshaw, C. *Dalton Trans.* **2013**, *42*, 8988.
- Boudier, A.; Breuil, P.-A. R.; Magna, L.; Olivier-Bourbigou, H.; Braunstein, P. *Chem. Commun.* **2014**, *50*, 1398.
- Deng, L.; Margl, P.; Ziegler, T. *J. Am. Chem. Soc.* **1999**, *121* (27), 6479-6487.
- Britovsek, G. J. P.; Cohen, S. A.; Gibson, V. C.; Maddox, P. J.; van Meurs, M. *Angew. Chem., Int. Ed.* **2002**, *41*, 489.
- Britovsek, G. J. P.; Cohen, S. A.; Gibson, V. C.; van Meurs, M. *J. Am. Chem. Soc.* **2004**, *126*, 10701.
- Bouwkamp, M. W.; Lobkovsky, E.; Chirik, P. J. *J. Am. Chem. Soc.* **2005**, *127*, 9660.
- Kaul, F. A. R.; Puchta, G. T.; Frey, G. D.; Herdtweck, E.; Herrmann, W. A. *Organometallics* **2007**, *26*, 988.
- Small, B. L.; Rios, R.; Fernandez, E. R.; Carney, M. J. *Organometallics* **2007**, *26*, 1744.
- Small, B. L.; Rios, R.; Fernandez, E. R.; Gerlach, D. L.; Halfen, J. A.; Carney, M. J. *Organometallics* **2010**, *29*, 6723.
- Wallenhorst, C.; Kehr, G.; Luftmann, H.; Fröhlich, R.; Erker, G. *Organometallics* **2008**, *27*, 6547.
- Zhang, W.; Chai, W.; Sun, W.-H.; Hu, X.; Redshaw, C.; Hao, X. *Organometallics* **2012**, *31*, 5039.
- Zhang, D.; Zhang, Y.; Hou, W.; Guan, Z.; Huang, Z. *Organometallics* **2017**, *36* (19), 3758-3764.
- Kawakami, T.; Ito, S.; Nozaki, K. *Dalton Trans.* **2015**, *44* (47), 20745-20752.
- Bolm, C.; Legros, J.; Le Paih, J.; Zani, L. *Chem. Rev.* **2004**, *104*, 6217-6254.
- Correa, A.; Garcia Mancheno, O.; Bolm, C. *Chem. Soc. Rev.* **2008**, *37*, 1108-1117.

43. Riener, K.; Haslinger, S.; Raba, A.; Högerl, M. P.; Cokoja, M.; Herrmann, W. A.; Kühn, F. E. *Chem. Rev.* **2014**, *114*, 5215–5272.
44. Zhang, Z. Y.; Zhang, H. J.; Ma, H. M.; Wu, Y. J. *Mol. Catal.* **1982**, *17* (1), 65–76.
45. Bazzini, C.; Giarrusso, A.; Porri, L. *Macromol. Rapid Commun.* **2002**, *23* (15), 922–927.
46. Ricci, G.; Sommazzi, A.; Masi, F.; Ricci, M.; Boglia, A.; Leone, G. *Coord. Chem. Rev.* **2010**, *254* (5), 661–676.
47. De, S. K.; White, J. R. *Rubber Technologist's Handbook*; Smithers Rapra Technology Limited: Shawbury, U.K., 2001.
48. McNeill, E.; Ritter, T. *Acc. Chem. Res.* **2015**, *48* (8), 2330–2343.
49. Raynaud, J.; Wu, J. Y.; Ritter, T. *Angew. Chem., Int. Ed.* **2012**, *51*, 11805–11808.
50. Luo, L.; Kang, X.; Zhou, G.; Chen, S.; Luo, G.; Qu, J.; Luo, Y. *Int. J. Quantum Chem.* **2016**, *116* (17), 1274–1280.
51. Zhiqian, S.; Jun, O.; Fusong, W.; Zhenya, H.; Fusheng, Y.; Baogong, Q. *J. Polym. Sci. Polym. Chem. Ed.* **1980**, *18* (12), 3345–3357.
52. Evans, W. J.; Giarikos, D. G.; Ziller, J. W. *Organometallics* **2001**, *20* (26), 5751–5758.
53. Evans, W. J.; Giarikos, D. G. *Macromolecules* **2004**, *37* (13), 5130–5132.
54. Fischbach, A.; Klimpel, M. G.; Widenmeyer, M.; Herdtweck, E.; Scherer, W.; Anwender, R. *Angew. Chem. Int. Ed.* **2004**, *43* (17), 2234–2239.
55. Kaita, S.; Doi, Y.; Kaneko, K.; Horiuchi, A. C.; Wakatsuki, Y. *Macromolecules* **2004**, *37* (16), 5860–5862.
56. Arndt, S.; Beckerle, K.; Zeimentz, P. M.; Spaniol, T. P.; Okuda, J. *Angew. Chem. Int. Ed.* **2005**, *44* (45), 7473–7477.
57. Ajellal, N.; Furlan, L.; Thomas, C. M.; Casagrande, O. L.; Carpentier, J.-F. *Macromol. Rapid Commun.* **2006**, *27* (5), 338–343.
58. Zhang, L.; Suzuki, T.; Luo, Y.; Nishiura, M.; Hou, Z. *Angew. Chem. Int. Ed.* **2007**, *46* (11), 1909–1913.
59. Gao, W.; Cui, D. *J. Am. Chem. Soc.* **2008**, *130* (14), 4984–4991.
60. Jian, Z.; Cui, D.; Hou, Z.; Li, X. *Chem. Commun.* **2010**, *46* (17), 3022–3024.
61. Liu, S.; Du, G.; He, J.; Long, Y.; Zhang, S.; Li, X. *Macromolecules* **2014**, *47* (11), 3567–3573.
62. Bonnet, F.; Visseaux, M.; Pereira, A.; Barbier-Baudry, D. *Macromolecules* **2005**, *38* (8), 3162–3169.
63. Zimmermann, M.; Törnroos, K. W.; Anwender, R. *Angew. Chem. Int. Ed.* **2008**, *47* (4), 775–778.
64. Yang, Y.; Lv, K.; Wang, L.; Wang, Y.; Cui, D. *Chem. Commun.* **2010**, *46* (33), 6150–6152.
65. Liu, H.; He, J.; Liu, Z.; Lin, Z.; Du, G.; Zhang, S.; Li, X. *Macromolecules* **2013**, *46* (9), 3257–3265.
66. Ricci, G.; Battistella, M.; Porri, L. *Macromolecules* **2001**, *34* (17), 5766–5769.
67. Zhang, L.; Luo, Y.; Hou, Z. *J. Am. Chem. Soc.* **2005**, *127* (42), 14562–14563.
68. Du, G.; Wei, Y.; Ai, L.; Chen, Y.; Xu, Q.; Liu, X.; Zhang, S.; Hou, Z.; Li, X. *Organometallics* **2011**, *30* (1), 160–170.
69. Suminoe, T. *Chem. high Polymers Tokyo* **1963**, *20*, 467. Or Suminoe, T. *Kobunshi Kagaku* **1963**, *20*, 467–471.
70. Falk, J. C.; Schlott, R. J. *Angew. Makromol. Chem.* **1972**, *21* (1), 17–23.
71. Rodrigues, A. S.; Kirillov, E.; Vuillemin, B.; Razavi, A.; Carpentier, J. F. *Polymer* **2008**, *49*, 2039.
72. Li, X.; Nishiura, M.; Hu, L.; Mori, K.; Hou, Z. *J. Am. Chem. Soc.* **2009**, *131* (38), 13870–13882.
73. Capacchione, C.; Saviello, D.; Avagliano, A.; Proto, A. *J. Polym. Sci. Part Polym. Chem.* **2010**, *48* (19), 4200–4206.
74. Chenal, T.; Visseaux, M. *Macromolecules* **2012**, *45* (14), 5718–5727.
75. Du, G.; Xue, J.; Peng, D.; Yu, C.; Wang, H.; Zhou, Y.; Bi, J.; Zhang, S.; Dong, Y.; Li, X. *J. Polym. Sci. Part Polym. Chem.* **2015**, *53* (24), 2898–2907.
76. Hu, X.; Kang, X.; Zhou, G.; Wang, X.; Hou, Z.; Luo, Y. *Chin. J. Chem.* **2017**, *35* (5), 723–732.
77. Britovsek, G. J. P.; Bruce, M.; Gibson, V. C.; Kimberley, B. S.; Maddox, P. J.; Mastroianni, S.; McTavish, S. J.; Redshaw, C.; Solan, G. A.; Strömberg, S.; et al. *J. Am. Chem. Soc.* **1999**, *121* (38), 8728–8740.
78. Han, C. J.; Lee, M. S.; Byun, D.-J.; Kim, S. Y. *Macromolecules* **2002**, *35* (24), 8923–8925.
79. Sun, J.; Wang, F.; Li, W.; Chen, M. *RSC Adv.* **2017**, *7* (87), 55051–55059.
80. Gao, W.; Cui, D. *J. Am. Chem. Soc.* **2008**, *130*, 4984.
81. Zimmermann, M.; Törnroos, K. W.; Anwender, R. *Angew. Chem., Int. Ed.* **2008**, *47*, 775.
82. Zhang, L.; Nishiura, M.; Yuki, M.; Luo, Y.; Hou, Z. *Angew. Chem., Int. Ed.* **2008**, *47*, 2642.
83. Britovsek, G. J. P.; Bruce, M.; Gibson, V. C.; Kimberley, B. S.; Maddox, P. J.; Mastroianni, S.;

Chapter IV

McTavish, S. J.; Redshaw, C.; Solan, G. A.; Strömberg, S.; et al. *J. Am. Chem. Soc.* **1999**, *121* (38), 8728–8740.

E. Experimental Part.

Table of Contents

E.1. Experimental Section of Chapter II	247
E.1.1. Polymerization Method in Supercritical CO ₂	247
E.1.2. Polymerization Method in Dimethylcarbonate	248
E.2. Experimental Section of Chapter III	249
E.2.1. Conventional Ethylene Free Radical Polymerization	249
E.2.2. Polymerization Method of Ethylene Radical Polymerization in Presence of Triethylaluminum	249
E.2.2.1. Quenching the Polymerization Reaction by Iodine	250
E.2.3. Polymerization Method of Ethylene Radical Polymerization in scCO ₂ in Presence of Triethylaluminum	250
E.2.4. Hydrolysis of the CO ₂ -Functionalized Polyethylene	251
E.3. Experimental Section of Chapter IV	251
E.3.1. Synthesis of Iron Complexes	251
E.3.1.1. Synthesis of Catalysts A and C	251
E.3.1.2. Synthesis of Catalyst B	253
E.3.2. Homo-Polymerization of Ethylene Using Catalyst A	254
E.3.3. Homo-Polymerization of Isoprene Using Catalyst B	254
E.3.4. Ethylene-Isoprene Copolymerization Test Using Catalyst A	254
E.3.5. Copolymerization Test Using Catalyst B	255
E.3.6. Ethylene-Isoprene Chain Shuttling Random Copolymerization	255
E.3.7. Ethylene-Isoprene Chain Shuttling Block Copolymerization	256
E.3.8. Iron-Catalyzed Ethylene Polymerization in scCO ₂	256
E.3.9. Iron-Catalyzed Isoprene Polymerization in scCO ₂	257

E.4. Analytical Methods	258
E.4.1. Nuclear Magnetic Resonance (NMR)	258
E.4.2. Size-Exclusion Chromatography (SEC)	258
E.4.3. Differential Scanning Calorimetry (DSC)	258
E.4.4. Fourier Transform Infrared Spectroscopy (FTIR)	259
E.4.5. Electron Paramagnetic Resonance (EPR)	259

All chemicals were handled using standard Schlenk procedures under argon atmosphere. Organic solvents were distilled or dried and degassed under argon. Heptane and toluene were dried by MBRAUN Solvent Purification Systems (MB-SPS) which operate by pushing the solvents through a series of drying columns resulting in moisture levels down to the ppm range. Any other solvents used were dried over CaH_2 and distilled.

Ethylene (purity 99.95%) and CO_2 (purity 99.95%) were purchased from "Air Liquide" and used without any further purification. Isoprene was purchased from "Sigma-Aldrich" and dried over CaH_2 . Radical initiators, AIBN and lauroyl peroxide, were purchased from "Acros", and benzoyl peroxide from "Fluka", and used without any further purification.

Syntheses of catalysts were performed under inert atmosphere and products are stored in a glove box.

CAUTION: *Most of the polymerizations involve high pressures and explosive gas (ethylene).*

E.1. Experimental Section of Chapter II

E.1.1. Polymerization Method in Supercritical CO_2

All experiments are done in a 160 mL high-pressure reactor from "PARR INSTRUMENT COMPANY", connected to a main ballast (1.5 L) which in role is connected to two intermediate ballasts 2 L each, one for ethylene and the other for CO_2 . The main ballast is used for condensation of gases to get high pressures up to 340 bars; the temperature varies in the ballast *via* oil circulation using an oil bath from "LAUDA", the oil has a temperature range from $-60\text{ }^\circ\text{C}$ to $80\text{ }^\circ\text{C}$. Heating the reactor is done using another oil bath from "JULABO" with an oil of temperature range from $30\text{ }^\circ\text{C}$ to $200\text{ }^\circ\text{C}$; all the apparatus details are presented in chapter II.

In each reaction, 0.3 mmol (50 mg) of the initiator is added into the reactor, then the reactor is closed and set under vacuum for 15 min. After that, the reactor temperature is set at $35\text{ }^\circ\text{C}$ for AIBN- and lauroyl peroxide-initiated reactions, and at $45\text{ }^\circ\text{C}$ for benzoyl peroxide-initiated reactions.

After condensing ethylene in the main ballast (42 bar at $-20\text{ }^\circ\text{C}$ to obtain 200 bar at 20

°C), the reactor is pressurized by this supercritical ethylene (110 bar for AIBN- and lauroyl peroxide-initiated reactions; 90 bar for benzoyl peroxide-initiated reactions). Next, the main ballast is depressurized, evacuated, and pressurized by CO₂ which is condensed to achieve high pressure (39 bar at -20 °C to obtain 200 bar at 20 °C). Then, the reactor is pressurized with CO₂, and the temperature is set at 70 °C for AIBN- and lauroyl peroxide-initiated reactions and at 90 °C for benzoyl peroxide-initiated reactions. Each reaction lasts for 3 hours after CO₂ addition. The stirrer is set at 600 rpm.

At the end of the reaction, the reactor is cooled *via* a cold water line and depressurized slowly through the depressurizing valve connected to a central fume hood. A dry white polyethylene is obtained (**Figure 1**). The obtained polyethylene is washed with methanol, then filtered and dried during 4 hours in a vacuum oven at 70 °C.



Figure 1. Dry polyethylene obtained from ethylene free radical polymerization in scCO₂.

E.1.2. Polymerization Method in Dimethylcarbonate

All experiments are done in the 160 mL high-pressure reactor.

In a Schlenk (100 mL), 0.3 mmol of the initiator is added, the Schlenk is dried under vacuum for 10 min. Then, under argon atmosphere, 50 mL of dimethylcarbonate "DMC" (dried over molecular sieves) is added using cannula. All initiators are readily soluble in DMC.

The reactor is closed and set under vacuum for 15 min. Then, under argon, the initiator/DMC solution is transferred using a cannula into the reactor through the inlet chamber. After that, the reactor temperature is set at 35 °C for AIBN- and lauroyl peroxide-initiated reactions, and at 45 °C for benzoyl peroxide-initiated reactions.

After condensing ethylene in the main ballast, the reactor is pressurized by this

supercritical ethylene (110 bar for AIBN- and lauroyl peroxide-initiated reactions; 90 bar for benzoyl peroxide-initiated reactions). Then, the reactor temperature is set at 70 °C for AIBN- and lauroyl peroxide-initiated reactions, and at 90 °C for benzoyl peroxide-initiated reactions (the pressure in the reactor reached \approx 200 bar). Each reaction lasts for 3 hours after pressurizing the reactor with ethylene. The stirrer is set at 600 rpm.

At the end of the reaction, the reactor is cooled *via* a cold water line and depressurized slowly through the depressurizing valve connected to a central fume hood. The obtained polyethylene is washed with methanol, then filtered and dried during 5 hours in a vacuum oven at 70 °C.

E.2. Experimental Section of Chapter III

E.2.1. Conventional Ethylene Free Radical Polymerization

The AIBN initiator (0.6 mmol; 100 mg) is added into the high-pressure reactor, then the reactor is closed and stripped from air and moisture. Then, under argon, 50 mL of dry heptane is added by a cannula into the reactor through the inlet chamber. This way is used because of the difficult direct solubilization of AIBN in heptane.

After that, the reactor temperature is set at 90 °C and pressurized by 200 bar of ethylene after condensing ethylene in the main ballast (42 bar at -20 °C to obtain 200 bar at 20 °C). The reaction lasts for 3 hours after ethylene addition. The stirrer is set at 600 rpm.

At the end of the reaction, the reactor is cooled *via* a cold water line and depressurized slowly through the depressurizing valve connected to a central fume hood. The obtained polyethylene is washed with methanol, then filtered and dried during 5 hours in a vacuum oven at 70 °C.

E.2.2. Polymerization Method of Ethylene Radical Polymerization in Presence of Triethylaluminum

In a 100 mL Schlenk, a 1 M solution of triethylaluminum (TEA) in heptane (50 mL) is prepared carefully under inert atmosphere.

In another Schlenk (100 mL), the desired amount of AIBN is added, and the Schlenk is

dried under vacuum for 10 min. Next, under argon atmosphere, 50 mL of dry heptane and the desired amount of TEA are added into the Schlenk. Then, the AIBN/heptane/TEA solution is stirred for 10 min, a pale yellow solution is obtained (the depth of the solution increases by increasing the amount of TEA). AIBN become soluble in heptane in presence of TEA.

The reactor is closed and set under vacuum for 10 min. Then, under argon, the AIBN/heptane/TEA solution is transferred using a cannula into the reactor through the inlet chamber. After that, the temperature is set at 90 °C, and the reactor is pressurized by 200 bar of ethylene after condensing ethylene in the main ballast (42 bar at -20 °C to obtain 200 bar at 20 °C). Each reaction lasts for the desired time after pressurizing the reactor by ethylene. The stirrer is set at 600 rpm.

At the end of the reaction, the reactor is cooled *via* a cold water line and depressurized slowly through the depressurizing valve connected to a central fume hood. The obtained polyethylene is washed with water, then filtered and dried during 5 hours in a vacuum oven at 70 °C.

E.2.2.1. Quenching the Polymerization Reaction by Iodine

After the passage of the desired time (3 hours) of the reaction of ethylene radical polymerization in presence of TEA, the reactor is depressurized from ethylene slowly till a pressure of 1 bar (to avoid any entrance of air into the reactor). Then, the argon valve is opened to purge all the remaining ethylene. After that, 2 equiv. of I₂ (with respect to TEA) are introduced into the reactor under argon atmosphere, and the reaction lasts for extra 1 hour.

At the end of the reaction, the reactor is cooled *via* a cold water line and depressurized slowly through the depressurizing valve connected to a central fume hood. The obtained polymer is washed with methanol, then filtered and dried during 5 hours in a vacuum oven at 70 °C.

E.2.3. Polymerization Method of Ethylene Radical Polymerization in scCO₂ in Presence of Triethylaluminum

In a Schlenk (100 mL), 0.6 mmol of AIBN is added, and the Schlenk is dried under

vacuum for 10 min. Then, under argon atmosphere, 50 mL of dry heptane and 5 equiv. of TEA (with respect to AIBN) are added into the Schlenk. The AIBN/heptane/TEA solution is stirred for 10 min, a pale yellow solution is obtained.

The reactor is closed and set under vacuum for 15 min. Then, under argon, the AIBN/heptane/TEA solution is transferred using a cannula into the reactor through the inlet chamber. After that, the reactor temperature is set at 70 °C.

After condensing a 1:1 mixture of CO₂/ethylene in the main ballast, the reactor is pressurized by 250 bar (at 70 °C) of this mixture. The stirrer is set at 600 rpm and the reaction lasts for 3 hours.

At the end of the reaction, the reactor is cooled *via* a cold water line and depressurized slowly through the depressurizing valve connected to a central fume hood. The obtained polymer is washed with methanol, then filtered and dried during 3 hours in a vacuum oven at 70 °C.

E.2.4. Hydrolysis of the CO₂-Functionalized Polyethylene

A sample (0.3 g) of the polymer obtained from the reaction of ethylene radical polymerization in scCO₂ in presence of TEA is added into a Schlenk. Then, 10 mL of a solution of hydrochloric acid (35 %) and 70 mL of distilled H₂O are added. The Schlenk is heated at 60 °C for 5 hours. Then, the polymer is filtered and dried during 5 hours in a vacuum oven at 70 °C.

E.3. Experimental Section of Chapter IV

E.3.1. Synthesis of Iron Complexes

The synthesis of the used complexes is well known in the literature, one of the papers that mentioned this synthesis in details is : "Britovsek, G. J. P.; Bruce, M.; Gibson, V. C.; Kimberley, B. S.; Maddox, P. J.; Mastroianni, S.; McTavish, S. J.; Redshaw, C.; Solan, G. A.; Strömberg, S.; et al. *J. Am. Chem. Soc.* **1999**, *121* (38), 8728–8740."

Here, we will mention the general synthesis of these complexes.

E.3.1.1. Synthesis of Catalysts A and C

Synthesis of ligands: To a solution of 2,6-diacetylpyridine in absolute ethanol are added

2 equiv. of 2,6-dimethylaniline (*for ligand of catalyst A*) or 2,6-diisopropylaniline (*for ligand of catalyst C*). After the addition of a few drops of glacial acetic acid, the solution is refluxed overnight at 130 °C with azeotropic removal of water using a Dean-Stark trap. Upon cooling to room temperature, the product crystallized from the solvent (yellow crystals). After filtration, the yellow powder is washed with pentane in order to remove the excess of 2,6-diacetylpyridine (^1H -NMR analysis is done after each wash to check the neatness of the ligand). Then, the product is dried under vacuum to give the corresponding ligand with a yield of approximately 80% (**Scheme 1**).

Ligand of catalyst A: 2,6-diacetylpyridinebis(2,6-dimethylanil).

Ligand of catalyst C: 2,6-diacetylpyridinebis(2,6-diisopropylanil).

Scheme 1. Synthesis of the bis(imino)pyridine ligands.

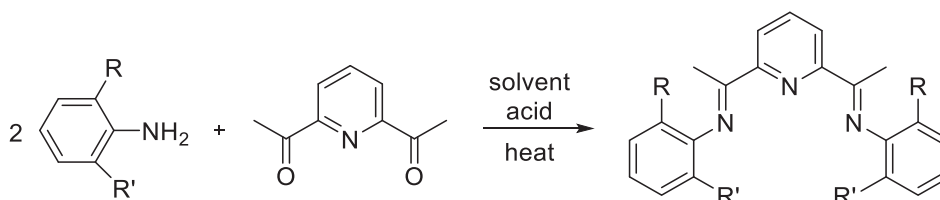


Figure 2 shows the proton NMR spectrum of the 2,6-diacetylpyridinebis(2,6-diisopropylanil) ligand as an example.

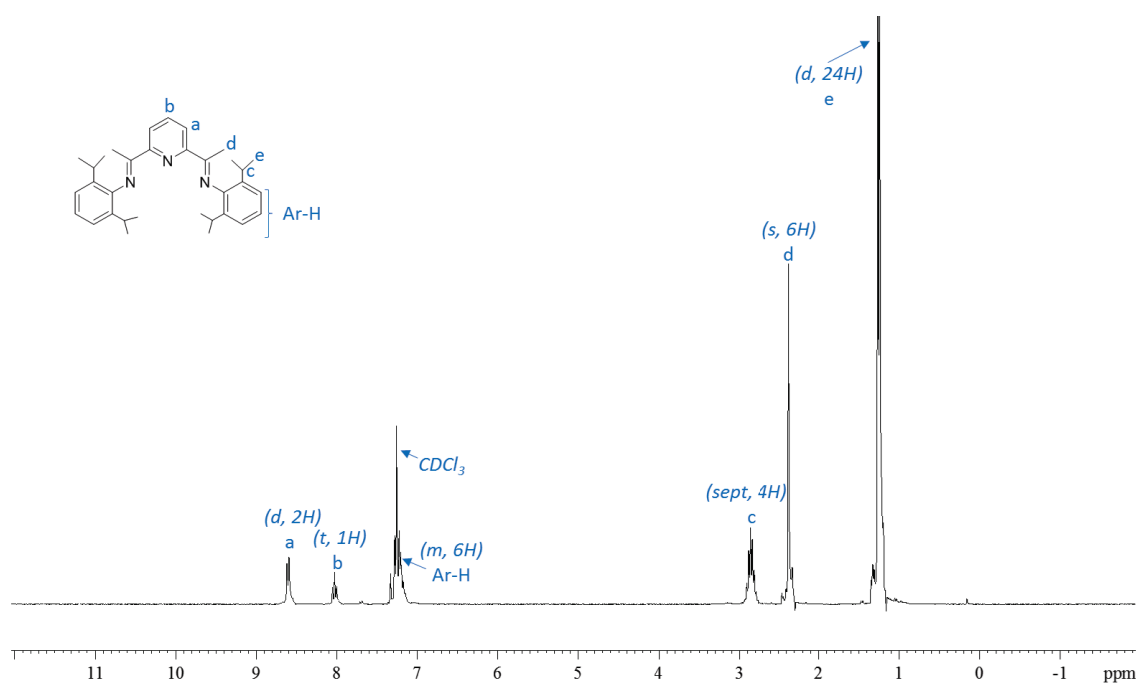
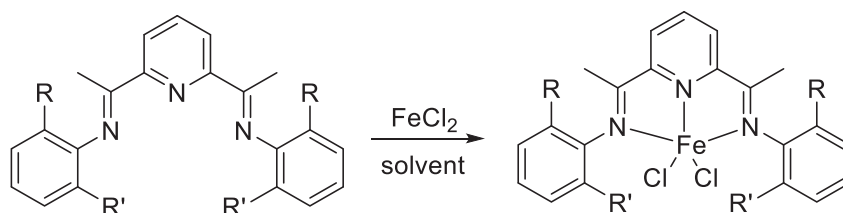


Figure 2. ^1H -NMR spectrum of the 2,6-diacetylpyridinebis(2,6-diisopropylanil) ligand.

Synthesis of the complex: Under inert atmosphere, a solution of the ligand in dichloromethane is added to FeCl₂ beads (99.99% purity) with a 1:1 mixture. The mixture is stirred for one week (**Scheme 2**). Then, the solution is filtered, dried under vacuum, and then washed by diethyl ether to remove the excess of ligand. Then it is re-filtered and dried under vacuum overnight. A navy colored complex is obtained.

Scheme 2. Synthesis of the bis(imino)pyridine iron(II) complex.

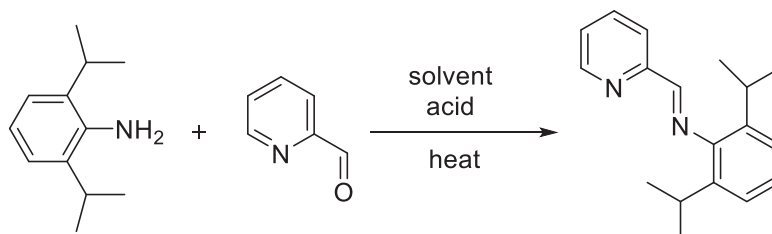


E.3.1.2. Synthesis of Catalyst B

Synthesis of ligand: To a solution of 2-pyridinecarboxaldehyde in dichloromethane is added 1 equiv. of diisopropylaniline. After the addition of a few drops of glacial acetic acid, the solution is refluxed overnight at 130 °C with azeotropic removal of water using a Dean-Stark trap. Upon cooling to room temperature, the product crystallized from the solvent (yellow crystals). After filtration the yellow solid is washed with pentane in order to remove the excess of 2-pyridinecarboxaldehyde (¹H-NMR analysis were done after each wash to check the neatness of the ligand). Then, the product is dried under vacuum to give the corresponding ligand (**Scheme 3**).

Ligand of catalyst B: (2-pyridinecarboxaldehyde(2,6-diisopropylanil)).

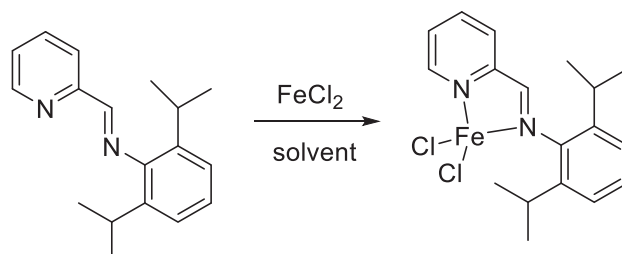
Scheme 3. Synthesis of the iminopyridine ligand.



Synthesis of the complex: Under inert atmosphere, a solution of the ligand in dichloromethane is added to FeCl₂ beads (99.99% purity) with a 1:1 mixture. The mixture is stirred for one week (**Scheme 4**). Then, the solution is filtered, dried under

vacuum, and then washed by diethyl ether to remove the excess of ligand. Then it is re-filtered and dried under vacuum overnight. A dark brown colored complex is obtained.

Scheme 4. Synthesis of catalyst B.



E.3.2. Homo-Polymerization of Ethylene Using Catalyst A

To a solution of 10 mg of catalyst A in 25 mL of toluene is added 20 mg (1 equiv.) of tritylBARf (trityl tetra(pentafluorophenyl)borate). This mixture is transferred by cannula into a balloon charged with 300 mL of heptane and 34 equiv. of triethylaluminum (TEA). Then the solution in the balloon is transferred through a cannula into a 1 L reactor which is stripped from air and moisture. After that, the temperature is set at 70 °C at which the reactor is pressurized by 7 bar of ethylene. The stirrer is set at 400 rpm. The reaction lasts 1 hour after which the reactor is cooled and depressurized. The obtained polyethylene is washed by methanol, filtered and dried for 3 hours in a vacuum oven at 70 °C.

E.3.3. Homo-Polymerization of Isoprene Using Catalyst B

To a solution of 10 mg of catalyst B in 25 mL of toluene is added 26.7 mg (1 equiv.) of tritylBARf. This mixture is transferred by cannula into a balloon charged with 100 mL of toluene and 27 equiv. of TEA. Then, 10 mL of isoprene is added into the balloon. The solution is stirred by a magnetic stirrer (400 rpm). The reaction lasts 2 hours at room temperature. The obtained polyisoprene is dried under vacuum, and stored in a fridge at 8 °C.

E.3.4. Ethylene-Isoprene Copolymerization Test Using Catalyst A

To a solution of 10 mg of catalyst A in 25 mL of toluene is added 20 mg (1 equiv.) of tritylBARf. This mixture is transferred by cannula into a balloon charged with 300 mL of heptane and 34 equiv. of TEA. Then, under argon, the solution in the balloon is

transferred through a cannula into a 1 L reactor which is dried under vacuum. After that, the desired amount of isoprene is added into the reactor. Then, the temperature is set at 70 °C at which the reactor is pressurized by 7 bar of ethylene. The stirrer is set at 400 rpm. The reaction lasts 30 min after which the reactor is cooled and depressurized. The obtained polymer is washed by methanol, filtered and dried under vacuum.

E.3.5. Copolymerization Test Using Catalyst B

To a solution of 10 mg of catalyst B in 25 mL of toluene is added 26.7 mg (1 equiv.) of tritylBARf. This mixture is transferred by cannula into a balloon charged with 300 mL of heptane and 34 equiv. of TEA. Then, under argon, the solution in the balloon is transferred through a cannula into a 1 L reactor which is dried under vacuum. After that, the desired amount of isoprene (2500 equiv.) is added into the reactor. Then, the temperature is set at 70 °C at which the reactor is pressurized by 7 bar of ethylene. The stirrer is set at 400 rpm. The reaction lasts 2 hours after which the reactor is cooled and depressurized. The obtained polymer is dried under vacuum.

E.3.6. Ethylene-Isoprene Chain Shuttling Random Copolymerization

Two Schlenks are used.

In Schlenk 1: To a solution of 20 mg of catalyst A in 25 mL of toluene is added 40 mg (1 equiv.) of tritylBARf under inert atmosphere. The mixture is stirred for 5 min.

In Schlenk 2: To a solution of the desired amount of catalyst B (1 or 5 equiv. with respect to catalyst A) in 25 mL of toluene is added 1 equiv. of tritylBARf under inert atmosphere. The mixture is stirred for 5 min.

Both mixtures are transferred by cannula into a balloon charged with 300 mL of heptane and desired amount of TEA (number of equiv. with respect to both catalysts). Then, the solution in the balloon is transferred through a cannula into a 1 L reactor which is stripped from air and moisture. After that, the desired amount of isoprene is added into the reactor. Then, the temperature is set at 70 °C at which the reactor is pressurized by 7 bar of ethylene. The stirrer is set at 400 rpm. Each reaction lasts 50 minutes after which the reactor is cooled and depressurized. The obtained copolymer is washed by methanol, filtered and dried under vacuum.

E.3.7. Ethylene-Isoprene Chain Shuttling Block Copolymerization

It is a two steps procedure. Two Schlenks are used.

In Schlenk 1: To a solution of 20 mg of catalyst A in 25 mL of toluene is added 40 mg (1 equiv.) of tritylBARF under inert atmosphere. The mixture is stirred for 5 min.

In Schlenk 2: To a solution of the desired amount of catalyst B (1 or 2 equiv. with respect to catalyst A) in 25 mL of toluene is added 1 equiv. of tritylBARF under inert atmosphere. The mixture is stirred for 5 min.

In step 1: The mixture of Schlenk 2 is transferred by cannula into a balloon charged with 100 mL of toluene and desired amount of TEA (number of equiv. with respect to both catalysts). Then the solution in the balloon is transferred through a cannula into a 1 L reactor which is stripped from air and moisture. After that, the desired amount of isoprene is added into the reactor. The stirrer is set at 400 rpm. At this point, the reaction of isoprene polymerization starts at room temperature.

In step 2: After the desired time, 200 mL of heptane and the mixture of Schlenk 1 are transferred by cannula into the reactor. The temperature is set at 70°C, and the reactor is pressurized by the desired pressure of ethylene.

At the end of the reaction, the reactor is cooled and depressurized. The obtained copolymer is washed by methanol, filtered and dried under vacuum.

For entry 8: Same procedure was followed but the reaction is done in a 0.5 L glass reactor from which a sample of the polyisoprene produced in step 1 is taken through sampling valve.

E.3.8. Iron-Catalyzed Ethylene Polymerization in scCO₂

To a solution of 10 mg of catalyst C in 5 mL of toluene are added 15.2 mg (1 equiv.) of tritylBARF and 50 equiv. of TEA. This mixture is stirred for 5 min then transferred by cannula into the high pressure reactor.

The reactor is pressurized by 2 bar of ethylene and 100 bar of CO₂ at 70 °C. The stirrer is set at 600 rpm. The reaction lasts 1 hour. The obtained polymer is washed by methanol, filtered and dried under vacuum.

E.3.9. Iron-Catalyzed Isoprene Polymerization in scCO₂

Isoprene (10 mL, 625 equiv.) is transferred by cannula into the high pressure reactor. Then, to a solution of 10 mg of catalyst B in 5 mL of toluene is added 26.7 mg (1 equiv.) of tritylBARF and 50 equiv. of TEA. This mixture is transferred by cannula into reactor.

The reactor is pressurized by 100 bar of CO₂ at room temperature. The stirrer is set at 600 rpm. The reaction lasts 2 hour. The obtained polymer is washed by methanol and dried under vacuum.

E.4. Analytical Methods

E.4.1. Nuclear Magnetic Resonance (NMR)

NMR analyses (^1H , Heteronuclear Single-Quantum Correlation (HSQC), and Diffusion-Ordered Spectroscopy (DOSY)) were recorded using a Bruker Avance III 400 MHz spectrometer, equipped with a 5mm multinuclear broad band probe (BBFO+) with z-gradient coil. All samples (50 mg) were dissolved in 0.5 mL of $\text{C}_6\text{D}_6/\text{TCE}$ "deuterated benzene/tetrachloroethylene" (1:2). The spectra were recorded at 90°C (363 K) with 256 scans for ^1H -NMR, and 16 scans and 256 increments for HSQC. Chemical shifts (in ppm) were expressed relative to the resonance of tetramethylsilane TMS ($\delta = 0$ ppm).

NMR analyses (^{13}C , DEPT-135, and HMBC) were recorded using a Bruker Avance II 400 MHz spectrometer, equipped with a 10mm ^{13}C - ^1H selective probe (PSEX13C) with z-gradient coil. All samples (100-200 mg) were dissolved in 3 mL of $\text{C}_6\text{D}_6/\text{TCE}$ (1:2). The spectra were recorded at 90°C (363 K) with 4096 scans for ^{13}C -NMR, and 16 scans and 256 increments for HMBC. Chemical shifts (in ppm) were expressed relative to the resonance of tetramethylsilane TMS ($\delta = 0$ ppm).

We thank the NMR Polymer Center of Institut de Chimie de Lyon for assistance and access to the NMR facilities.

E.4.2. Size-Exclusion Chromatography (SEC)

The high temperature size-exclusion chromatography (gel-permeation chromatography (GPC)) analyses were performed using a "Viscotek-Malvern instrument high temperature GPC system" equipped with a differential refractive index detector, viscometer and light scattering detector: Column set: 4 x PLgel Olexis 20 μm columns; Injection volume: 200 μL ; Eluent: 1,2,4 trichlorobenzene at 150°C + 2,6-di-*tert*-butyl-4-methylphenol (0.2 $\text{g}\cdot\text{L}^{-1}$); flow rate: 1.0 ml/min; OmniSEC software (ver. 5.12) was used for data interpretation.

E.4.3. Differential Scanning Calorimetry (DSC)

DSC analyses were carried out on a DSC 3+- Differential Scanning Calorimetry apparatus from METTLER TOLEDO equipped with an auto sampler. This device has a wide temperature range from -70 to 700°C . A computer controls the device and

retrieves the results using STARe software from METTLER TOLEDO.

For the polyethylene samples, a heating-cooling-heating ($25\text{ }^{\circ}\text{C} \leftrightarrow 180\text{ }^{\circ}\text{C}$) process was performed with a heating rate of $10\text{ }^{\circ}\text{C}/\text{min}$ and N_2 flow of $30\text{ mL}/\text{min}$. For ethylene-isoprene copolymers samples, a double cooling-heating ($-90\text{ }^{\circ}\text{C} \leftrightarrow 180\text{ }^{\circ}\text{C}$) process with stabilizing for 5 min at $-90\text{ }^{\circ}\text{C}$ was performed, the heating rate was $20\text{ }^{\circ}\text{C}/\text{min}$ and N_2 flow was $30\text{ mL}/\text{min}$. We consider the data obtained during the last heating.

E.4.4. **Fourier Transform Infrared Spectroscopy (FTIR)**

The device used for infrared analysis is a Nicolet iS50 infrared spectrometer from Thermo Fisher Scientific. The infrared spectra were recorded from 400 cm^{-1} to 4000 cm^{-1} with 32 scans and a resolution of 4. A background spectrum is collected and subtracted from the spectrum of the sample. Samples do not require any prior preparation and were analyzed directly by the ATR module. The software used here for the analysis is OMNIC from Thermo Fisher Scientific.

E.4.5. **Electron Paramagnetic Resonance (EPR)**

The EPR analyses were done in "Laboratoire de Chimie" at ENS-Lyon. It bears the following characteristics: Band X (Bruker 9.4GHz), liquid nitrogen temperature control (Bruker), liquid helium temperature control (Oxford), sperX microwave (ER049X).

Conclusion and Perspectives

Conclusion

The main goal of this thesis has been to utilize carbon dioxide in radical and catalytic polymerizations of olefins. For this purpose, we used ethylene, the simplest and most industrially applicable olefinic monomer, to polymerize it *via* a radical process, in which we use CO₂ as a polymerization medium and as a functionalization agent. On the other hand, we used ethylene and isoprene as monomers in iron-catalyzed polymerization processes. Both monomers were exploited for two purposes. The first purpose was to copolymerize ethylene and isoprene through an iron-catalyzed chain shuttling copolymerization, such copolymers could have several applications mainly in tire manufacturing. The second purpose is to polymerize each monomer in supercritical CO₂ (scCO₂) using its corresponding iron catalyst in order to aim at sustainable processes and potentially chain-end functionalization. Both monomers produce polymers that are crucial from an industrial point of view, polyethylene is the most common thermoplastic and polyisoprene can be derivatized into a mimic of natural rubber.

In the section of ethylene radical polymerization, the first achievement was the polymerization of ethylene *via* a free radical process in scCO₂ (as a polymerization medium) under mild conditions (< 100 °C, < 300 bar) without addition of any initiator diluent (co-solvent). This work has been done using three different initiators, AIBN, lauroyl peroxide, and benzoyl peroxide, to investigate different initiation modes. The decarboxylation of the latter was suppressed in scCO₂ and yielded ester-functionalized polyethylene.

Thus, CO₂ was successfully used as a polymerization medium in ethylene free radical polymerization process.

Triethylaluminum (AlEt₃) has been found to be an agent that interacts with CO₂ as mentioned in the literature.^{1,2} Here, we evidenced its interaction with radicals and its role as an irreversible chain transfer agent in ethylene radical polymerization.

Relying on both characteristics of AlEt₃ (interaction with CO₂ and radicals), this chain-transfer agent was utilized in CO₂-mediated ethylene radical polymerization to obtain a

CO₂-functionalized polyethylene. This work showed that AlEt₃ acts as a CO₂-incorporating agent in CO₂-mediated ethylene radical polymerization. CO₂ was incorporated within the LDPE chains in the form of a ketal (a primary proposition).

Thus, the LDPE produced in the radical polymerization process has been functionalized by CO₂ within its chains using AlEt₃.

Therefore, CO₂ can be advantageously utilized as a polymerization medium and a functionalization agent in ethylene radical polymerization.

In the catalytic section, the ethylene-isoprene random and block copolymerizations *via* an iron-catalyzed chain shuttling process have been achieved. In this method, a dual-catalyst process was applied in order to synthesize ethylene-isoprene copolymers using two iron complexes, each one is exclusively active in the polymerization of one specific monomer. By varying the procedure, either a random or a block copolymer has been produced. The produced copolymers were analyzed extensively to insure the synthesis of the proposed architectures and study their microstructure. This process represents an innovative route for the synthesis of such copolymers using the environmentally friendly iron complexes; ethylene-isoprene copolymer could be used in manufacture of tires and golf balls for example.

Then, successful tests have been done for ethylene and isoprene iron-catalyzed polymerizations in scCO₂, showing that CO₂ could be used as an alternative to organic solvents in the catalytic synthesis of these polymers that are the precursors in our daily-used materials (plastics and rubbers).

Perspectives

In this thesis, each chapter opens the door for a series of new projects.

Ethylene free radical polymerization in scCO₂:

The free radical polymerization of other olefins, such as styrene, in scCO₂ could be investigated. Polystyrene is of high industrial importance, it is used for producing disposable plastic cutlery and dinnerware, small hardware such as smoke detector housings, etc., in addition to its medical applications in tissue culture trays and test tubes manufacture for example. Thus polymerizing such an industrially applicable monomer in

CO₂, a waste product that is affecting the climate, without addition of any petro-derived organic solvents constitutes a real improvement toward sustainable production of polystyrene.

Also, polymerization of some polar monomers could be tested in scCO₂, such as vinyl acetate polymerization. Poly(vinyl acetate) has several end-uses, as a wood glue and a paper adhesive for example. This homo-polymerization could be continued towards the copolymerization of ethylene and vinyl acetate in scCO₂ since both monomers feature close reactivity ratios. Until now, this copolymerization is only achieved in conventional free radical polymerization processes. Ethylene-vinyl acetate copolymer (EVA) production refers to different processes and different EVA classes. Very high-pressure bulk polymerization process yields EVA with high ethylene contents (semi-crystalline EVA), low-pressure emulsion polymerization process yields EVA with high vinyl acetate content (amorphous EVA), and solution polymerization in organic solvent yields EVA with properties in between those of the EVA produced in bulk and in emulsion processes. In scCO₂, EVA bearing common properties of that produced in emulsion process and that produced in solution process could be expected.

Such copolymer is frequently required due to its wide range of applications, in hot melt adhesives, drug delivery devices, ski boots, hockey pads, encapsulation materials for crystalline silicon solar cells, etc. The synthesis of this copolymer in scCO₂ is again an alternative to organic-solvent based processes. (This is an area of research at C2P2 laboratory)

Effect of triethylaluminum on ethylene radical polymerization:

The role of AlEt₃ as an irreversible chain transfer agent shows that it could be possible to have compounds that are structurally related to AlEt₃ (BEt₃, ZnEt₂, MgR₂...) acting as controlling agents in ethylene radical polymerization. Thus, several compounds that bear a Lewis acid character could be tested in ethylene radical polymerization, especially metal alkyls, such as dialkylzinc or dialkylmagnesium. If the control is achieved using these compounds they will be an interesting alternative to other controlling agents, such as RAFT agents (which contain sulfur) and tellurium compounds in tellurium-mediated radical polymerization, in particular thanks to their functionalizable M-C bond. An emphasis on the fragmentation of the M-C bond is here essential, to develop a suitable

controlling agent.

In case of success of the control of ethylene radical polymerization using one of the agents, the investigations could continue towards the synthesis of ethylene/co-monomer block copolymers through the living polyethylene chain-ends. The co-monomers could vary from olefins, such as styrene, to polar monomers, such as vinyl acetate, but it must be taken into account the reactivity of the ester functional group in vinyl acetate with controlling agents such as AlEt_3 . As aforementioned, such copolymers are of huge interest from an industrial point of view.

Incorporation of CO_2 within the polyethylene chains using triethylaluminum:

The percentage of the CO_2 incorporated could be improved by scanning different compounds that are structurally related to AlEt_3 , such as dialkylzinc and dialkylmagnesium. By increasing this percentage, new LDPE-type bearing CO_2 -derived motifs with improved polarity will be produced, this would help its compatibilization with fillers for instance, while retaining its intrinsic mechanical and chemical properties.

Other aluminum-based Lewis acids, such as aluminum chloride, could be also tested in CO_2 -mediated ethylene radical polymerization to check their efficiency in incorporating CO_2 within the polyethylene chains, speculating some ligand exchange *via* single-electron transfer processes. This test must be preceded by an investigation of the interaction between the Lewis acid and radicals. Note that, even though some Lewis acids of this family are hard to solubilize in the solvents used in radical polymerization reactions, it could be possible to solubilize them in a small amount of a co-solvent taking into account the overall miscibility of solvents, for example, solubilizing AlCl_3 in toluene for a reaction done in heptane.

On the other hand, AlEt_3 could be utilized in the incorporation of CO_2 within other common polymer chains, such as polystyrene. This incorporation will give these apolar polymers a partially polar characteristic, helping in their compatibilization within blends of polymers, or with fillers in their industrial applications.

Other methods could be applied to incorporate CO_2 within polyethylene and other polyolefins. One of these methods is the use of frustrated Lewis pairs (P-B or N-B Lewis pairs) as CO_2 -incorporating agents in ethylene (olefin) radical polymerization. It has been

proved in the literature that this type of Lewis pairs is able to "catch" CO_2 ,^{3,4} thus, there will be non-symmetrical CO_2 molecules in the polymerization medium which will facilitate its incorporation within the polyethylene (polyolefin) chain.

Iron-catalyzed ethylene-isoprene chain shuttling copolymerization:

The chain shuttling copolymerization process using the environmentally friendly iron complexes could be exploited in other ethylene/co-monomer copolymerizations, such as ethylene-butadiene. These copolymers will be produced using an environmentally benign metal (iron) which is also the cheapest among transition metals. In addition, this process will give access to the production of a series of random and block copolymers that are of huge industrial interest. Ethylene-butadiene copolymer is used in tires for instance.

Also, we could have access to other copolymers that couldn't be synthesized using strictly iron catalysts but using other metal complexes. For example, ethylene-styrene block copolymer could be synthesized using a dual metal-based iron/nickel catalyzed chain shuttling copolymerization.

Iron-catalyzed polymerizations of ethylene and isoprene in scCO_2 :

Further investigations must be conducted for the iron-catalyzed polymerizations of ethylene and isoprene in scCO_2 in order to optimize all the kinetics to achieve better activities (comparable to the activities in the conventional polymerizations).

On the other hand, the investigations could continue towards the incorporation of CO_2 within the polymer chains. One of the key steps to achieve this incorporation is to have the concentration of ethylene in the medium equal to triple of that of CO_2 , as it was proved by kinetic studies in the literature. Other strategies could be investigated to overcome the kinetic barriers of this process, such as adjusting the temperature.

A route to copolymerize ethylene and CO_2 could be tested using a hybrid radical/catalytic process. First, by the aid of a Lewis base, iron complexes could be able to produce acrylates from ethylene and CO_2 via an ironalactone intermediate in the same manner of nickel-catalyzed reactions which have been studied thoroughly in the literature (see chapter I). Then, the formed acrylates could be polymerized using a radical initiator that will be added into the medium. Thus, ethylene and CO_2 could be copolymerized through an acrylate intermediate using a hybrid catalytic/radical process; this process is

an analogue to what has been proposed by Nozaki and co-workers about butadiene-CO₂ copolymerization *via* a lactone intermediate using a palladium/AIBN hybrid process.⁵

Finally, this thesis forms a basis towards the activation of CO₂ in the polymerizations of olefins. Also, it represents a path towards the development of more sustainable olefin polymerization processes, either by utilizing a waste and readily available product (carbon dioxide) in these processes or by utilizing cheap and environmentally friendly raw materials (iron complexes). Therefore, it is really attractive for both academic and industrial domains for the new chemistries that it presents (especially in CO₂ activation) and for the dual benefit that it provides in the olefin polymerization processes (versatile and environmentally benign processes).

References

1. J. Weidlein *Angew. Chem.* **1969**, *81*, 947.
2. Yur'ev, V. P.; Kuchin, A. V.; Tolstikov, G. A. *Bull. Acad. Sci. USSR Div. Chem. Sci.* **1974**, *23* (4), 817.
3. Peuser, I.; Neu, R. C.; Zhao, X.; Ulrich, M.; Schirmer, B.; Tannert, J. A.; Kehr, G.; Fröhlich, R.; Grimme, S.; Erker, G.; et al. *Chem. - Eur. J.* **2011**, *17* (35), 9640–9650.
4. Voss, T.; Mahdi, T.; Otten, E.; Fröhlich, R.; Kehr, G.; Stephan, D. W.; Erker, G. *Organometallics* **2012**, *31* (6), 2367–2378.
5. Nakano, R.; Ito, S.; Nozaki, K. *Nat. Chem.* **2014**, *6* (4), 325–331.